

City Research Online

City St George's, University of London

Citation: Brown, A. J. (1972). The gas phase oxidation of N.butane. (Unpublished Doctoral thesis, The City University)

This is the accepted version of the paper.

This version of the publication may differ from the final published version. To cite this item please consult the publisher's version.

Permanent repository link: https://openaccess.city.ac.uk/id/eprint/38474/

Copyright and Reuse: Copyright and Moral Rights remain with the author(s) and/or copyright holders. Copies of full items can be used for personal research or study, educational, or not-for-profit purposes without prior permission or charge, unless otherwise indicated, provided that the authors, title and full bibliographic details are credited, a hyperlink and/or URL is given for the original metadata page and the content is not changed in any way. For full details of reuse please refer to City Research Online policy.

City Research Online: http://openaccess.city.ac.uk/ publications@citystgeorges.ac.uk

A THESIS

entitled

THE GAS PHASE OXIDATION OF n-BUTANE

by

ANDREW JAMES BROWN

Submitted for the

Degree of Doctor of Philosophy

of The City University

THE CITY UNIVERSITY LIBRARY,
ST. JOHN STREET, LONDON, E.C.1.

68374

ABSTRACT

The gas phase oxidation of n-butane has been studied at sub-atmospheric pressures in the temperature range 280 - 420°C. The effect of the variation of initial temperature and initial pressure on the mechanism of oxidation has been assessed from observations of the kinetic changes and the variation of the nature and distribution of products.

Section 1 examines the most recent theories on the mechanism of oxidation of hydrocarbons and particular attention is focussed on the primary chain-propagation reactions. The effect of molecular structure on the mechanism of oxidation is considered in detail and it is shown that high molecular weight hydrocarbons oxidise by different routes from low molecular weight hydrocarbons. The morphological phenomenon of cool flames is considered in the light of the foregoing variation in mechanism of oxidation.

Section 2 describes the experimental techniques used in the present study. A standard static vacuum system was employed in which pressure changes were monitored by means of a strain-gauge pressure transducer and temperature changes by micro-thermocouples. Reaction products were identified and estimated by gas chromatography.

The kinetic and analytical results are presented in Section 3. Changes in physical parameters are related to the initial temperature and pressure. It is shown that at temperatures below ca. 330°C cool flames propagate from the walls of the reactor, whereas above this temperature they propagate from the centre of the reactor. Details of the variation of the concentration of reaction products with time are given and the percentage yields of these products, during the early stages of reaction, are related to the initial reaction conditions.

The results are discussed in Section 4 in which it is concluded that the major chain-propagation sequence involves α- and β-hydroperoxybutyl radicals at low initial temperatures. Further oxidation of β-hydroperoxybutyl radicals gives rise to acetaldehyde and acetone in relatively large yields, whereas the β-scission decomposition of α-hydroperoxybutyl radicals, which occurs predominantly at the reactor walls, is responsible for the formation of but-1-ene and but-2-ene. At higher initial temperatures, however, the chain-propagation cycle involves principally α-hydroperoxybutyl radicals which undergo homogeneous β-scission decomposition reactions to form the major products but-1-ene and but-2-ene. Furthermore, at high initial temperatures the further oxidation of β-hydroperoxybutyl radicals is of minor importance.

CONTENTS

		Page No.
ABSTRACT		2
ACKNOWLEDGEMENTS		5
SECTION 1	INTRODUCTION	6
SECTION 2	EXPERIMENTAL	69
SECTION 3	RESULTS	105
SECTION 4	DISCUSSION	198
REFERENCES		259

ACKNOWLEDGEMENTS

I wish to acknowledge the advice and encouragement given to me throughout my work by my supervisor Dr. R.T. Pollard and by [redacted]. Furthermore, I am particularly grateful to Dr. Pollard for arranging a visit to the University of Lille where I was able to have informative discussions with the members of [redacted] research team. I also wish to express my appreciation to my colleagues in the Combustion Research Group for providing a congenial working atmosphere and to [redacted] and [redacted] for their technical help.

Finally, I am grateful to the Science Research Council who provided a grant and a Research Studentship for this work.

A.J.B.

SECTION 1

INTRODUCTION

SECTION 1

		Page No.
1.1	Introduction	9
1.2	Phenomena associated with gas phase hydrocarbon oxidation	13
1.2.1	Ignition diagram	13
1.2.2	Slow combustion	15
1.2.3	Cool flames	17
	1.2.3.1 The single cool-flame region	17
	1.2.3.2 The multiple cool-flame region	17
1.2.4	Hot ignition	18
	1.2.4.1 Single-stage ignition	18
	1.2.4.2 Two-stage ignition	19
	1.2.4.3 Multi-stage ignition	19
1.2.5	Negative temperature coefficient regions	19
1.2.6	Pic d'arrêt	20
1.3	Modern theories of the mechanism of the gas phase oxidation of hydrocarbons	21
1.3.1	The low temperature mechanism	22
	1.3.1.1 Initiation	22
	1.3.1.2 Propagation	24
	1.3.1.3 Branching	37
	1.3.1.4 Termination	44
1.3.2	The high temperature mechanism	48
	1.3.2.1 Initiation	48
	1.3.2.2 Propagation and branching	48
	1.3.2.3 Termination	52

		Page No.
1.4	Consequences of the low temperature mechanism	53
1.4.1	Cool flames and two-stage ignitions	53
1.4.2	Knock and run-on	55
1.4.3	Preparative applications	56
1.5	The influence of molecular structure on the mechanism of oxidation	58
1.5.1	Hydrocarbons with five or more carbon atoms	59
1.5.2	Hydrocarbons with four or less carbon atoms	63
1.6	The present work	67

1.1 Introduction

Two of Man's principal natural resources, oil and natural gas, consist essentially of hydrocarbons. At present these are used mainly for combustion, the energy released being converted to heat and mechanical energy. The rapid growth of industry during the past forty years has led to an approximately threefold increase in the demand for energy and much of this increased demand has necessarily been met by oil, and to a lesser extent by natural gas. The important role of these sources of energy can clearly be seen from Table 1.1 which shows the Free World Energy Consumption over the last thirty years[1].

Another increasingly important use of these hydrocarbon resources is as feedstocks for the large-scale production of petrochemicals. The petrochemical industry which began in the U.S. in the early 1920's, has now become internationally important, largely as a result of naphtha assuming a dominating position as a feedstock for the production of ethylene. An attractive feature of producing petrochemicals by direct oxidation methods is the relatively low cost of the raw materials. Oxygen can be separated from air very cheaply and hydrocarbon feedstocks are both inexpensive and plentiful. This is clearly illustrated by the fact that in 1969 more than 84% of the U.S. industry's ethylene oxide[2] and practically all of the acetic acid[3] were produced by direct oxidation methods. The worldwide expansion of the petrochemical industry has been further encouraged by the increasing demands of three growth industries namely nitrogen fertilisers, high polymers and man-made fibres. In a review of the future of petroleum processing, Uhl[4] indicates that a far heavier emphasis will continue to be placed on the production of even larger tonnages of petrochemicals.

Table 1.1

Free World Energy Consumption
(Million metric tons coal equivalent)

Year	Coal	Oil†	Natural Gas	Hydroelectric & Nuclear Power	Total
1937	1,133	320	92	21	1,566
	72.4	20.4	5.9	1.3	100%
1948	1,212	506	191	35	1,944
	62.4	26.0	9.8	1.8	100%
1955	1,191	932	360	55	2,538
	46.9	36.7	14.2	2.2	100%
1960	1,128	1,228	534	76	2,966
	38.0	41.4	18.0	2.6	100%
1966	1,213	1,888	742	109	3,952
	30.6	47.8	18.8	2.8	100%
1968	1,220	2,170	850	120	4,360
	28.0	49.8	19.5	2.7	100%

† based on 1 ton of oil = 1.5 tons coal equivalent

The increasing importance and widespread use of hydrocarbons in the twentieth century has naturally been paralleled by a vast amount of research into the nature of the reaction between hydrocarbons and oxygen or air. Since the combustion of hydrocarbons is used primarily as a source of heat and mechanical energy, maximum efficiency can be attained only by subjecting the combustion processes to the necessary control. In this context it is possible to exert both physical and chemical control and it is in the latter case that detailed studies of combustion reactions are important. Furthermore, abnormal combustion phenomena, such as 'knock' and 'run-on' in internal combustion engines, lead to a general loss of power and efficiency and these phenomena have, therefore, been subjected to considerable research in order to eliminate or at least minimise their detrimental effects. Directly associated with the increased use of internal combustion engines is the problem of automobile exhaust emissions [5]. This form of pollution results from incomplete reaction in the combustion chamber which leads to the release into the atmosphere of obnoxious partial oxidation products, such as unsaturated carbonyl compounds [6]. Legislation is now being introduced, and indeed is already in force in some countries, to control exhaust emissions and this has led to detailed studies of the means by which complete combustion may be enhanced.

The expansion of the petrochemical industry has also involved extensive research into the partial and selective oxidation of hydrocarbons. Direct oxidation, as previously mentioned, constitutes a most important method of production of petrochemicals. However, the partial oxidation of hydrocarbons, even for simple compounds such as methane and benzene, usually gives rise to a multiplicity of products by a series of consecutive reactions. Careful control of the experimental conditions can, however, improve selectivity, as can the use of homogeneous catalysts such as hydrogen bromide and nitrogen oxides.

Alternatively, heterogeneous oxidation reactions offer the advantage that they may be carried out at lower temperatures and thus with improved selectivity although they suffer from the fact that the catalysts, which are generally expensive, tend to undergo various forms of physical and chemical deterioration. From the foregoing considerations it is clear, however, that an overall understanding of the mechanism of hydrocarbon oxidation and the precise experimental conditions under which the reaction concerned may be controlled, is of vital importance to industry.

1.2 Phenomena associated with gas phase hydrocarbon oxidation

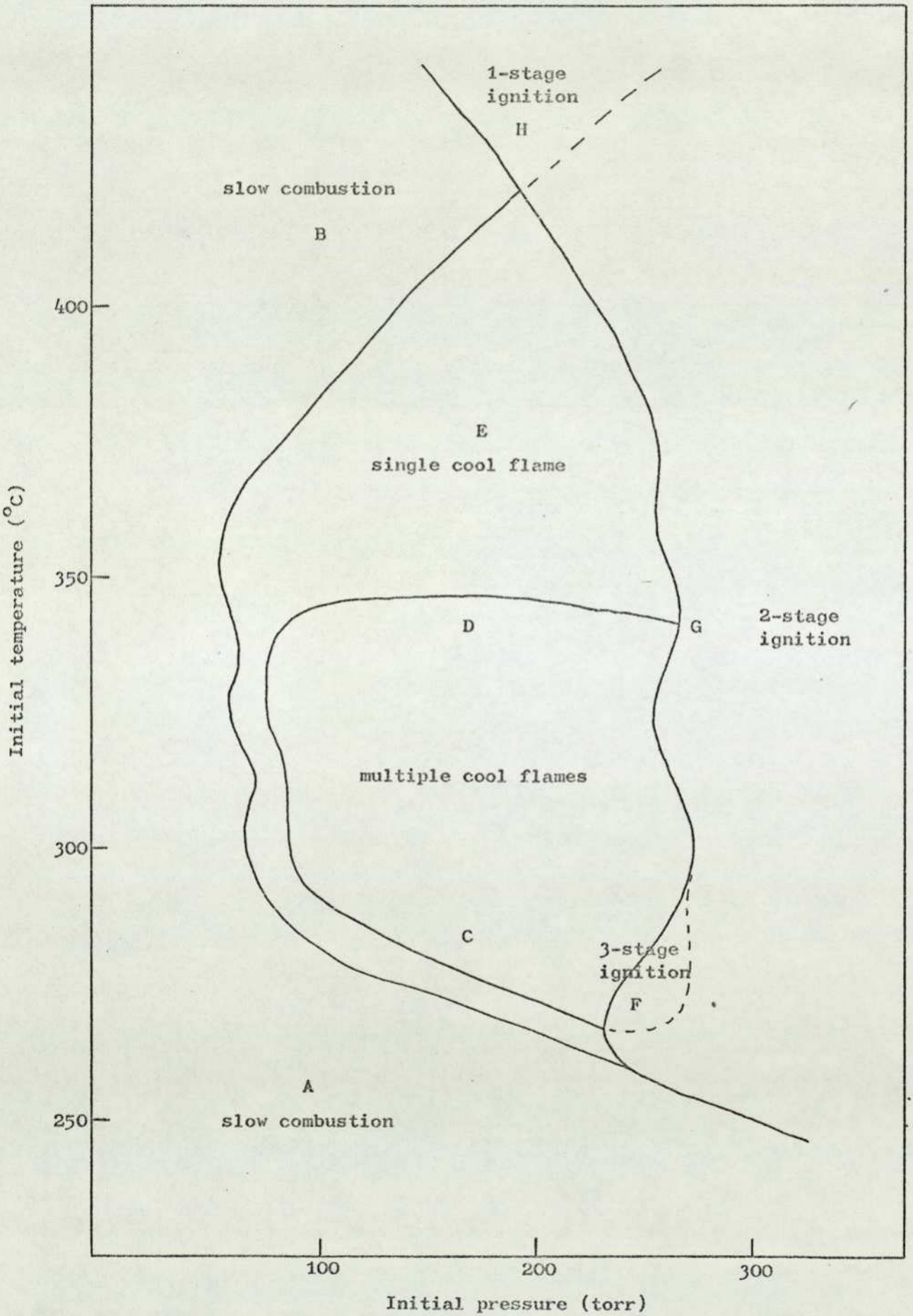
The gaseous oxidation of a hydrocarbon is a complex free-radical chain reaction which involves a proliferation of chain carriers and branching agents with widely differing lifetimes and modes of reaction. It is also one of the best known examples of a degenerately branched chain reaction [7], a concept first introduced by Semenov in 1933. The oxidation mechanism, which manifests itself in the variation of reaction rate with the initial temperature and pressure conditions, leads to a complex temperature/pressure ignition diagram that exhibits distinct high temperature and low temperature regions with an intermediate region of negative temperature coefficient of reaction rate. The nature of the various phenomena, such as slow combustion, cool flames and hot ignitions, exhibited by hydrocarbon + oxygen systems are described below.

1.2.1 Ignition diagram

The physical manifestations of the various combustion phenomena are usually observed as changes in pressure, temperature and light emission. It is convenient, therefore, to illustrate the initial conditions under which these phenomena occur in terms of a temperature/pressure diagram, an example of which is shown in figure 1.1. The major features of this diagram are the regions of slow combustion, cool flames and spontaneous ignition. The position and shape of the boundaries between these regions are extremely dependent upon the molecular structure of the hydrocarbon, the stoichiometry, the reaction vessel dimensions and the nature of the reactor surface. These diagrams usually exhibit lobes in the cool flame/ignition boundary which are sometimes reflected at the slow combustion/cool flame boundary. The number of lobes that occur, depends principally on the molecular weight and structure of the hydrocarbon.

Figure 1.1

A typical ignition diagram for hydrocarbon + oxygen mixtures



1.2.2 Slow combustion

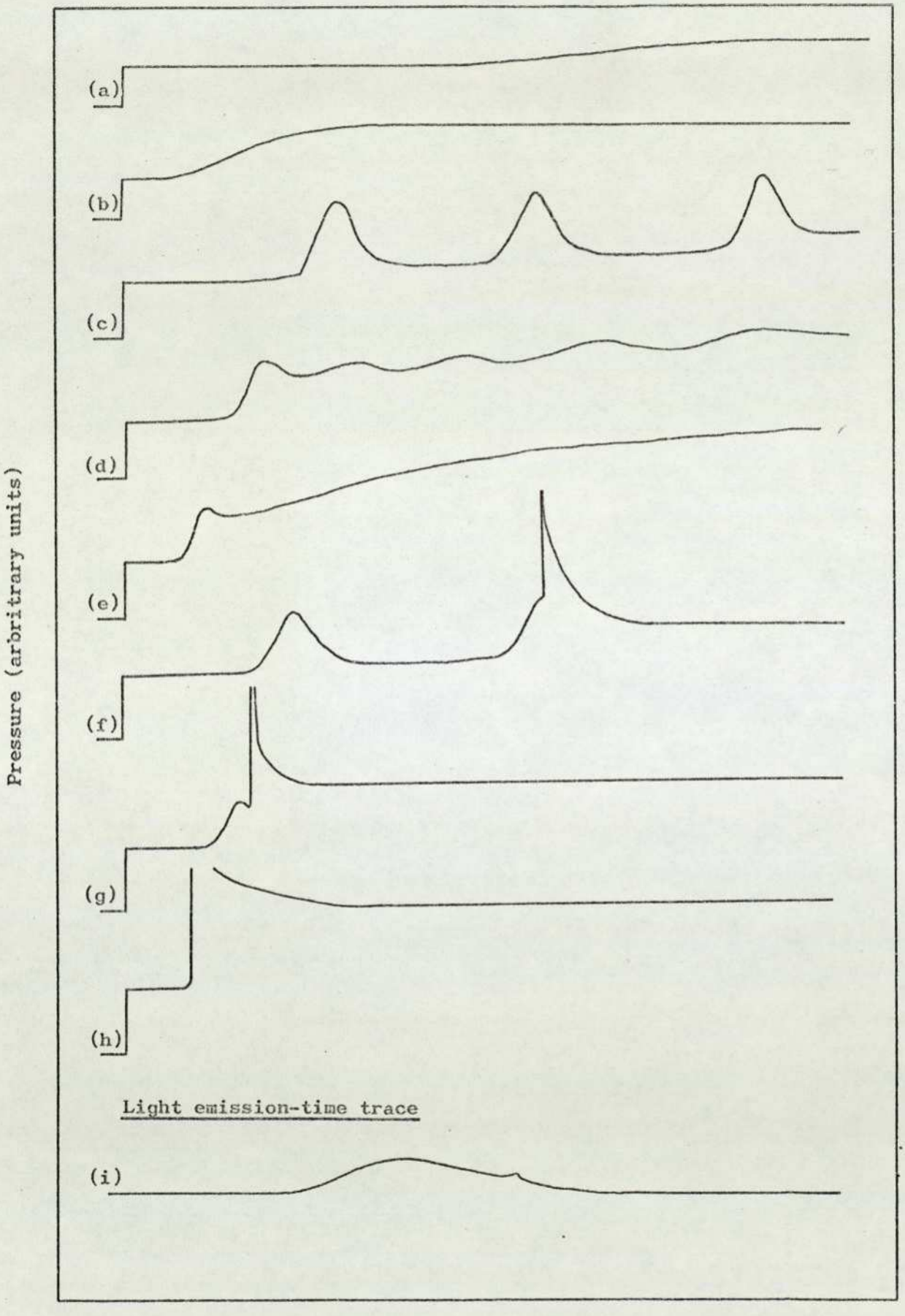
The region of slow combustion can conveniently be considered in two parts, namely the high-temperature region above 350 - 400°C and the low-temperature region below 350°C, although the observed phenomena change continuously as this region is traversed isobarically.

In the low temperature region, hydrocarbons begin to oxidise slowly above limiting temperatures and pressures and the reaction is characterised by an induction period during which no appreciable reaction occurs. The pressure then rises exponentially until a maximum rate of change is attained after which the rate falls and the pressure finally reaches a stationary value (a typical pressure-time recording is shown in figure 1.2(a) for initial conditions corresponding to point A on the ignition diagram). The slow combustion process is essentially isothermal and is accompanied by a faint luminescence, although this cannot be detected without the use of a photocell. The reaction, during which the hydrocarbon is only partially consumed, leads to an overall increase in pressure and this represents the increase in molecular concentration.

The physical characteristics of slow combustion in the high-temperature region are similar to those in the lower region except that the reaction is considerably faster and a greater consumption of reactants occurs. The induction periods are considerably shorter and the sinusoidal pressure rise is more pronounced as shown in figure 1.2(b) (point B on the ignition diagram). Likewise, the intensity of the luminescence accompanying the reaction is markedly increased.

Figure 1.2

Pressure-time recordings of oxidation phenomena



1.2.3 Cool flames

The cool-flame region in the ignition diagram can also be divided into two distinct parts. At temperatures below ca. 300 - 350°C (depending on the molecular structure of the hydrocarbon), multiple cool flames are observed for the majority of hydrocarbons, whereas above this temperature a single cool flame propagates and is followed by rapid slow combustion.

1.2.3.1 The single cool-flame region

A cool flame in this region is associated with a transient pressure pulse ($\Delta p_{c.f.}$) of ca. 10 - 50 torr and a transient temperature pulse ($\Delta T_{c.f.}$) of ca. 10 - 100°C. At initial temperatures close to the upper cool flame limit, the intensities of the cool flames,(as defined by

$$I = \frac{\Delta p_{c.f.}}{p_o + \Delta p_{c.f.}}$$

where p_o is the initial pressure), are much smaller than those at lower temperatures near to the multiple cool flame limit. The passage of the cool flame is also accompanied by a sudden increase in the light emission, which is manifested as a pale blue glow that slowly fades as the following fast combustion ensues. A typical pressure-time recording is shown in figure 1.2(e) (point E). Throughout this region, the overall increase in pressure ($\Delta p_{c.f.\infty}$), which is indicative of the extent of reaction during the cool flame, is large in comparison with the transient pressure rise associated with the cool flame ($\Delta p_{c.f.}$).

1.2.3.2 The multiple cool-flame region

The intensities of cool flames in this region are noticeably greater than those of cool flames in the upper region and pressure rises of ca. 10 - 90 torr and temperature pulses of ca. 10 - 200°C are observed. Multiple cool flames are also accompanied by periodic blue glows which are

generally observed to propagate from the centre of the reaction vessel [8]. Induction periods at initial temperatures close to the lower limit can vary between minutes and hours, whereas near the upper limit of multiple cool flames they are usually only of the order of seconds. Furthermore, at low initial temperatures $\Delta p_{c.f.}{}^{\infty}$ is small in comparison with $\Delta p_{c.f.}$ but as the temperature is increased, $\Delta p_{c.f.}{}^{\infty}$ increases whilst $\Delta p_{c.f.}$ decreases. Another noticeable variation is that at low initial temperatures (point C) the cool flames are clearly resolved, the pressure pulses having large amplitudes and relatively low frequencies (as shown in figure 1.2(c)), whereas at higher temperatures (point D) they have small amplitudes and high frequencies and are superimposed on the fast combustion following the first cool flame, as shown in figure 1.2(d). The number of successive cool flames depends largely on the nature of the hydrocarbon, the stoichiometry and the nature and extent of the reactor surface, the maximum reported being seven [9, 10].

1.2.4 Hot ignition

Three types of hot ignition may occur, depending on the initial conditions as shown in figure 1.1.

1.2.4.1 Single-stage ignition

This type of ignition generally occurs at temperatures above ca. 400°C and is characterised by an extremely rapid increase in pressure and temperature and a large overall pressure increase. The temperature rise is usually considerably greater than that observed during cool flame propagation. This type of ignition is preceded by an induction period of the order of milliseconds and is accompanied by a bright orange flame. The pressure-time trace of a one-stage ignition is shown in figure 1.2(h) which corresponds to point H.

1.2.4.2 Two-stage ignition

Two-stage ignition occurs on the high pressure side of the cool flame/ignition boundary. In this case, the hot ignition described above is preceded by the propagation of a cool flame as shown in figure 1.2(g) (point G). The two-stage process is accompanied by a pale blue glow which is rapidly superseded by a bright blue or orange flame at low and high initial temperatures respectively. The ignition stage is again associated with a large increase in pressure and temperature and a large overall pressure rise, indicating a high consumption of reactants.

1.2.4.3 Multi-stage ignition

Three, four and five-stage ignitions can occur under certain initial conditions although these are very limited. This type of phenomenon is found at low temperature in pockets along the cool flame/ ignition boundary. A multi-stage ignition consists of the propagation of between one and three cool flames followed by a two-stage ignition as shown in figure 1.2(f)(point F). This type of ignition is accompanied by pulsating light blue glows culminating in a slightly more intense glow which corresponds to the final ignition stage. The intensity of this final stage is notably less than that of either single or two-stage ignition since considerable consumption of reactants has already occurred in the preceding cool flames.

1.2.5 Negative temperature coefficient regions

A feature peculiar to all regions of hydrocarbon oxidation is the occurrence of temperature ranges within which the rate of the overall reaction possesses a negative temperature coefficient. Thus, as the initial temperature is raised, the rate of the reaction falls until a temperature is reached where a positive value is restored to the coefficient and the reaction rate again increases. The principal

negative temperature coefficient region for most hydrocarbon + oxygen systems is found to extend over about 50° above ca. 300 - 350°C and as this region is traversed from low to high temperature, the kinetic phenomena accompanying the reaction become noticeably less pronounced. Smaller regions of negative temperature coefficient also exist in the low temperature region where the cool flame/ignition boundary displays lobes.

1.2.6 Pic d'arrêt

This phenomenon occurs in the final stages of the slow reaction between 250 and 600°C and is characterised by a sharp increase in light emission and a sudden, but temporary, acceleration of the rate of reaction. Two distinct regions, one at high and the other at low temperatures, can be identified for the occurrence of the phenomenon, which becomes more pronounced as the oxygen content of the reactant mixture is lowered. The interval of time between the point at which the reaction rate is a maximum and the occurrence of the pic d'arrêt is also dependent on the oxygen concentration and decreases as the oxygen content is lowered. A typical light emission-time trace showing the pic d'arrêt is shown in figure 1.2(j).

1.3 Modern theories of the mechanism of the gas phase oxidation of hydrocarbons

The past decade has seen many significant changes in the approach to the elucidation of the complex mechanism of hydrocarbon oxidation. First, improved analytical techniques such as gas-liquid chromatography and mass spectrometry have allowed far more detailed information regarding intermediate products to be obtained at all stages of the reaction. Secondly, thorough investigations have been made into the oxidation of the various intermediate oxidation products such as alkenes, aldehydes and ketones. Thirdly, and perhaps most important, the development of mass spectrometric techniques has led to the positive identification of free radicals, such as hydroperoxy and alkylperoxy radicals, which have been proposed as participants in oxidation mechanisms and for which only circumstantial evidence had previously existed. Fourthly, specific radical reactions have been studied using new techniques such as kinetic spectroscopy and low temperature cryostat investigations and finally, the expansion of thermochemical and kinetic knowledge has led to the accumulation of a vast quantity of data concerning the elementary reactions occurring in hydrocarbon oxidation. This quantitative data takes the form of specific rate constants at stated temperatures as well as the associated Arrhenious parameters. It has become possible, therefore, to suggest likely sequences of reactions for a given oxidation and in many cases semi-quantitative tests on these schemes give excellent results [11,12]. Even so, unanimous agreement as to the complete mechanism has yet to be reached, although it is generally accepted that two distinct mechanisms can be distinguished, namely a low temperature and a high temperature mechanism. During the past forty years numerous mechanisms have been proposed [13-18], but the current theories will now be discussed.

1.3.1 The low temperature mechanism

This mechanism, which is considered to operate below ca.400°C, must be capable of explaining not only the variation of the nature and distribution of the reaction products with respect to the initial conditions, but also the observed morphological phenomena such as cool flames, hot ignitions, regions of negative temperature coefficient and lobes in the cool flame/ignition boundary.

1.3.1.1 Initiation

At temperatures below 450°C the initiation step is generally believed to involve the abstraction of a hydrogen atom by an oxygen molecule:

$$C_nH_{2n+2} + O_2 \longrightarrow \dot{C}_nH_{2n+1} + \dot{H}O_2 \qquad (1.1)$$

This mode of initiation was first suggested by Cullis and Hinshelwood [19] and later substantiated theoretically by Semenov [20]. The ease of the initial hydrogen abstraction depends on the nature of the C-H bond, and as Walsh [21] has pointed out, in view of the electrophilic nature of the oxygen molecule, the probability of attack at a C-H bond is in the order $3^o > 2^o > 1^o$. It can clearly be seen from the C-H bond strengths (Table 1.2) that the initiation is likely to be selective, endothermic and slow. Mayer and Schiller [22] computed the activation energy and rate constants of reaction (1.1) for methane and found $E_{1.1} = 57$ kcal.mole^{-1}, $k_{1.1}(300^oK) = 6 \times 10^{-33}$ l.mole.$^{-1}$ sec.$^{-1}$ and $k_{1.1}(1000^oK) = 6 \times 10^{-3}$ l.mole.$^{-1}$ sec.$^{-1}$. For higher hydrocarbons the overall value of $E_{1.1}$ is likely to be slightly lower due to the presence of 2° or 3° C-H bonds and a value of $E_{1.1}$ of 45-50 kcal.mole^{-1} is generally accepted. This endothermic reaction was originally thought to occur homogeneously, but several workers have illustrated the existence of a heterogeneous mode of initiation [23, 24].

Table 1.2

C-H bond strengths

Bond	$D[C\text{-}H]$ kcal. $mole^{-1}$
primary	98.0
secondary	94.5
tertiary	91.7
	$D[H\text{-}O_2^{\cdot}] = 45$ kcal. $mole^{-1}$

1.3.1.2 Propagation

Alkyl radicals formed in the initiation step may undergo several modes of subsequent reaction viz:- isomerisation, recombination, abstraction, decomposition or further reaction with oxygen as shown below.

$$CH_3\dot{C}H(CH_2)_nCH_3 \longrightarrow CH_3CH_2\dot{C}H(CH_2)_{n-1}CH_3 \quad (1.2)$$

$$\dot{C}_nH_{2n+1} + \dot{C}_nH_{2n+1} \longrightarrow C_{2n}H_{4n+2} \quad (1.3)$$

$$\dot{C}_nH_{2n+1} + C_mH_{2m+2} \longrightarrow C_nH_{2n+2} + \dot{C}_mH_{2m+1} \quad (1.4)$$

$$\dot{C}_nH_{2n+1} \longrightarrow C_mH_{2m} + \dot{C}_{(n-m)}H_{2(n-m)+1} \quad (1.5)$$

$$\dot{C}_nH_{2n+1} + O_2 \longrightarrow C_nH_{2n+1}\dot{O}O \quad (1.6)$$

$$\dot{C}_nH_{2n+1} + O_2 \longrightarrow C_nH_{2n} + \dot{H}O_2 \quad (1.7)$$

However, in the gaseous oxidation of hydrocarbons at temperatures between 150 and 450°C, reaction with oxygen is generally considered to be the major fate of alkyl radicals. The nature of this reaction has, however, led to a considerable divergence of opinion.

Below 250°C it is generally agreed that reactions (1.6) and (1.8) constitute the primary chain cycle:

$$\dot{C}_nH_{2n+1} + O_2 \longrightarrow C_nH_{2n+1}\dot{O}O \quad (1.6)$$

$$C_nH_{2n+1}\dot{O}O + C_nH_{2n+2} \longrightarrow C_nH_{2n+1}OOH + \dot{C}_nH_{2n+1} \quad (1.8)$$

This alkyl hydroperoxide mechanism is accepted for liquid phase oxidations in which the monohydroperoxide is the major initial product. Since the chain is completed by alkylperoxy radical attack on the alkane, the reaction is selective and produces mainly 2° and 3° alkyl hydroperoxides. Reaction (1.6) which has been widely studied is known to be fast and proceeds with an activation energy very close to zero [25]. In the case of methyl radicals it has been shown to be termolecular [26].

$$CH_3 + O_2 + M \longrightarrow CH_3\dot{O}O + M \quad (1.9)$$

This may also be true for ethyl radicals but for higher molecular weight alkyl radicals this process is bimolecular, since a greater number of degrees of freedom are available for the distribution of energy released during the reaction. By consideration of the enthalpy and entropy changes, Fish [27] has estimated that the rate constant and pre-exponential factor for reaction (1.6) are $k_{1.6}(550^{o}K) = 10^{-13}$ cc. molecule^{-1}sec.$^{-1}$ and $A_{1.6} = 1.1 \times 10^{-13}$ cc.molecule^{-1} sec.$^{-1}$.

Between 250 and 400°C, however, where the alkylperoxy radical is less stable, two conflicting theories of chain propagation have recently been proposed.

(a) Alkene-hydroperoxy radical addition theory

Following a series of studies of the oxidation of ethane [28] and propane [29, 30] in the early stages of reaction, Knox postulated that the major propagation sequence in the oxidation of lower alkanes, is reaction (1.7) followed by reaction (1.10):

$$\dot{C}_nH_{2n+1} + O_2 \longrightarrow C_nH_{2n} + \dot{H}O_2 \qquad (1.7)$$

$$C_nH_{2n+2} + \dot{H}O_2 \longrightarrow \dot{C}_nH_{2n+1} + H_2O_2 \qquad (1.10)$$

At temperatures in the range 250 - 400°C the hydrogen peroxide was considered to be inert and so the hydroperoxy radical was the main chain propagating radical. However, consideration of the competition of reaction (1.11),

$$\dot{H}O_2 + \dot{H}O_2 \longrightarrow H_2O_2 + O_2 \qquad (1.11)$$

especially after the early stages of reaction, together with the results of competitive experiments [31] which indicated that the main radical attacking the hydrocarbon molecule was unselective, led Knox to a reappraisal of his ideas in 1965 [32]. He considered that in order to explain the observed oxidation rates, the hydroperoxy radical must be converted into a more reactive species in the intermediate and later stages of the reaction. Thus, he was forced to derive a mechanism for

the conversion of hydroperoxy radicals to hydroxyl radicals. He considered that this conversion must involve some intermediate product and the most obvious choice was the conjugate alkene which he had shown to be the major intermediate in the oxidation of these low molecular weight hydrocarbons. The conversion scheme he considered is:

$$C_nH_{2n} + \dot{H}O_2 \longrightarrow \dot{C}_nH_{2n}OOH \qquad (1.12)$$

$$\dot{C}_nH_{2n}OOH + O_2 \longrightarrow \dot{O}OC_nH_{2n}OOH \qquad (1.13)$$

$$\dot{O}OC_nH_{2n}OOH + \dot{H}O_2 \longrightarrow HOOC_nH_{2n}OOH + O_2 \qquad (1.14)$$

$$HOOC_nH_{2n}OOH \longrightarrow 2\dot{O}H + \text{carbonyl compounds} \qquad (1.15)$$

In this scheme two hydroperoxy radicals are converted to two hydroxyl radicals which can propagate the primary chain as in reaction (1.16):

$$C_nH_{2n+2} + \dot{O}H \longrightarrow \dot{C}_nH_{2n+1} + H_2O \qquad (1.16)$$

Knox drew considerable support for this scheme from work on alkene oxidation which had shown that in the temperature range 300 - 350°C, approximately 80% of the primary products were carbonyl compounds [33, 34]. Furthermore, the existence of dihydroperoxides had been illustrated by Cartlidge and Tipper [35], although only for relatively high molecular weight hydrocarbons.

An important consequence of this scheme was that it offered an explanation of the negative temperature coefficient phenomenon. Knox calculated that at initial temperatures up to 370°C, hydroperoxy radicals were converted to reactive hydroxyl radicals whereas above this temperature their major fate became disproportionation (reaction (1.11)), which thus accounted for the observed decrease in the rate of reaction.

These considerations allowed him to formulate a mechanism for low temperature hydrocarbon oxidation as follows:

$$\dot{C}_nH_{2n+1} + O_2 \longrightarrow C_nH_{2n} + \dot{H}O_2 \quad (80\%) \qquad (1.7)$$

$$\dot{C}_nH_{2n+1} + O_2 \longrightarrow C_nH_{2n+1}\dot{O}O \quad (20\%) \qquad (1.6)$$

$$C_nH_{2n+2} + \dot{H}O_2 \longrightarrow \dot{C}_nH_{2n+1} + H_2O_2 \quad \text{(initial stages)} \qquad (1.10)$$

$$C_nH_{2n+2} + \dot{O}H \longrightarrow \dot{C}_nH_{2n+1} + H_2O \quad \text{(later stages)} \qquad (1.16)$$

$$C_nH_{2n+1}\dot{O}O \longrightarrow \text{wall destruction} \qquad (1.17)$$

The minor products were thought to arise largely through the destruction of alkylperoxy radicals at the walls of the reactor (reaction (1.17)) since their distribution showed a marked dependence on the nature of the reactor surface [36, 37].

The importance of the conjugate alkenes as intermediate products has received support from many workers, notably Cullis et al [38] who showed by C^{14}- tracer techniques that during the oxidation of n-butane at 315°C, at least 35% of the fuel had been converted to the two conjugate alkenes after 50 seconds of reaction. These workers also considered that the mode of formation of the alkene is via reaction (1.7) and not via isomerisation of the alkylperoxy radical (reaction 1.18)) and subsequent decomposition of the α-hydroperoxybutyl radical (reaction (1.19)),

$$CH_3-CH_2-\underset{\dot{O}-O}{\underset{|}{CH_2}}-CH_2 \longrightarrow CH_3-CH_2-\dot{C}H-\underset{HO-O}{\underset{|}{CH_2}} \qquad (1.18)$$

$$CH_3-CH_2-\dot{C}H-\underset{HO-O}{\underset{|}{CH_2}} \longrightarrow CH_3-CH_2-CH=CH_2 + \dot{H}O_2 \qquad (1.19)$$

because the predominant isomerisation of the but-1-ylperoxy radical would be expected to involve 1:5 hydrogen transfer due to the lower strain energy involved.

Benson also considered this problem of the mode of alkene formation theoretically and arrived at the same conclusion [39]. His reasoning was as follows. From the simple scheme:

$$\dot{C}_nH_{2n+1} + O_2 \rightleftharpoons C_nH_{2n+1}\dot{O}O \quad (1.6)$$

$$C_nH_{2n+1}\dot{O}O \rightleftharpoons \dot{C}_nH_{2n}OOH \quad (1.20)$$

$$\dot{C}_nH_{2n}OOH \rightleftharpoons C_nH_{2n} + \dot{H}O_2 \quad (1.21)$$

$$C_nH_{2n+1}\dot{O}O + C_nH_{2n+2} \longrightarrow C_nH_{2n+1}OOH + \dot{C}_nH_{2n+1} \quad (1.8)$$

it can be seen that the maximum fraction of the alkylperoxy radicals converted to the alkene is given by the ratio:

$$k_{1.20} / (k_{1.20} + k_{-1.6} + k_{1.8}[C_nH_{2n+2}])$$

Benson estimated that $A_{1.20} = 10^{11.5}$ sec.$^{-1}$, $E_{1.20} = 27$ kcal.mole^{-1}, $A_{-1.6} = 10^{15.3}$ sec.$^{-1}$ and $E_{-1.6} = 27$ kcal.mole^{-1} and hence that the fraction converted $\ll k_{1.20}/k_{-1.6} = 10^{-3.8}$. For the competing path to alkene formation (reaction (1.7)) $A_{1.7} \gg$ ca. $10^{8.7}$ l.mole^{-1} sec.$^{-1}$; $E_{1.7}$ is not known but Benson believes it is ca.3kcal.mole^{-1}. He points out, however, that even if it is as high as 6 kcal.mole^{-1} the rate of alkene production via reaction (1.7) at 300°C would be ca. 8 times faster than the maximum rate via the intramolecular rearrangement. Unfortunately, his argument rests on the high activation energy (16~18 kcal.mole^{-1}) he uses for bimolecular 2° hydrogen abstraction by $C_nH_{2n+1}\dot{O}O$ in his estimation of $E_{1.20}$ (sum of the endothermicity + strain energy + activation energy of bimolecular 2° hydrogen abstraction). There is no direct experimental evidence to substantiate this value, but comparison with 2° hydrogen abstraction by Br atoms [40], for which E = 10.2 kcal. mole^{-1}, suggests that this value is too high.

Reaction (1.6) is of course reversible and the values of the equilibrium constant, which have been summarised by Benson[41] as shown in Table 1.3, show that the relative importance of reaction (1.7) will depend on the temperature and the nature of the alkyl radical. More accurate thermokinetic data is required, however, before the mode of formation of the alkene at a given temperature can be assessed

Table 1.3

Estimated values of K_{eq} for the bimolecular association of oxygen with alkyl radicals

$$\dot{C}_nH_{2n+1} + O_2 \rightleftharpoons C_nH_{2n+1}\dot{O}O$$

Alkyl Group	Log K_{eq} atm.$^{-1}$		
	300°K	500°K	700°K
H	30.4	16.4	10.6
$\dot{C}H_3$	12.3	4.6	1.35
$\dot{C}_2H_5$	13.5	5.2	1.50
i-$\dot{C}_3H_7$	14.1	5.5	1.85
t-$\dot{C}_4H_9$	13.0	4.6	0.97

unequivocally.

More recently Knox has investigated the slow combustion of n-pentane [42] and has shown that the yields of many of the reaction products, particularly acetone, are very susceptible to the nature of the reactor surface. For this hydrocarbon he considers that reactions of alkylperoxy radicals explain the formation of not only 2-methyltetrahydrofuran but of the pentenes as well. The formation of carbonyl compounds is believed to involve intermolecular hydrogen abstraction by the pentylperoxy radicals to form an unstable hydroperoxide which diffuses to the reactor walls where it decomposes.

In his more recent work, therefore, Knox has modified his views concerning the importance of the alkene-hydroperoxy radical addition theory and has moved closer to the alkylperoxy radical isomerisation theory.

(b) Alkylperoxy radical isomerisation theory

The main chain-propagating cycle may be summarised in general terms by the following reactions:

$$\dot{C}_nH_{2n+1} + O_2 \longrightarrow C_nH_{2n+1}\dot{O}O \qquad (1.6)$$

$$C_nH_{2n+1}\dot{O}O \longrightarrow \dot{C}_nH_{2n}OOH \qquad (1.20)$$

$$\dot{C}_nH_{2n}OOH \longrightarrow \text{Products} + \dot{O}H \qquad (1.22)$$

$$C_nH_{2n+2} + \dot{O}H \longrightarrow \dot{C}_nH_{2n+1} + H_2O \qquad (1.16)$$

In contrast to the alkene theory, the predominant mode of oxidation of the alkyl radicals is by oxygen addition and the alkylperoxy radical so formed then undergoes homogeneous intramolecular rearrangement, reaction (1.20). Decomposition of the rearranged radical (reaction (1.22)) usually leads to a hydroxyl radical and stable products which include O-heterocycles, alkenes, carbonyl compounds and alcohols with rearranged carbon skeletons relative to the fuel. The chain-cycle is then completed by unselective attack on the fuel by the hydroxyl radical.

The isomerisation of alkylperoxy radicals involves the formation of a cyclic transition complex in which a bond forms between the terminal oxygen atom possessing the free valency and a hydrogen atom attached to a carbon atom in the hydrocarbon skeleton. Several modes of hydrogen transfer can occur via the formation of different size transition ring complexes. Thus for example, hept-2-ylperoxy radicals can isomerise to form four different hydroperoxyhept-2-yl radicals through the formation of four transition complexes (as shown on Page 32). The α-, β-, γ-and δ-hydroperoxyheptyl radicals so formed arise via 5, 6, 7 and 8 membered transition ring complexes respectively. The associated strain energies for these rings are approximately 6.5, 0.6, 6.5 and 10 kcal.mole^{-1} and it can be seen, therefore, that the most favourable mode of isomerisation is 1:5 hydrogen transfer which leads to the formation of a β-hydroperoxyheptyl radical. The corresponding 1:4 and 1:6 hydrogen transfers are less favourable and the 1:7 hydrogen transfer is most difficult of all. However, the relative rates of the various modes of hydrogen transfer for alkylperoxy radicals in general will depend not only on the size of the transition ring but also on the nature of the C-H bond broken. The pre-exponential factor for these isomerisations has been estimated by Benson [39] to be $10^{11.5 \pm 0.3}$ sec.$^{-1}$ and Fish [43] has estimated the activation energies and the rate constants at 550°K as shown in Table 1.4.

The hydroperoxyalkyl radicals formed in reaction (1.20) may subsequently reisomerise, decompose or add oxygen:

$$\dot{C}_nH_{2n}OOH \longrightarrow C_nH_{2n+1}\dot{O}O \qquad (-1.20)$$

$$\dot{C}_nH_{2n}OOH \longrightarrow \text{products} + \text{radical} \qquad (1.22)$$

$$\dot{C}_nH_{2n}OOH + O_2 \longrightarrow \dot{O}OC_nH_{2n}OOH \qquad (1.23)$$

In general, the reverse isomerisation of γ- and δ-hydroperoxyalkyl radicals

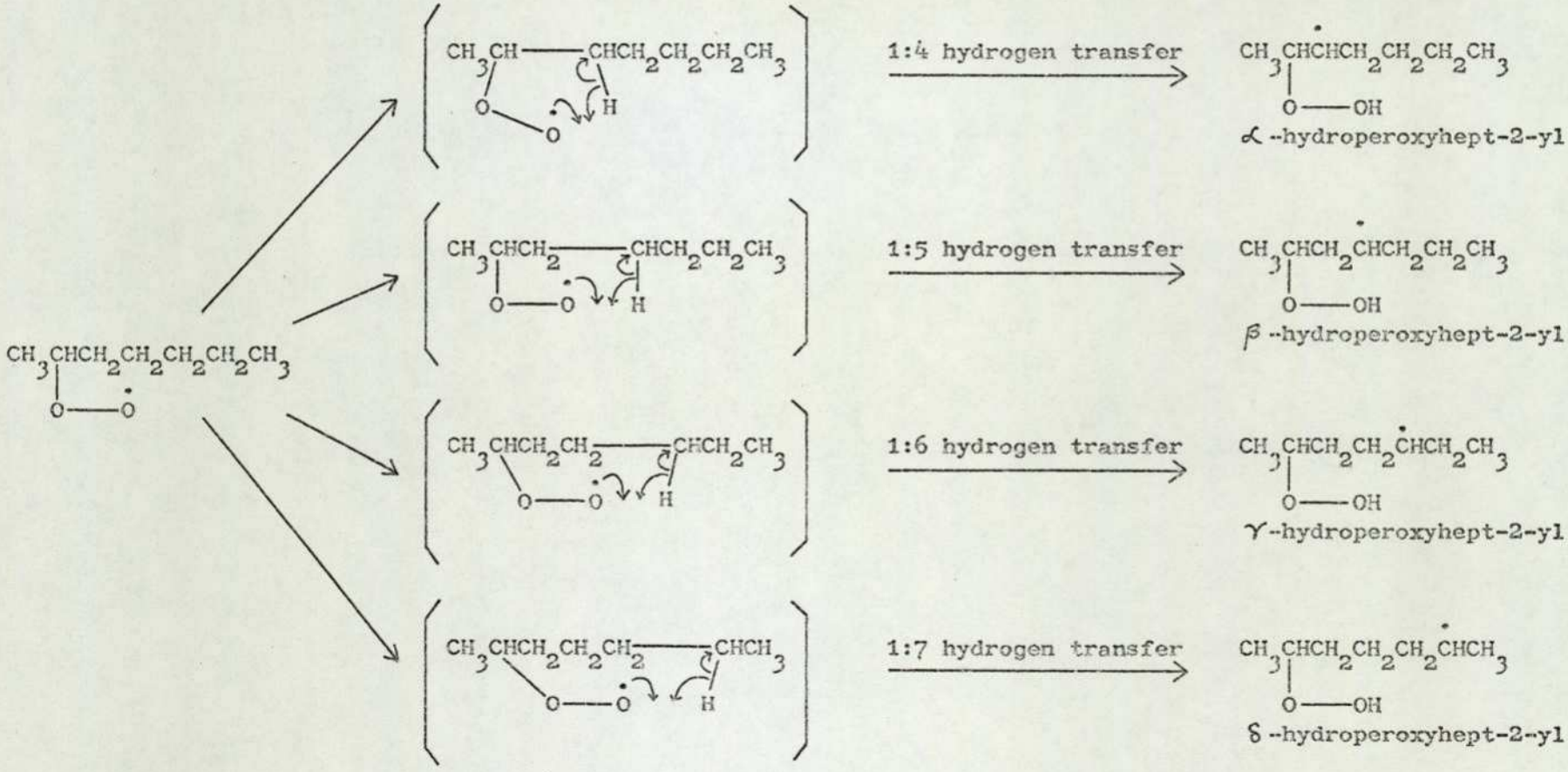

1:4 hydrogen transfer
α-hydroperoxyhept-2-yl
1:5 hydrogen transfer
β-hydroperoxyhept-2-yl
1:6 hydrogen transfer
γ-hydroperoxyhept-2-yl
1:7 hydrogen transfer
δ-hydroperoxyhept-2-yl

Table 1.4

Thermodynamic and kinetic parameters of alkylperoxy radical isomerisation at 550°K

Nature of C-H Bond Broken	Class of H-Transfer Reaction	Transition State Ring Size (Including H)	ΔH (kcal.mole^{-1})	E (kcal.mole^{-1})	Log k* (k in sec.$^{-1}$)
Primary	1:3	4	8	40	-5.0
	1:4	5	8	21	2.9
	1:5	6	8	15	5.2
	1:6	7	8	21	2.9
	1:7	8	8	24	1.5
Secondary	1:3	4	4.5	37	-3.6
	1:4	5	4.5	17	4.3
	1:5	6	4.5	11	6.6
	1:6	7	4.5	17	4.3
	1:7	8	4.5	21	2.9
Tertiary	1:3	4	1.7	34	-2.5
	1:4	5	1.7	14	5.4
	1:5	6	1.7	8	7.7
	1:6	7	1.7	14	5.4
	1:7	8	1.7	18	4.0

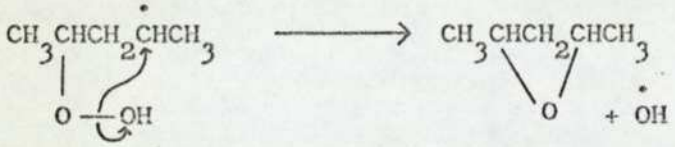
* for A = 10^{11} sec.$^{-1}$

is considered to be slow compared with their decompositions and as such is not important [43]. Under certain circumstances this reverse isomerisation for α-and β-hydroperoxyalkyl radicals may be competitive although results from a recent C^{14} - tracer study of the oxidation of n-butane [38] suggest that this isomerisation is also unimportant for α-hydroperoxybutyl radicals.

The various modes of decomposition of hydroperoxyalkyl radicals may be summarised as follows:

(i) cyclisation to give an O-heterocycle and a hydroxyl radical

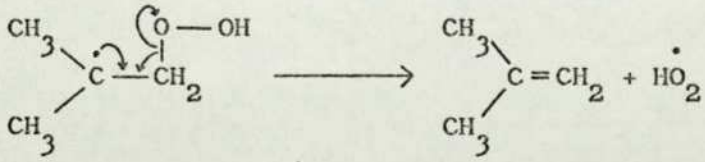
α-, β-, γ- and δ-hydroperoxyalkyl radicals cyclise to form oxirans, oxetans, tetrahydrofurans and tetrahydropyrans respectively, e.g.



(1.24)

(ii) β-scission of the C - O bond to give the conjugate alkene and a hydroperoxy radical

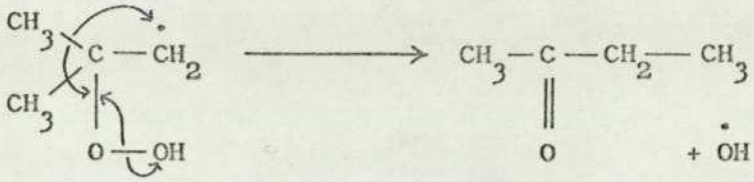
This mode of decomposition is restricted to α-hydroperoxyalkyl radicals, e.g.



(1.25)

(iii) homolysis of the O - O bond and intramolecular transfer of an alkyl group to give a rearranged carbonyl compound and a hydroxyl radical

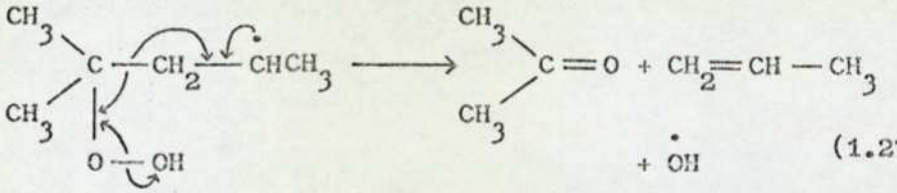
Group shifts have been confirmed in studies of the oxidation of 3-methylpentane, 3-ethylpentane and isobutane, e.g.



(1.26)

(iv) β-scission of a C - C bond and homolysis of the O - O bond to give an alkene, a hydroxyl radical and either a carbonyl compound or an O-heterocycle

β-Hydroperoxyalkyl radicals undergo this mode of decomposition to form alkenes and carbonyl compounds in pairs e.g.



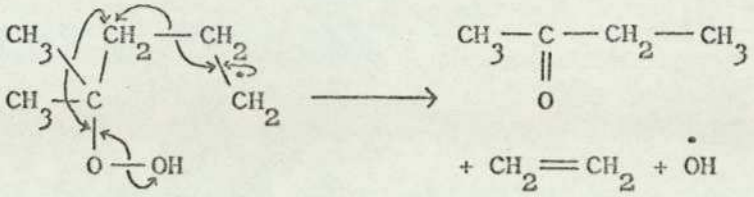
(1.27)

This type of decomposition is energetically less favourable for γ- and δ-hydroperoxyalkyl radicals which form alkenes and O-heterocycles in pairs.

(v) β-scission of a C - C bond and homolysis of the O - O bond accompanied by group transfer to give rearranged scission compounds and a hydroxyl radical

This mode of decomposition is exemplified in the oxidation of 2-methylpentane and can explain

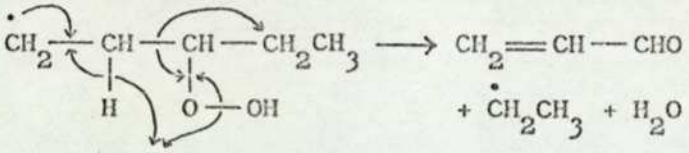
the formation of methyl ethyl ketone and ethylene as shown below:



(1.28)

(vi) homolysis of O - O bond and two other bonds to give an unsaturated carbonyl compound, an alkyl radical and water

This mode of decomposition is complex and may not occur in a single step, e.g.



(1.29)

Of these decomposition reactions, the most common are the cyclisation and β-scission reactions, modes (i), (ii) and (iv). The importance of cyclisation is clearly demonstrated by the considerable yields of O-heterocycles found in the oxidation of high molecular weight hydrocarbons [44]. The β-scission decomposition of β-hydroperoxyalkyl radicals has been shown to be more important for branched-chain hydrocarbons [12] whilst the same decomposition for α-hydroperoxyalkyl radicals becomes increasingly more important as the molecular weight of the alkane is decreased [45].

The further oxidation of hydroperoxyalkyl radicals has been studied by Calvert and Dingledy [25] and shown to be fast, the activation energy being close to zero.

$$\dot{C}_nH_{2n}OOH + O_2 \longrightarrow \dot{O}OC_nH_{2n}OOH \qquad (1.23)$$

A dihydroperoxide or possibly a trihydroperoxide may subsequently be formed by intermolecular hydrogen abstraction:

$$C_nH_{2n+2} + \dot{O}OC_nH_{2n}OOH \longrightarrow HOOC_nH_{2n}OOH + \dot{C}_nH_{2n+1} \qquad (1.30)$$

The existence of dihydroperoxides is well documented in the work of Cartlidge and Tipper [35], Crandall and Thomas [46] and Rust [47].

The various competing reactions of hydroperoxyalkyl radicals have been assessed by Fish [43] who concludes that, neglecting the reverse isomerisation reaction, further oxidation competes effectively with the formation of conjugate alkenes, oxirans and oxetans i.e. α-hydroperoxyalkyl radicals and to a lesser extent β-hydroperoxyalkyl radicals will add on oxygen while γ- and δ-hydroperoxyalkyl radicals preferentially decompose.

The identification of all the possible O-heterocycles in the oxidation of n-butane [38] clearly indicates that the radical attack on the hydrocarbon is indeed unselective as would be expected since the hydroxyl radical is formed in many of the decomposition reactions above. In order to describe the propagation mechanism in detail it is necessary, therefore, to consider the reactions of each and every alkylperoxy radical formed from the fuel. From such a consideration Fish has been able to describe qualitatively the product distribution found during the oxidation of 2-methylpentane [48], neopentane [49], n-hexane [50] and 2,3-dimethylbutane [51] over a wide range of initial reaction conditions.

1.3.1.3 Branching

There has been considerable controversy over the nature of the intermediate directly responsible for degenerate branching during the oxidation of hydrocarbons; the two compounds most commonly believed to be involved in this step being hydroperoxides and aldehydes. Since the common precursor of both of these compounds is an alkylperoxy radical,

$$C_nH_{2n+1}\dot{O}O + C_nH_{2n+2} \longrightarrow C_nH_{2n+1}OOH + \dot{C}_nH_{2n+1} \quad (1.8)$$

$$C_nH_{2n+1}\dot{O}O \longrightarrow \dot{C}_nH_{2n}OOH \quad (1.20)$$

$$\dot{C}_nH_{2n}OOH \longrightarrow AH + \dot{O}H \quad (1.31)$$

(where AH is a compound with a labile hydrogen e.g. an aldehyde), the conflict has arisen from the differing opinions as to the nature of its subsequent reaction. At temperatures below 250°C, alkyl hydroperoxides are relatively stable and constitute the major oxidation product, however as the temperature is increased, the possibility of branching by their homogeneous decomposition is substantially increased (reaction 1.32)).

$$C_nH_{2n+1}OOH \longrightarrow C_nH_{2n+1}\dot{O} + \dot{O}H \quad (1.32)$$

Benson [39] has estimated the stability of alkyl hydroperoxides with regard to their unimolecular decomposition. Assuming $D\left[C_nH_{2n+1}O - OH\right]$ to be about 43kcal. mole^{-1} and a pre-exponential factor of 10^{15} sec.$^{-1}$, he estimates the half-life of $C_nH_{2n+1}OOH$ at 330°C to be of the order of 1 second and at 290°C to be 10 seconds. He therefore concludes that hydroperoxides can justifiably be considered as branching intermediates up to about 350°C. However, above this temperature, the rate of the alkylperoxy radical isomerisation is such that the stationary concentration of alkylperoxy radicals is considerably reduced and it is doubtful whether alkyl hydroperoxides may be formed at all.

For fuel lean mixtures where the further oxidation of hydroperoxyalkyl radicals is important, branching may also occur via the decomposition of dihydroperoxides:

$$HOOC_nH_{2n}OOH \longrightarrow 2\dot{O}H + \text{carbonyl compounds} \quad (1.15)$$

In the oxidation of n-pentane, for example, Bastow [52] has described the branching process below 315°C in terms of the unimolecular decomposition of pentyl dihydroperoxides.

Aldehydes may lead to branching in two ways. Shtern, Tcherniak and Antonovski [52*] suggested that the reaction of acetaldehyde with oxygen, to give an acyl radical and a hydroperoxy radical, could explain the branching process.

$$CH_3CHO + O_2 \longrightarrow CH_3\dot{C}O + \dot{H}O_2 \qquad (1.33)$$

An alternative role of aldehydes in the branching process was suggested by Enikolopyan [53] based on the ideas of Bawn, Mullen and Skirrow [54] concerning the importance of peracetic acid during the oxidation of propylene. In this scheme the branching reaction is the unimolecular decomposition of peracetic acid as shown below:

$$CH_3CHO + \dot{O}H \longrightarrow CH_3\dot{C}O + H_2O \qquad (1.34)$$

$$CH_3\dot{C}O + O_2 \longrightarrow CH_3COO\dot{O} \qquad (1.35)$$

$$CH_3COO\dot{O} + AH \longrightarrow CH_3COOH + \dot{A} \qquad (1.36)$$

$$CH_3COOH \longrightarrow CH_3CO\dot{O} + \dot{O}H \qquad (1.37)$$

A similar scheme has recently been shown to be capable of explaining branching during the oxidation of n-butane [55] above 330°C, particularly for fuel lean mixtures. Furthermore, peracetic acid is believed to be responsible for degenerate branching during the oxidation of acetaldehyde [56]. An important consequence of this mode of branching is that it is capable of explaining the occurrence of the large negative temperature coefficient region between 350 - 400°C for most hydrocarbons. In this temperature range the homogeneous decompositions of acyl and acylperoxy radicals become increasingly competitive.

$$CH_3\dot{C}O \longrightarrow \dot{C}H_3 + CO \qquad (1.38)$$

$$CH_3COO\dot{O} \longrightarrow CH_3\dot{O} + CO_2 \qquad (1.39)$$

Thus as the initial temperature is raised above 350°C these reactions gradually predominate over reaction (1.36) and the stationary concentration of the peracid decreases with a concommitant decrease

in the reaction rate.

The variation of the mode of branching and the reactions leading to the formation of the branching intermediate, has been considered as an explanation of the lobes that appear on the cool flame/ ignition boundary. Walsh [57] designated the three lobes he found with n-heptane and n-octane L_1, L_2 and L_3 in order of increasing temperature and ascribed their occurrence to various modes of alkylperoxy radical isomerisation. He considered that the three important isomerisations involved hydrogen abstraction from a 2° carbon in the β-position, a 2° carbon in the δ-position and a 1° carbon in the ϵ-position. Walsh suggested that these isomerisations involved progressively higher activation energies and this could account for the temperature dependence of the lobes. The branching process was considered to be due to the decomposition of dihydroperoxides formed by the further oxidation of the subsequent hydroperoxyalkyl radicals followed by intermolecular hydrogen abstraction. The negative temperature coefficient region associated with each lobe, was seen as the increasing competition of the decomposition of the hydroperoxyalkyl radical which leads to non-branching intermediates as the temperature is increased.

In 1968 Fish [58] modified these ideas and suggested that a correlation existed between the number of lobes and the number of possible modes of alkylperoxy radical isomerisation. From a study of the data available at the time, Fish concluded that for the majority of hydrocarbons this relationship certainly seemed valid. The explanation of the lobes given by him was that 1:6 and 1:5 hydrogen transfer accounted for the L_1 and L_2 lobes respectively, whilst 1:4 and 1:n (where $n > 6$) hydrogen transfer accounted for the L_3 lobe. From detailed studies of neopentane [49] and 2,3-dimethylbutane [51], which exhibit two and five lobes respectively, it is now clear, however, that a given mode of hydrogen transfer cannot be assigned exclusively to a given lobe.

In addition, Lucquin [59] observed that the lower lobe found for 2-methylpentane + oxygen mixtures [48], and assigned L_1 by Fish, occurs at a lower temperature than that found by Walsh for straight chain hydrocarbons. He suggested, therefore, that this lower lobe should be called L_o thus enabling a nomenclature of lobes to be ascribed with respect to temperature.

A more recent suggestion for the occurrence of lobes is that proposed by Antonik and Lucquin [60]. The basis of their theory is that the competing reactions of the alkylperoxy radical change as the initial temperature is raised and the various branching steps can be identified as follows:

(i) L_o mechanism

This is a mechanism of pure peroxidation which is important at low temperatures, but can only occur when the fuel itself has a labile hydrogen atom (such as 2-methylpentane and acetaldehyde)

$$C_nH_{2n+1}\dot{O}O + C_nH_{2n+2} \longrightarrow C_nH_{2n+1}OOH + \dot{C}_nH_{2n+1} \qquad (1.8)$$

$$C_nH_{2n+1}OOH \longrightarrow C_nH_{2n+1}\dot{O} + \dot{O}H \qquad (1.32)$$

(ii) L_1 mechanism

The L_1 mechanism involves primary peroxidation which is catalysed by hydrogen donors, such as aldehydes, formed in the primary chain cycle:-

$$C_nH_{2n+1}\dot{O}O \longrightarrow \dot{C}_nH_{2n}OOH \qquad (1.20)$$

$$\dot{C}_nH_{2n}OOH \longrightarrow AH + \text{alkene} + \dot{O}H \qquad (1.41)$$

(where AH represents an aldehyde)

$$C_nH_{2n+1}\dot{O}O + AH \longrightarrow C_nH_{2n+1}OOH + \dot{A} \qquad (1.42)$$

$$C_nH_{2n+1}OOH \longrightarrow C_nH_{2n+1}\dot{O} + \dot{O}H \qquad (1.32)$$

Evidence for this mechanism has recently been obtained from a study of the oxidation of neopentane [61]. The addition of 1% HBr to the neopentane

+ oxygen system was shown to induce the appearance of an L_1 lobe and the mode of action of the additive was considered to be:

$$C_nH_{2n+1}\dot{O}O + HBr \longrightarrow C_nH_{2n+1}OOH + \dot{B}r \quad (1.40)$$

$$C_nH_{2n+1}OOH \downarrow \text{degenerate branching}$$

Since D $\left[H - Br\right]$ is of the order of 87 kcal.mole^{-1}, reaction (1.40) is responsible for the production of the branching agent at lower temperatures than in the absence of the additive. Furthermore, variation of the stoichiometry shows that the L_1 mechanism is favoured by a high hydrocarbon to oxygen ratio, as might be expected from the proposed mechanism, since the hydroperoxyalkyl radicals are less likely to undergo further oxidation.

(iii) L_2 mechanism

Antonik and Lucquin consider this to be a process of secondary peroxidation, possibly that of aldehydes. The branching step is the decomposition of peracids formed by further oxidation of the aldehydes as shown below:

$$AH + O_2 \longrightarrow \dot{A} + \dot{H}O_2 \quad (1.43)$$

$$\dot{A} + O_2 \longrightarrow \dot{A}O_2 \quad (1.44)$$

$$\dot{A}O_2 + C_nH_{2n+2} \longrightarrow AOOH + \dot{C}_nH_{2n+1} \quad (1.45)$$

$$AOOH \longrightarrow \dot{A}O + \dot{O}H \quad (1.46)$$

The changeover in branching mechanism with increase of temperature, L_1 to L_2, is considered by the authors to be the competition between reaction (1.42) and reaction (1.43) with the latter predominating at higher temperatures.

$$AH + C_nH_{2n+1}\dot{O}O \longrightarrow C_nH_{2n+1}OOH + \dot{A} \quad (1.42)$$

$$AH + O_2 \longrightarrow \dot{A} + \dot{H}O_2 \quad (1.43)$$

Since reaction (1.42) is a radical/molecule reaction, its activation

energy will be lower and this reaction will predominate at lower temperatures.

The L_2 mechanism is, therefore, favoured by low fuel to oxygen ratios and receives considerable substantiation from the observation of the dramatic fall in the concentration of aldehydes during the cool flames of neopentane [61] for example.

(iv) L_3 mechanism

This mechanism is similar to the L_2 mechanism except that formaldehyde is believed to be involved in the branching step:

$$\dot{HCO}_3 + C_nH_{2n+2} \longrightarrow HCO_3H + \dot{C}_nH_{2n+1} \qquad (1.47)$$

$$HCO_3H \longrightarrow \dot{HCOO} + \dot{OH} \qquad (1.48)$$

Thus, the foregoing considerations certainly seem to reconcile the apparently contradictory hydroperoxide and aldehyde theories of branching, indicating that in general aldehydes are important above 300°C whereas hydroperoxides and possibly dihydroperoxides are important below this temperature. Furthermore, this theory incorporates the explanation suggested by Yenikolopyan of the major negative temperature coefficient region in terms of the competition of reactions (1.38) and (1.39) with reaction (1.36), (when acetaldehyde is the aldehyde in question).

$$\dot{CH_3CO} \longrightarrow \dot{CH_3} + CO \qquad (1.38)$$

$$\dot{CH_3CO_3} \longrightarrow \dot{CH_3O} + CO_2 \qquad (1.39)$$

$$\dot{CH_3CO_3} + AH \longrightarrow CH_3CO_3H + \dot{A} \qquad (1.36)$$

Additional support for the theory is gained from the identification of peracetic and perpropionic acids above 300°C in the reaction products of the oxidation of propane and n-butane respectively [35].

1.3.1.4 Termination

Termination reactions may take place with the participation of one or two free radicals. In the latter case (quadratic termination), chain breaking can occur through either recombination or disproportionation. Thus, for example, under the conditions towards the end of hydrocarbon oxidation reactions when the concentration of oxygen is very low, alkyl radicals may recombine to form saturated molecules. In the oxidation of propane [6], the appearance of ethane in the final stages of the reaction is considered to be due to the recombination of methyl radicals:

$$\dot{C}H_3 + \dot{C}H_3 + M \longrightarrow C_2H_6 + M \qquad (1.49)$$

Recombination between atoms and simple radicals often requires a third body for the necessary stabilisation of the product, whereas recombination reactions of more complex radicals occur by a simple bimolecular collision.

It is generally considered that in the low temperature region where the formation of alkylperoxy radicals is important, chain termination reactions often involve the destruction of these radicals. A variety of reactions have been considered viz:-

$$C_nH_{2n+1}\dot{O}O \longrightarrow \text{destruction at wall} \qquad (1.17)$$

$$C_nH_{2n+1}OOH \longrightarrow \text{destruction at wall} \qquad (1.50)$$

$$C_nH_{2n+1}\dot{O}O + \dot{H}O_2 \longrightarrow C_nH_{2n+1}OOH + O_2 \qquad (1.51)$$

$$C_nH_{2n+1}\dot{O}O + C_nH_{2n+1}\dot{O}O \longrightarrow C_nH_{2n+1}O_4C_nH_{2n+1} \qquad (1.52)$$

$$C_nH_{2n+1}\dot{O}O + C_nH_{2n+1}\dot{O} \longrightarrow C_nH_{2n+1}O_3C_nH_{2n+1} \qquad (1.53)$$

There is considerable support for the view that reactions (1.17) and (1.50) constitute major termination reactions in the low temperature region [32, 63]. Furthermore, studies of the addition of inert gas, variation of the nature of the reactor surface and the surface to

volume ratio, all indicate the importance of heterogeneous termination reactions. For example, Bonner and Tipper [64] consider that the inhibition exerted on the oxidation of propane, cyclohexane and n-heptane by potassium chloride and lead monoxide surface coatings, is due to the increased rates of destruction of various peroxy radicals and hydroperoxides at the surface. Seakins [65] also considers the destruction of alkyl hydroperoxides at the walls to form stable products to be of importance.

Reaction (1.51) is known to occur in the liquid phase and its occurrence in the gas phase depends on the stability of the alkyl hydroperoxide so formed. Calculations of the half-life of hydroperoxides[39] indicate that above 250°C this cannot be accepted as a termination step. Moreover, the concentration of hydroperoxy radicals is likely to be low due to reaction (1.11):

$$\dot{H}O_2 + \dot{H}O_2 \longrightarrow H_2O_2 + O_2 \qquad (1.11)$$

Below 400°C the hydrogen peroxide formed may be considered to be inert [66] and therefore under these circumstances reaction (1.11) may become an important homogeneous termination reaction.

Benson [41, 67] has carried out a detailed study of reactions (1.51), (1.52) and (1.53) and concludes that very little evidence exists for termination reactions involving alkylperoxy radicals in the gas phase. The products of reactions (1.51), (1.52) and (1.53) are all extremely unstable and as such have a greater propensity for propagating rather than terminating the chain.

Nevertheless, radical - radical interactions can be shown to have some important consequences. Lucquin and his co-workers consider that the pic d'arrêt is due to the reaction of alkylperoxy radicals with alkyl radicals and that these reactions are particularly favoured by low oxygen concentrations, as found in the final stages of reaction. The analogy has been drawn between the pic d'arrêt and oxygen "cut-off" in

liquid phase studies [68]. Thus the basic sequence of reactions considered is:

$$\dot{C}_nH_{2n+1} + C_nH_{2n+1}\dot{O}O \longrightarrow C_nH_{2n+1}OOC_nH_{2n+1} \quad (1.54)$$

$$C_nH_{2n+1}OOC_nH_{2n+1} \longrightarrow \text{oxygenated products} \quad (1.55)$$

The significant yields of aldehydes and alcohols detected at the time of the appearance of the pic d'arrêt are considered to be due to further reactions of alkoxy radicals formed from the decomposition of dialkyl peroxides.

$$C_nH_{2n+1}\dot{O} \longrightarrow AH + \dot{C}_mH_{2m+1} \quad (1.56)$$

$$C_nH_{2n+1}\dot{O} + AH \longrightarrow C_nH_{2n+1}OH + \dot{A} \quad (1.57)$$

The burst of luminescence which also accompanies the pic d'arrêt is attributed to termination reactions which are highly energetic and produce excited formaldehyde. Sochet, Sawerysyn and Lucquin [62], for example, have suggested three radical - radical reactions which can account for its production during the oxidation of propane.

$$CH_3\dot{O} + CH_3\dot{O} \longrightarrow CH_3OH + HCHO^* \quad (1.58)$$

$$\Delta H = -81 \text{ kcal.mole}^{-1}$$

$$CH_3\dot{O} + \dot{O}H \longrightarrow H_2O + HCHO^* \quad (1.59)$$

$$\Delta H = -101 \text{ kcal.mole}^{-1}$$

$$CH_3\dot{O} + \dot{C}H_3 \longrightarrow CH_4 + HCHO^* \quad (1.60)$$

$$\Delta H = -81 \text{ kcal.mole}^{-1}$$

Similar highly energetic radical - radical interactions are considered to be capable of explaining the luminescence accompanying slow combustion and more particularly cool flames. Excited formaldehyde has been shown to be responsible for this luminescence [69] and since the reaction producing the excited formaldehyde must be exothermic to the extent of 77 kcal.mole^{-1}, radical - radical reactions are the most probable source. Minkoff and Tipper [63] suggest that the most likely

reaction, considering the large concentration of alkylperoxy radicals present under cool flame conditions, is reaction (1.61) which is exothermic by ca. 85-90 kcal.mole^{-1}.

$$\dot{CH_3}O\dot{O} + \dot{HO_2} \longrightarrow HCHO^{*} + H_2O + O_2 \qquad (1.61)$$

Sokolik [70] has suggested that reactions (1.62) and (1.63), which are both exothermic by ca. 100 kcal.mole^{-1}, can also account for the production of excited formaldehyde.

$$\dot{CH_3} + \dot{HO_2} \longrightarrow HCHO^{*} + H_2O \qquad (1.62)$$

$$\dot{CH_3} + \dot{HCO_3} \longrightarrow HCHO^{*} + H_2O + CO \qquad (1.63)$$

In any event, it is clear that in view of the relatively low number of quanta emitted during a cool flame, the reaction producing the excited formaldehyde must be a secondary reaction involving infrequent radical - radical interactions and plays no part in the propagation reactions.

1.3.2 The high temperature mechanism

This mechanism of hydrocarbon oxidation is considered to be important above ca. 400°C and is, in general, far simpler than the low temperature mechanism. However, in comparison with studies carried out at lower temperatures, very little work has been performed in the high temperature region. The most outstanding contributions towards elucidating the high temperature mechanism have been made by Sampson, who has studied the oxidation of hydrocarbons in a flow reactor and by Baldwin and Walker who have devised a novel scheme for oxidising hydrocarbons in a controlled radical environment. These studies have allowed a detailed mechanism to be considered and the elementary reactions which have been identified are discussed below.

1.3.2.1 Initiation

The initiation reaction is considered to be the same as that at lower temperatures (reaction 1.1):

$$C_nH_{2n+2} + O_2 \longrightarrow \dot{C}_nH_{2n+1} + \dot{H}O_2 \qquad (1.1)$$

A further mode of initiation which may be envisaged above 600°C, particularly with low partial pressures of oxygen, is the unimolecular pyrolysis of the hydrocarbon molecule, reaction (1.64):

$$C_nH_{2n+2} \longrightarrow \dot{C}_mH_{2m+1} + \dot{C}_{(n-m)}H_{2(n-m)+1} \qquad (1.64)$$

1.3.2.2 Propagation and branching

At these temperatures the predominant reaction between alkyl radicals and oxygen is abstractive and not additive.

$$\dot{C}_nH_{2n+1} + O_2 \longrightarrow C_nH_{2n} + \dot{H}O_2 \qquad (1.7)$$

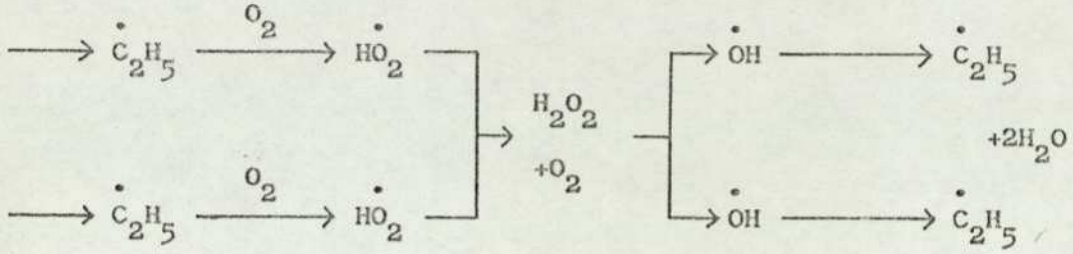
The hydroperoxy radicals so formed are capable of disproportionation to form hydrogen peroxide which at high temperature has been shown to undergo considerable homogeneous decomposition [71]. Thus in the high

temperature region it can act as the agent of degenerate branching.

$$\dot{H}O_2 + \dot{H}O_2 \longrightarrow H_2O_2 + O_2 \qquad (1.11)$$

$$H_2O_2 + M \longrightarrow 2\dot{O}H + M \qquad (1.65)$$

Baldwin [72] has shown that these reactions are an important source of hydroxyl radicals in the $H_2 + O_2$ system. Similarly, Sampson [73] has proposed a route for the conversion of $\dot{H}O_2$ to $\dot{O}H$ in the high temperature oxidation of ethane as follows:



Cullis, Fish and Gibson [74] consider that in the early stages of reaction the major initial attack on the hydrocarbon involves hydroperoxy radicals,

$$C_nH_{2n+2} + \dot{H}O_2 \longrightarrow \dot{C}_nH_{2n+1} + H_2O_2 \qquad (1.10)$$

but in the later stages following the homogeneous decomposition of the peroxide, the propagation is then continued by the unselective attack by hydroxyl radicals:

$$C_nH_{2n+2} + \dot{O}H \longrightarrow \dot{C}_nH_{2n+1} + H_2O \qquad (1.16)$$

Reaction with oxygen is not the only important fate of alkyl radicals at these temperatures, however. Sampson [75] has shown that they also pyrolyse to a large extent. Thus, for example, during the oxidation of isobutane at 532 - 625°C, he found that although isobutene is still an important product, the pyrolysis of iso- and tert-butyl radicals accounts for 50% of the isobutane reacting. Several thermal decompositions can be considered for alkyl radical pyrolysis, but the particular mode of decomposition depends principally on the structure

of the alkyl radical viz:-

$$\dot{C}_3H_7 \longrightarrow \dot{C}H_3 + C_2H_4 \qquad (1.66)$$

$$n\text{-}\dot{C}_4H_9 \longrightarrow \dot{C}_2H_5 + C_2H_4 \qquad (1.67)$$

$$i\text{-}\dot{C}_4H_9 \longrightarrow \dot{C}H_3 + C_3H_6 \qquad (1.68)$$

Sampson also found that in general, the reactivity of alkanes increases in the order $C_5 > C_4 > C_3 > C_2$, although not nearly as markedly as at low temperatures. He ascribed the increase in reactivity to the proportion of methyl radicals produced by pyrolysis of the alkyl radical. The methyl radicals thus formed were considered to be important in propagating the reaction, either by abstracting hydrogen from the hydrocarbon, or by reacting with oxygen to give formaldehyde and a hydroxyl radical:

$$CH_3 + C_nH_{2n+2} \longrightarrow CH_4 + \dot{C}_nH_{2n+1} \qquad (1.69)$$

$$CH_3 + O_2 + (M) \longrightarrow CH_3\dot{O}O + (M) \qquad (1.70)$$

$$CH_3\dot{O}O \longrightarrow HCHO + \dot{O}H \qquad (1.71)$$

Sampson considered, therefore, that the alkyl radicals producing the greatest proportion of methyl radicals will be the most reactive.

Important kinetic and mechanistic data concerning the high temperature mechanism has been obtained from studies of the addition of trace quantities of hydrocarbons to slowly reacting H_2+O_2 mixtures in aged boric-acid vessels at 500°C. Baldwin and Walker have used this method to study the high temperature oxidation of methane [76], ethane [76], propane [77], n-butane [77], isobutane [77] and neopentane [76]. Two methods of investigation can be carried out using this technique:

(i) examination of the rates of consumption of the hydrocarbon and formation of water allow the relative rates of attack by H, O, $\dot{O}H$ and $H\dot{O}_2$ to be determined and

(ii) analysis of the reaction products at various stages in the reaction allows the fate of the radicals produced in the primary

attack to be deduced.

The additions of hydrocarbons are kept below 0.1% so that the known relative concentrations of H, O, $\dot{O}H$ and $H\dot{O}_2$ radicals formed in the $H_2 + O_2$ reaction are kept stationary. The hydrocarbon thus added competes with reactions involving these radicals and since the mechanism of the $H_2 + O_2$ reaction is known in detail, the major competing reactions may be assessed. For example, the two competing reactions of the hydroxyl radical are:

$$C_nH_{2n+2} + \dot{O}H \longrightarrow \dot{C}_nH_{2n+1} + H_2O \qquad (1.16)$$

$$H_2 + \dot{O}H \longrightarrow H + H_2O \qquad (1.72)$$

The rates of consumption of hydrocarbon and formation of water may be substituted in the expression below and since $k_{1.72}$ is known accurately, a value for the rate constant of hydroxyl radical attack on the hydrocarbon $k_{1.16}$ can be calculated.

$$\frac{d\left[C_nH_{2n+2}\right]}{d\left[H_2O\right]} = \frac{k_{1.16}\left[C_nH_{2n+2}\right]}{k_{1.72}\left[H_2\right]}$$

Thus, by studying a range of hydrocarbons it is possible to estimate Arrhenious parameters for specific radical attacks by assuming that the velocity constants for attack at equivalent C - H bonds are the same.

The analytical results of these studies have highlighted the importance of reaction (1.7) in the early stages of reaction at 500°C. Thus the studies of ethane, propane, isobutane and n-butane oxidation have revealed that 95%, 80%, 80% and 65% respectively of the hydrocarbon consumed in the early stages is converted to the conjugate alkene. Furthermore, these studies indicate that alkyl radical pyrolysis becomes increasingly important as the molecular weight of the hydrocarbon increases.

1.3.2.3 Termination

Little work has been carried out on the nature of the termination steps at high temperature, although it is generally considered that reactions (1.73) and (1.74) are the major terminating steps.

$$\dot{O}H \xrightarrow{\text{walls}} \text{inactive products} \qquad (1.73)$$

$$\dot{H}O_2 \xrightarrow{\text{walls}} \text{inactive products} \qquad (1.74)$$

The important contribution of heterogeneous termination has been illustrated by Cullis et al [74] who showed that increasing the reaction vessel diameter leads to a lowering of the spontaneous ignition limit with respect to pressure.

Thus, although not all of the aspects of high temperature oxidation are yet fully understood, the foregoing studies nevertheless contribute important information regarding the mechanism as well as valuable rate constant data.

1.4 Consequences of the low temperature mechanism

1.4.1 Cool flames and two-stage ignitions

The important reactions which lead to and occur during the propagation of cool flames and the first stage of two-stage ignition have been discussed in section 1.3.1. Since it is generally recognised that cool flames play a significant part in the onset of low temperature ignition it is important to understand their self-quenching nature and the transition to two-stage ignition in terms of the physico-chemical implications of the low temperature mechanism.

A cool flame can be considered as a chain-thermal explosion. The propagation reactions occurring in the induction period, during which there is no appreciable self-heating of the reaction mixture, lead to a build-up of the degenerate branching agent. When the reaction conditions are such that ϕ (the net branching factor) exceeds a small positive value, the concentration of chain carriers increases exponentially and the reaction mixture suffers considerable self-heating. This leads to a chain-thermal ignition which manifests itself as a cool flame. As mentioned previously, this process is self-quenching and the explanation of this phenomenon may be found by considering the stationary concentration of the branching agent. The increase in reaction rate and the accompanying self-heating that occurs causes a corresponding increase in the rate of consumption of the branching agent. Furthermore, as the temperature of the reacting mixture increases, the reactions in which the branching agent is produced suffer increasing competition from other non-branching reactions, with the net result that the stationary concentration of the branching agent decreases. The rate of branching and hence the rate of reaction subsequently fall. As a result, the rate of heat evolution falls below that of heat dissipation to the surroundings and the mixture rapidly cools thus returning almost

to the initial temperature conditions. This cycle may be repeated to give rise to further cool flames until insufficient fuel is left to form the critical concentration of branching agent necessary for the evolution of a cool flame. The series of cool flames is then followed by slow combustion which completes the reaction. Since the first cool flame produces numerous intermediate products, the branching agent(s) responsible for subsequent cool flames is not necessarily the same and it is in this respect that the transition to two-stage ignition can be understood. The important role of the products formed during the first cool flame in the mechanism leading to a subsequent ignition is clearly demonstrated in the work of Fish et al [78], who studied the two-stage ignition of a range of alkanes with the aim of determining the mechanism in detail. The experiments were carried out in an arrested piston rapid compression machine and clearly indicate that an inverse relationship exists between the induction period of the second ignition stage τ_i, (measured from the time at which the maximum rate of pressure increase during the cool flame stage occurs) and the magnitude of the pressure rise accompanying the cool flame as shown below:

$$\tau_i \propto \Delta p_{c.f.}^{-x}$$

This relationship holds over considerable ranges of temperature and pressure which suggests that the cool flame stage actually controls the hot ignition. The fact that the ignition delay depends on the intensity of the cool flame, rather than on conditions of temperature and pressure existing prior to its propagation, is chemically very significant. Indeed the product concentration/time curves obtained in these studies show that many of the products which are formed at the onset of the cool flame are formed again just prior to the hot ignition. Thus, although hot ignition commences in a similar manner to a cool flame, the value of the net branching factor must be larger in the hot ignition. Fish et al conclude that this is probably due to additional branching

agents being available following the passage of the cool flame.

A unique feature of the low temperature ignition diagram is the existence of regions of multi-stage ignition (see section 1.2.4.3). This phenomenon was first reported by Bardwell[79] for n-butane + oxygen mixtures and has more recently been confirmed for the propane + oxygen system by Griffiths et al [80] and by Antonik [81]. This type of ignition seems to be restricted to low molecular weight hydrocarbons and as yet the mechanism of its occurrence is not fully understood.

1.4.2 Knock and run-on

The phenomena of 'knock' and 'run-on' in internal combustion engines reduce their efficiency and hence in recent years considerable attention has been paid to elucidating the mechanism by which they occur. The idea that knock could be directly correlated to the shape and extent of the low temperature cool flame region of hydrocarbon oxidation was by no means new when Affleck and Fish [82] produced compelling evidence that the mechanism leading to knock is identical to that leading to low temperature two-stage ignition. In their work with a rapid compression machine they showed, like Voinov and his co-workers [83], that the two-stage ignition is maintained at pressures far into the high pressure region and at pressures and temperatures similar to those experienced in a combustion engine. A study of the pressure rise/time curves for a spark-induced ignition showed that two distinctly different phenomena occurred. The first consisted of the smooth propagation of a flame front which lead discontinuously to a second, wholly different rapid spontaneous phenomenon which exhibited the property of knock. This latter phenomenon was shown to be identical to the high pressure two-stage spontaneous ignition and was therefore related to the sub-atmospheric two-stage ignition process. The similarity of the nature of the mechanism of two-stage ignition of 2-methylpentane + oxygen mixtures at

both high and low pressure was clearly indicated by the nature of the reaction products from the first stage in both regions [11, 48]. Despite the considerable differences in conditions, the chemical products were almost identical and included considerable quantities of O-heterocycles. The very low surface to volume ratio and the high initial pressure used in the compression machine experiments strongly suggest, therefore, that alkylperoxy radical isomerisation occurs homogeneously. Affleck and Fish have concluded that a reduction in the tendency of a fuel to knock can be brought about by the use of additives which inhibit cool flame propagation or at least decrease the intensity of the cool flame so that the hot ignition delay is correspondingly increased.

Similar work on the problem of 'run-on' led Affleck et al [84] to conclude that like knock, this phenomenon results from a two-stage ignition of part of the fuel + air charge. In this work, a study of the effect on run-on of numerous additives indicated that a detailed knowledge of the mechanism of hydrocarbon oxidation is essential in order that the model requirements of an effective additive can be assessed. Furthermore, the authors illustrated that the Research Octane Number (RON) is closely related to the molecular structure of the fuel and that the run-on performance of a fuel can be reasonably described by its octane rating.

1.4.3 Preparative applications

It has frequently been suggested that the cool flame oxidation of hydrocarbons may be a viable route to the production of useful chemicals such as O-heterocycles and carbonyl compounds. This is an attractive suggestion since both the raw materials and the processing costs are low compared with alternative methods of production. Cullis et al [44] have shown that under suitable conditions relatively large conversions to O-heterocycles may be achieved. High conversions (ca. 25 - 55% by weight of hydrocarbon feed) have also been obtained in

the 'falling solids' reactor designed by Jones and Fenske [85]. A major drawback of this method, however, is the difficulty and cost of separating the complex mixture of products formed, but it is hoped that homogeneous additives may considerably improve the selectivity of the method.

1.5 The influence of molecular structure on the mechanism of oxidation

The first attempt to relate the influence of molecular structure and the mechanism of the gaseous oxidation of hydrocarbons was made by Cullis and Hinshelwood[19] in 1947. They studied the oxidation of a range of hydrocarbons and found that the ease of oxidation increases as the length of the carbon chain increases, but decreases as the degree of branching in the carbon skeleton increases. They pointed out that this behaviour directly parallels the tendency of a paraffin hydrocarbon to exhibit the phenomenon of knock. An investigation of the minimum spontaneous ignition temperatures for a variety of hydrocarbons, led Affens et al[86] to the same conclusion. In both cases the authors suggested that the ease of oxidation depends primarily on the stability of the hydroperoxide formed during the oxidation, this in turn being related to the molecular structure of the hydroperoxide and hence to that of the parent hydrocarbon.

Following these preliminary investigations, Walsh[57] made a detailed study of the relationship between molecular structure and knock ratings of hydrocarbon fuels. In common with many other workers he considered that the mechanism leading to knock was the same as the low temperature mechanism of hydrocarbon oxidation and therefore concluded that the knock resistance of a fuel was related to the resistance to cool flame formation. Walsh recognised that an important propagation step was the isomerisation of alkylperoxy radicals and suggested that several modes of isomerisation could occur, each with a different activation energy. In this way, as the molecular weight of the hydrocarbon is increased, more modes of isomerisation with progressively lower activation energies become possible and so the tendency to form cool flames is increased. Using these ideas he was able to explain the dependence of the knock

rating of a fuel on its molecular structure and although these ideas have been modified in view of more recent information, they nevertheless provide a basis for considerations of the influence of molecular structure on the mechanism of hydrocarbon oxidation.

Numerous detailed reports on various alkane and oxygen systems have been made during the last decade and from these a clear picture of the effect of molecular structure has emerged.

It has been shown in section 1.3.1.2 that in the temperature range 250 - 400°C, low molecular weight hydrocarbons, with the exception of methane, tend to form the conjugate alkene as the predominant reaction product during the early stages of reaction, whereas higher molecular weight hydrocarbons form reaction products such as O-heterocycles and carbonyl compounds under the same conditions. It seems clear, therefore, that the structural constraints placed upon the ability of a particular alkylperoxy radical to isomerise, dictate the mechanism by which the hydrocarbon will oxidise. Consideration of these constraints allows the identification of two categories of hydrocarbons which exhibit different behaviour, namely:

(i) hydrocarbons with five or more carbon atoms and

(ii) hydrocarbons with four or less carbon atoms.

However, the change in behaviour as the homologous series is ascended is gradual and hydrocarbons such as n-butane and n-pentane exhibit properties common to both categories.

1.5.1 Hydrocarbons with five or more carbon atoms

The predominant mode of propagation for hydrocarbons in this category involves alkylperoxy radical isomerisation and reactions of the hydroperoxyalkyl radicals so formed. Theoretical considerations suggest that both the isomerisations and subsequent decompositions proceed with fairly low activation energies as shown in Tables 1.4 and 1.5.

(See p.33 for Table 1.4)

Table 1.5

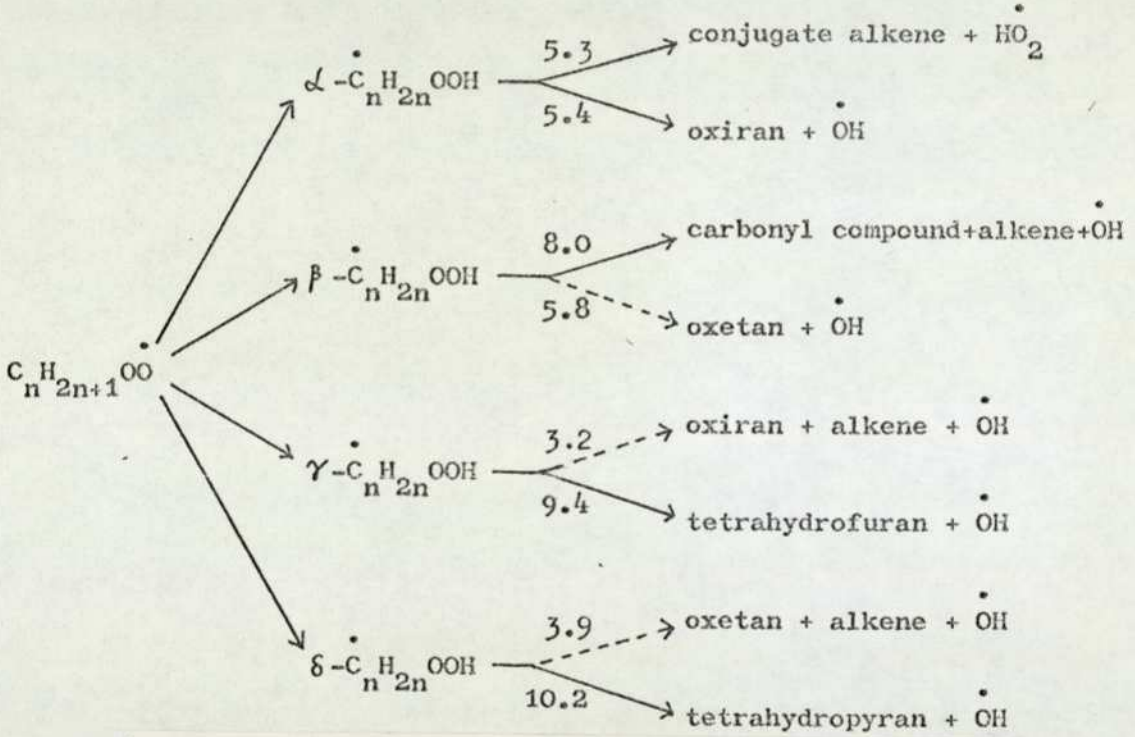
Kinetic parameters of hydroperoxyalkyl radical decompositions (at 550°K)

Mode of decomposition	Product(s)	Log k (k in $sec.^{-1}$)	Log A (A in $sec.^{-1}$)	E ($kcal.mole^{-1}$)
Cyclisation	oxiran	5.4	11	14
	oxetan	5.8	11	13
	tetrahydrofuran	9.4	11	4
	tetrahydropyran	10.2	11	2
β - Scission of C-O bond	conjugate alkene	5.3	12	14.5
β - Scission of C-C bond	alkene + carbonyl compound	8.0	12.7	12.0

(from reference 43)

Furthermore, this mode of propagation has been shown to be important at temperatures as high as 400°C and the apparently negligible effect of deposits of carbon formed during ignition [87] and pressure [11] suggests that these reactions proceed homogeneously.

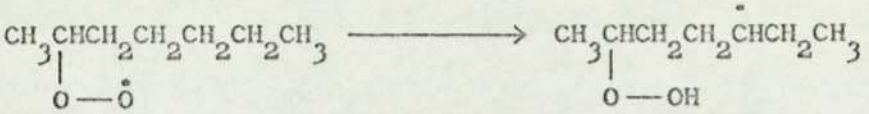
Considerable variation in the nature of the product distribution, however, is observed for different hydrocarbons in this category and this may be attributed to the various fates of different hydroperoxyalkyl radicals which are illustrated by the following generalised scheme and estimated rate constants:



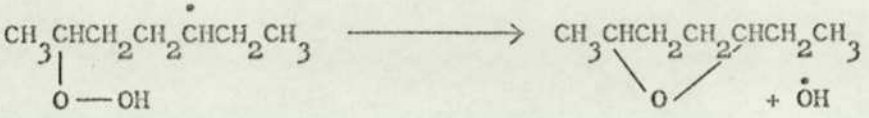
(The values of $\log_{10}k$ at 550°K are estimated [43,101])

Straight chain hydrocarbons in this category, with the exception of n-pentane, can form γ-hydroperoxyalkyl radicals by the relatively easy initial attack at a secondary C - H bond, addition of oxygen, and subsequent 1:6 hydrogen transfer from another secondary C - H bond. Since the decomposition of these radicals is fast, tetrahydrofurans would be expected to be important products for these hydrocarbons and indeed, this has been shown to be the case in the cool flame oxidation of n-heptane [88]; cis and trans 2-ethyl-5-methyltetra-

hydrofuran accounting for ca. 30% of the products.



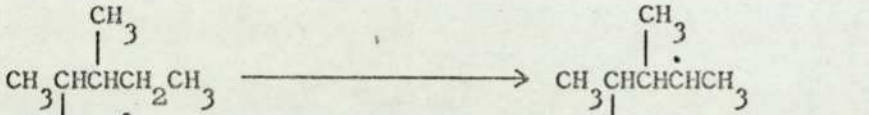
(1.75)



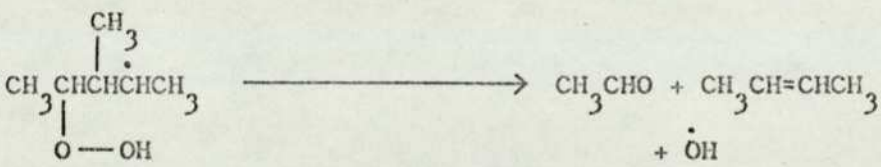
(1.76)

Similarly as the length of the carbon chain increases, the possibility of forming δ-hydroperoxyalkyl radicals, which undergo fast cyclisation reactions to form tetrahydropyrans, is enhanced.

In contrast, branched-chain hydrocarbons such as 2-methylpentane, 3-methylpentane and 3-ethylpentane, for which the formation of γ-hydroperoxyalkyl radicals involves either initial attack at a primary C - H bond or alkylperoxy radical isomerisation via 1:6 hydrogen transfer from a primary C - H bond, oxidise principally via the formation of β-hydroperoxyalkyl radicals. As shown in the above scheme, the predominant mode of decomposition of these radicals involves β-scission of a C - C bond to form carbonyl compounds and alkenes. The production of similar amounts of acetaldehyde and but-2-ene in the oxidation of 3-methylpentane [12], for example, may be accounted for by the following reaction sequence:



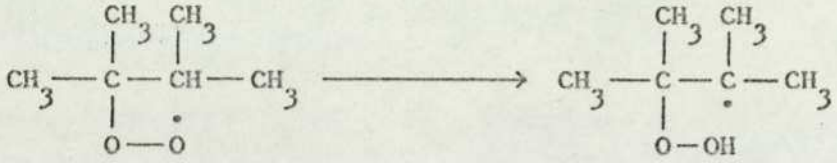
(1.77)



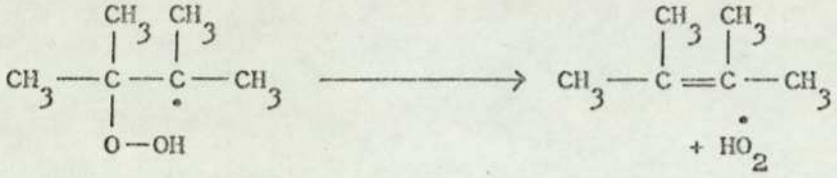
(1.78)

Thus, for these branched-chain hydrocarbons the yields of scission compounds are greater than the yields of the corresponding O-heterocycles. For highly branched hydrocarbons, the formation of α-hydroperoxyalkyl radicals will be important. Thus, for example, the structure of

2,3-dimethylbutane favours the formation of these radicals and since their principal mode of decomposition is by β-scission of the C - O bond to form the conjugate alkene and a hydroperoxy radical, 2,3-dimethylbut-2-ene would be expected to be an important product in the oxidation of 2,3-dimethylbutane, as has been found experimentally [51]:



(1.79)

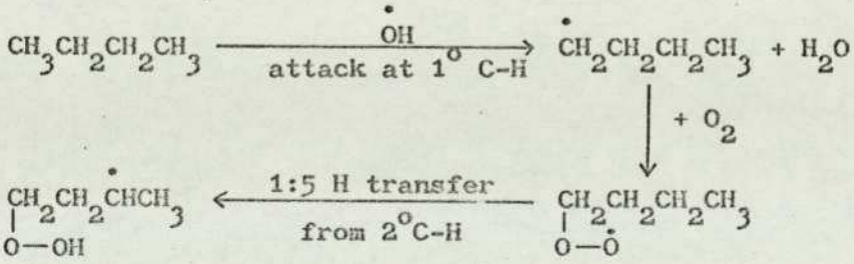


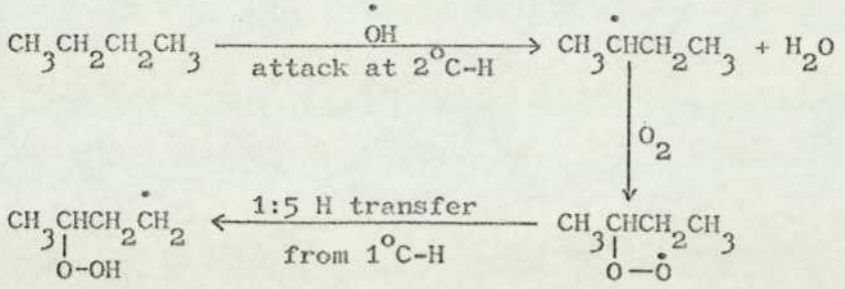
(1.80)

It can thus be seen that the nature of the product distribution is dependent on the relative rates of formation and decomposition of the α-, β-, γ- and δ-hydroperoxyalkyl radicals which in turn depend on the molecular structure of the parent hydrocarbon.

1.5.2 Hydrocarbons with four or less carbon atoms

An important limitation placed upon the isomerisation of alkylperoxy radicals formed from these hydrocarbons is that, with the exception of the but-1-ylperoxy radical, they cannot form γ-hydroperoxyalkyl radicals. Furthermore, 1:5 hydrogen transfer to form a β-hydroperoxyalkyl radical involves attack at a primary C - H bond either in the initial attack on the hydrocarbon or in the isomerisation step:





Thus for hydrocarbons of this category alkylperoxy radical isomerisations are severely restricted.

Another most important aspect is the influence of the reactor surface on the mechanism of oxidation of these low molecular weight hydrocarbons. Batten, Gardner and Ridge [89] who studied the oxidation of isobutane, concluded that the primary propagating reactions during the induction period of cool flames occurred at the reactor surface. Similarly the work of Hay, Knox and Turner [36] indicated an important heterogeneous contribution to the cool flame oxidation of isobutane. Recent studies of the oxidation of both isobutane [45] and n-butane [55] suggest that the conjugate alkene is formed heterogeneously. Thus, for example, Luckett and Pollard have shown that in the early stages of reaction (<1% conversion of isobutane) the yield of isobutene decreases as the initial pressure of the reactants is increased towards the ignition limit. They conclude that the conjugate alkene formation occurs by a selective heterogeneous decomposition of α-hydroperoxy-t-butyl radicals. In contrast, the yields of ethylene and propene remain sensibly constant whilst the yield of tert-butyl hydroperoxide increases, suggesting that the decomposition of β-hydroperoxy-iso-butyl radicals proceeds homogeneously. Furthermore, the yield of isobutene, over the temperature range 310 - 380°C, passes through a minimum at ca. 350°C which suggests that the mode of production of isobutene is different at low and high temperatures. Luckett and Pollard have therefore concluded that as the initial temperature is raised, the heterogeneous mode of isobutene formation becomes increasingly less important and the

homogeneous decomposition of hydroperoxyalkyl radicals becomes the predominant reaction. Similarly, Dechaux [55], who has studied the oxidation of n-butane, showed that the yields of the butenes, ethylene and hydrogen peroxide all decrease as the initial pressure is increased. He also concludes that the results provide strong evidence for a heterogeneous mode of formation of alkenes via the decomposition of hydroperoxyalkyl radicals.

Recently, evidence has been presented for a small heterogeneous contribution in the low temperature mechanism of n-pentane oxidation [52], although this hydrocarbon does not strictly belong to this category. Bastow found that the yields of pent-2-ene and 2-methyltetrahydrofuran decrease as the initial pressure of the reactants is increased. Knox [42] has also found that the yield of acetone, a major product in the oxidation of n-pentane at low temperatures, is strongly sensitive to changes of the reactor surface. Finally, the absence of conjugate alkenes in the products of the oxidation of n-pentane in a shock tube[90,91], which is virtually a wall-less reactor, gives strong support to the suggestion that these compounds are formed heterogeneously.

The substantial yields of the conjugate alkene reported for hydrocarbons of this category clearly indicate the importance of α-hydroperoxyalkyl radicals in the propagation sequence and the foregoing considerations show that the decomposition of the radicals via β-scission of the C - O bond may well occur at the walls of the reactor.

It can be seen, therefore, that marked differences in behaviour occur for these two categories of hydrocarbons. A simple generalisation is that alkylperoxy radicals derived from higher molecular weight hydrocarbons have virtually unrestricted modes of isomerisation and subsequent reactions of the hydroperoxyalkyl radicals proceed quickly and homogeneously, whilst alkylperoxy radicals derived from lower molecular weight hydrocarbons have highly restricted

isomerisations and further reactions of the hydroperoxyalkyl radicals are slower and may occur heterogeneously. Similarly an increase in branching of the hydrocarbon skeleton will again restrict the alkylperoxy radical isomerisations thus reducing the overall rate of oxidation and increasing the possibility of a heterogeneous contribution to the mechanism. Clearly, the correlation between the molecular structure of a hydrocarbon fuel and its knock rating is not surprising in view of these foregoing considerations.

1.6 The present work

In the foregoing discussion it has been seen that the nature and mechanism of chain propagation, during the gaseous oxidation of hydrocarbons, depend on the molecular structure of the fuel. Indeed, recent analytical investigations of the oxidation of n-butane and isobutane suggest that, for low molecular weight hydrocarbons, there is an important heterogeneous contribution to the propagating sequence at low temperatures. Furthermore, it has been seen that for the majority of hydrocarbon + oxygen systems, alkylperoxy radical isomerisation plays an important role in the propagation reactions in the low temperature region and studies of the oxidation of 2-methylpentane and 3-ethylpentane indicate that this isomerisation may be important even at temperatures of ca. 400°C.

It is desirable, therefore, to study in depth the oxidation of n-butane in order to investigate and test specific aspects of the alkylperoxy radical isomerisation theory. A detailed kinetic survey of the n-butane + oxygen system has not been previously reported and clearly, if there is a changeover from heterogeneous to homogeneous propagation as the initial temperature is increased, this should be reflected in the kinetics of the system. It was anticipated that analytical studies of the variation with the initial reactant conditions of the nature and distribution of reaction products in the early stages of reaction, when the effect of secondary reactions can be considered negligible, would provide valuable information regarding the propagation reactions and that correlation with the results of studies of the oxidation of higher hydrocarbons and

branched-chain hydrocarbons, such as isobutane and 2,3-dimethylbutane, would throw more light on the effect of molecular weight and structure.

Throughout this study the n-butane:oxygen ratio was maintained at 1:2 and strict regard was paid to the reactor surface.

SECTION 2

EXPERIMENTAL

SECTION 2

		Page No.
2.1	The apparatus	71
2.1.1	The vacuum system	71
2.1.2	The furnace and line heating	74
2.1.3	The reactant and product gates	76
2.1.4	The pressure transducer	79
2.1.5	Thermocouples	81
2.1.6	Signal amplification and recording equipment	83
2.1.7	Calibration of vessels and line	85
2.2	Reactants	86
2.3	General procedure	87
2.3.1	Preparation of fuel + oxygen mixtures	87
2.3.2	Introduction of reactants into the reaction vessel	87
2.3.3	Conditioning of the reaction vessel	87
2.3.4	Evacuating the reaction vessel	88
2.3.5	Measurement of the kinetic parameters from traces	88
2.3.6	Product sampling	90
2.4	Gas-chromatographic analysis of reaction products and reactants	93
2.4.1	The gas chromatograph	93
2.4.2	Preparation of columns	93
2.4.3	Column conditions	93
2.4.4	Sample introduction	96
2.4.5	Identification and calibration of products	96
2.4.6	Operating procedure	101

2.1 The apparatus

2.1.1 The vacuum system

A conventional static vacuum system was constructed of Pyrex glass and is shown schematically in figure 2.1. The spherical reaction vessel, volume ca. 550 ml, was thoroughly cleaned with nitric acid, distilled water and finally acetone prior to use. It was then suspended in an electrically heated furnace and a pressure transducer was fitted vertically above it. The reaction section, enclosed by stop-cock R_1 and the reactant gate in figure 2.1, was constructed of 3 mm capillary tubing and was kept as compact as possible in order to minimise 'dead-space'. Greaseless P.T.F.E. Rotaflo stop-cocks were fitted in this section of the apparatus to prevent the adsorption of reaction products. Moreover, since high-vacuum greases are silicone-based, the risk of contaminating the reaction vessel surface was eliminated. The reaction section was completed with a mercury manometer, a removable sample trap, a calibrated vessel and electronically operated reactant and product gates. A product gate by-pass B_2 was incorporated into the reaction section to prevent unnecessary use of the gate whilst conditioning and kinetic runs were performed. The reaction product sample trap was attached to the apparatus by greaseless ball and cup joints and held in position by spring clips.

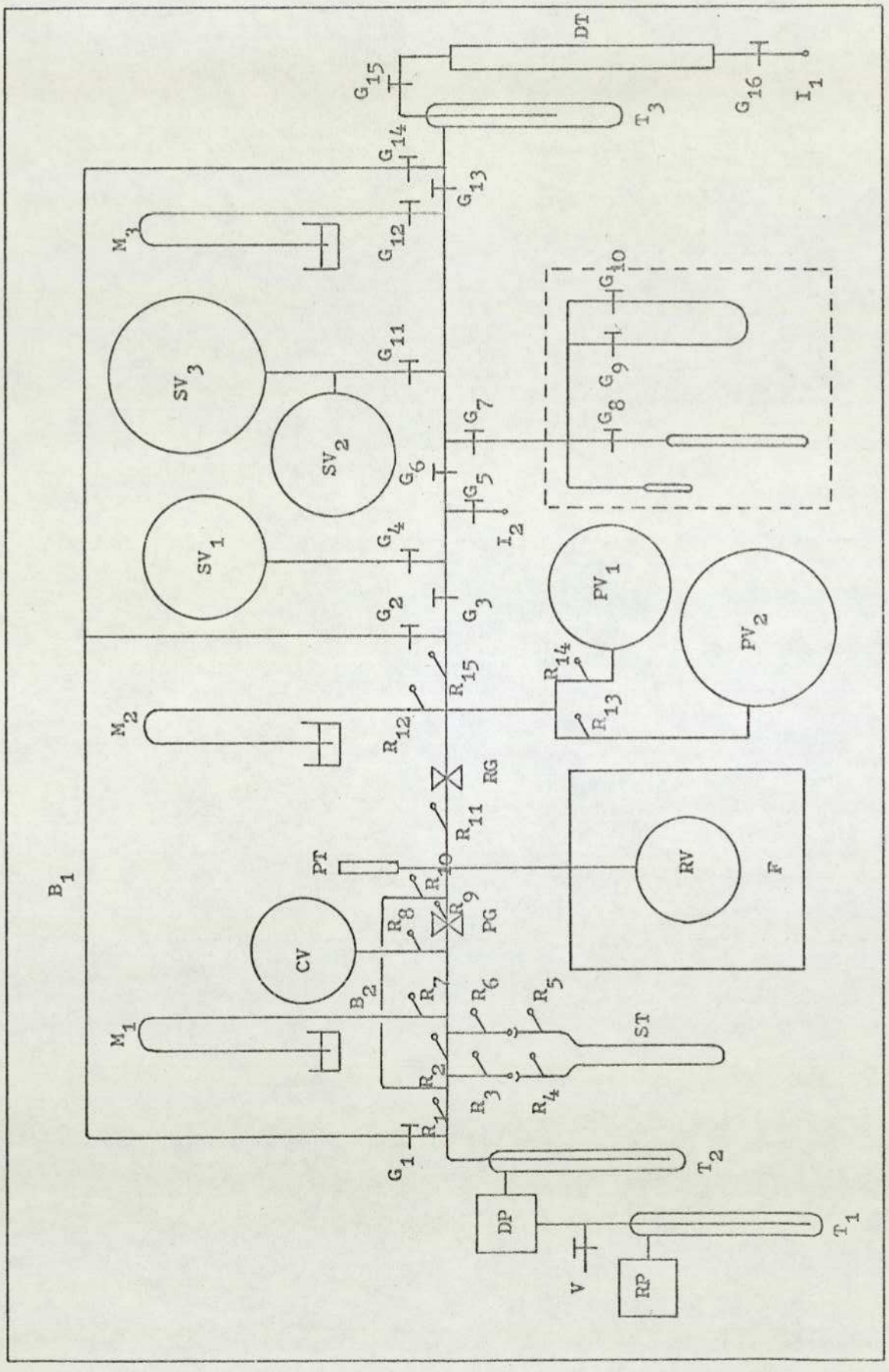
The gas-handling section, bounded by stop-cocks G_3, G_5, G_{14} and G_{16} in figure 2.1, was constructed of 5 mm tubing and incorporated conventional vacuum stop-cocks greased with Edwards high vacuum silicone grease. Permanent gases were introduced at the inlet I_1 and passed through a drying tower containing molecular sieve (grade 4A) to a cold trap T_3, maintained at -196°C, where they were condensed and fractionated. Cylinders of n-butane and other hydrocarbon gases were connected to the section at the inlet I_2 by means of a ball and cup joint.

Key to figure 2.1

RV	Reaction vessel
F	Furnace
RG	Reactant gate
PG	Product gate
PT	Pressure transducer
ST	Sample trap
CV	Calibrated vessel
PV_1, PV_2	Premix vessels (2 and 5 litres)
SV_1, SV_2, SV_3	Gas storage vessels (2, 2 and 5 litres)
T_1, T_2, T_3	Cold traps
M_1, M_2, M_3	Mercury manometers
B_1, B_2	By-passes
DT	Drying tower containing molecular sieve
DP	Mercury diffusion pump
RP	Rotary oil pump
V	Vent
⊣ G	Grease stop-cock
⟋ R	Rotaflo greaseless stop-cock
	Ball and cup joint
-----	Active-compound handling section
I_1	Inlet for permanent gases
I_2	Inlet for hydrocarbon gases

Figure 2.1

The static vacuum apparatus



Three gas storage vessels of 2, 2 and 5 litres were attached to this section and were wrapped with insulation tape as a protection against implosion. This section was also completed by a mercury manometer.

The reactant premix section, bounded by stop-cock R_{15} and the reactant gate, incorporated a 2 litre and a 5 litre premix vessel and a mercury manometer. These premix vessels were enclosed in metal jackets as a protection against explosion and were maintained at ambient temperature. Rotaflo greaseless stop-cocks were also used throughout this section.

A by-pass B_1, constructed of wide bore tubing, was attached to the apparatus at stop-cocks G_1, G_2 and G_{14}. This increased the pumping efficiency of the mercury diffusion pump which was backed by an Edwards rotary oil pump. In order to prevent undue contamination of the oil and diffusion of mercury vapour into the apparatus, two cold traps, T_1 and T_2, were incorporated in the line on either side of the diffusion pump. Provided these traps were properly maintained, a vacuum of ca. 10^{-3} torr could easily be achieved.

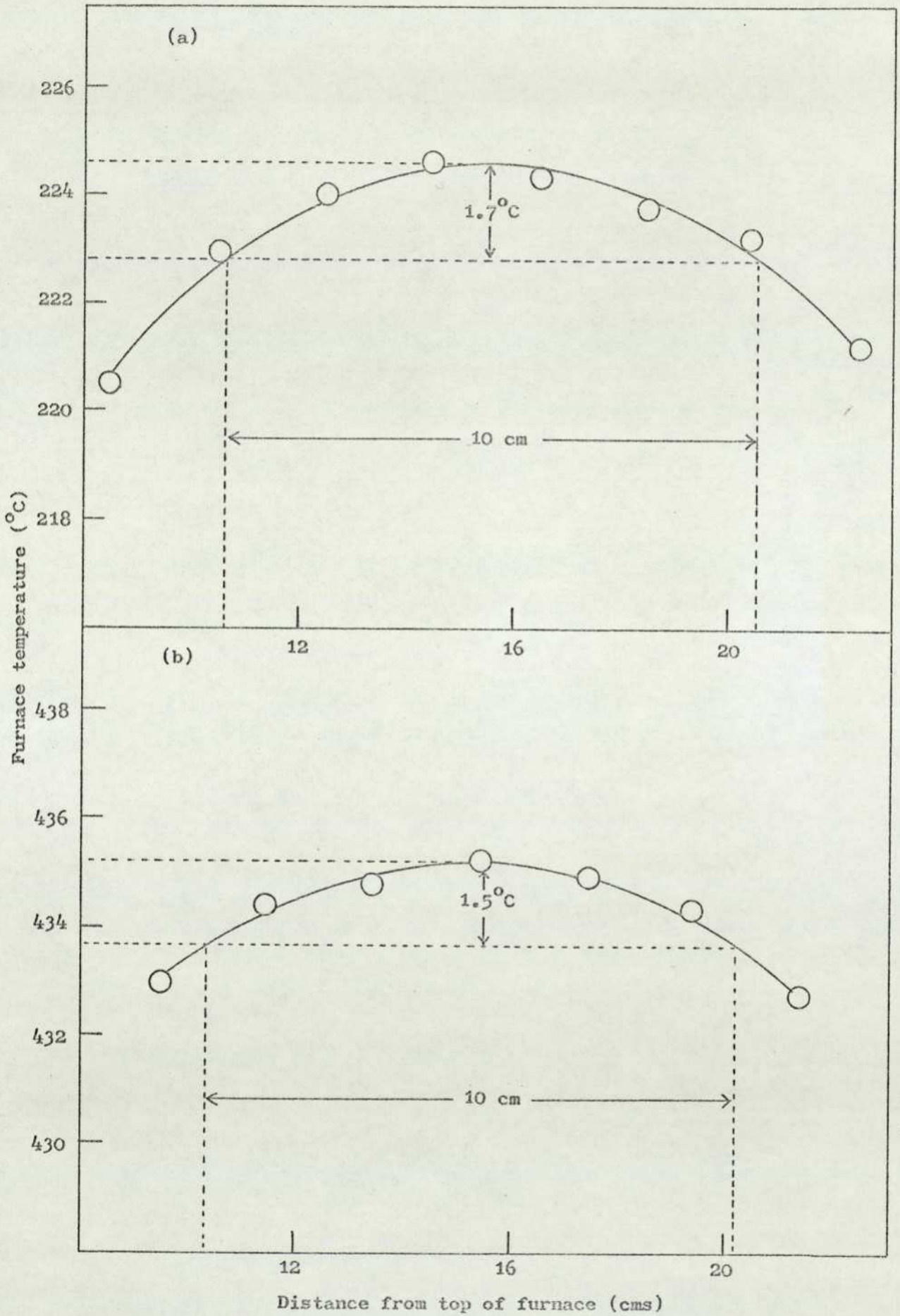
2.1.2 The furnace and line heating

The furnace was powered by a silicon controlled rectifier which in turn was connected to a Sirect Mark II Proportional Temperature Controller. Temperature fluctuations in the furnace were automatically compensated for by the proportional controller which compared the feedback signal from a platinum resistance thermometer with the desired set temperature and adjusted the furnace current accordingly. Control was possible to within $\pm 0.2^{\circ}C$ of the desired temperature.

A temperature profile of the furnace well was constructed using a chromel/alumel thermocouple which had previously been compared with a standard platinum/platinum-rhodium thermocouple. Figure 2.2 shows that over an optimum 10 cm distance (reaction vessel diameter) along the

Figure 2.2

Furnace temperature profiles at (c) 224°C (b) 435°C



vertical axis of the furnace well, the temperature gradient was no more than 1.7°C at the two temperatures investigated. This determination dictated the position of the reaction vessel, and the chromel/alumel thermocouple hot junction was positioned adjacent to the mid-point of the reaction vessel.

The line and calibration vessel in the reaction section were maintained at 80°C, using thermal tape, in order to prevent high-boiling reaction products condensing out. The manometer in this section was wrapped with nichrome wire which, in parallel with the thermal tape, was connected to an a.c. power supply. The sample trap was maintained at the termperature of the line by means of Electrothermal heating cord connected to a portable power supply.

2.1.3 The reactant and product gates

The construction of the reactant gate is shown in figure 2.3 and its mode of action depends on the principle of the solenoid. Its operation was such that on energising the 240 volt a.c. solenoid coil (SC), the iron core (C) was lifted out of its cup seating and thus permitted reactant mixture to flow to the evacuated reaction vessel. As soon as the current was stopped the iron core dropped quickly into its seating under the action of gravity and the coiled spring (S) thus preventing further flow through the gate. The seal between the iron core and its cup seating was made by a silicone rubber O-ring and the gate was arranged so that the pressure differential across it acted to improve the seal. The opening time of the gate, and therefore the pressure of reactants admitted to the reaction vessel, was controlled using the timing circuit illustrated in figure 2.4. By selecting different capacitors the circuit was made to discharge across the a.c. relay for different time intervals, thus activating the solenoid coil for corresponding times. The timing circuit was powered by a 9 volt battery and could be triggered with a micro-switch.

Figure 2.3

The reactant gate

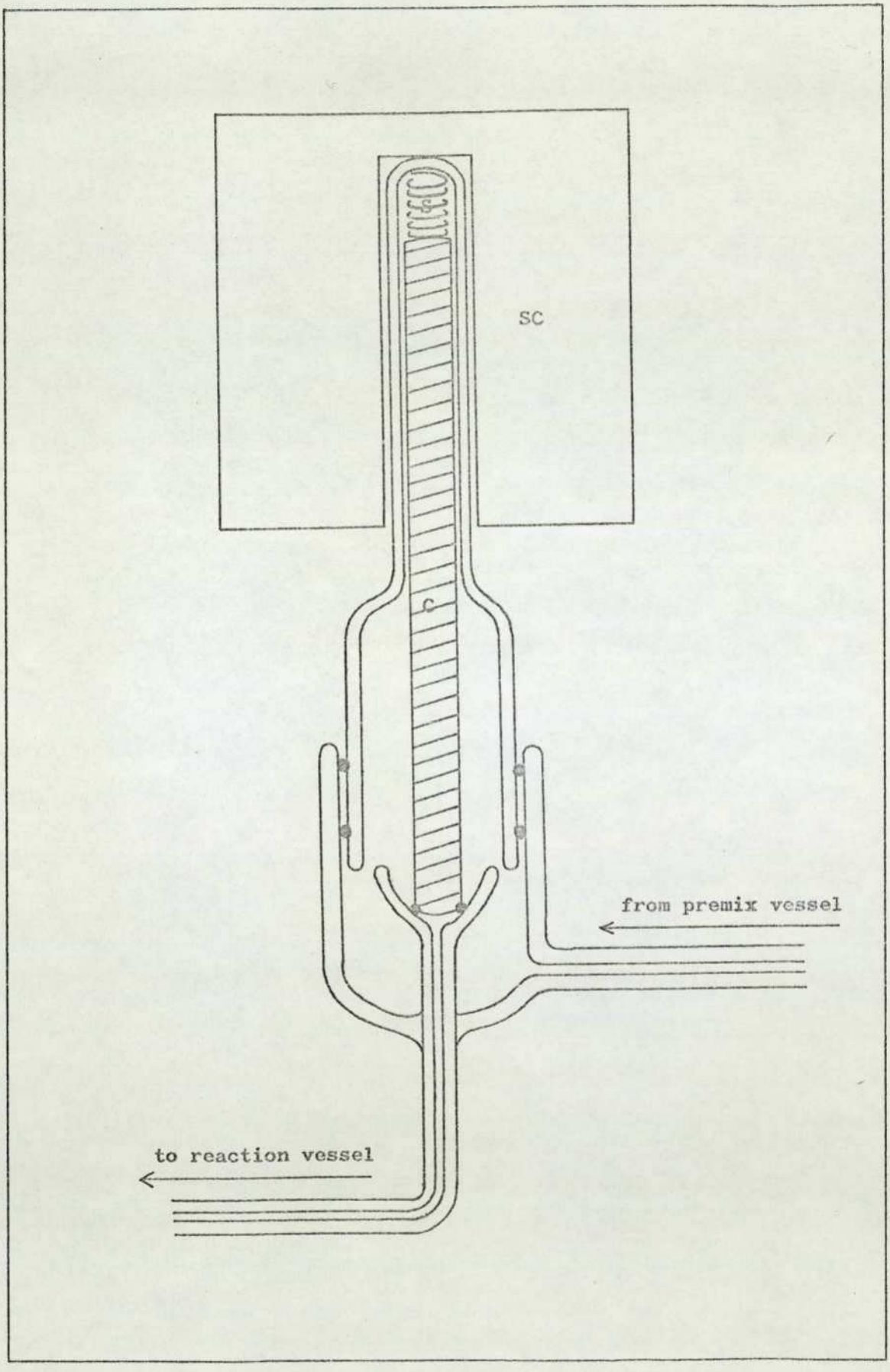
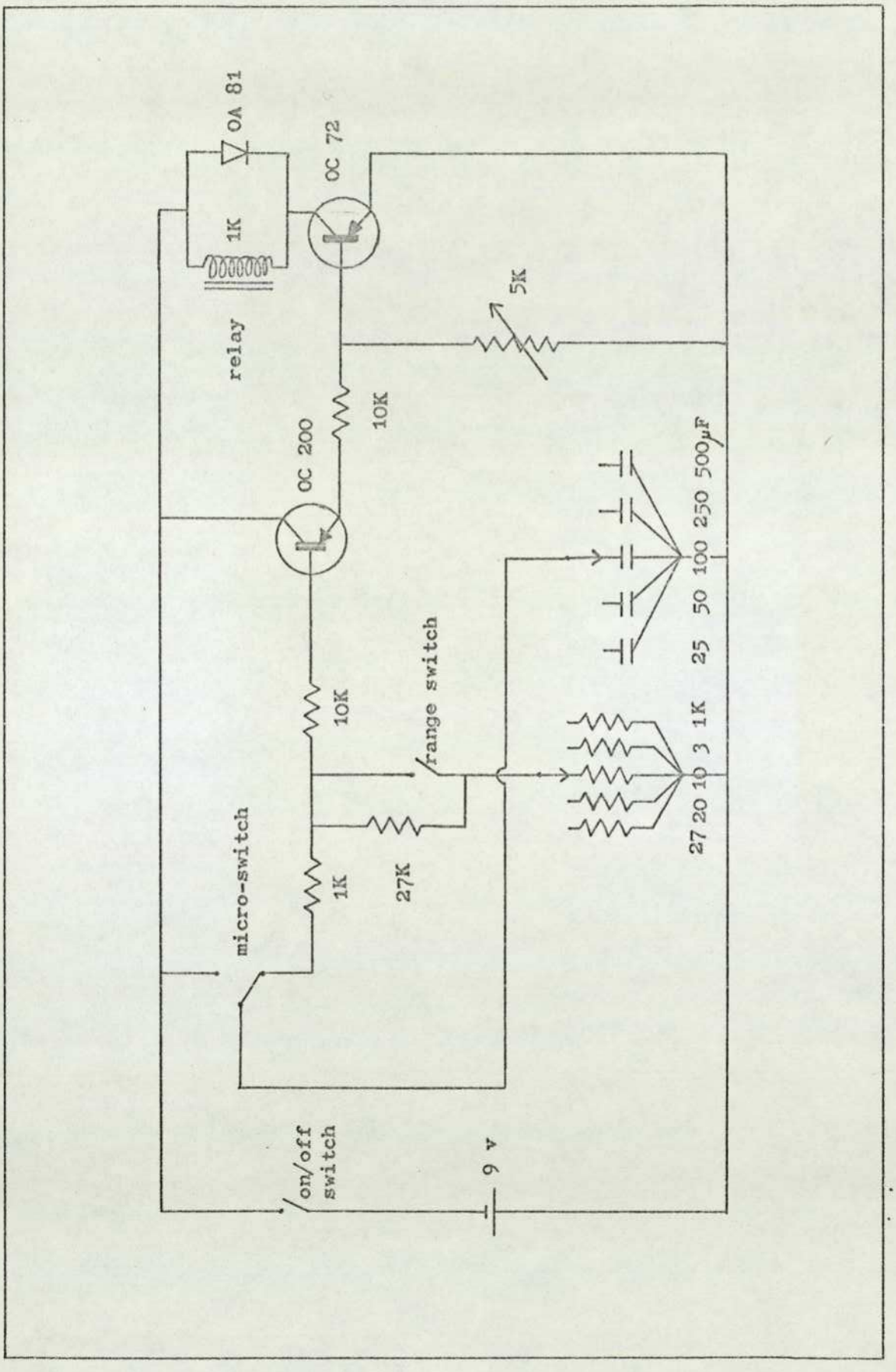


Figure 2.4

The solenoid gate timing circuit



The product gate was identical in construction to the reactant gate although since it was positioned in the line to minimise 'dead-space', the pressure differential across it acted to the detriment of the seal and this necessitated the use of a stronger coiled spring. The product gate was operated with a similar timing circuit to that of the reactant gate except that a smaller relay was employed in order to improve the speed of response.

The advantages of these gates were that they allowed rapid admission of reactants into the reaction vessel and rapid withdrawal of samples of the reacting mixtures. Furthermore, the product gate could be operated whilst observing the data displayed on the recording apparatus thus enabling accurate sampling to be performed. The reactant gate was calibrated at an appropriate setting of the timing circuit so that any desired initial pressure of reactants in the reaction vessel could be achieved by adjusting the pressure of the reactants in the premix vessel. This procedure gave reproducible initial pressures as well as standardising the time for introducing reactants into the reaction vessel.

2.1.4 The pressure transducer

Pressure changes in the reaction vessel were followed by means of a 0-10 p.s.i.a. strain-gauge transducer (Bell and Howell type 4-326-L101). The supply voltage for the transducer was provided by a stabilised 10 volt d.c. transformer (Bell and Howell type 3-142). Pressure changes acting on the diaphragm of the transducer were converted to controlled strains in a Wheatstone bridge circuit in which all four arms are active strain-gauge windings. The signal generated by the pressure transducer was amplified and the output fed to a recording instrument (section 2.1.6). A zero balance circuit was incorporated between the transducer and the stabilised power supply as shown in

Figure 2.5

The zero balance circuit

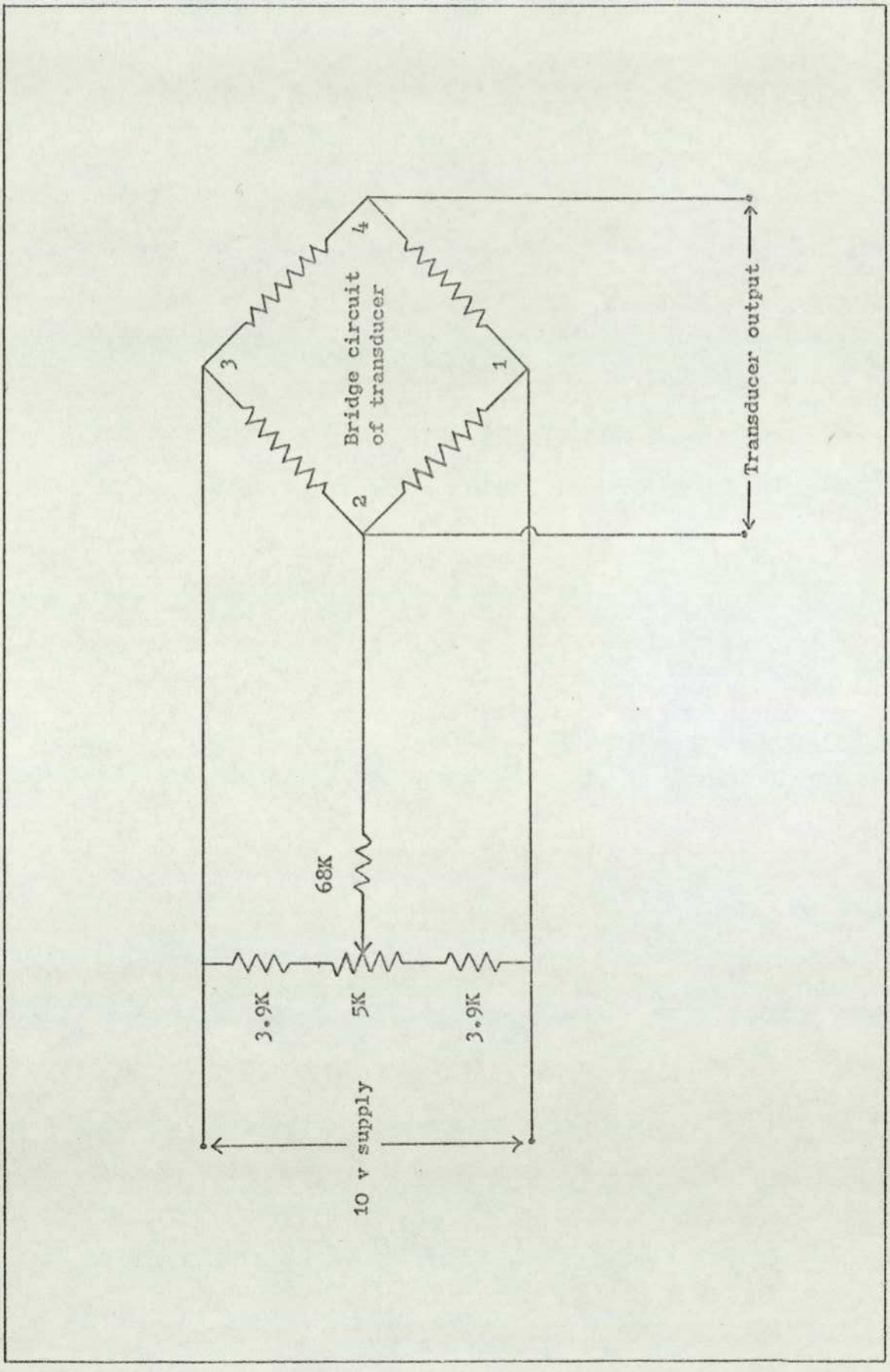


figure 2.5. The transducer was calibrated against a mercury manometer using dry nitrogen and its output was shown to be linear over a pressure range 0-500 torr.

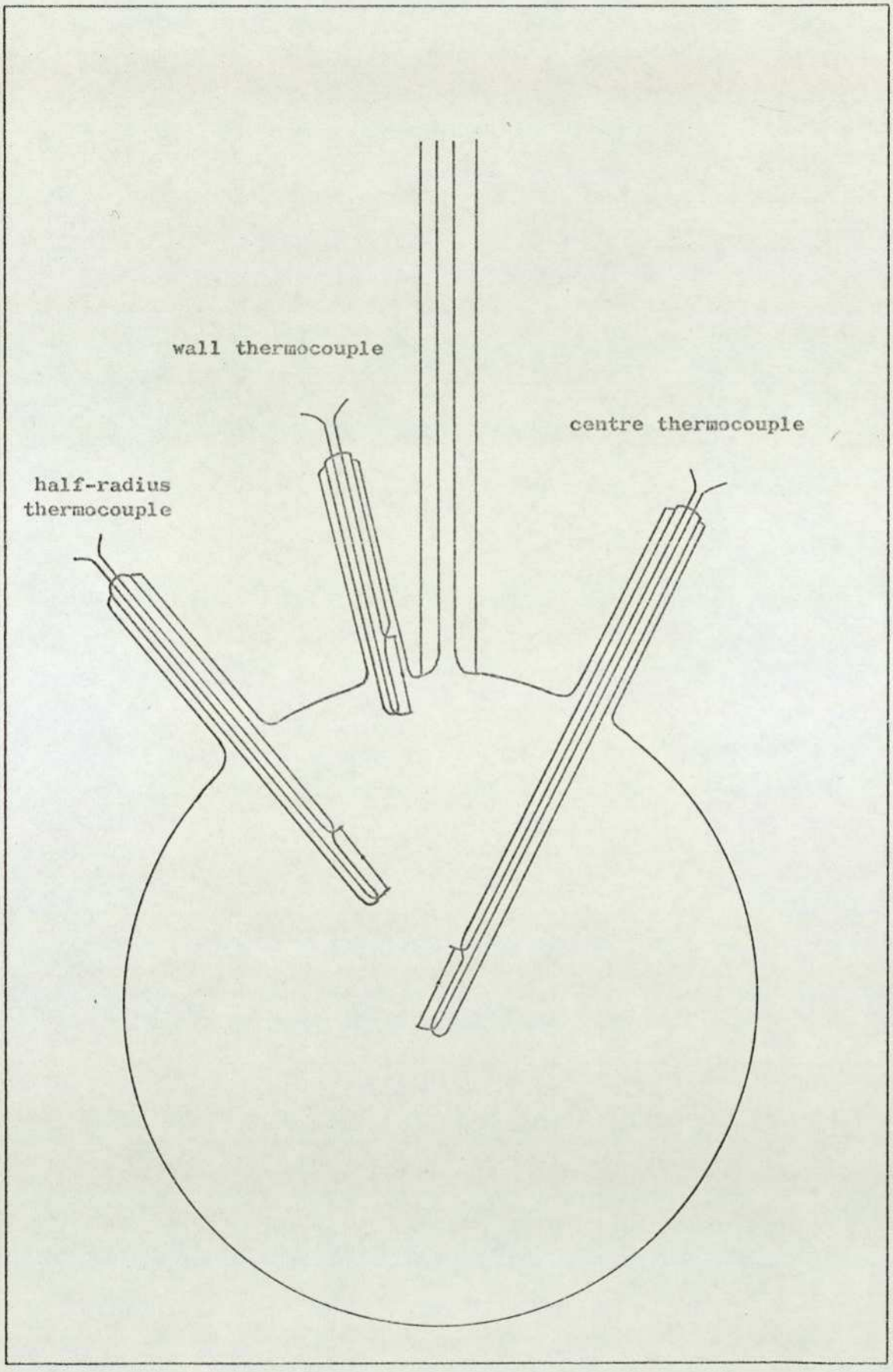
2.1.5 Thermocouples

Temperature changes occurring within the reaction vessel were monitored using specially developed micro-thermocouples. The thermocouples were constructed of 0.025 mm platinum and platinum-13% rhodium wires butt-welded together and supported on 0.25 mm wires of the same material. The support wires were sealed into twin-bore capillary Pyrex sheaths which led to the outside of the reaction vessel. To prevent any catalytic action due to the platinum, those parts of the thermocouples which extended into the reaction vessel were coated with a thin layer of silica using the method developed by Kaskan [92]. The hot junctions of the three micro-thermocouples were positioned at the centre, at the half-radius and adjacent to the wall of the reaction vessel as shown in figure 2.6. The cold junctions were maintained at 0°C and the outputs from the thermocouples were led via three d.c. amplifiers to the recorder.

The advantage of the micro-thermocouples is that since their thermal capacity is very small, their frequency response is high and allows temperature fluctuations, such as those accompanying the passage of cool flames, to be followed faithfully. Indeed, it has been shown that such thermocouples with 0.05 mm diameter junction beads, are capable of responding to 75% of a step-change in the gas temperature in less than 0.2 sec.[93]. Furthermore, it has also been calculated that under steady-state conditions, heat loss by conduction along the support wires and by radiation result in only a 1% difference in temperature between the gas and the bead. In the present work, the temperature of the reacting gas mixture was followed using thermocouples whose bead

Figure 2.6

The position of the thermocouples in the reaction vessel



diameter was of the order of 0.04 mm.

2.1.6 Signal amplification and recording equipment

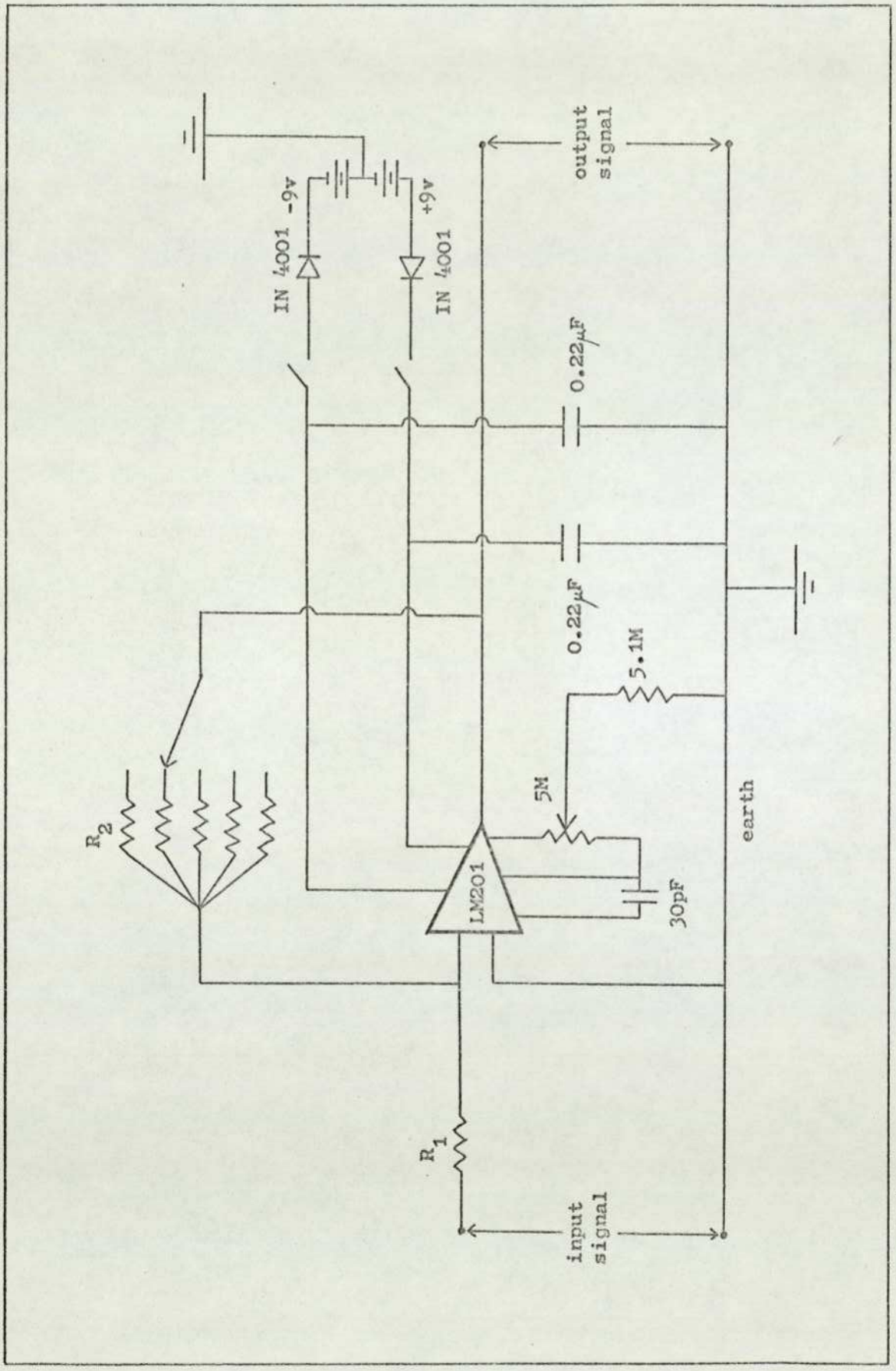
In order to record the transient pressure and temperature changes in the reaction vessel with fidelity, it was necessary to amplify the output signals of the pressure transducer and thermocouples. To achieve the desired amplification, a d.c. amplifier circuit was designed and one constructed for each of the four signals. This circuit is illustrated in figure 2.7, the principal component being a National Semiconductor LM201 operational amplifier module which is driven by a ± 9 volt power supply. The amplification factor or gain of the amplifier is derived from the ratio of the feedback resistor R_2 to the input resistor R_1 and by selecting suitable values of R_1 and R_2, a range of gains may be obtained. A balance circuit is included so that any intrinsic offset in the amplifier module may be nullified. The quoted frequency response of this amplifier circuit is of the order of kilocycles per second and therefore these amplifiers were considered to be capable of following any pressure or temperature oscillations likely to be encountered.

The amplified output signals were fed via a network of damping resistors to four Honeywell BB 130A sub-miniature optical galvanometers mounted in a Honeywell 1706 Visicorder. The values of the damping resistors were chosen to give a damping ratio of 0.64 which allows the optimum speed of response with a minimum oscillation and final value error. The movements of the galvanometer mirrors, caused by fluctuations of the signals, were recorded on U.V. photo-sensitive chart paper from which kinetic measurements could be made.

The flat frequency response of the BB 130A galvanometers is 80 c.p.s. which means that any pressure or temperature oscillations with rise-times greater than 0.003 seconds can be followed accurately.

Figure 2.7

The d.c. amplifier circuit



Since quoted rise-times for cool flames are considerably longer than this value it was considered that the complete monitoring, amplification and recording system was capable of responding to any changes in the reaction vessel with fidelity.

2.1.7 Calibration of vessels and line

The volume of the calibration vessel was determined prior to its incorporation in the reaction section by weighing the quantity of acetone required to fill it at 25°C. Similarly the volume of the reaction product sample trap was determined by weighing the quantity of clean mercury necessary to fill it at 25°C. Other parts of the reaction section including the reaction vessel, product gate and reaction line were calibrated by sharing dry nitrogen between them and the calibration vessel.

2.2 Reactants

All investigations were carried out using 'instrument' grade n-butane which was obtained from the Matheson Corporation. This gas was shown to be better than 99.8% pure by gas liquid chromotography, the main impurities being isobutane, but-2-ene (cis and trans) and propane.

Oxygen, supplied by the British Oxygen Company, was taken from a cylinder, passed through the drying tower and condensed in a cold trap (T_3) maintained at -196°C. The oxygen was purified by fractional distillation. The middle fraction was allowed to evaporate into the storage vessels, considerable head and tail fractions being rejected.

'Oxygen-free' nitrogen, also supplied by the British Oxygen Company, was taken from a cylinder, passed through the drying tower and through the cold trap. This dry nitrogen was then passed to storage vessels.

2.3 General procedure

2.3.1 Preparation of fuel + oxygen mixtures

n-Butane was passed directly from a lecture bottle into the two evacuated premix vessels. The 'working' premix vessel (2 litre) was filled to a pressure of 100 torr and the 'reservoir' premix vessel (5 litre) was filled to a third of the atmospheric pressure. Using the gas storage vessels as a buffer system, oxygen evaporated directly from the middle fraction of the distillation was mixed with the n-butane to give a final pressure of 300 torr and one atmosphere in the working and reservoir premix vessels respectively. The mixtures were then left for about one hour to become completely homogeneous.

2.3.2 Introduction of the reactants into the reaction vessel

The automatic reactant gate was initially calibrated (section 2.1.3) so that any desired initial pressure of reactants could be achieved by adjusting the pressure of the reactants in the working premix vessel, either by pumping some out or by adding some from the reservoir premix vessel. The majority of the experiments were performed using a gate opening time of 400 milliseconds. Reactants were admitted to the reaction vessel with stop-cocks R_9 and R_{10} closed and R_{11} open. Immediately this operation was completed, R_{11} was closed to prevent reaction products from attacking the O-ring seal in the reactant gate.

2.3.3 Conditioning of the reaction vessel

Prior to determining the temperate-pressure ignition profile, about 250 conditioning runs were performed. These experiments included mainly slow combustion and cool flame oxidations although some two-stage ignitions occurred. The carbon deposited on the reaction vessels by such ignitions drastically altered the kinetics of subsequent experiments and

it was necessary to remove it. This was achieved by leaving oxygen in the reaction vessel at 450°C for several days and the reaction vessel was considered to be conditioned when reproducible results were obtained at all temperatures (280 - 400°C).

Several reaction vessels were used throughout the investigations and so a standard procedure for conditioning, as outlined above, was rigorously applied. The majority of the kinetic studies and all of the analytical studies were carried out in carbon-free reaction vessels so that the results could be correlated.

2.3.4 Evacuating the reaction vessel

Upon the completion of a run, the reaction vessel was evacuated by pumping the products out through the by-pass B_2 with stop-cocks R_1 and R_{10} open. During the kinetic investigations it was found necessary to pump on the reaction vessel for at least 15 minutes before carrying out a further experiment. If such a procedure was not strictly adhered to, inconsistent results were obtained. Pumping times were increased to 1 hour whilst analytical studies were performed.

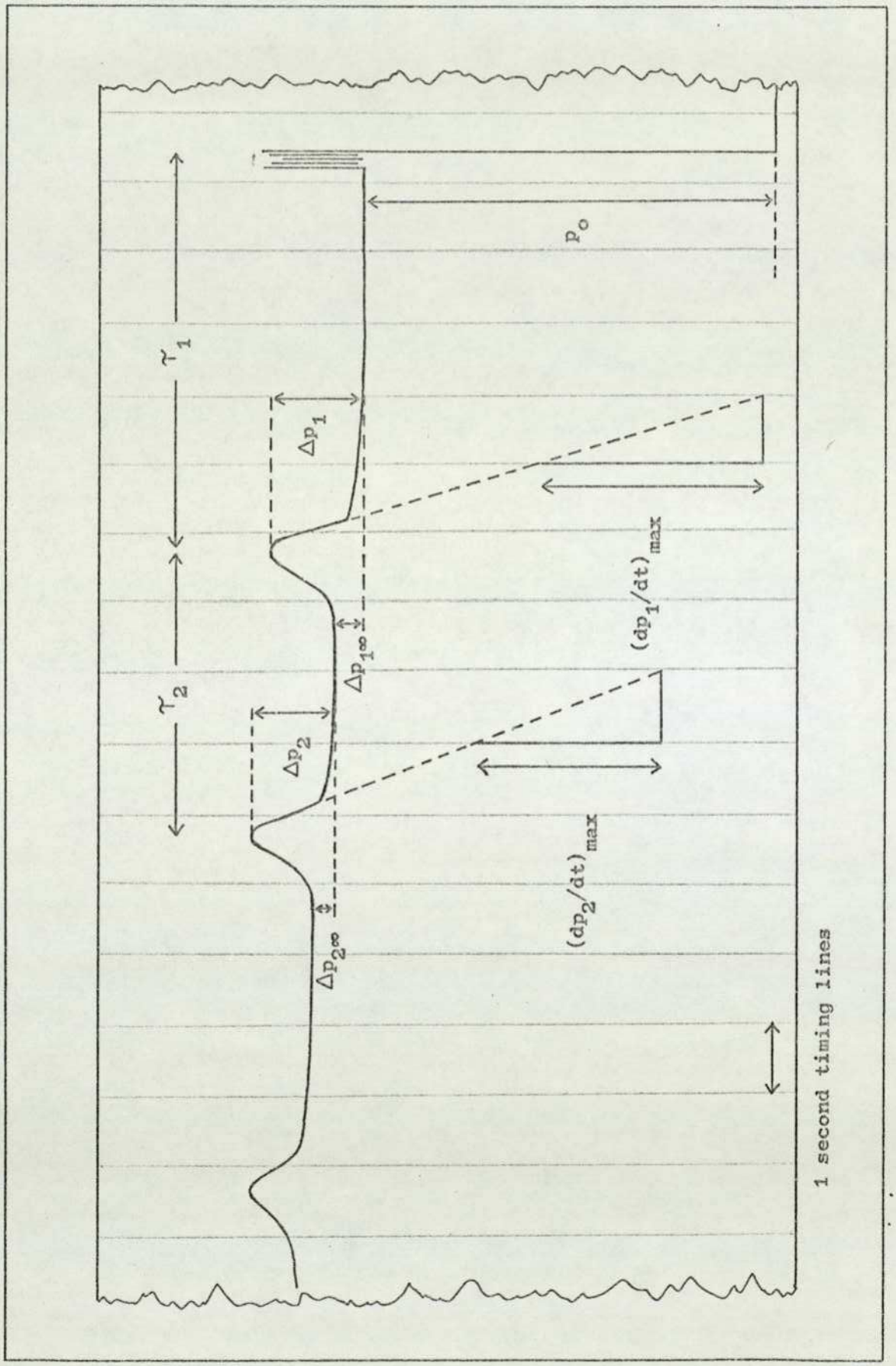
2.3.5 Measurement of the kinetic parameters from traces

Kinetic investigations were carried out in two parts. First, the ignition profile for a 1:2 n-butane/oxygen mixture was determined using pressure measurements only. Secondly, the ignition profile was determined using both pressure and temperature measurements.

A typical pressure-time recording for a multiple cool flame oxidation is shown in figure 2.8. The induction period of the first cool flame was measured from the time the reactant gate was opened to the time at which the pressure rise accompanying the cool flame reached its maximum value. All induction periods were recorded in seconds. The rate of pressure rise $(dp_1/dt)_{max}$ was measured by constructing a tangent to the

Figure 2.8

A typical pressure-time recording
illustrating the measurement of kinetic parameters



pressure trace at its maximum rate of rise and calculating its gradient in torr $sec.^{-1}$. The techniques used for measuring the maximum pressure rise during the cool flame (Δp_1), the initial reactant pressure (p_o) and the overall rise in pressure following the passage of the cool flame ($\Delta p_{1\infty}$), all measured in torr, are also shown in figure 2.8. Measurements made on subsequent cool flames were similar except that the induction period was measured from the pressure maximum of the preceding cool flame.

A typical recording showing pressure and temperature changes at the centre, half-radius and wall of the reaction vessel during a multiple cool flame oxidation is shown in figure 2.9. In these experiments, measurements were made of the usual pressure parameters together with the maximum temperature rise accompanying the first cool flame (ΔT_1) in ^{o}C, the maximum rate of temperature rise $(dT_1/dt)_{max}$ in $^{o}C\ sec.^{-1}$ and the time interval (Δt) in seconds, by which the temperature maximum either leads or follows the pressure maximum as recorded by each thermocouple. The technique for measuring temperature changes occurring at the wall of the reaction vessel is shown in figure 2.9.

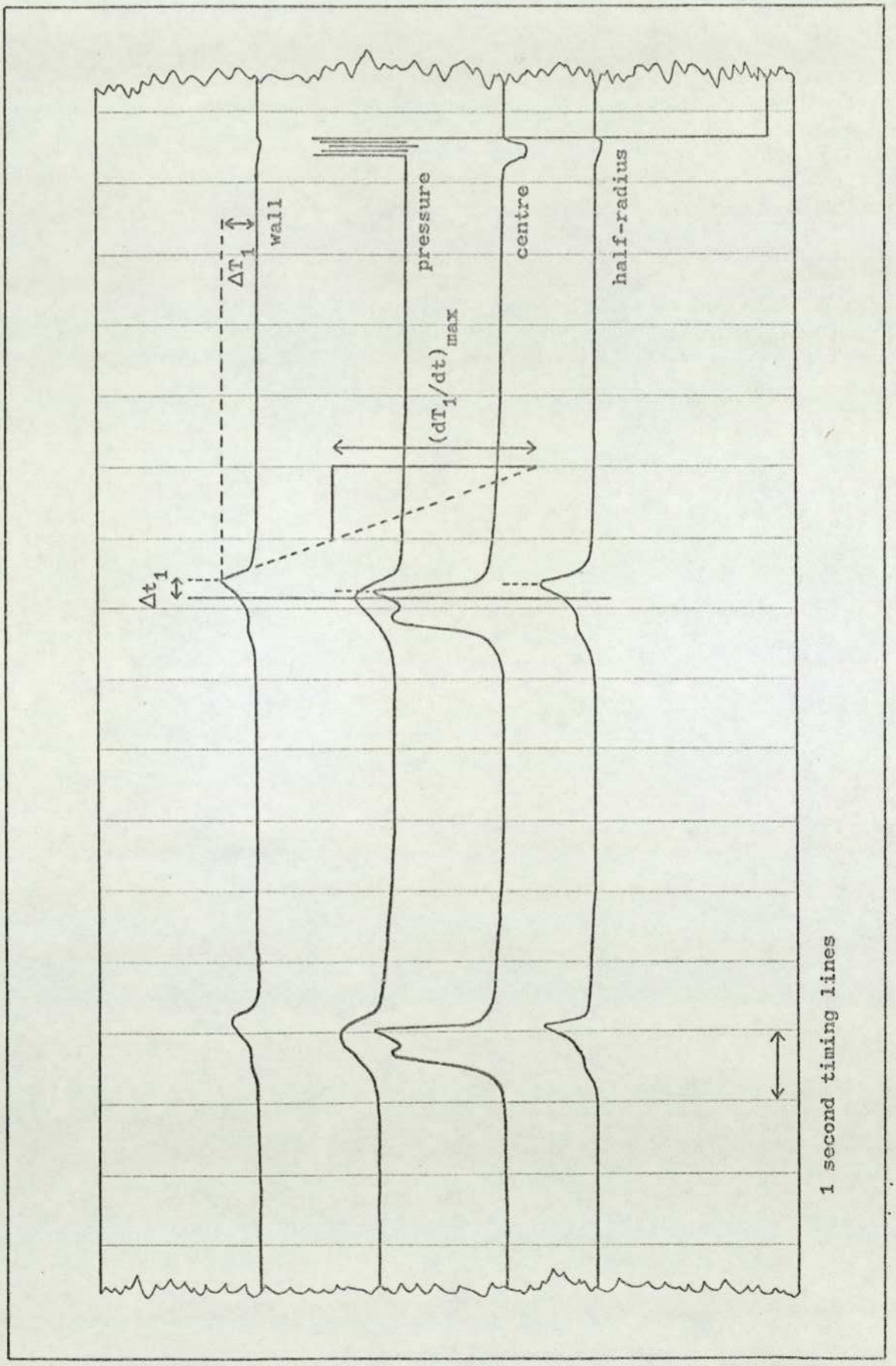
At initial temperatures above ca. $340^{o}C$, some difficulty was experienced in locating the precise position of the slow combustion/cool flame boundary since the changeover in behaviour, as determined from the kinetic parameters, was extremely indistinct. It was decided arbitrarily, therefore, that a cool flame occurred if the maximum rate of pressure rise exceeded 0.5 torr $sec.^{-1}$.

2.3.6 Product sampling

The reacting mixture was sampled using the automatic product gate with stop-cocks R_2, R_3, R_4 and R_{10} closed and R_5, R_6, R_7, R_8 and R_9 open. The product gate was activated at the desired sampling time for about 150 milliseconds so that a fraction of the reaction mixture was rapidly withdrawn into the evacuated calibration vessel and product sample trap.

Figure 2.9

A typical temperature/pressure-time recording illustrating the measurement of kinetic parameters



The pressure of the withdrawn sample and the temperature of the reaction line were recorded and stop-cocks R_5 and R_6 were closed. The sample trap was then removed from the reaction section and transferred to the chromatographic equipment. The calibration vessel was used in conjunction with the sample trap in order to withdraw a relatively large fraction of the reacting mixture, ca. a sixth, in as short a time as possible, so that the precise point in the reaction at which the products were sampled and analysed is known accurately. For some analytical experiments, part of the withdrawn sample was stored in the calibration vessel to enable separate product determinations to be made on the same sample.

2.4 Gas-chromatographic analysis of reaction products and reactants

2.4.1 The gas chromatograph

A Perkin-Elmer F11 gas chromatograph was used throughout the analytical investigations. This instrument incorporated dual flame ionisation detectors (F.I.D.) and therefore enabled dissimilar columns (one specifically for hydrocarbon determinations, another for oxygenate determinations), to be used for the analysis of product mixtures. A schematic diagram of the complete chromatographic system is shown in figure 2.10.

The output signal from the detector in use at a given time was led to an ionisation amplifier and subsequently recorded on a Honeywell chart recorder. Calculations of peak areas from the chromatograms obtained were performed using the triangulation method.

2.4.2 Preparation of columns

The column packing materials were obtained from Phase Separation Limited. The columns were constructed of $\frac{1}{8}$ inch internal diameter stainless steel tubing which, prior to use, was thoroughly cleaned with concentrated nitric acid, distilled water, acetone and finally the solvent appropriate to the packing material. The tubes were filled using a vibration technique so that the column material packed under the action of gravity. Metal sinters were used to close the ends of the columns and all gas joints were made using stainless steel Swagelok couplings. The columns were finally conditioned in situ at their operating temperatures by passing carrier gas through them for 48 hours.

2.4.3 Column conditions

The column conditions and specifications are shown in Table 2.1.

Figure 2.10

A schematic diagram of the gas chromatographic system

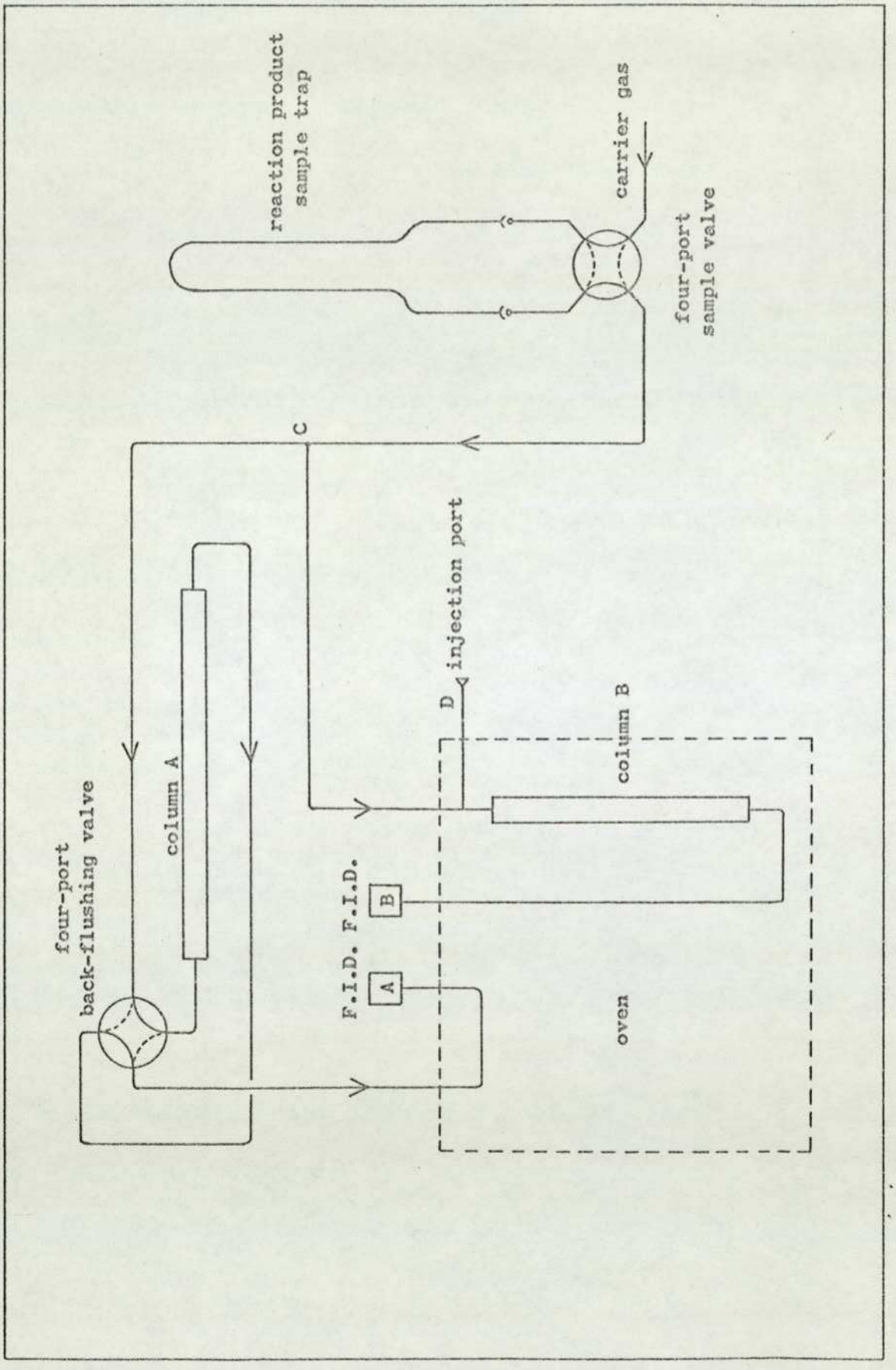


Table 2.1

Conditions and specifications of the columns

	Column A	Column B
Stationary phase	bis-methoxy ethyl adipate + di-ethyl n-hexyl sebacate	MS 550 silicone oil + polyethylene glycol 400
Loading	13.5% and 6.5% respectively	17.5% and 2.5% respectively
Support	Chromsorb P (80-100 mesh)	Chromosorb W
Solvent	acetone	methanol
Column length	10 m	6 m
Operating temperature	ambient	50°C
Flow rate	15 ml $min.^{-1}$	13 ml $min.^{-1}$
Pressure drop across column	40 p.s.i.a.	25 p.s.i.a.
Carrier gas	nitrogen	nitrogen
Detector	F.I.D.	F.I.D.
Detector supplies		
Air	20 p.s.i.a.	25 p.s.i.a.
Hydrogen	17 p.s.i.a.	17 p.s.i.a.

These conditions were found to give satisfactory separation with minimum elution times. The total analysis time for hydrocarbons using column A was 50 minutes whilst that for oxygenates using column B was 75 minutes.

2.4.4 Sample introduction

The reaction product sample trap was attached to the chromatograph at the four-port sample valve by means of greaseless cup and ball joints with spring clips to hold the trap in position. Manipulation of the sample valve caused the flow of carrier gas to the chromatograph to be diverted through the sample trap thus 'sweeping' the sample onto the columns as a plug. The sample was split in a fixed ratio of ca. 2:3 between columns A and B respectively at point C (see figure 2.10). All gas lines, with the exception of the detector and carrier gas supply lines, were wrapped with heating cord and maintained at ca. 80°C to prevent condensation of reaction products.

Liquid samples could only be introduced to column B (oxygenate column) at the injection port D shown in figure 2.10.

2.4.5 Identification and calibration of products

The reaction products were identified by comparison of retention times of standard components with those of the peaks in the chromatograms. In the case of oxygenates the identification was performed on two different columns for additional confirmation. Previous studies of the oxidation of n-butane [38] provided useful information with which the identifications were compared.

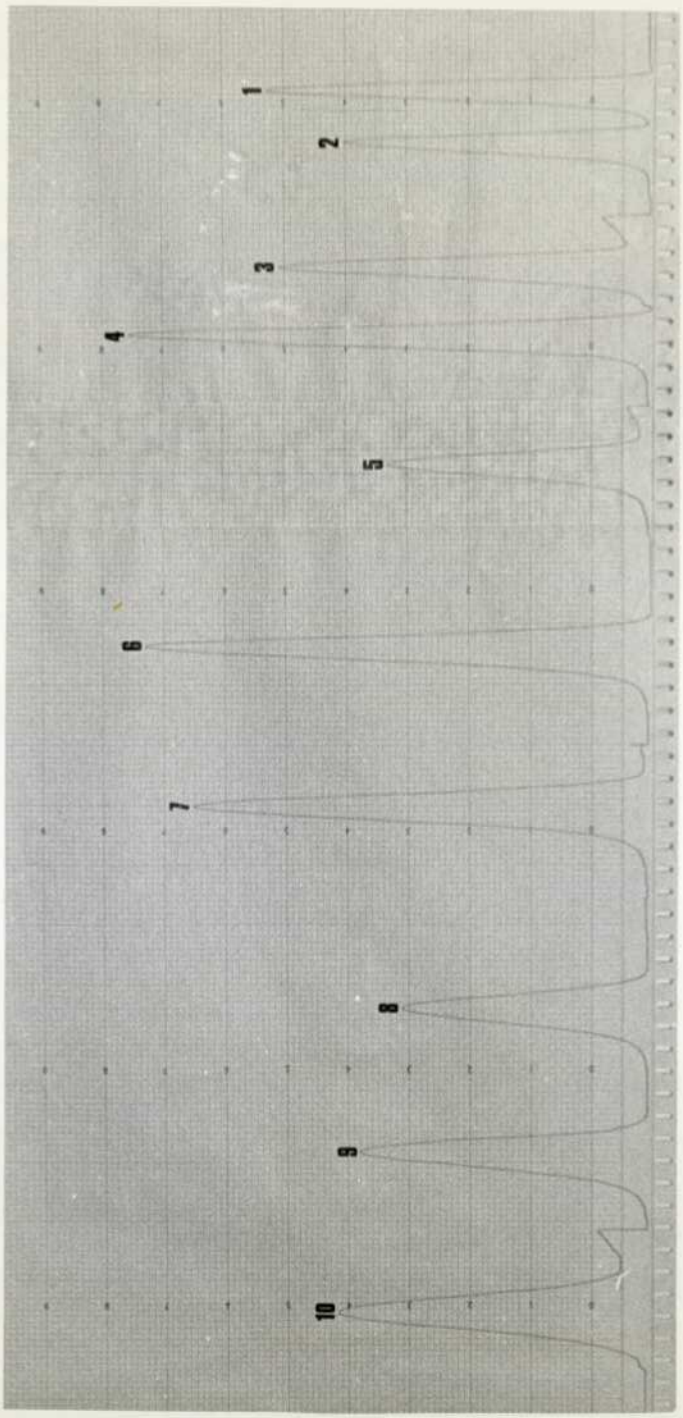
The hydrocarbon and oxygenate chromatograms obtained using columns A and B are shown in Plates 1 and 2 respectively.

Key to Plate 1

Column A

Peak	Compound
1	methane
2	ethylene
3	propane
4	propene
5	isobutane
6	n-butane
7	but-1-ene
8	but-2-ene (trans)
9	but-2-ene (cis)
10	buta-1,3-diene

Plate 1

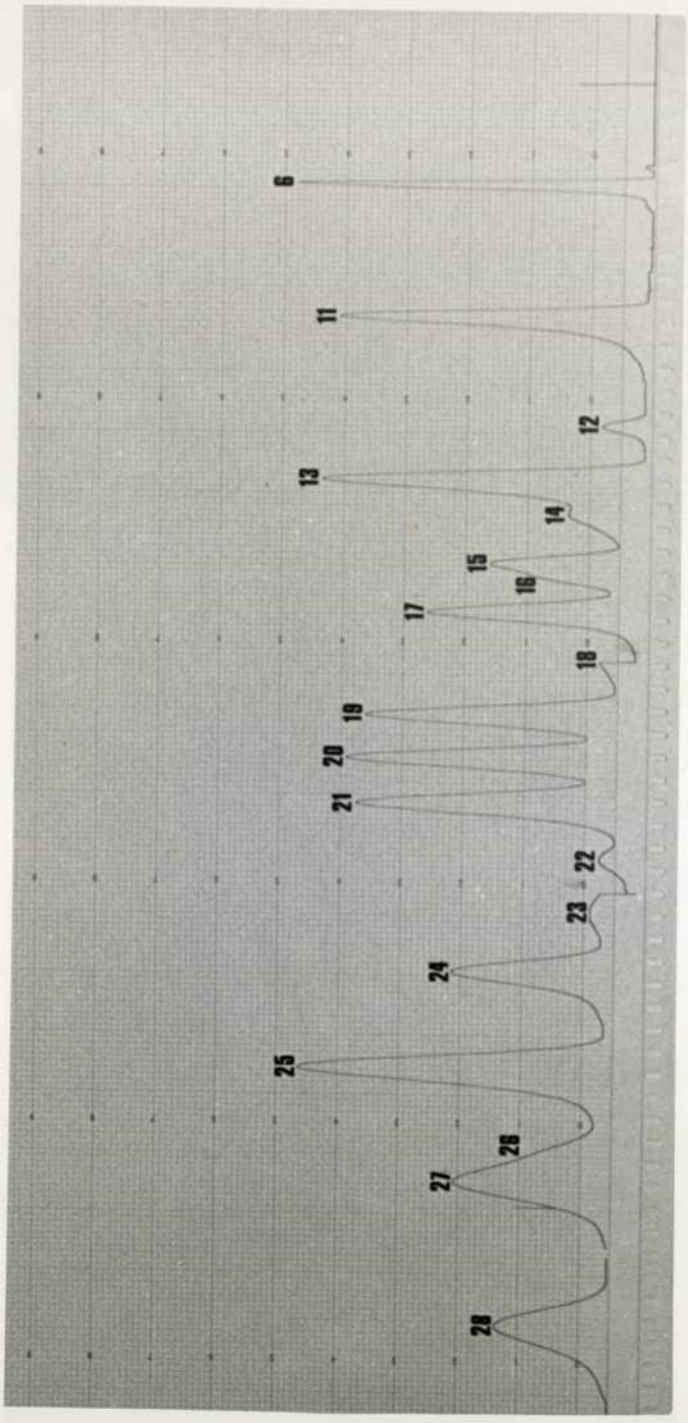


Key to Plate 2

Column B

Peak	Compound
6	n-butane
11	acetaldehyde
12	2-methyloxiran
13	methanol
14	propionaldehyde
15	2,3-dimethyloxiran (trans)
16	acrolein
17	acetone
18	unknown
19	2,3-dimethyloxiran (cis)
20	2-ethyloxiran
21	2-methyloxetan
22	unknown
23	n-butyraldehyde
24	tetrahydrofuran
25	methyl ethyl ketone
26	unknown
27	methyl vinyl ketone
28	unknown

Plate 2



Twenty eight compounds were found in samples of the product mixture and twenty four of these were positively identified. The sensitivities of the detectors to these compounds together with their respective retention times are shown in Tables 2.2 and 2.3.

The response of detector A to pure samples of hydrocarbons was determined by measuring the peak areas corresponding to known amounts of hydrocarbon introduced from the sample trap. The response of detector B to oxygenates was determined in a similar manner except that varying amounts of oxygenates were introduced onto the column through the septum injection port using a 0-10 microlitre Hamilton syringe. All oxygenate samples were obtained commercially except for 2-methyloxetan which was prepared using the method of Schmoyer and Case[94].

Since flame ionisation detectors were used throughout the analytical investigations, compounds such as water, hydrogen peroxide and carbon oxides were not detected. Furthermore, no determination of acids was performed, since the retention times of such compounds were prohibitively long. Formaldehyde was also not determined.

2.4.6 Operating procedure

The determination of hydrocarbons was achieved using column A and F.I.D. A with the appropriate detector supply conditions (as shown in Table 2.1). The sample was introduced onto the column as described in section 2.4.4 with the recorder chart speed set at 1 inch $min.^{-1}$. After the last hydrocarbon peak was eluted (ca. 25 minutes) the four-port back-flushing valve was manipulated so that the flow of carrier gas through column A was reversed. The back-flushing operation was carried out for 25 minutes and finally the valve was returned to its original position in readiness for the next determination.

The determination of oxygenates in the reaction mixture sample was achieved using column B and F.I.D. B with the relevant detector supply conditions. The sample was introduced in the manner previously described with the recorder chart speed set at 0.25 inch $min.^{-1}$. In this case no back-flushing procedure was necessary.

Table 2.2

Hydrocarbon calibrations

Compound	Retention time (minutes)	Relative sensitivity
methane	4.7	0.20
ethylene	5.5	0.47
propane	7.5	0.68
propene	8.7	0.70
isobutane	10.7	0.92
n-butane	13.8	1.00
but-1-ene	16.5	0.96
but-2-ene (t)	20.0	0.96
but-2-ene (c)	22.6	0.86
buta-1,3-diene	24.5	0.95

5.425×10^{-5} moles of n-butane ≡
peak area of 100 cm^2 (range 1×10^4)

Table 2.3

Oxygenate calibrations

Compound	Retention time (minutes)	Relative sensitivity
n-butane	6.2	-
acetaldehyde	14.3	0.56
2-methyloxiran	21.4	1.14
methanol	24.6	0.33
propionaldehyde	26.9	0.67
2,3-dimethyloxiran (t)	29.9	1.81
acrolein	30.7	0.72
acetone	32.6	1.00
unknown	34.8	-
2,3-dimethyloxiran (c)	38.6	1.21
2-ethyloxiran	42.0	1.71
2-methyloxetan	44.9	1.67
unknown	48.2	-
n-butyraldehyde	51.8	0.59
tetrahydrofuran	55.6	1.62
methyl ethyl ketone	61.7	1.45
unknown	66.6	-
methyl vinyl ketone	68.8	1.13
unknown	69.8	-

6.250×10^{-5} moles of acetone $\equiv$
peak area of 100 cm^2 (range 1×10^4)

SECTION 3

RESULTS

SECTION 3

		Page No.
3.1	The kinetic results	108
3.1.1	System I	108
3.1.1.1	The temperature-pressure ignition diagram	108
3.1.1.2	The induction period of the first cool flame	114
3.1.1.3	The pressure rise accompanying the first cool flame	118
3.1.1.4	The maximum rate of pressure rise accompanying the first cool flame	122
3.1.1.5	The induction period of the second cool flame	127
3.1.1.6	The pressure rise accompanying the second cool flame	127
3.1.1.7	The maximum rate of pressure rise accompanying the second cool flame	127
3.1.1.8	The induction period of the third cool flame	135
3.1.1.9	The pressure rise accompanying the third cool flame	135
3.1.1.10	The maximum rate of pressure rise accompanying the third cool flame	135
3.1.1.11	Transition to two-stage ignition	141
3.1.2	System II	144
3.1.2.1	The temperature-pressure ignition diagram	144
3.1.2.2	The temperature rise accompanying the first cool flame	149
3.1.2.3	The maximum rate of temperature rise accompanying the first cool flame	153
3.2	The analytical results	159
3.2.1	The variation of product distribution with time in the cool flame region	159
3.2.2	Product distribution during the early stages of reaction	188
3.2.2.1	The variation with respect to initial temperature	188
3.2.2.2	The variation with respect to initial pressure	195

Glossary

p_o	initial pressure
T_o	initial temperature
τ_n	induction period of the nth cool flame
Δp_n	pressure rise accompanying the nth cool flame
$\Delta p_{n\infty}$	overall increase in pressure immediately after the passage of the nth cool flame
$(dp_n/dt)_{max}$	maximum rate of pressure rise accompanying the nth cool flame
τ_s	induction period of the shoulder on the first cool flame
Δp_s	pressure rise accompanying the shoulder pulse
ΔT_1	temperature rise accompanying the first cool flame
$(dT_1/dt)_{max}$	maximum rate of temperature rise accompanying the first cool flame

3.1 The kinetic results

The kinetic investigations were carried out in two parts. In the first part, the combustion phenomena which occurred in the temperature range 280-420°C at initial reactant pressures of between 45 and 250 torr, were studied by following the associated pressure changes and the cool flame region was established for a spherical reaction vessel which was free from surface deposits of carbon. In the second part, a study was made of both the temperature and pressure changes which accompanied these phenomena for the same range of initial conditions. In this case the cool flame region was re-established for a reaction vessel which was not strictly spherical (as shown in figure 2.6) but was again free from carbon deposits. For convenience these two sections of work are subsequently referred to as System I and System II respectively. Some slight differences in behaviour were observed between the two systems and these are discussed in section 3.1.2.1.

3.1.1 System I

3.1.1.1 The temperature-pressure ignition diagram

Figures 3.1 and 3.2 show typical examples of the pressure-time recordings of combustion phenomena used to construct a detailed temperature-pressure ignition diagram, shown in figure 3.3. It can be seen from this diagram that the cool flame region is divided into two distinct parts. At low initial temperatures, between 285-345°C, a region of multiple cool flames exists within which up to seven consecutive cool flames are observed, whereas at higher temperatures, between 345-420°C, a single cool flame is followed by rapid slow combustion. The change in behaviour, as the cool flame region is traversed from low to high temperatures at constant pressure, is shown in figures 3.1(a) - 3.1(i).

At low temperatures, cool flames are intense and clearly resolved from each other (figures 3.1(a) and 3.1(b)). Furthermore, the overall rise in pressure after the propagation of a cool flame ($\Delta p_{c.f.\infty}$) is small in comparison with the transient pressure rise ($\Delta p_{c.f.}$) that attends the passage of the cool flame. However, as the temperature is increased, $\Delta p_{c.f.\infty}$ increases whilst at the same time $\Delta p_{c.f.}$ decreases. The multiple cool flames following the first cool flame also become progressively weaker and less clearly resolved although, as shown in figures 3.1(c), 3.1(d) and 3.1(e), their precise behaviour varies in a complex manner (see sections 3.1.1.5 - 3.1.1.10). At temperatures close to the upper limit of multiple cool flames, the weak cool flames are superimposed on the slow combustion following the first cool flame, as shown in figure 3.1(f). Pressure-time recordings in the upper single cool flame region, figures 3.1(g), 3.1(h) and 3.1(i), show that this slow combustion becomes considerably more intense as the temperature is raised towards the upper ignition limit. Another interesting feature of these recordings in the cool flame region is the pressure pulse which develops as a shoulder on the first cool flame (figures 3.1(c) - 3.1(h)). This pulse becomes noticeably more pronounced as the initial temperature is increased and develops into the second stage of two-stage ignition above ca.300°C (see section 3.1.1.11).

At initial pressures higher than those at which cool flames propagate, spontaneous ignition is observed. Typical recordings of two-stage ignition at progressively increasing initial temperatures are shown in figures 3.2(a), 3.2(d) and 3.2(e). These recordings illustrate that at low temperatures the hot ignition stage develops during the passage of the cool flame whereas at higher temperatures a discrete ignition delay separates the two stages. This delay increases as the temperature is increased and is of the order of ca.10 seconds at 400°C.

A region of multi-stage ignition is observed in the temperature range 285 - 310°C at initial pressures of between 170 and 230 torr. This region is principally three-stage ignition and a typical recording is shown in figure 3.2(b). Four-stage ignition (figure 3.2(c)) is also observed, although as can be seen in figure 3.3, the two regions in which it occurs are extremely limited and border the spontaneous ignition boundary. Single-stage ignition is not observed under any of the conditions investigated.

The cool flame/two-stage ignition boundary exhibits two lobes. The lower lobe, which occurs at about 285°C, is considerably more pronounced than the upper lobe which occurs at about 360°C. These lobes, however, are not reflected in the slow combustion/cool flame boundary.

Figure 3.1

Pressure-time recordings in the cool flame region

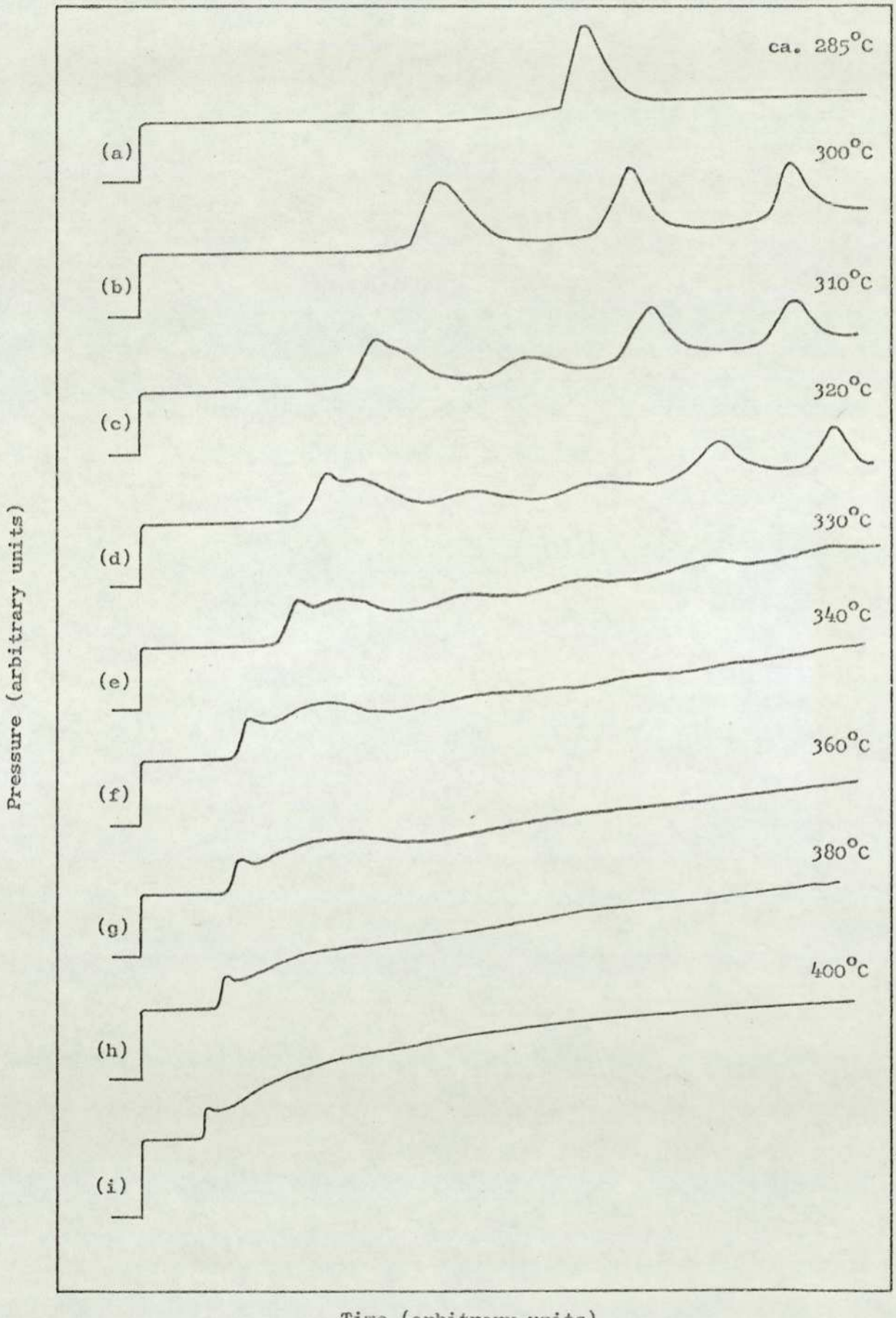


Figure 3.2

Pressure-time recordings of ignition phenomena

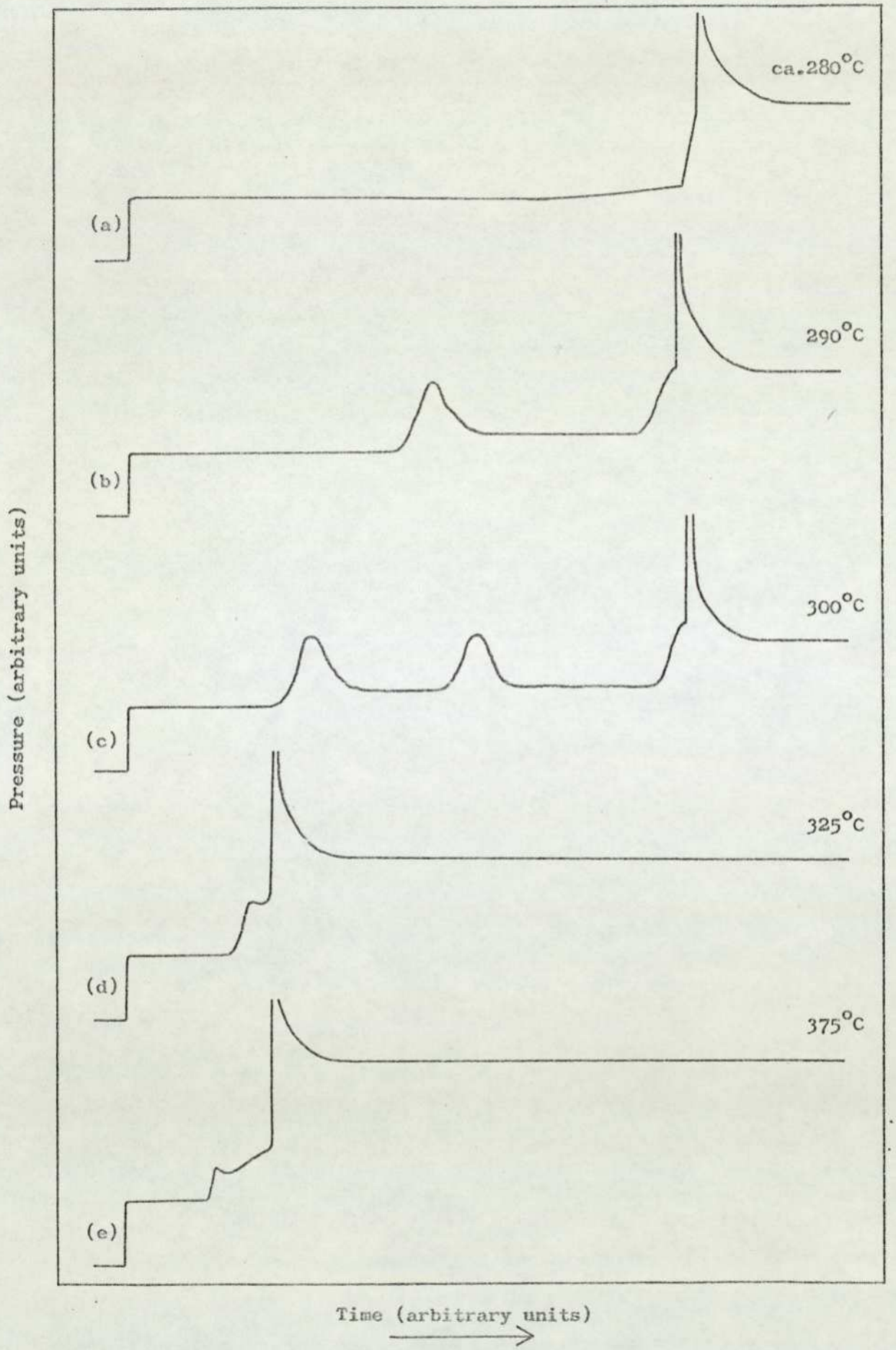
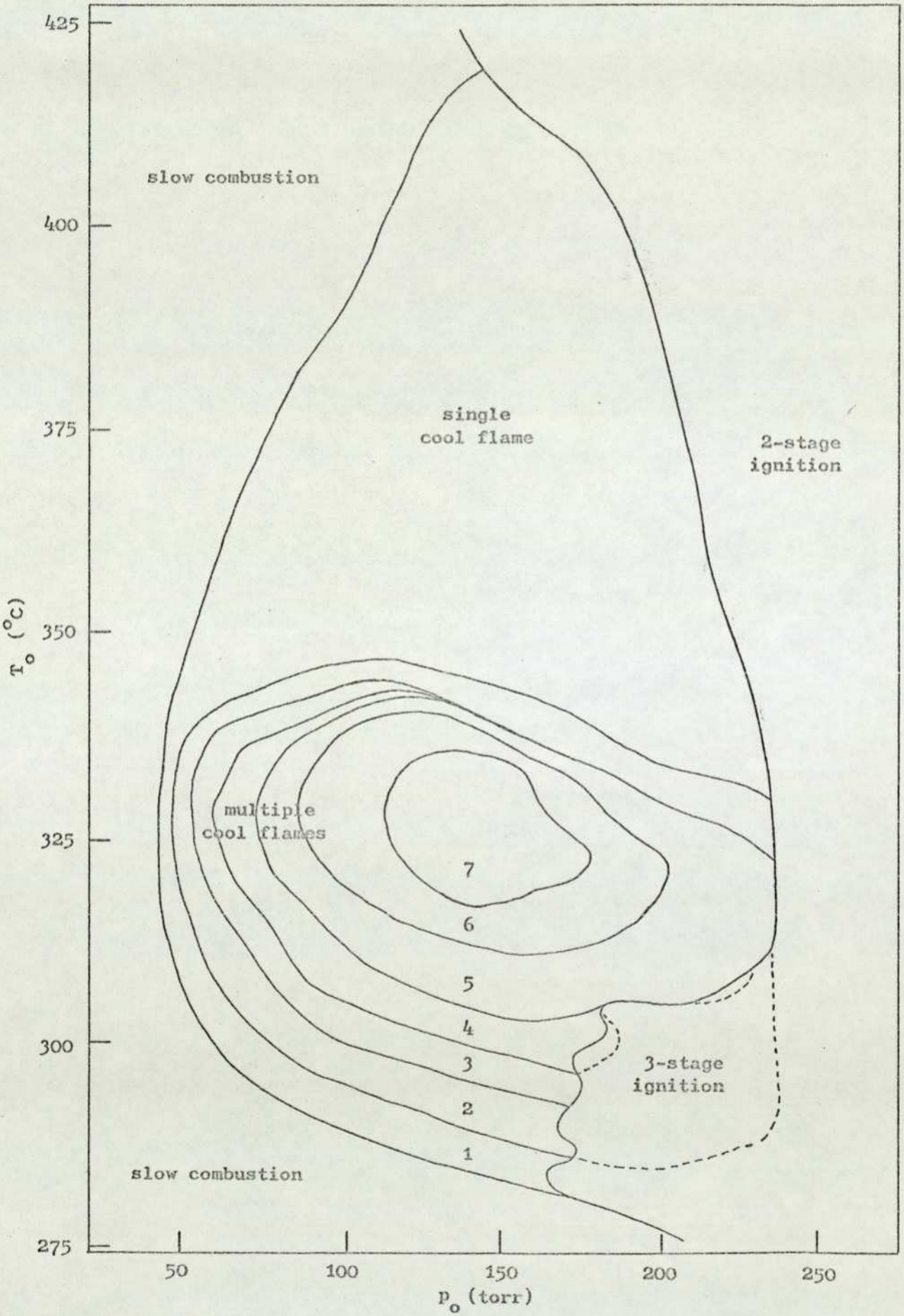


Figure 3.3

The temperature-pressure ignition diagram for n-butane and oxygen mixtures in the molar ratio 1:2



3.1.1.2 The induction period of the first cool flame

The variation of τ_1 with p_o in the multiple cool flame region and the single cool flame region is shown in figures 3.4 and 3.5 respectively. It can be seen that marked differences occur between the two regions. In the multiple cool flame region induction periods vary between minutes and hours whereas in the single cool flame region they are only of the order of seconds. Furthermore, it is clear that the reduction in τ_1 brought about by increasing p_o, becomes much less pronounced as the temperature is increased.

The curves illustrated in figures 3.4 and 3.5 show that at all temperatures investigated, the relationship:

$$\tau_1 = kp_o^{-n} + c$$

where k, c and n are constants at constant temperature, found for other hydrocarbons clearly holds for n-butane also.

Figure 3.6, which shows the variation of τ_1 with T_o at different initial pressures, also highlights the difference between the two regions. The change in behaviour, which is most marked at low initial pressures, is exemplified by the fact that an increase in the initial temperature above 330°C has only a small effect on τ_1, while a corresponding decrease leads to a considerable lengthening of τ_1.

Figure 3.4

The variation of τ_1 with p_o in the multiple cool flame region

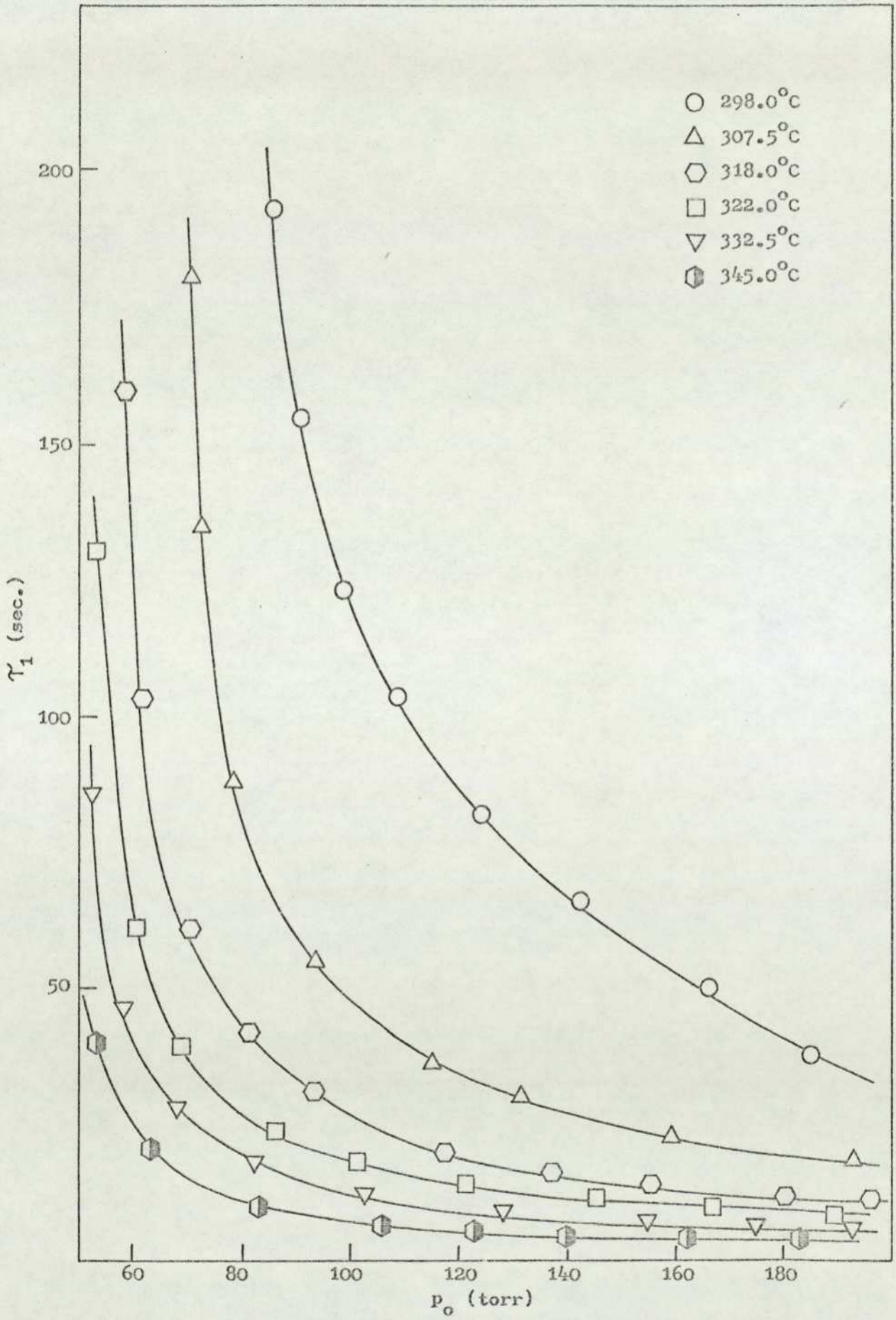


Figure 3.5

The variation of τ_1 with p_o in the single cool flame region

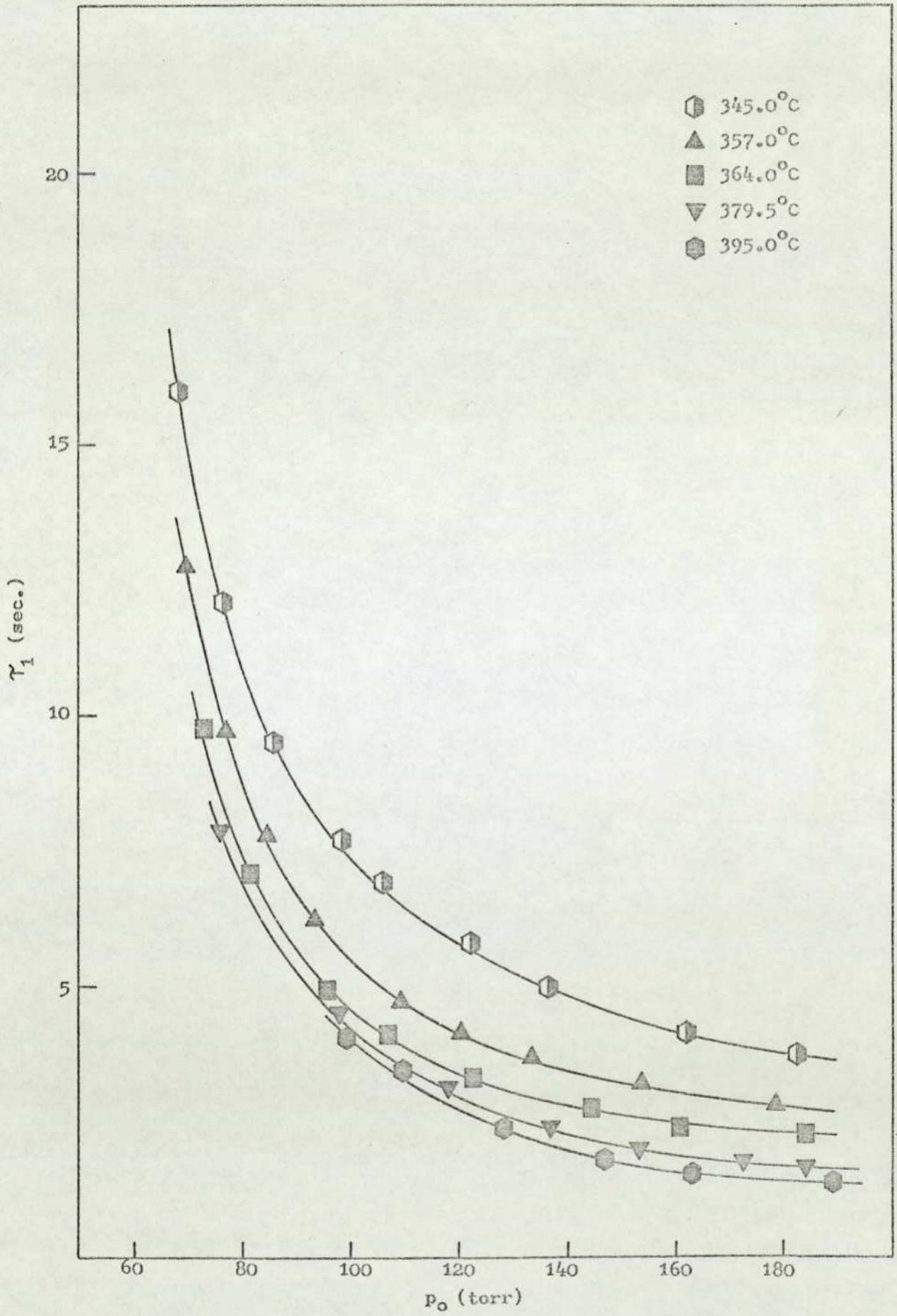
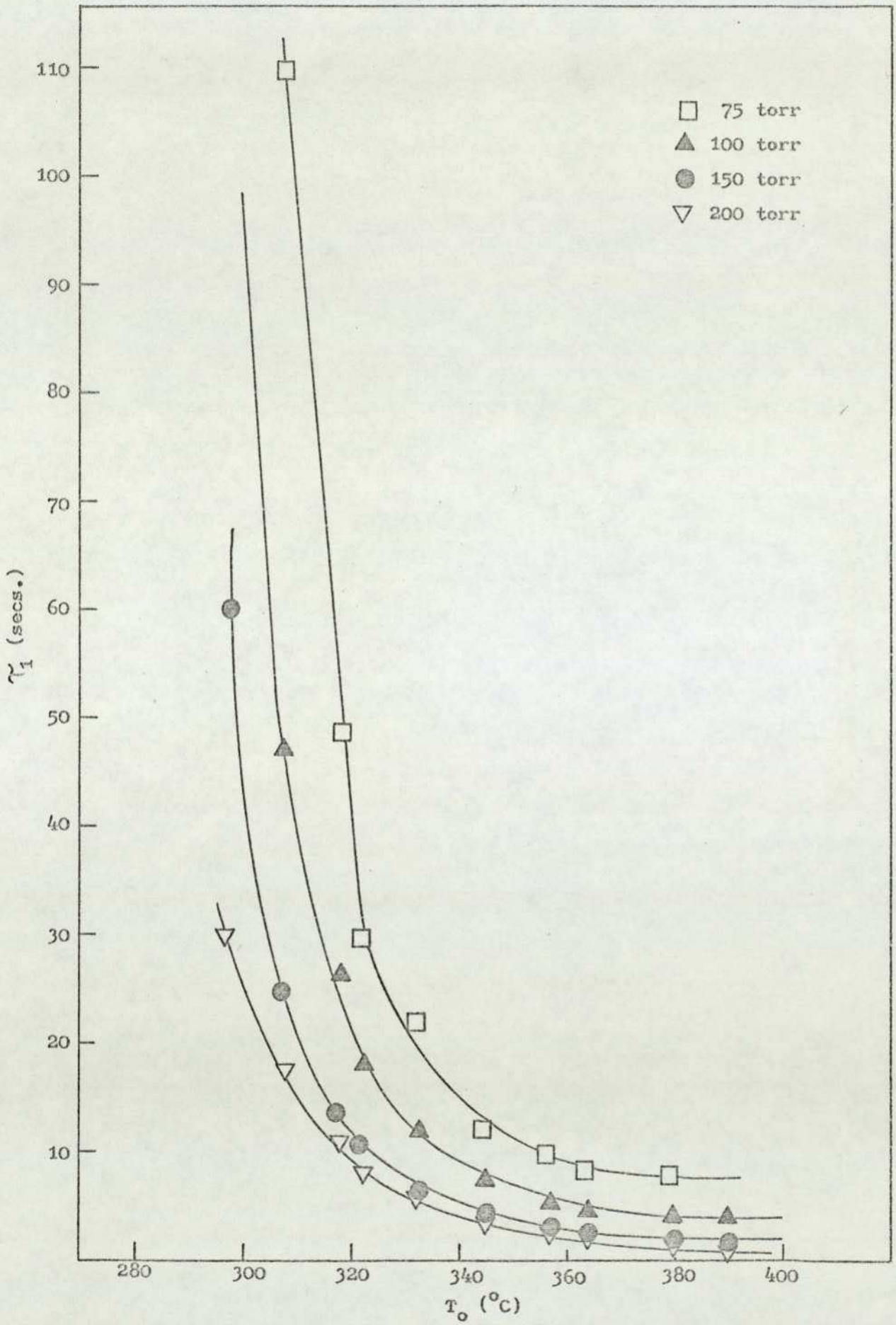


Figure 3.6

The variation of τ_1 with T_o



3.1.1.3 The pressure rise accompanying the first cool flame

The variation of Δp_1 with p_o is shown in figure 3.7 and it is clear that for a particular initial temperature, Δp_1 generally increases as the initial pressure is increased. An interesting feature of figure 3.7, however, is the appearance of a minimum in some of the curves. This occurs at low initial temperatures when the induction periods are comparatively long. During these induction periods, slow combustion occurs which leads to an increase in pressure and this increase is included in the computed values of Δp_1. Figure 3.7 also shows that the relationship between Δp_1 and p_o can be expressed as:

$$\Delta p = a p_o^{\,m}$$

where a and m are constants at constant temperature. Figure 3.8, which illustrates the logarithmic relationship between Δp_1 and p_o, shows that the value of m varies from 1.3 at 297°C to 3.8 at 390°C. Furthermore, it is interesting to note how the lines tend to converge towards a focal point which corresponds to a value of p_o of ca. 240 torr and a value of Δp_1 of ca. 69 torr.

Figure 3.9 shows the effect of temperature on Δp_1 at constant initial pressure. It can be seen that a point of inflection occurs in the curves at ca. 315°C.

Figure 3.7

The variation of Δp_1 with p_o

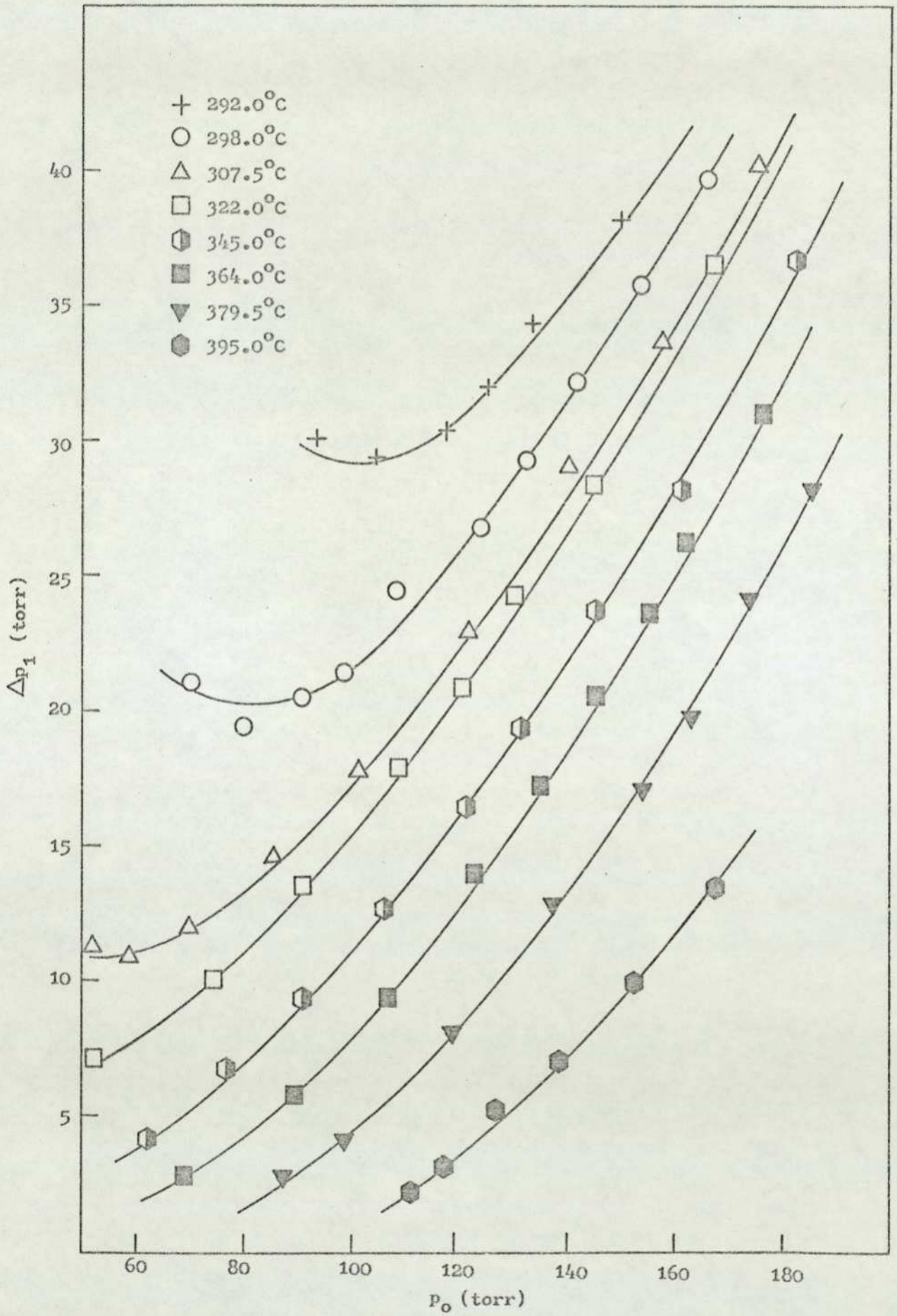


Figure 3.8

The logarithmic relationship of Δp_1 with p_o

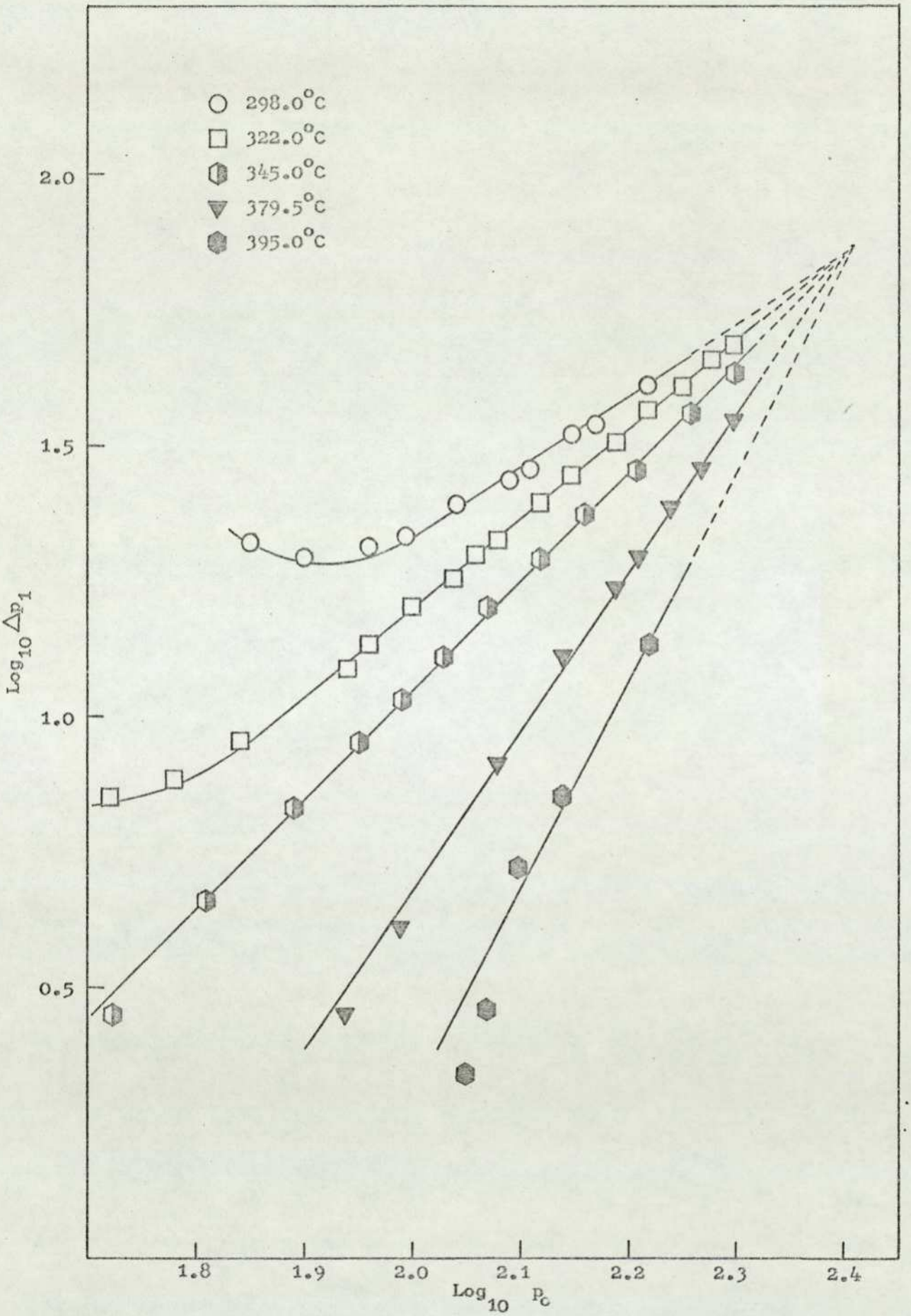
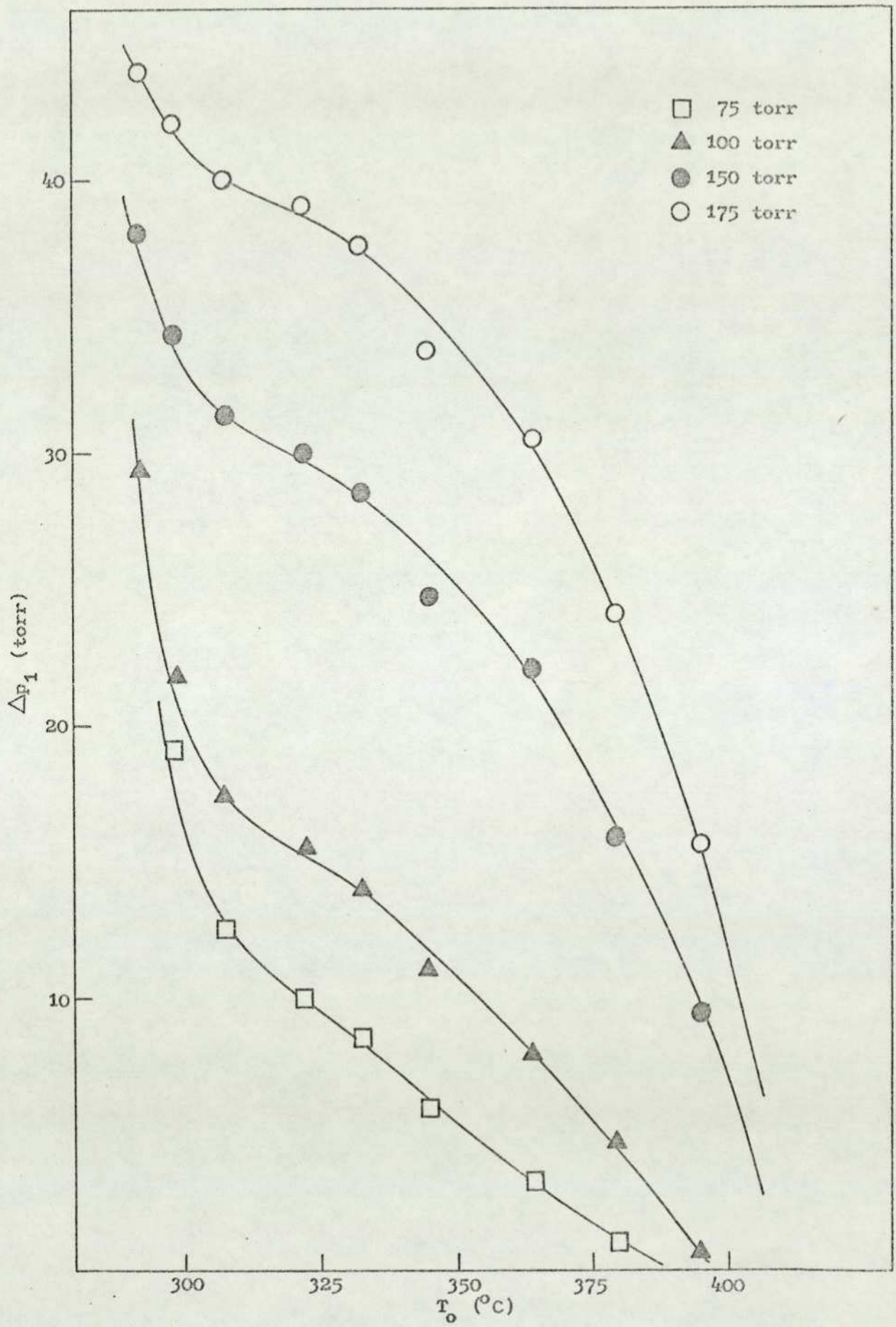


Figure 3.9

The variation of Δp_1 with T_o



3.1.1.4 The maximum rate of pressure rise accompanying the first cool flame

This parameter, which is indicative of the maximum rate of chemical transformation associated with the propagation of a cool flame, varies in a complex manner with the initial conditions. The variation of $(dp_1/dt)_{max}$ with p_o in the multiple cool flame region is shown in figure 3.10 and it is clear that the effect of increasing p_o becomes more pronounced as the initial temperature is increased. A feature of the curves corresponding to low initial temperatures is the point of inflection which occurs at low initial pressures. This reflects the distinct nature of the cool flame boundary at these pressures. Figure 3.11 illustrates the variation of $(dp_1/dt)_{max}$ with p_o in the single cool flame region and shows that $(dp_1/dt)_{max}$ increases smoothly with p_o. This in turn reflects the indistinct nature of the cool flame boundary at high temperatures. Figures 3.10 and 3.11 show that in the cool flame region values of $(dp_1/dt)_{max}$ range from 0.5 torr $sec.^{-1}$ to over 200 torr $sec.^{-1}$.

Two prominent regions of negative temperature coefficient are clearly illustrated in figure 3.12 which shows the relationship between $(dp_1/dt)_{max}$ and T_o at various initial pressures. These regions exist between 285 - 315°C and 360 - 420°C and correspond to the two lobes on the ignition diagram. It is interesting to note that the former is apparent at all initial pressures, whereas the latter is extremely prominent at high initial pressures but virtually non-existent at low initial pressures. Furthermore, the former can be associated with the region in which the first cool flame is followed by intense and clearly resolved multiple cool flames, whereas the latter can be roughly associated with the upper single cool flame region.

The fine structure of the cool flame/two-stage ignition boundary is clearly reflected in the loci of constant $(dp_1/dt)_{max}$ plotted on a temperature-pressure diagram as shown in figure 3.13. It can be seen that the larger the value of $(dp_1/dt)_{max}$, the more clearly the fine structure of the ignition boundary is reflected.

Figure 3.10

The variation of $(dp_1/dt)_{max}$ with p_o in the multiple cool flame region

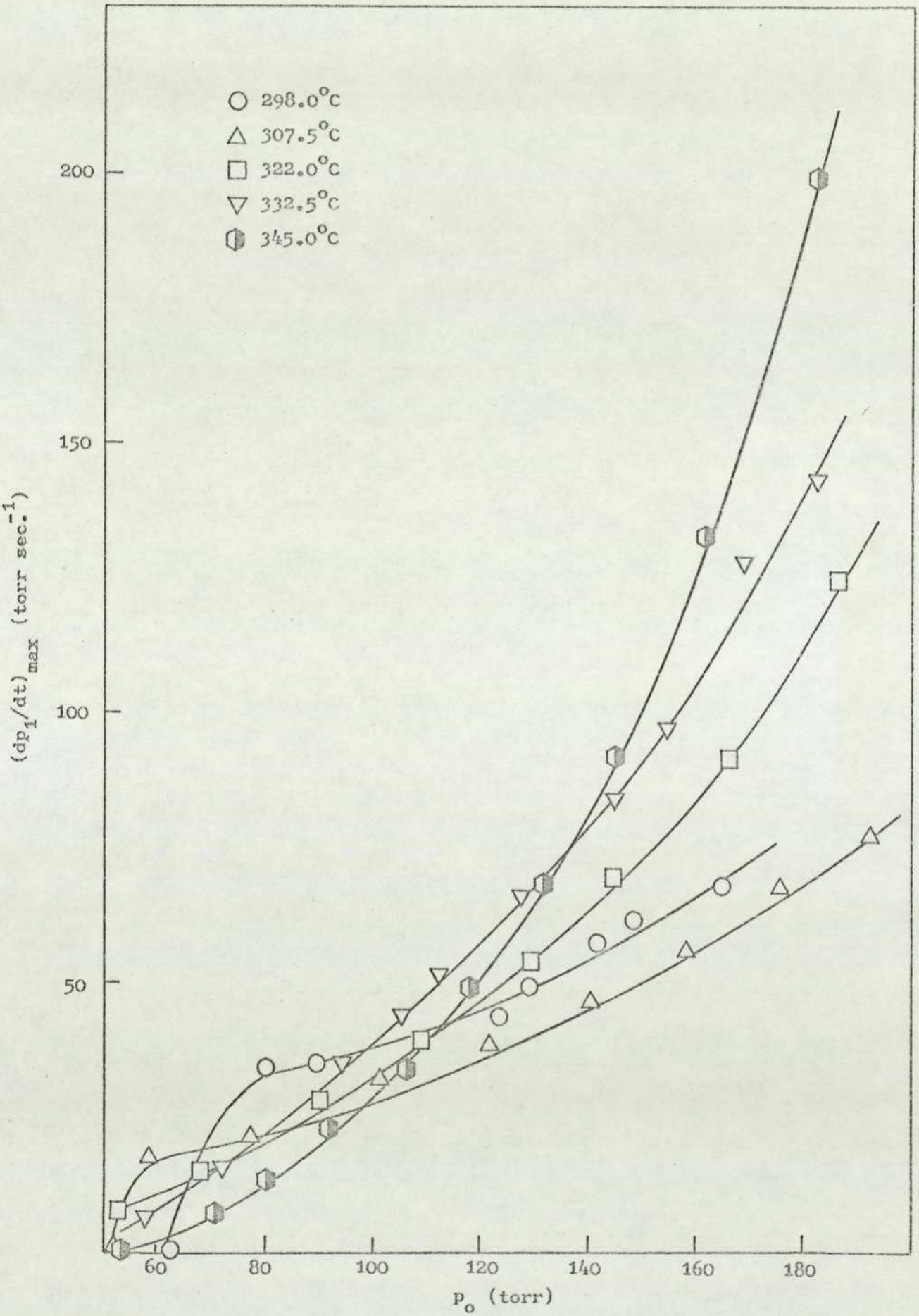


Figure 3.11

The variation of $(dp_1/dt)_{max}$ with p_o in the single cool flame region

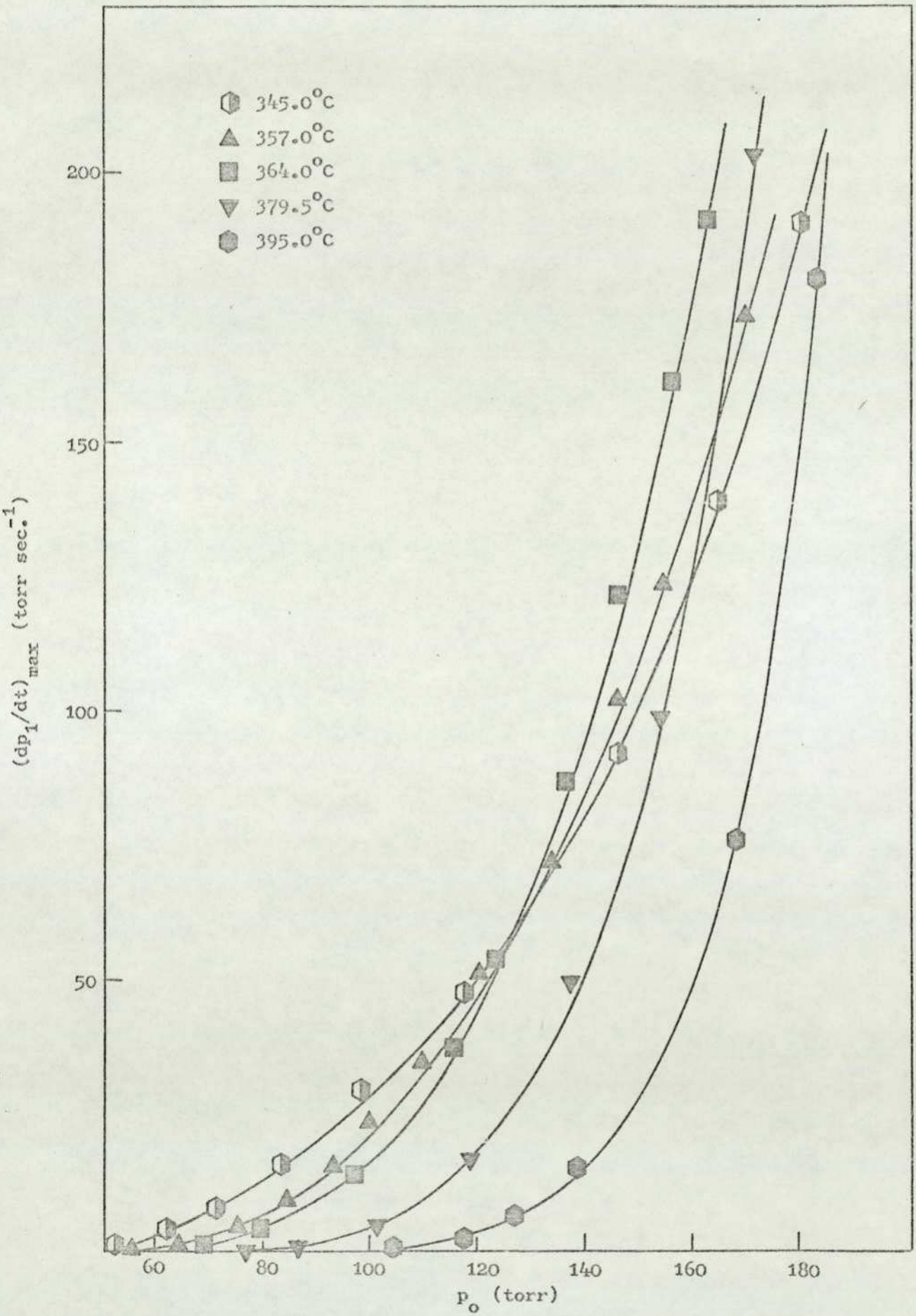


Figure 3.12

The variation of $(dp_1/dt)_{max}$ with T_o

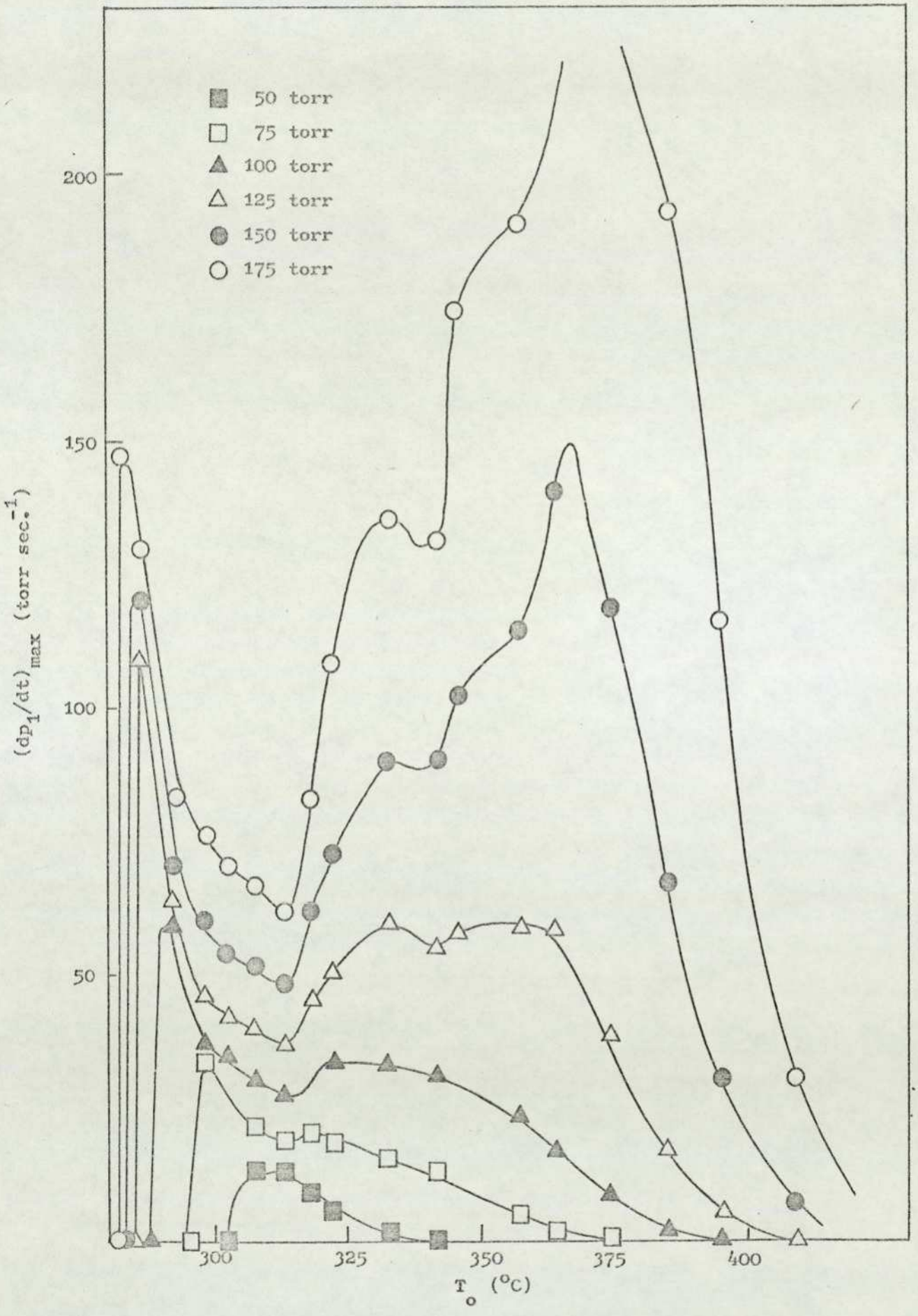
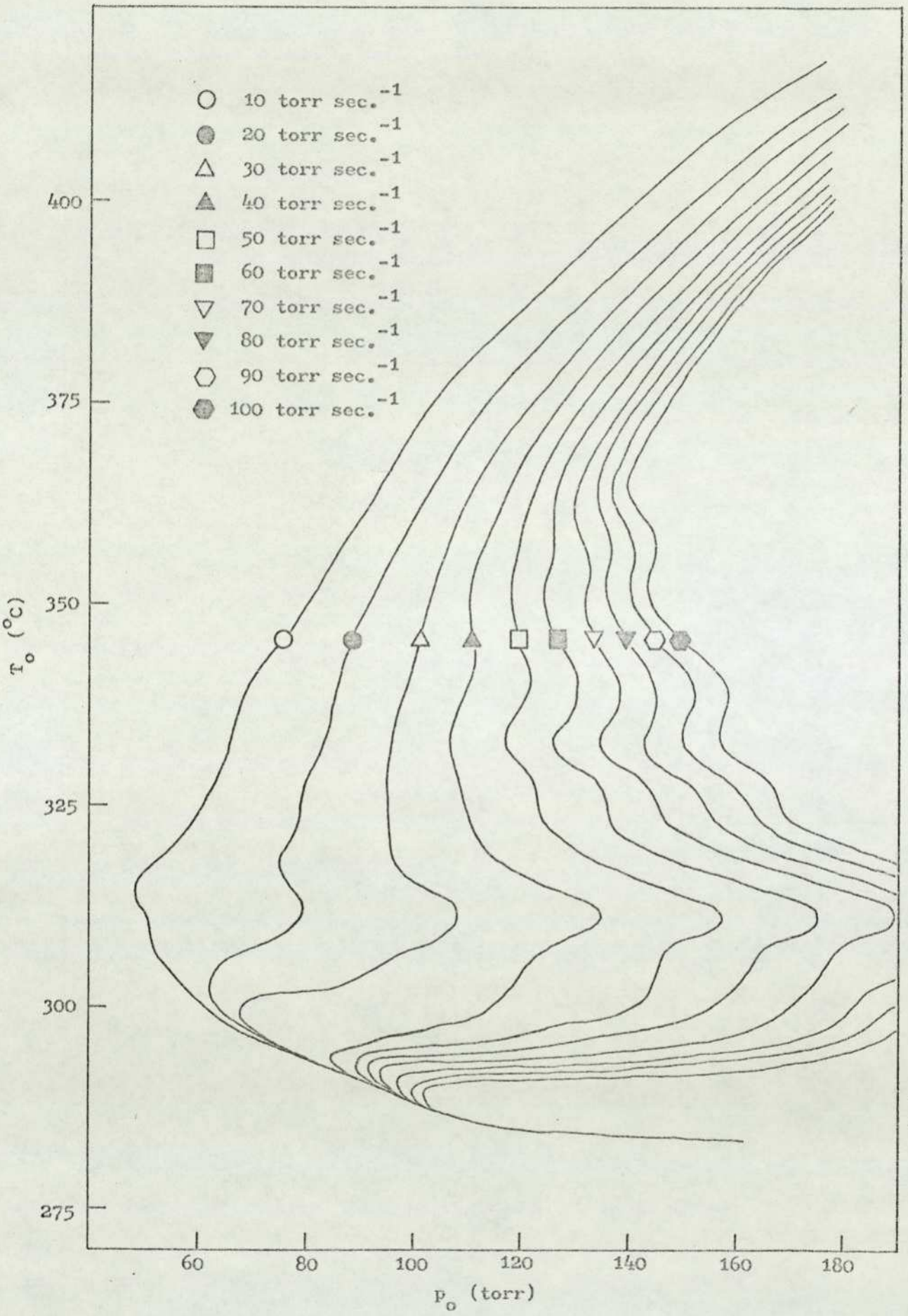


Figure 3.13

Loci of constant $(dp/dt)_{max}$ for the first cool flame



3.1.1.5 The induction period of the second cool flame

The variation of τ_2 with p_o is shown in figure 3.14. It can be seen that at low initial pressures, the relationship between τ_2 and p_o bears a close similarity with that between τ_1 and p_o in that an increase in p_o brings about a decrease in τ_2. However, at initial temperatures greater than 307.5°C further increase in p_o increases τ_2. Furthermore, it is apparent that the minimum in the curves occurs at progressively lower initial pressures as the temperature is increased.

Values of τ_2 throughout the multiple cool flame region are always less than those of the corresponding τ_1 and in contrast with τ_1, τ_2 never exceeds more than ca. 2 minutes at low initial temperatures.

3.1.1.6 The pressure rise accompanying the second cool flame

The variation of Δp_2 with p_o is shown in figure 3.15 and is remarkable for several reasons. It can be seen that above a limiting temperature, the curves exhibit one or more turning points which become less pronounced as the initial temperature is increased further. Another interesting feature of these curves is that at low temperatures, for example at 298°C, the value of Δp_2 actually exceeds that of Δp_1 at all initial pressures.

3.1.1.7 The maximum rate of pressure rise accompanying the second cool flame

The behaviour of $(dp_2/dt)_{max}$ as the initial pressure is increased is similar to that of Δp_2 in that above a limiting initial temperature, turning points occur in the curves shown in figure 3.16. Again it is clear that the pressure at which the maximum occurs decreases and the turning points become less pronounced as the temperature is raised. Furthermore, at low initial temperatures the value of $(dp_2/dt)_{max}$ exceeds that of $(dp_1/dt)_{max}$ at all initial pressures.

It is interesting to note the marked points of inflection in the curves at low initial pressures and their occurrence reflects the distinct nature of the lower two cool flame limit. This is also apparent in figure 3.17 which shows the variation of $(dp_2/dt)_{max}$ with T_o for various initial pressures. These curves show that for the second cool flame the whole multiple cool flame region can be considered as a region of negative temperature coefficient. Figure 3.18(a) shows that the lower lobe in the cool flame/two-stage ignition boundary is also reflected in the loci of constant $(dp_2/dt)_{max}$.

The variation with T_o of the limiting initial pressures, at which the relationships between p_o and τ_2, Δp_2 and $(dp_2/dt)_{max}$ exhibit turning points, is shown in figure 3.19. It can be seen that these curves diagonally bisect the two cool flame region and that in general $(dp_2/dt)_{max}$ is the first parameter to suffer a decline as the initial pressure is increased.

Figure 3.14

The variation of τ_2 with p_o

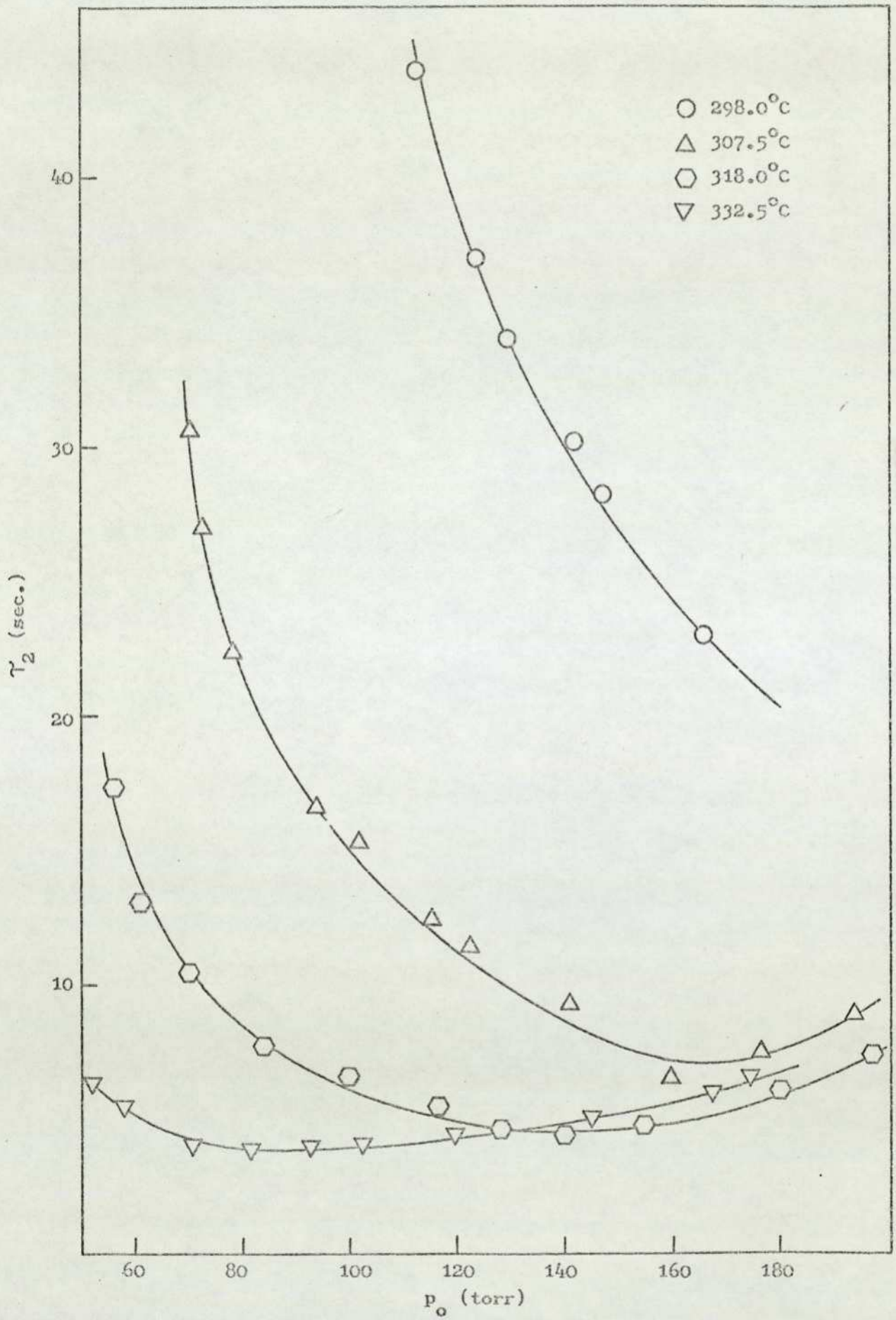


Figure 3.15

The variation of Δp_2 with p_o

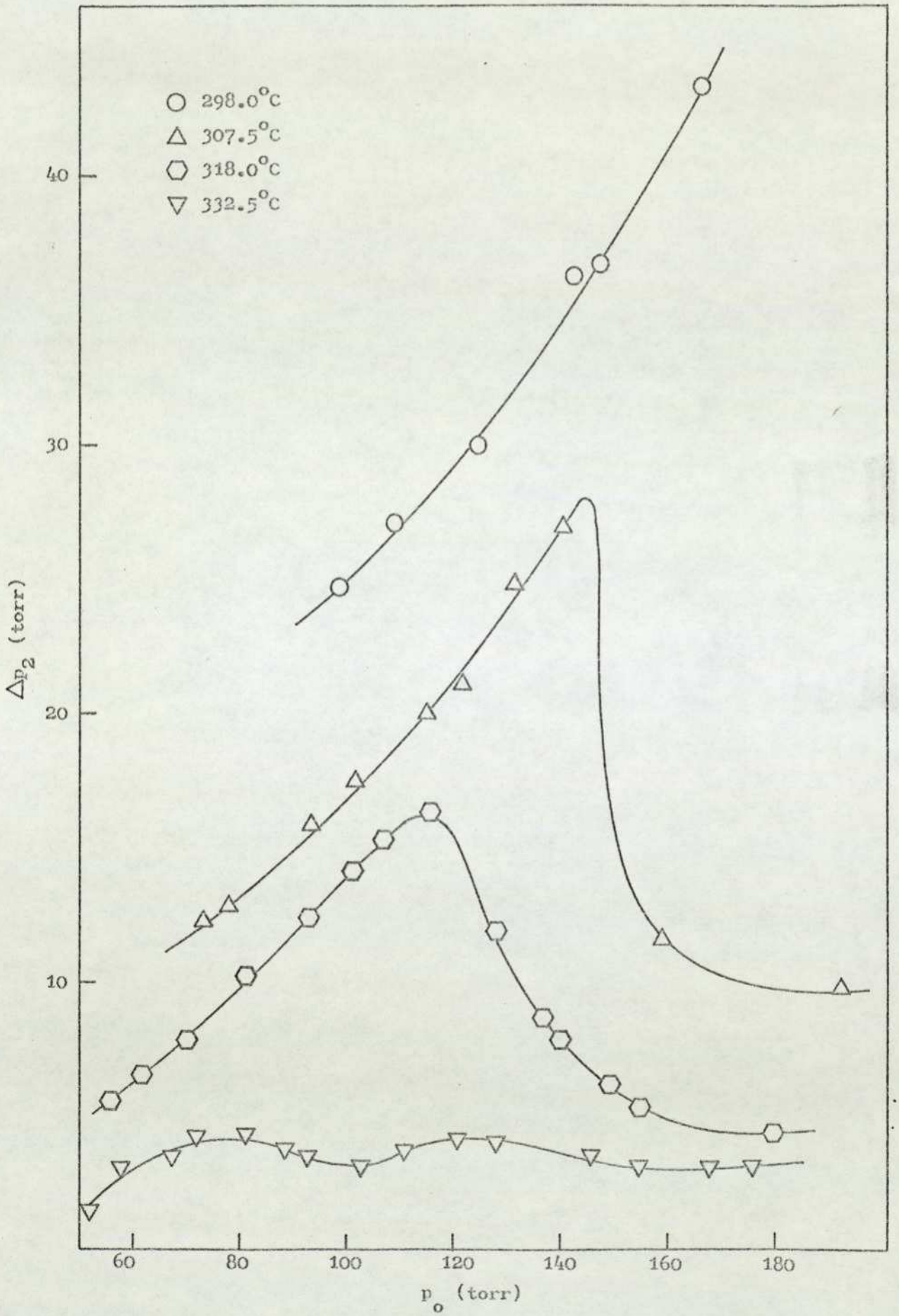


Figure 3.16

The variation of $(dp_2/dt)_{max}$ with p_o

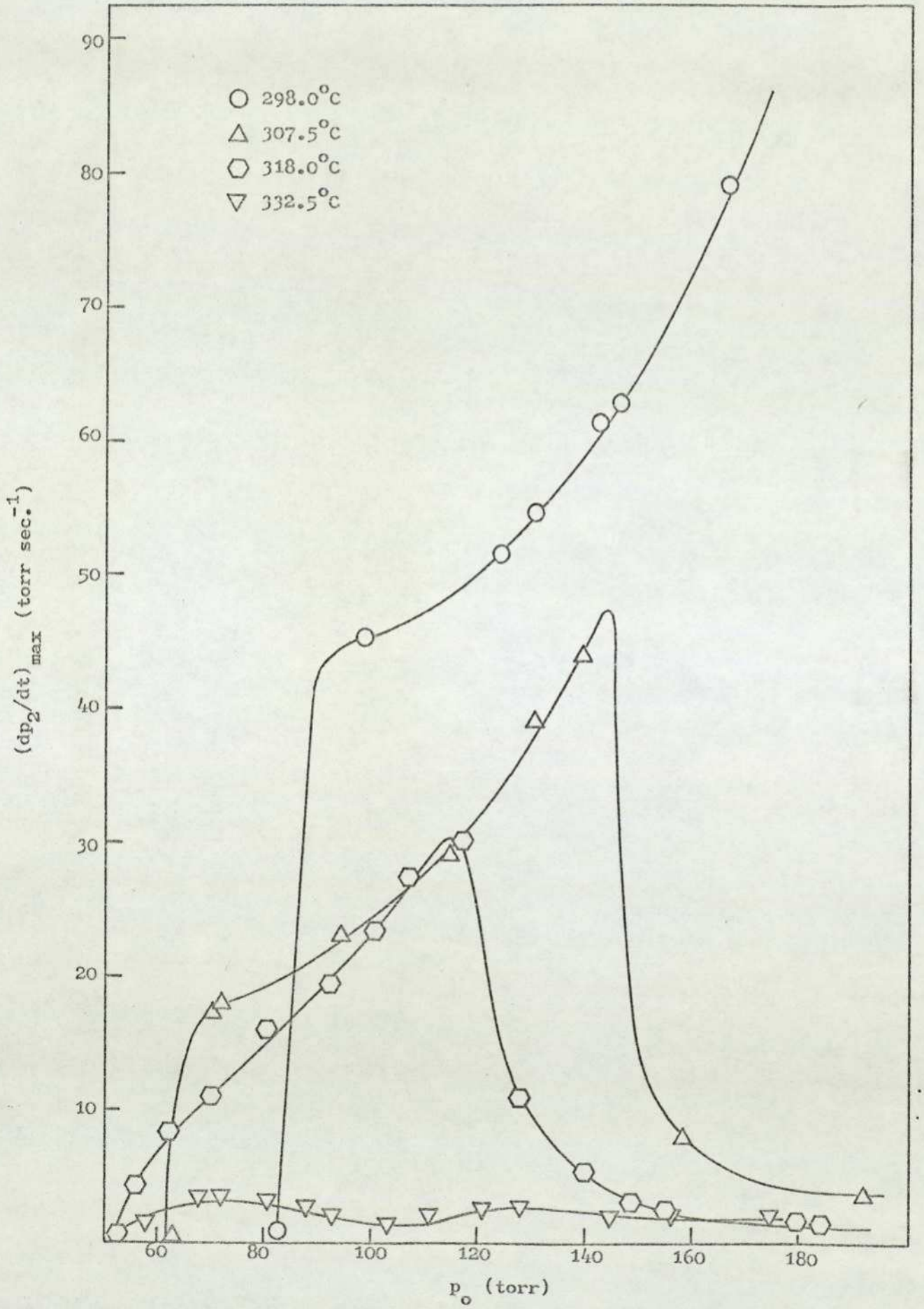


Figure 3.17

The variation of $(dp_2/dt)_{max}$ with T_o

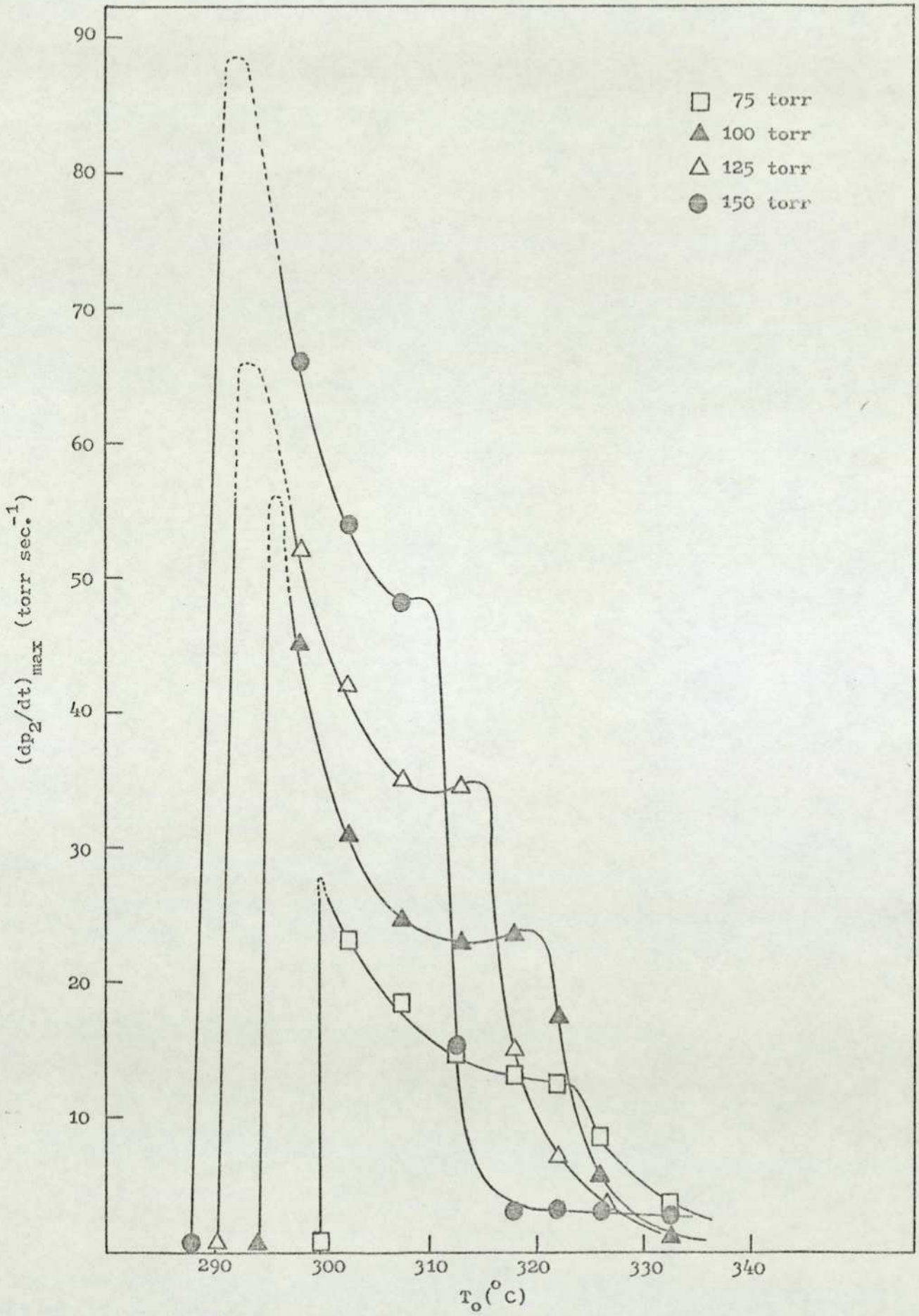


Figure 3.18

Loci of constant $(dp/dt)_{max}$ for
(a) the second cool flame and (b) the third cool flame

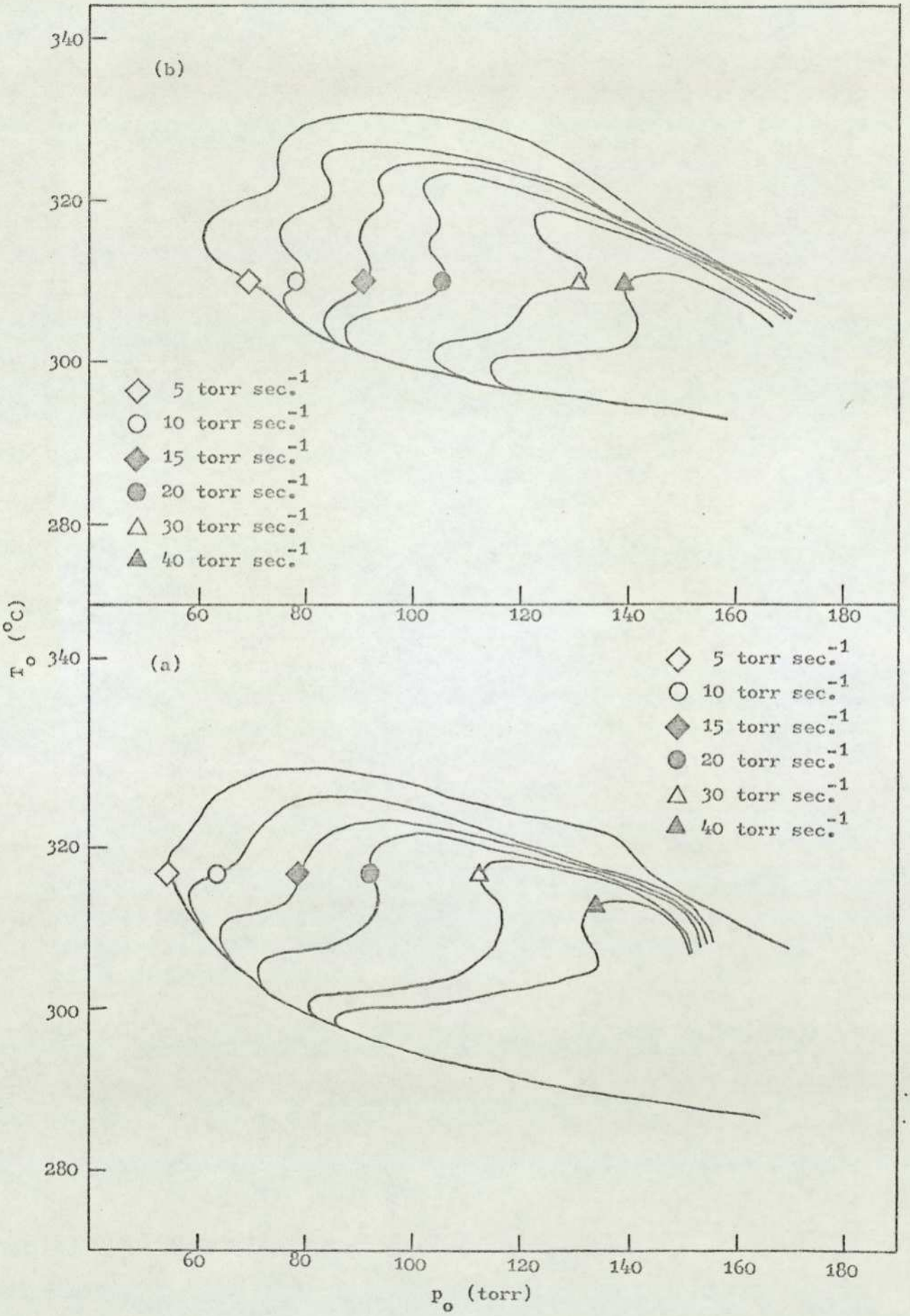
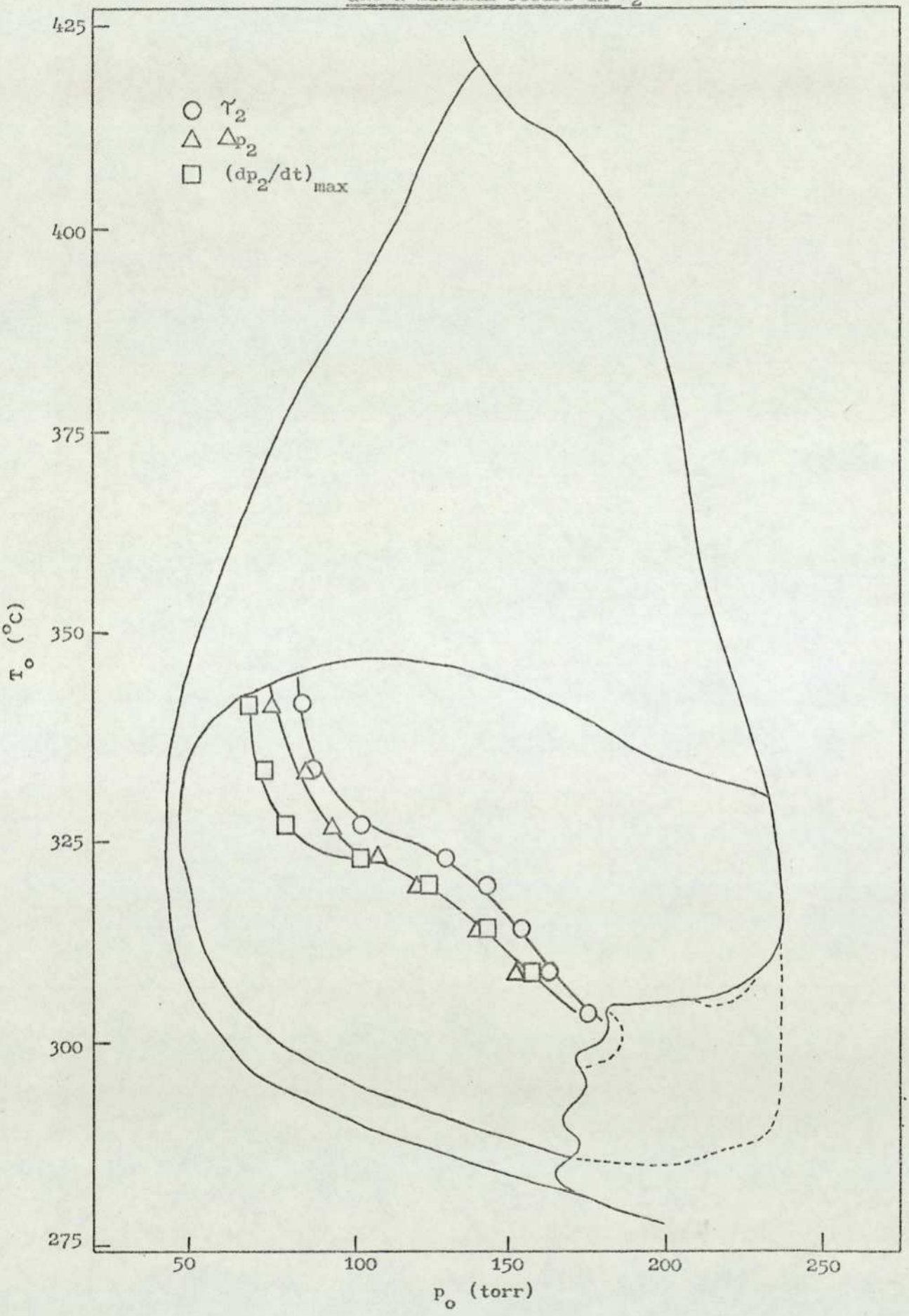


Figure 3.19

The variation with T_o of the initial pressure at which maxima occur in Δp_2 and $(dp_2/dt)_{max}$ and a minimum occurs in τ_2



3.1.1.8 The induction period of the third cool flame

The variation of τ_3 with p_o, as shown in figure 3.20, exhibits a similar behaviour to that of τ_2 with p_o. A comparison of figures 3.14 and 3.20 shows that in general τ_3 is greater than τ_2 except at high initial pressures. However, τ_3 is always less than τ_1 at all initial temperatures.

3.1.1.9 The pressure rise accompanying the third cool flame

The behaviour of Δp_3 as the initial pressure is increased (figure 3.21) is similar to that of Δp_2. Inspection of figure 3.21 also shows that at low initial temperatures, for example at 298°C, Δp_3 is greater than Δp_2.

3.1.1.10 The maximum rate of pressure rise accompanying the third cool flame

The variation of $(dp_3/dt)_{max}$ with p_o exhibits the same features as $(dp_2/dt)_{max}$ as shown in figure 3.22. Again the distinct nature of the lower limit for three cool flames can be seen from figures 3.22 and 3.23. It is also interesting to note that at 298°C, $(dp_3/dt)_{max}$ exceeds $(dp_2/dt)_{max}$. Figure 3.18(b) shows that the loci of constant $(dp_3/dt)_{max}$ also reflect the lower lobe in the cool flame/two-stage ignition boundary although it is less pronounced than in the loci of constant $(dp_2/dt)_{max}$.

The variation with T_o of the limiting initial pressures, at which the relationships between p_o and τ_3, Δp_3 and $(dp_3/dt)_{max}$ exhibit turning points, is shown in figure 3.24. It can be seen by comparison with figure 3.19 that for a given initial temperature the limiting initial pressures for the third cool flame parameters are higher than those for the second cool flame.

Figure 3.20

The variation of τ_3 with p_o

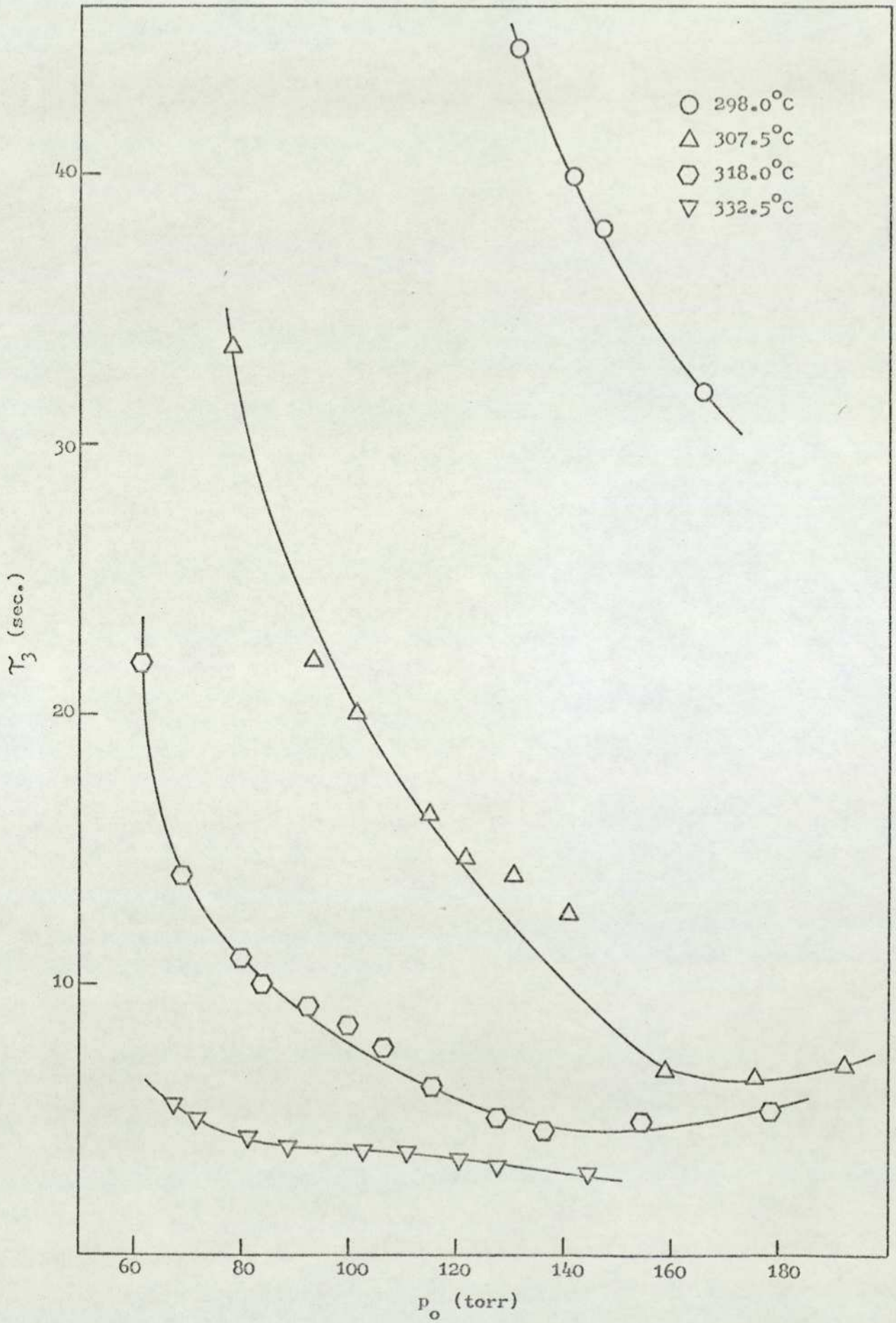


Figure 3.21

The variation of Δp_3 with p_o

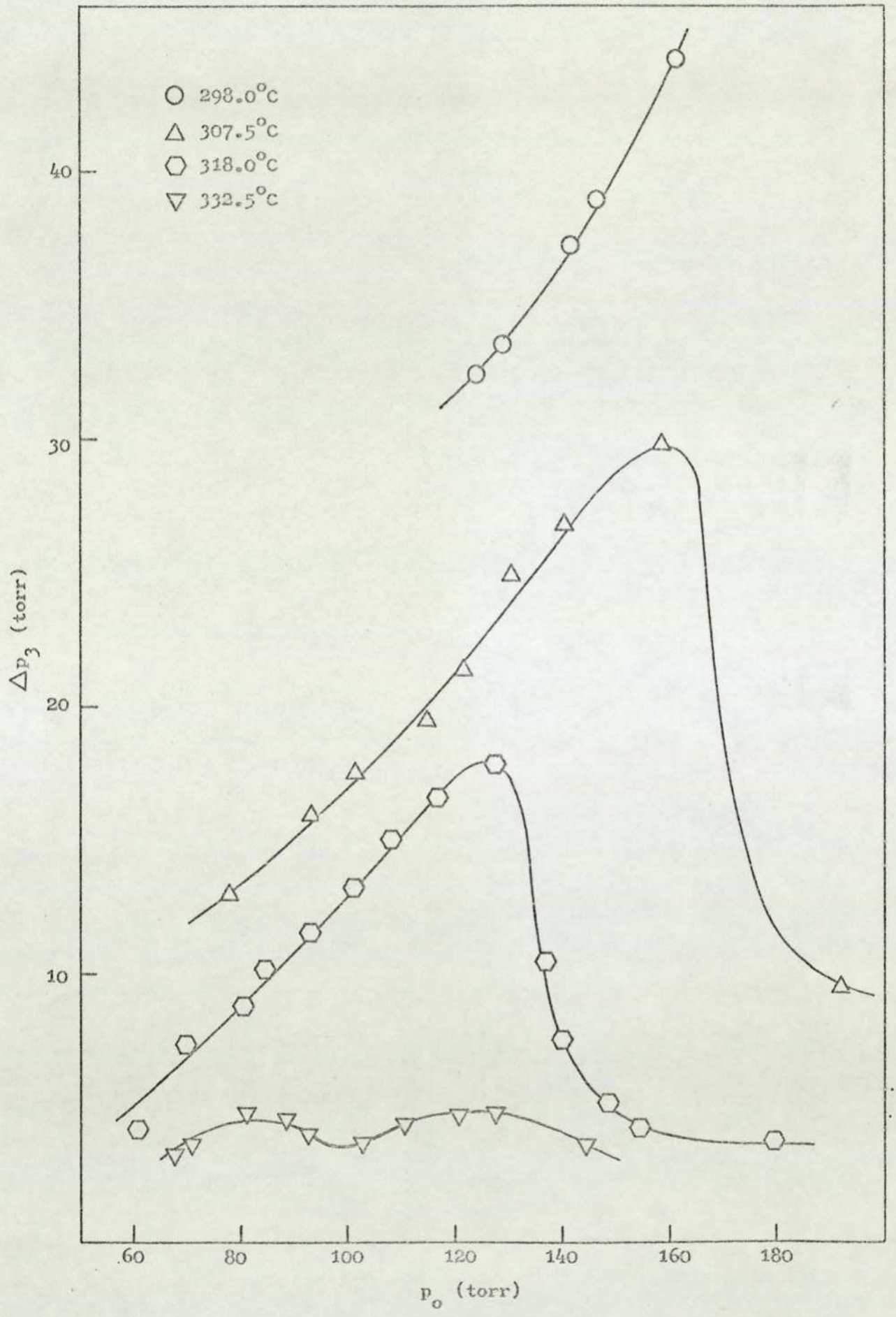


Figure 3.22

The variation of $(dp_3/dt)_{max}$ with p_o

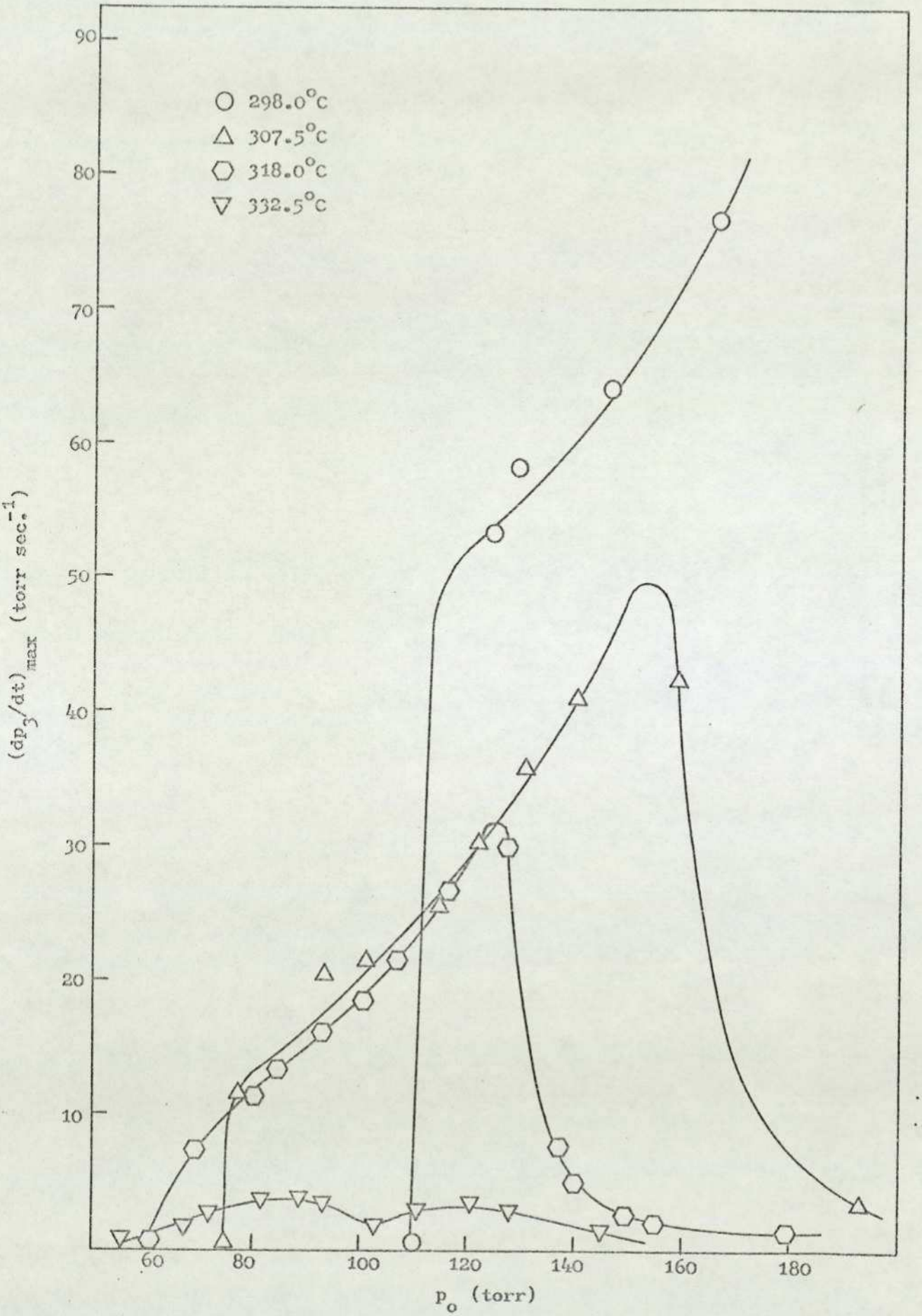


Figure 3.23

The variation of $(dp_3/dt)_{max}$ with T_o

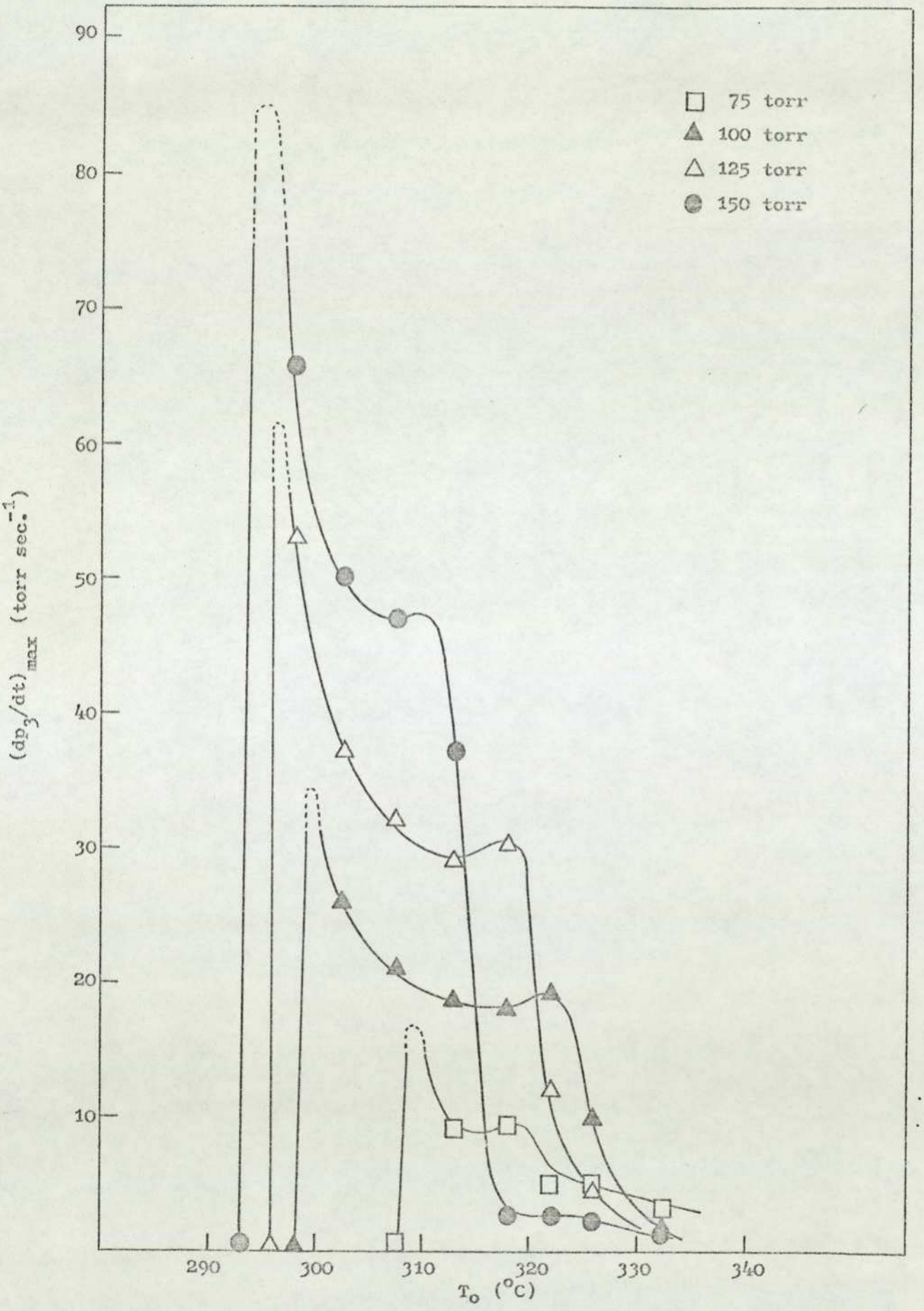
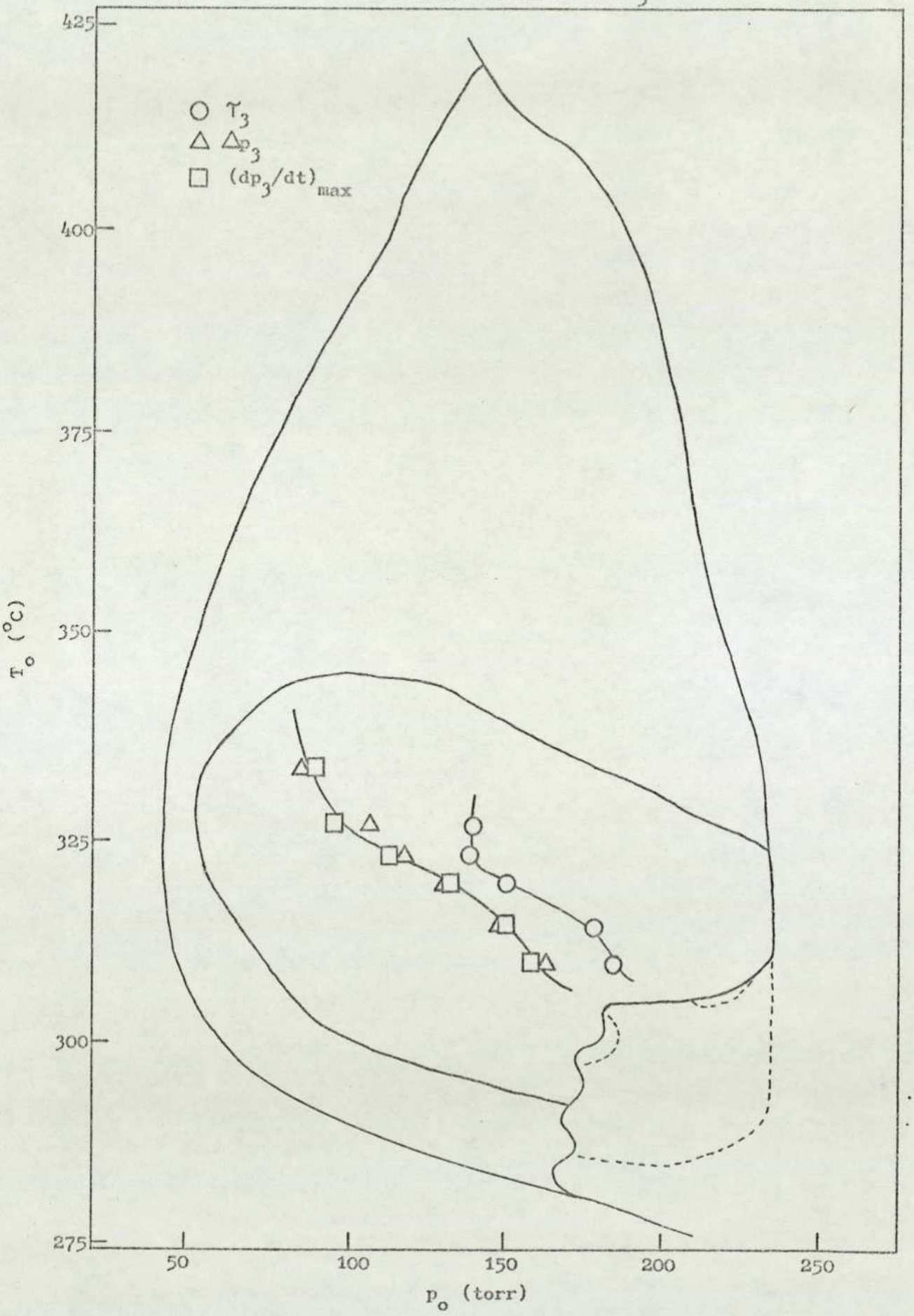


Figure 3.24

The variation with T_o of the initial pressure at which maxima occur in Δp_3 and $(dp_3/dt)_{max}$ and a minimum occurs in τ_3



3.1.1.11 Transition to two-stage ignitions

The remarkable change in behaviour of the second and subsequent cool flames above a limiting pressure can be associated with the appearance of a shoulder on the first cool flame (figure 3.1(c)). This shoulder grows into a pronounced pulse as either the temperature or initial pressure is increased. At initial temperatures greater than ca. 300°C, the hot ignition stage takes off from this pulse as shown in figure 3.2(e). The variation with p_o of the induction period of this shoulder, measured from the time at which the pressure rise accompanying the first cool flame is at a maximum, is shown in figure 3.25. It can be seen that in general τ_s increases as the initial pressure is increased towards the ignition limit. Furthermore, it is clear that as the initial temperature is increased, τ_s increases and this reflects the behaviour of the ignition delay at the ignition limit. Figure 3.26 shows the variation of Δp_s with p_o in the multiple cool flame region and it is interesting to note that Δp_s varies little with T_o.

Figure 3.25

The variation of τ_s with p_o

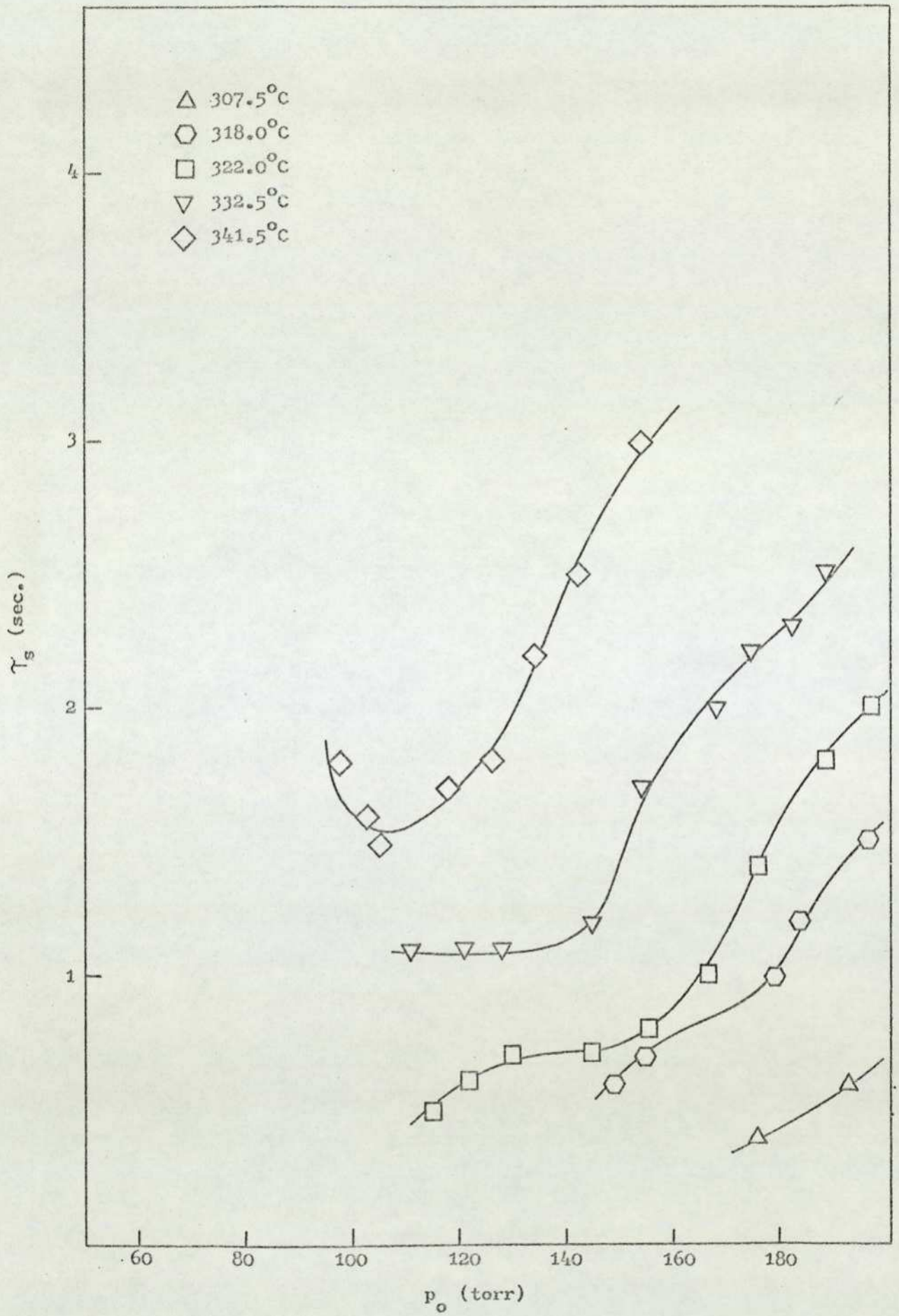
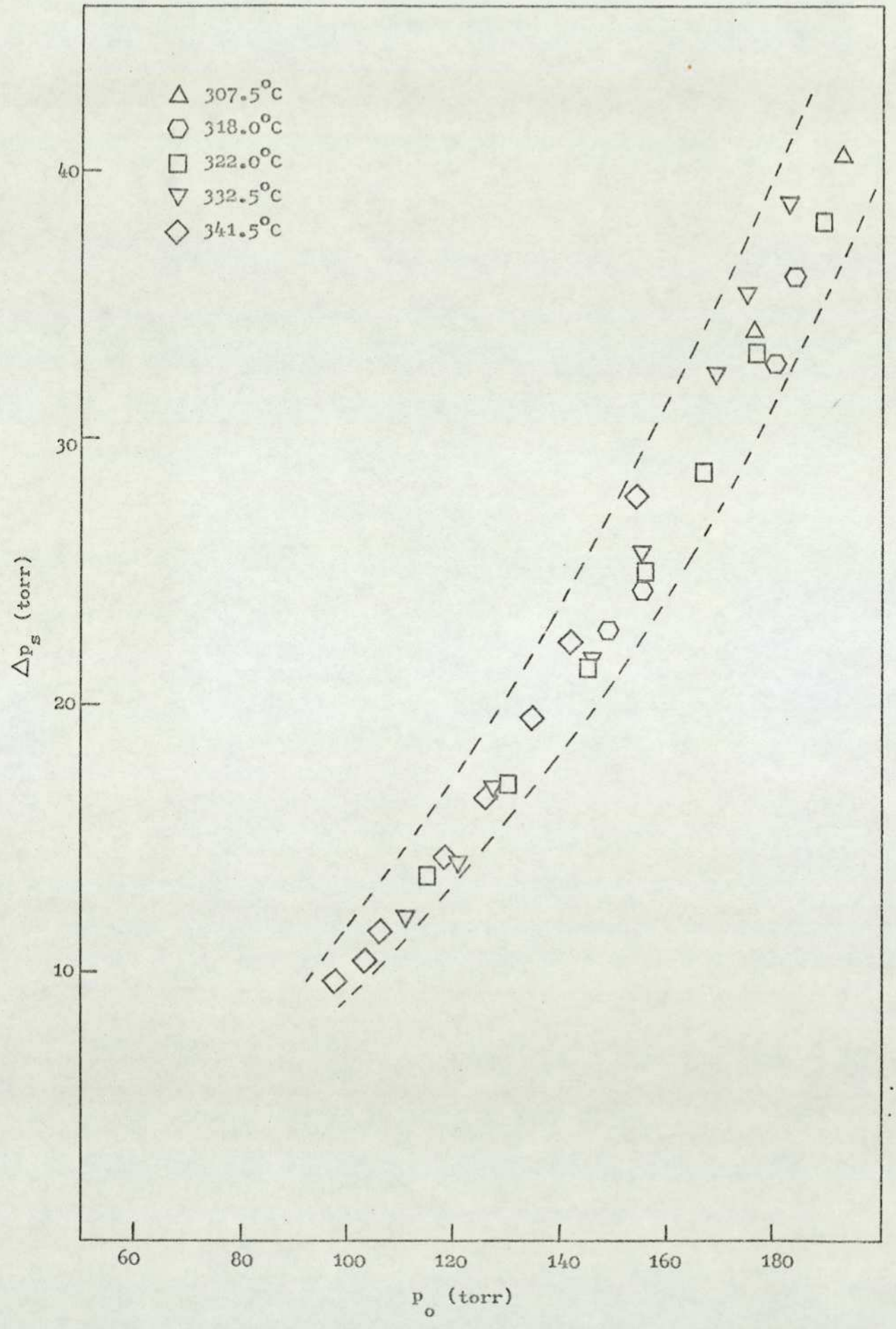


Figure 3.26

The variation of Δp_s with p_o



3.1.2 System II

3.1.2.1 The temperature-pressure ignition diagram

Figure 3.27 shows the ignition diagram obtained from a study of the combustion phenomena in a reaction vessel incorporating thermocouple probes. The cool flame/two-stage ignition boundary was not established because it was considered that repeated ignitions would damage the micro-thermocouples. It can be seen that although the general shape of the boundaries is similar to that obtained in a spherical reaction vessel (system I), their positions are shifted to higher initial pressures, particularly at temperatures below ca. 360°C. Furthermore, the multiple cool flame boundaries are considerably closer together in System II. Again, as in System I, the slow combustion/cool flame boundary is a smooth curve with no indication of any fine structure.

The kinetic parameters show the same features as those observed for System I except that, in general, the induction periods are longer and the rates of pressure rise are smaller. These differences are particularly pronounced at low initial temperatures where, for example, the induction periods at low initial pressures may be up to ten times longer and the rates of pressure rise may be reduced by 50%. Typical temperature-time recordings at the wall, half-radius and centre of the reaction vessel in the multiple cool flame region and the single cool flame region are illustrated in figures 3.28(a) and 3.28(b) respectively.

An interesting feature of these recordings is that above limiting initial temperatures and pressures, the order in which the temperature maximises during the first cool flame is at the centre, half-radius and wall while below these limiting values this order is reversed. These temperature measurements indicate that at high initial temperatures, for example above ca. 330°C, the first cool flame propagates from the centre of the vessel, whereas below this temperature the cool flame propagates

from the walls. The precise variation with p_o of the initial temperature at which all three temperature readings maximise together is shown in figure 3.29.

In System II measurements were made on the first cool flame only, since temperature changes in the vessel after the passage of the first cool flame were often extremely complex.

Figure 3.27

The temperature-pressure ignition diagram for n-butane and oxygen mixtures (1:2) obtained in a reaction vessel incorporating thermocouples

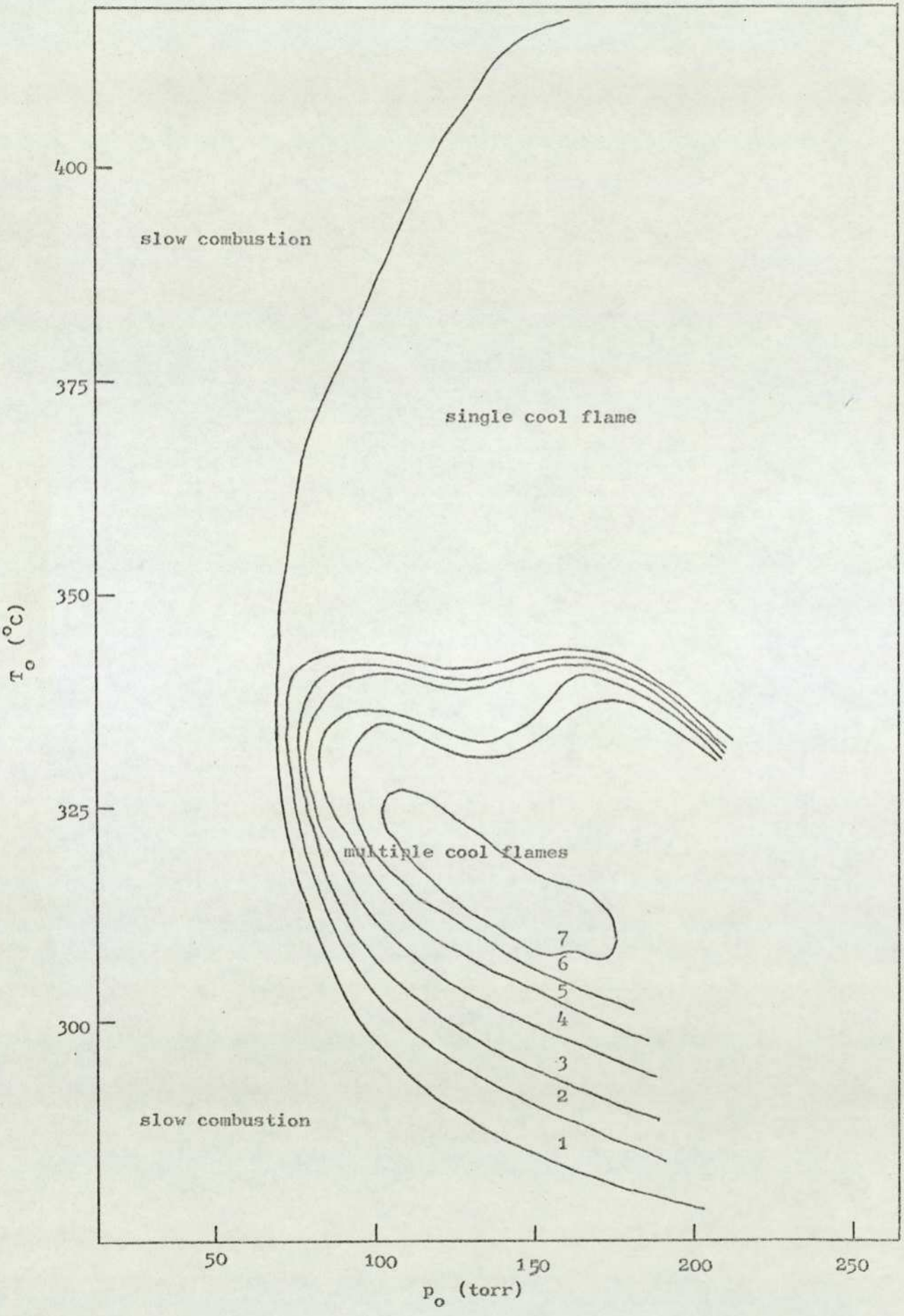


Figure 3.28

Typical temperature/pressure-time recordings in (a) the multiple cool flame region and (b) the single cool flame region

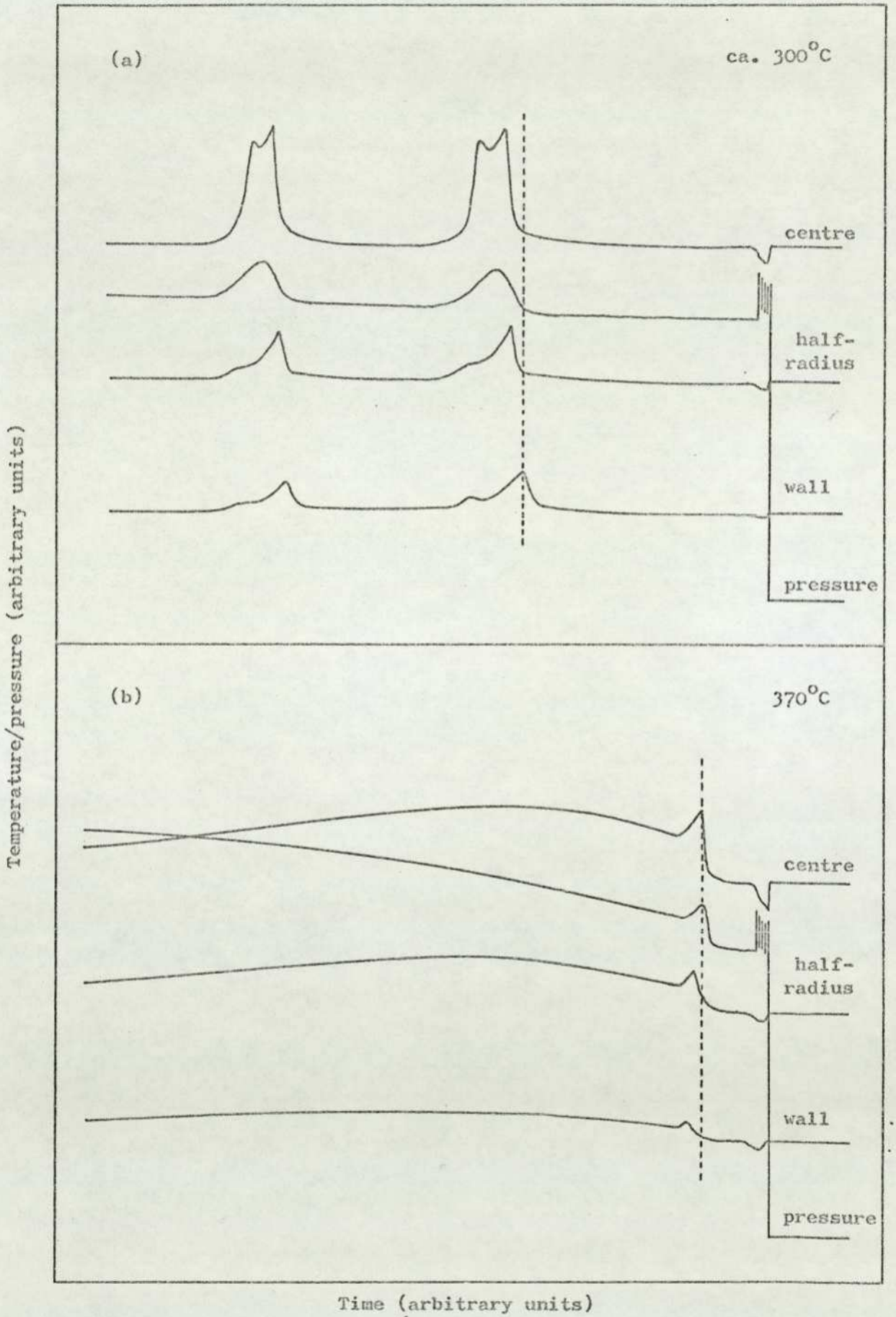
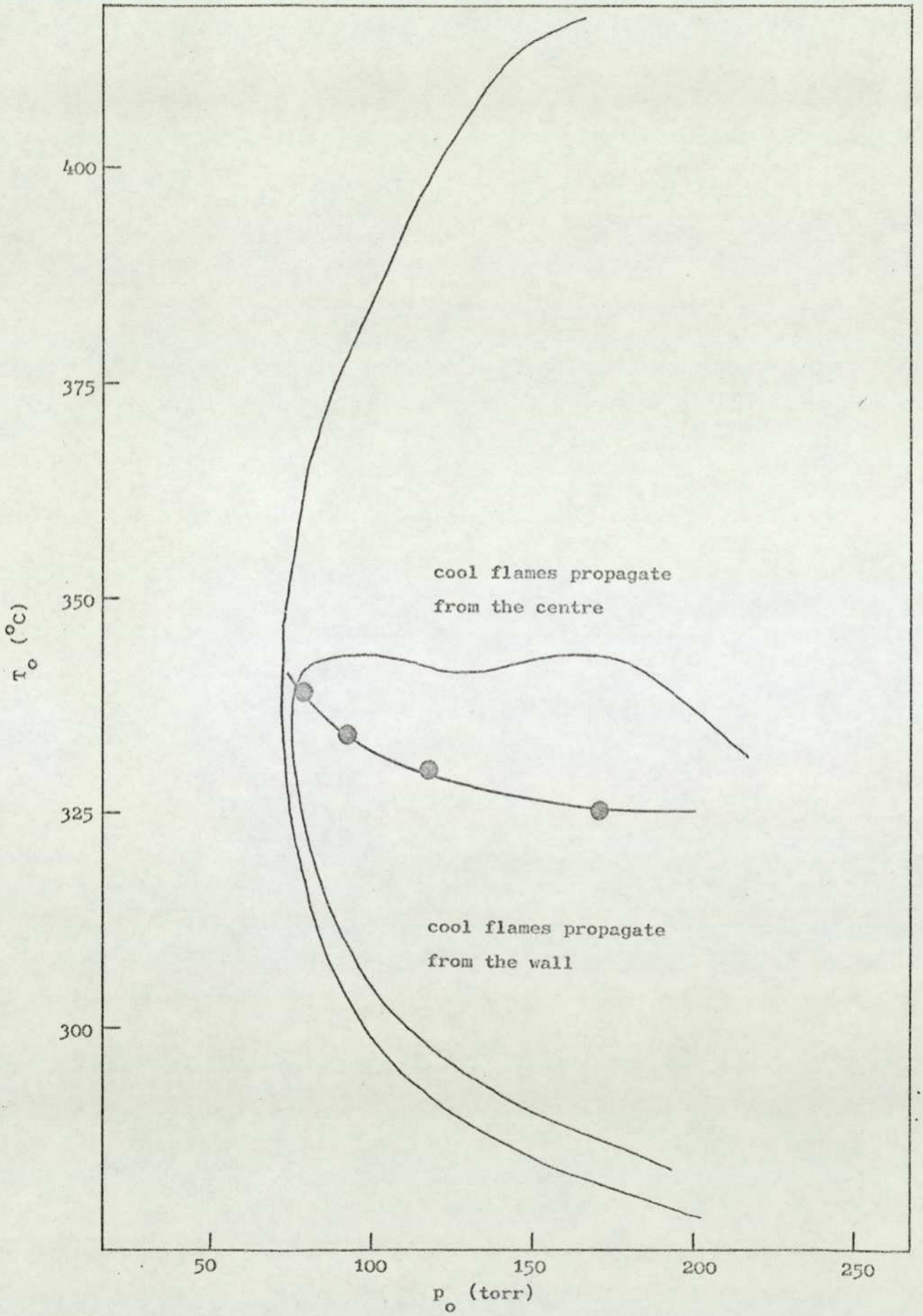


Figure 3.29

The variation with T_o of the initial pressure at which the changeover from centre to wall propagation occurs



3.1.2.2 The temperature rise accompanying the first cool flame

Figures 3.30 - 3.32 show the relationship between p_o and ΔT_1 measured at the wall, half-radius and centre of the reaction vessel respectively. It can be seen that during the passage of the first cool flame there is parabolic temperature distribution across the reaction vessel and that the values of ΔT_1 range from ca. 40°C at the wall to ca. 200°C at the centre of the vessel.

The relationship between p_o and ΔT_1 at the wall (figure 3.30) is linear and of the form:

$$\Delta T_1 = Mp_o + C$$

Throughout the cool flame region the value of M is ca. 0.18 and although the value is C is clearly dependent on temperature in the multiple cool flame region, this temperature dependence is considerably less pronounced at temperatures above 345°C i.e. the upper single cool flame region. At the half-radius (figure 3.31), the relationship is also linear but in this case the value of M is ca. 0.70 in the single cool flame region and varies from 0.50 to 0.60 in the multiple cool flame region. Furthermore, the constant C is temperature dependent throughout the cool flame region. It can be seen from figure 3.32 that the relationship at the centre of the vessel is not linear, however, but of the form:

$$\Delta T_1 = Mp_o^x + C$$

In this case the temperature dependence of the constant C is more pronounced in the single cool flame region (c.f. temperature dependence of C at wall of vessel).

Figure 3.30

The variation with p_o of ΔT_1 at the wall of the reaction vessel

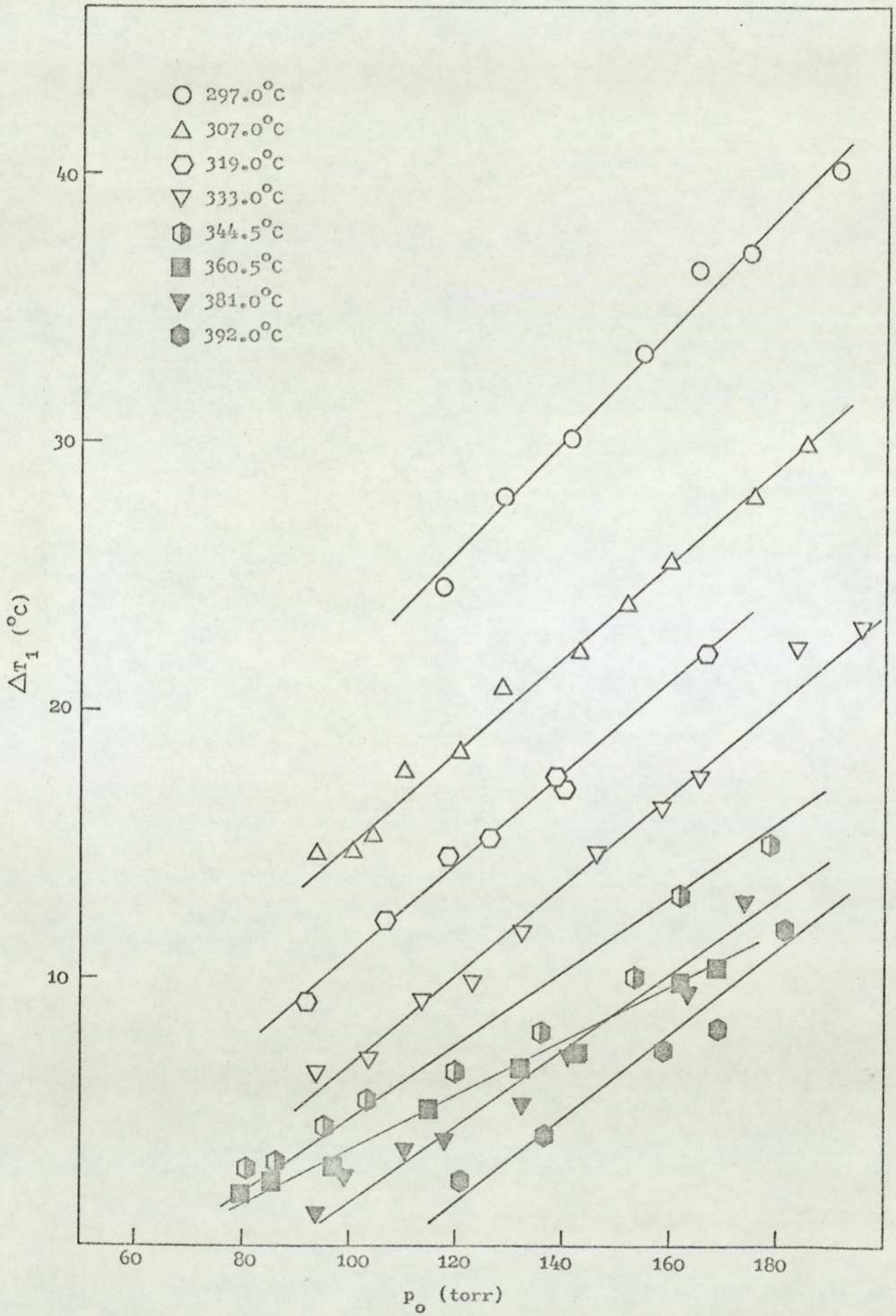


Figure 3.31

The variation with p_o of ΔT_1 at the half-radius of the reaction vessel

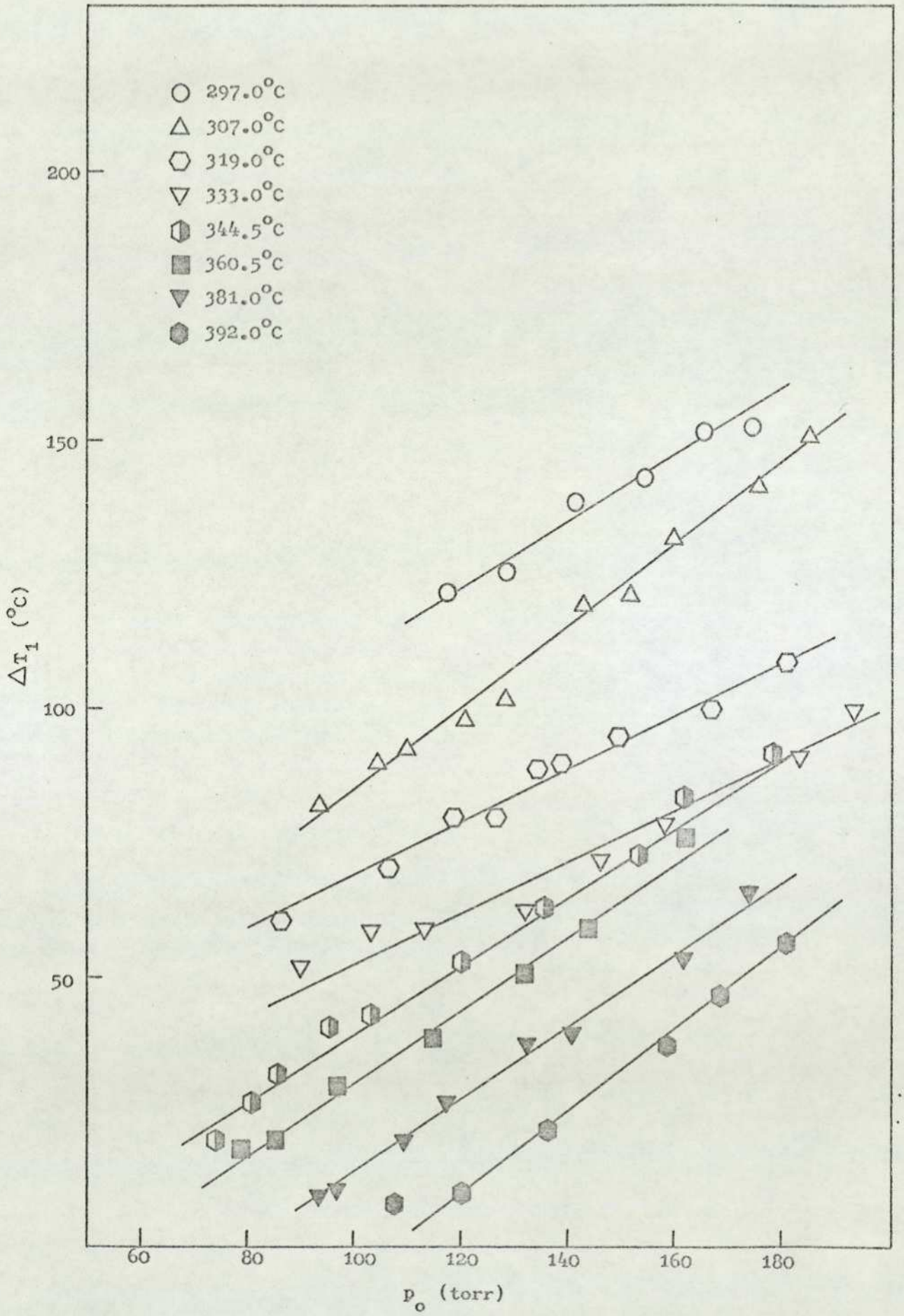
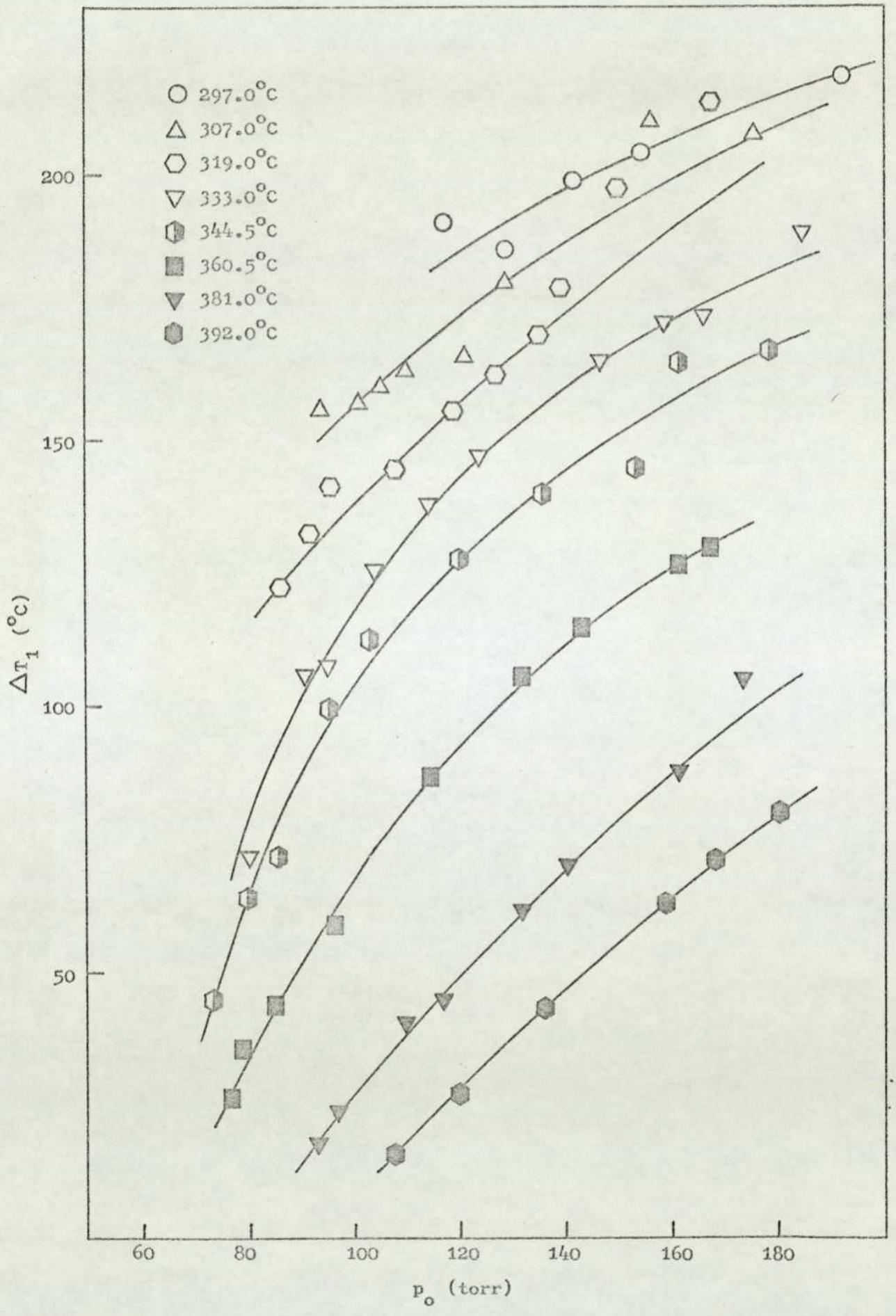


Figure 3.32

The variation with p_o of ΔT_1 at the centre of the reaction vessel



3.1.2.3 The maximum rate of temperature rise accompanying the first cool flame

Figures 3.33 - 3.35 show the variation with p_o of $(dT_1/dt)_{max}$ at the three positions in the vessel. The curves are similar to those obtained for the variation of $(dp_1/dt)_{max}$ with p_o (figures 3.10 and 3.11). Again, the points of inflection at low initial temperatures and pressures indicate the clearly defined nature of the lower cool flame limit. Furthermore, it can be seen that the values of $(dT_1/dt)_{max}$ range from ca. 300°C $sec.^{-1}$ at the wall to well over 2000°C $sec.^{-1}$ at the centre of the vessel.

The variation with T_o of $(dT_1/dt)_{max}$ at the wall and centre of the vessel is shown in figures 3.36 and 3.37 respectively. It can be seen that the whole of the cool flame region i.e. between 290 and 420°C, can be considered as a region of negative temperature coefficient with respect to the rate of the reaction occurring in the vicinity of the wall of the vessel, particularly at high initial pressures. Figure 3.37 reveals a more complex variation of $(dT_1/dt)_{max}$ with p_o at the centre of the vessel. At initial temperatures between 290 and 310°C there is a marked negative temperature coefficient region at all initial pressures, but as the temperature is increased from 310 to 340°C the value of $(dT_1/dt)_{max}$ passes through several maxima and minima which are most pronounced at high initial pressures. Above ca. 340°C the rate again falls as the initial temperature is increased.

Figure 3.33

The variation with p_o of $(dT_1/dt)_{max}$ at the wall of the reaction vessel

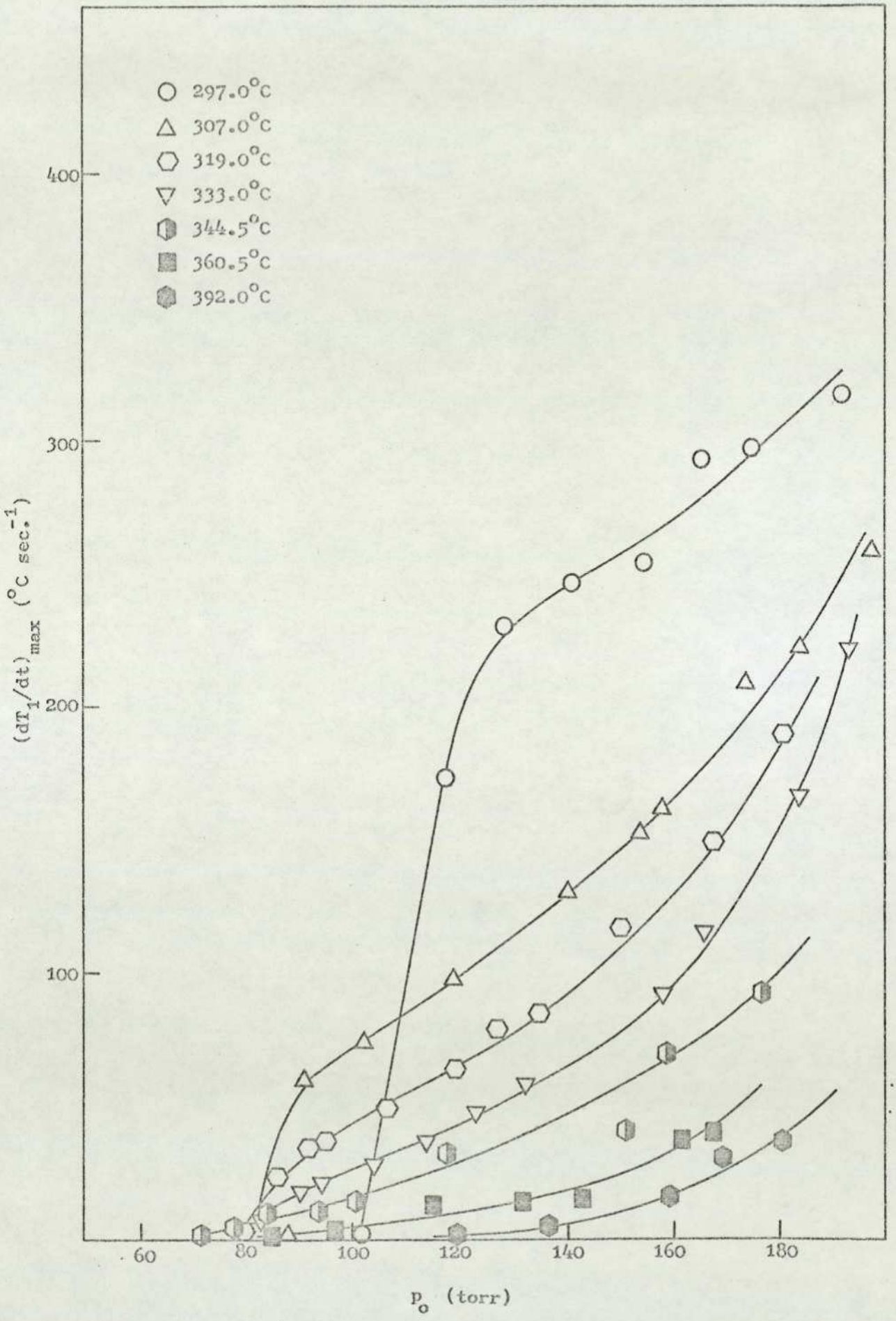


Figure 3.34

The variation with p_o of $(dT_1/dt)_{max}$ at the half-radius of the reaction vessel

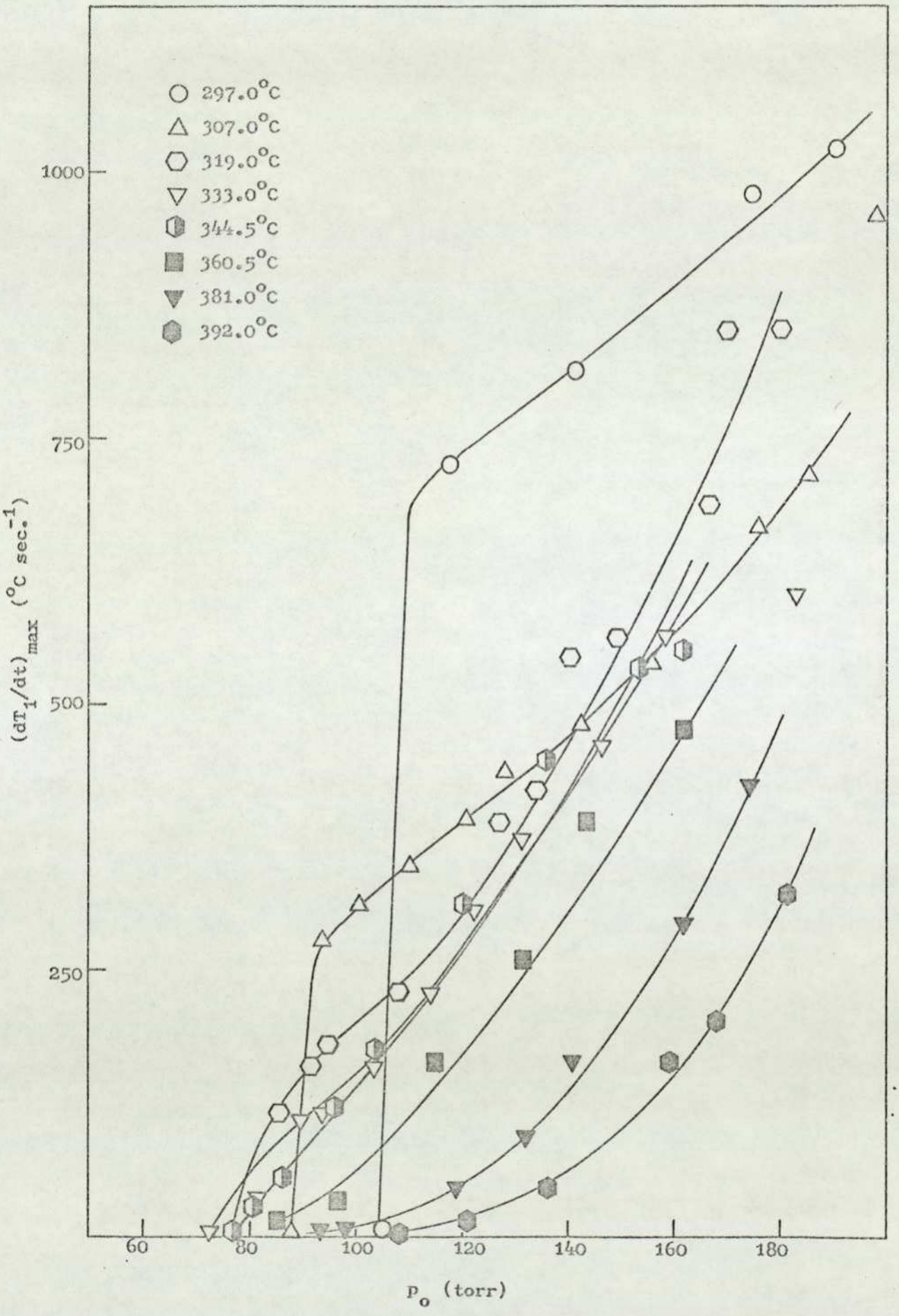


Figure 3.35

The variation with p_o of $(dT_1/dt)_{max}$ at the centre of the reaction vessel

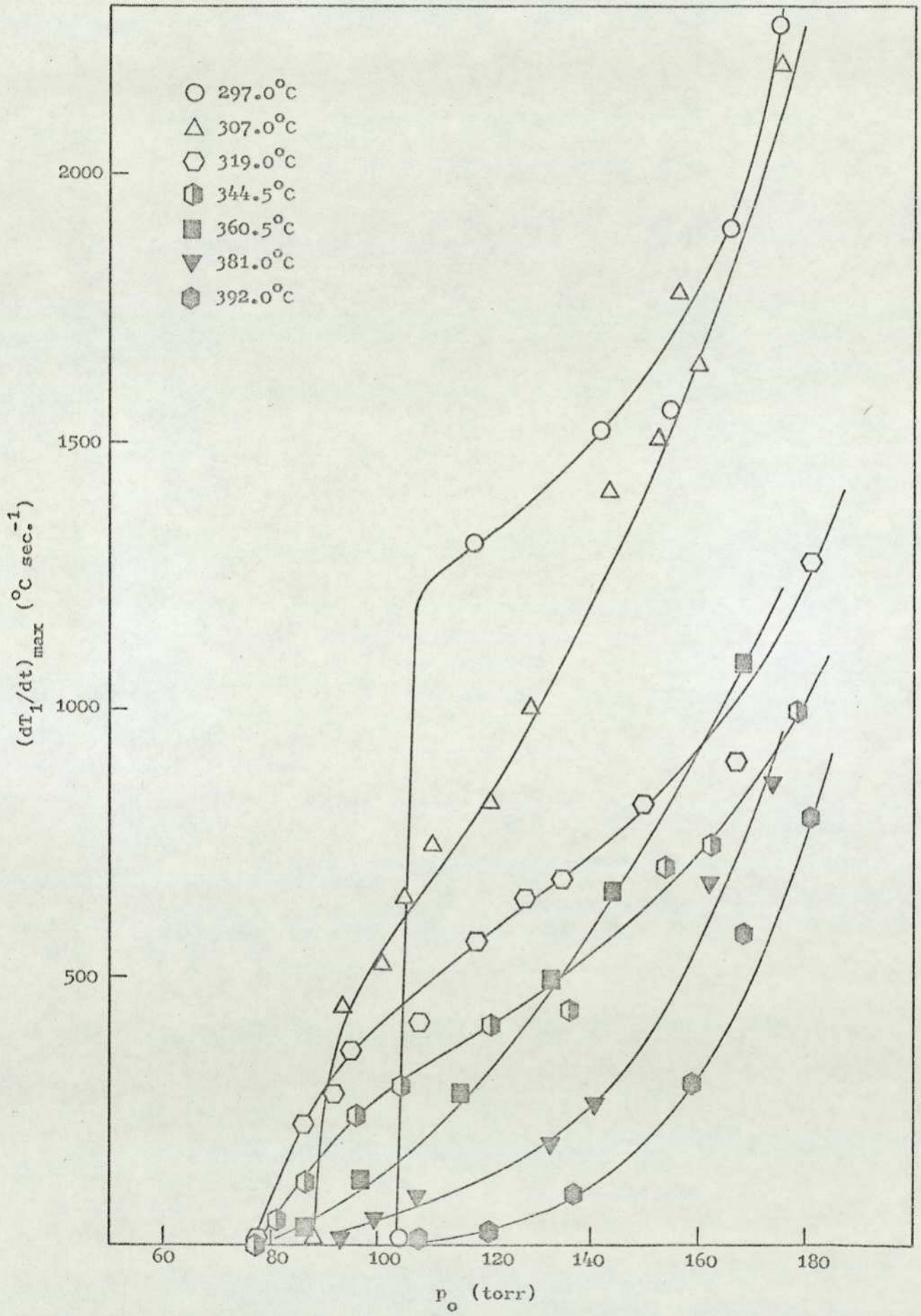


Figure 3.36

The variation with T_o of $(dT_1/dt)_{max}$ at the wall of the reaction vessel

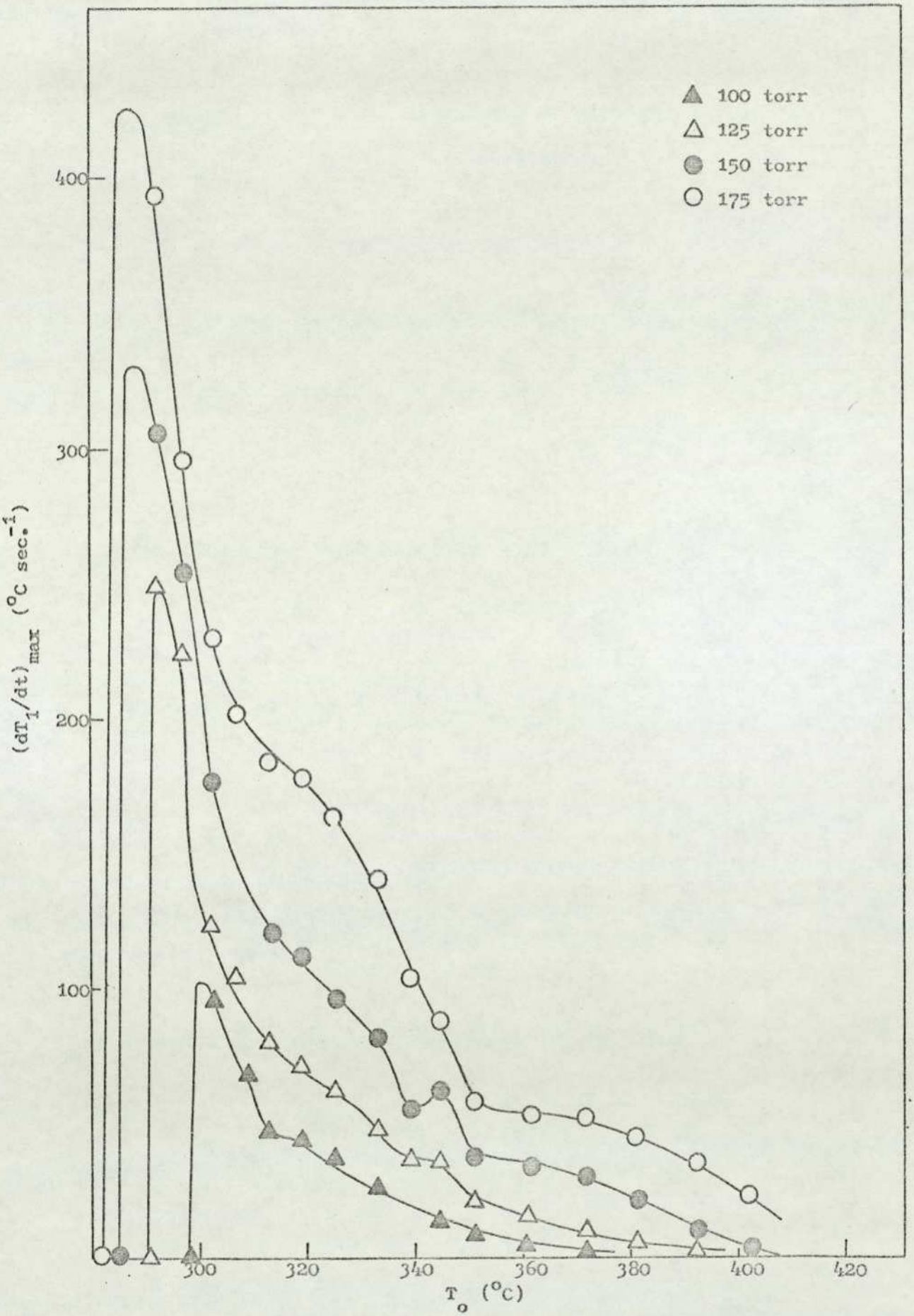
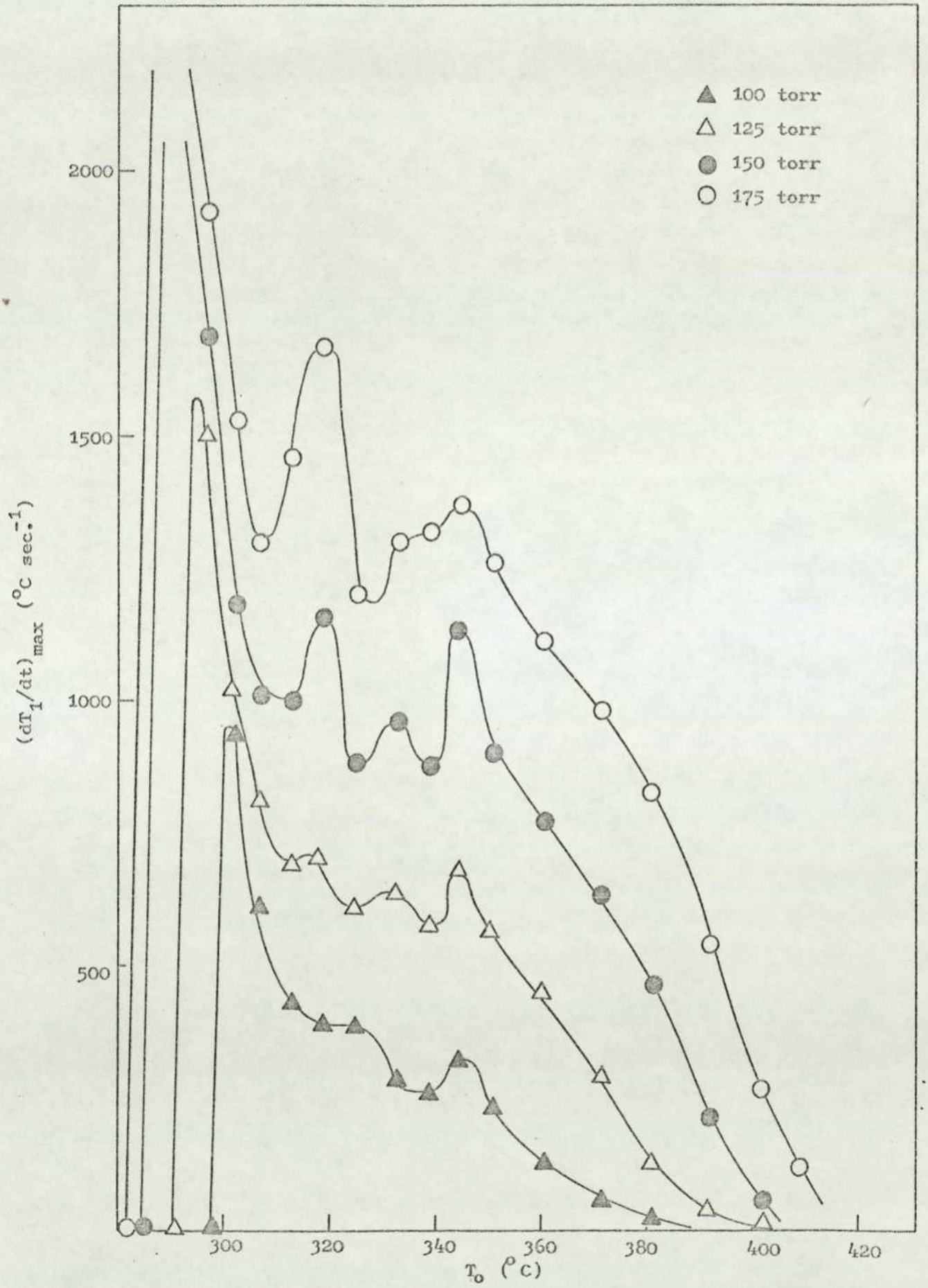


Figure 3.37

The variation with T_o of $(dT_1/dt)_{max}$ at the centre of the reaction vessel



3.2 The analytical results

The analytical investigations were carried out after the kinetics of the system had been established. They were performed using a new reaction vessel which was conditioned in the usual manner (section 2.3.3) and which was free of carbon deposits. The kinetic parameters obtained were similar to those of System I except that the induction periods were slightly longer and the rates of pressure change were fractionally smaller. The conditions under which the analytical investigations were carried out were almost identical, therefore, to those under which the kinetics were determined and so a direct correlation between the two sets of results can be made.

3.2.1 The variation of product distribution with time in the cool flame region

The kinetic results indicated that an initial pressure of 150 torr was the most useful at which to study the variation of the product distribution with respect to both time and the initial temperature. Furthermore, at this pressure the first cool flame was well developed at all temperatures.

Carbon balances performed during the induction period preceding the first cool flame and immediately after its passage at two different initial temperatures are shown in Tables 3.1 and 3.2 respectively. It can be seen that in the early stages of reaction the balances are very close to 100%, whereas after the passage of the first cool flame they are ca. 93% and 86% at 300°C and 360°C respectively. This apparent loss of carbon can most probably be attributed to the formation of formaldehyde and carbon oxides as the cool flame propagates. Furthermore, Table 3.2 shows that the ratio:

$$\frac{\text{g. atoms of carbon detected in products}}{\text{g. atoms of carbon in n-butane consumed}}$$

decreases by a factor of about two between 300°C and 360°C and this indicates that the yields of these scission products increase as the initial temperature is increased.

Table 3.1

Carbon balances during the induction period of the first cool flame (initial pressure = 150 torr)

reaction product	g.atoms of carbon ($\times 10^{+6}$)	
	300°C	360°C
methane	-	-
ethylene	5.6	4.2
propene	0.5	1.1
but-1-ene	58.6	47.0
but-2-ene(t)	34.3	26.5
but-2-ene(c)	19.4	18.4
buta-1,3-diene	0.2	0.1
acetaldehyde	53.7	5.2
2-methyloxiran	2.1	0.5
methanol	2.2	0.6
propionaldehyde	2.2	0.3
2,3-dimethyloxiran(t)	3.7	1.0
acrolein	0.7	0.3
acetone	46.6	1.8
2,3-dimethyloxiran (c)	2.4	0.7
2-ethyloxiran	0.5	0.3
2-methyloxetan	1.7	1.1
n-butyraldehyde	-	0.6
tetrahydrofuran	0.7	0.5
methyl ethyl ketone	11.7	1.2
methyl vinyl ketone	3.7	0.1
total products	251	112
n-butane unconsumed	36189	32980
total carbon detected	36440	33092
carbon introduced	36890	33410
carbon balance	98.8%	99.1%

Table 3.2

Carbon balances immediately after the passage of the first cool flame (initial pressure = 150 torr)

reaction product	g.atoms of carbon ($\times 10^{+6}$)	
	300°C	360°C
methane	18.0	6.0
ethylene	206.5	126.1
propane	1.4	0.7
propene	133.1	96.2
but-1-ene	858.8	804.0
but-2-ene(t)	396.0	432.0
but-2-ene(c)	264.0	300.0
buta-1,3-diene	12.9	9.6
acetaldehyde	579.0	159.7
2-methyloxiran	21.6	3.6
methanol	202.8	33.0
propionaldehyde	82.7	18.0
2,3-dimethyloxiran(t)	103.2	36.0
acrolein	73.7	45.0
acetone	223.1	25.2
2,3-dimethyloxiran(c)	53.8	22.1
2-ethyloxiran	39.9	14.4
2-methyloxetan	182.4	84.0
n-butyraldehyde	7.7	2.9
tetrahydrofuran	62.4	14.4
methyl ethyl ketone	29.8	6.7
methyl vinyl ketone	28.8	2.9
total products	3582	2243
n-butane unconsumed	30735	26610
total carbon detected	34317	28853
carbon introduced	36890	33410
carbon balance	93.0%	86.4%
$\frac{\text{total products detected}}{\text{n-butane consumed}} \times 100$	58.1%	33.0%

The variation with time of the concentrations of individual products was studied at 300, 309 and 360°C and is shown in figures 3.38 - 3.56.

At 300°C four intense, well resolved, cool flames propagate and are followed by slow combustion (figure 3.57). Acetaldehyde, acetone, but-1-ene and but-2-ene are the only products formed in appreciable quantities during the induction period (figures 3.38 - 3.44). The rates of formation of these and other products increase exponentially however about two seconds before the first cool flame and reach maximum values concurrently with the maximum rate of pressure rise $(dp_1/dt)_{max}$ accompanying the cool flame. The major products found immediately after the passage of the first cool flame are acetaldehyde, but-1-ene, but-2-ene, methanol, ethylene and acetone and together these account for ca. 80% of the total products detected.

During the induction periods of subsequent cool flames the concentrations of most products remain sensibly constant and only show a marked increase as the cool flame propagates. Thus a step-wise accumulation of the products occurs as exemplified by methanol (figure 3.39). Some products, however, such as the butenes, propylene, 2-methyloxetan, tetrahydrofuran, methyl ethyl ketone and but-1,3-diene show a marked deviation from this behaviour and their concentrations fluctuate throughout the course of the reaction. This behaviour is most clearly illustrated by that of 2-methyloxetan (figure 3.42) and indicates the involvement of these products in further oxidation or decomposition reactions. The behaviour of methyl ethyl ketone is particularly interesting since its concentration falls dramatically as each cool flame begins to propagate, although its overall rate of accumulation remains reasonably constant throughout the reaction as shown in figure 3.43. The concentration of acetone also builds up at a fairly steady rate throughout the reaction.

After the passage of the final cool flame and during the slow combustion which completes the reaction, the concentration of products such as methanol, methane, acetone, propionaldehyde, oxirans and propane continues to increase whereas the other products apparently undergo further reaction.

Figure 3.44 shows that the fuel consumption is ca. 18%, 14% and 9% at the first, second and third cool flames respectively. Furthermore, it can be seen that there is negligible fuel consumption during the passage of the fourth cool flame or during the subsequent slow combustion (see figure 3.57).

Key to analytical results

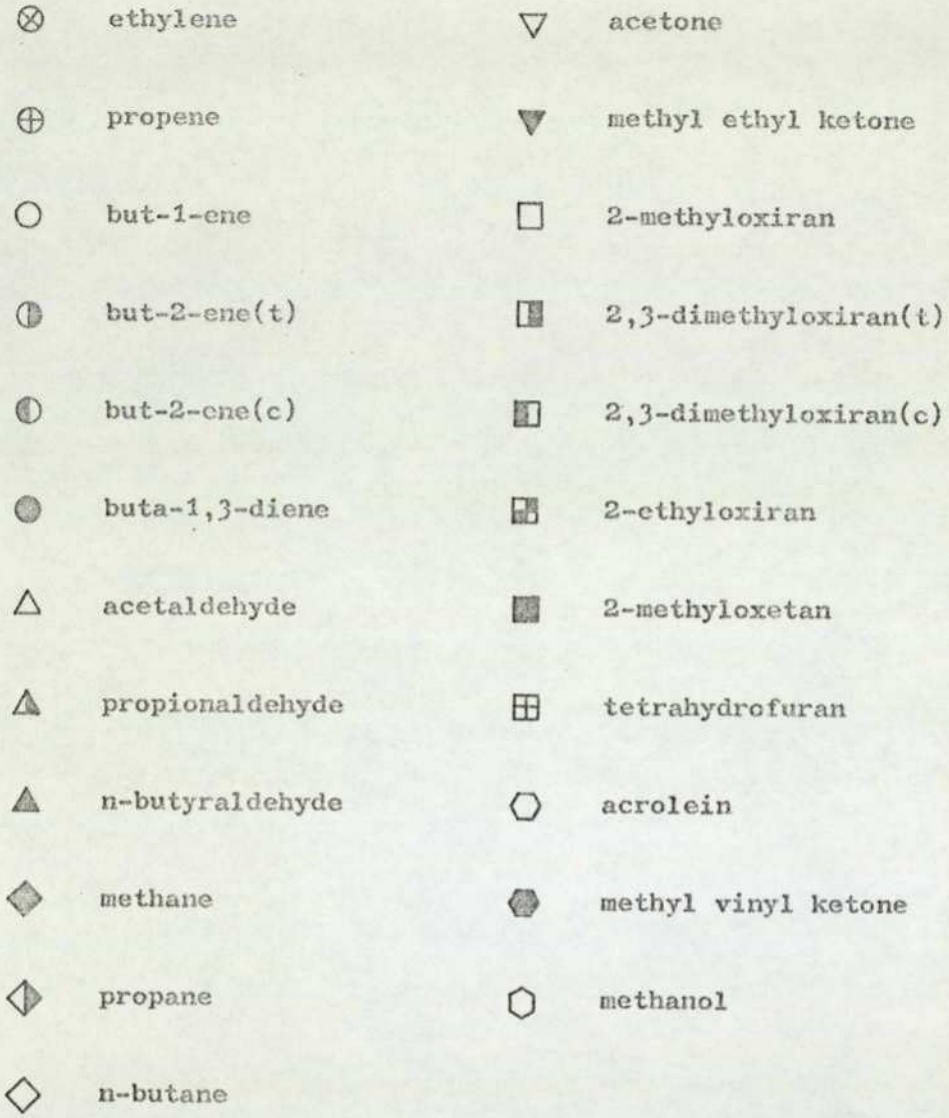


Figure 3.38

The variation with time of the yields of acetaldehyde, ethylene and methane (300 °C, 150 torr)

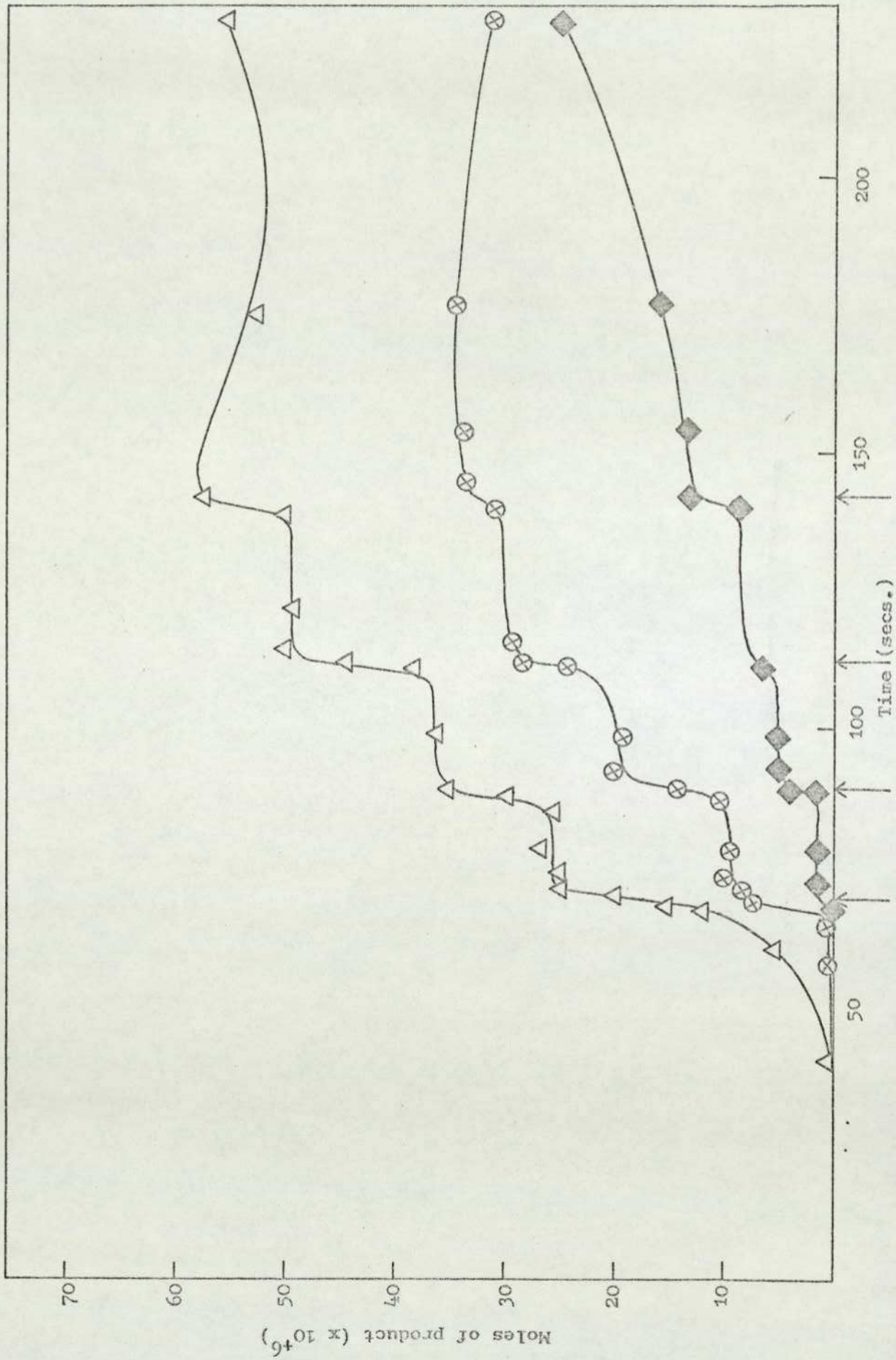


Figure 3.39

The variation with time of the yields of but-1-ene, trans but-2-ene, cis but-2-ene and methanol (300°C, 150 torr)

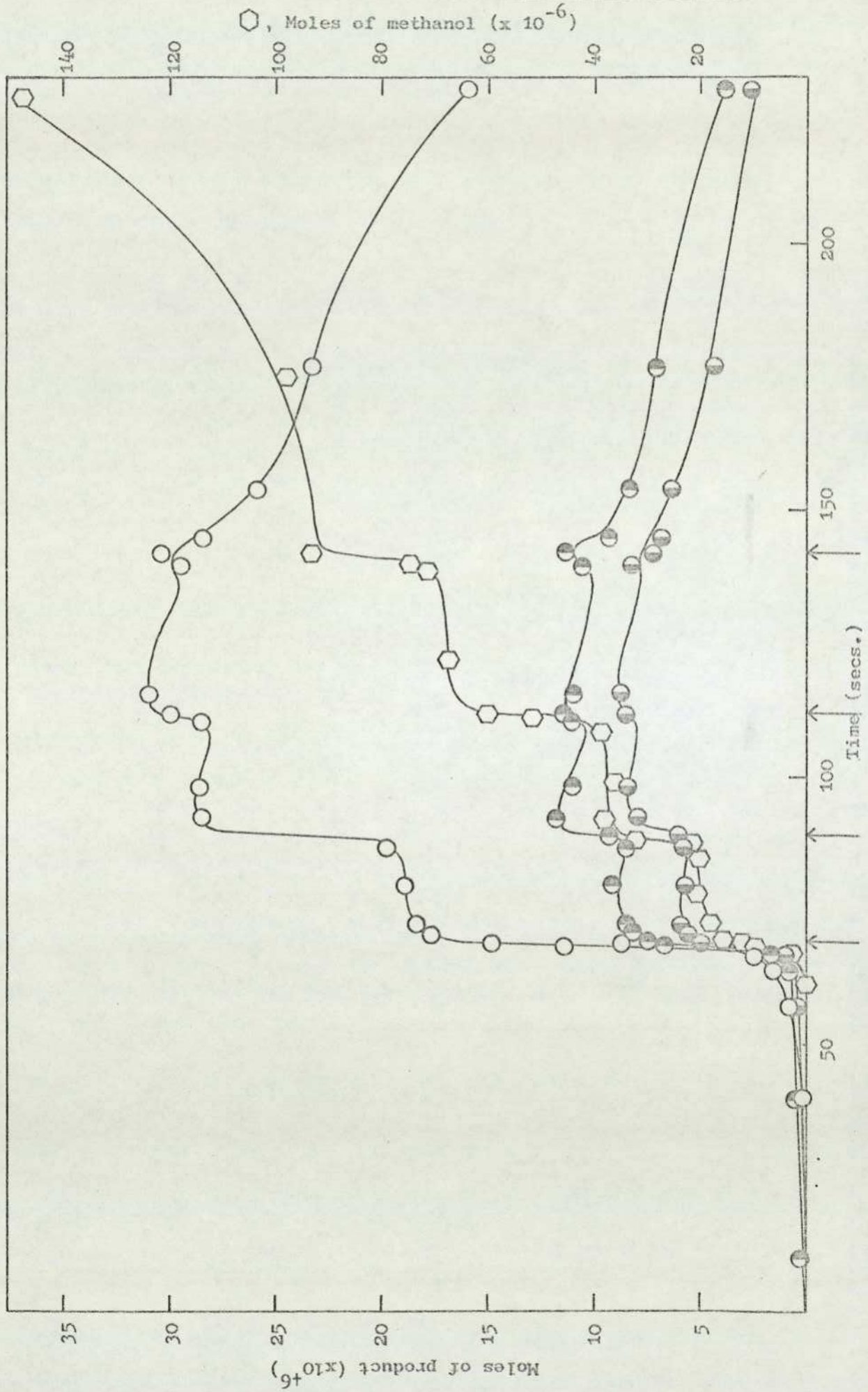


Figure 3.40

The variation with time of the yields of acetone, propene and acrolein (300°C, 150 torr)

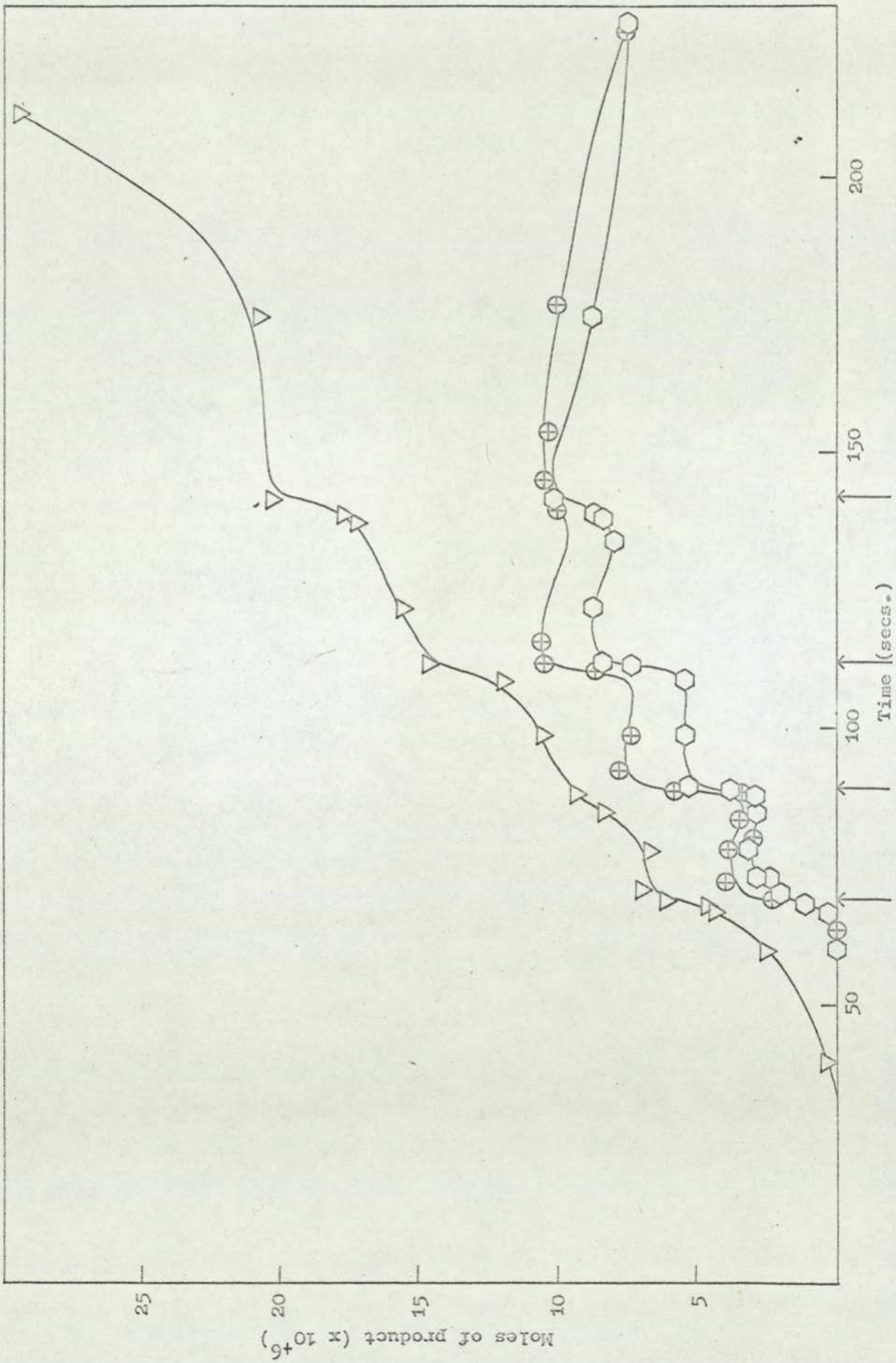


Figure 3.41

The variation with time of the yields of propionaldehyde, trans 2,3-dimethyloxiran and cis 2,3-dimethyloxiran (300°C, 150 torr)

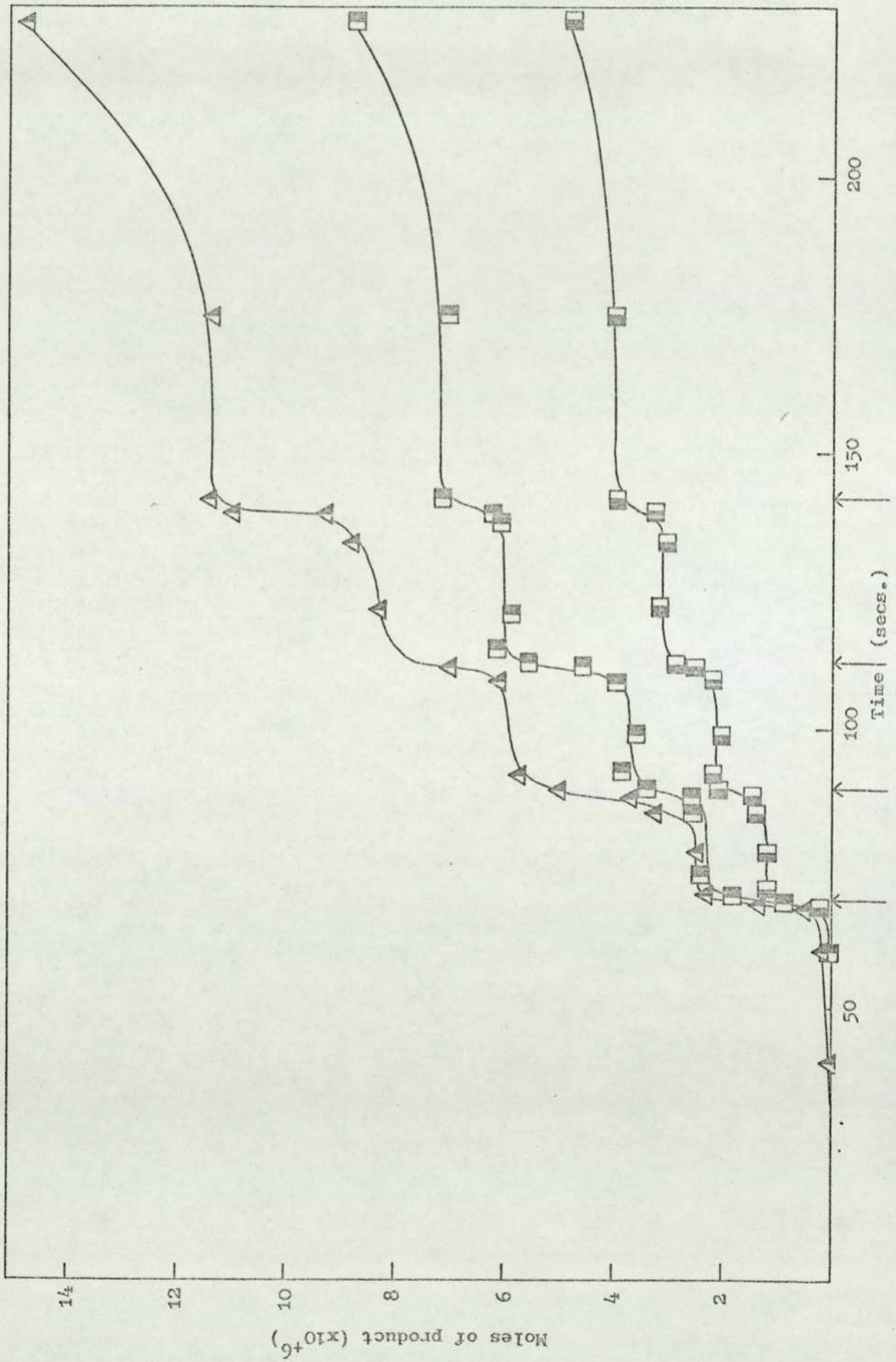


Figure 3.42

The variation with time of the yields of 2-ethyloxiran, 2-methyloxetan, tetrahydrofuran and 2-methyloxiran (300°C, 150 torr)

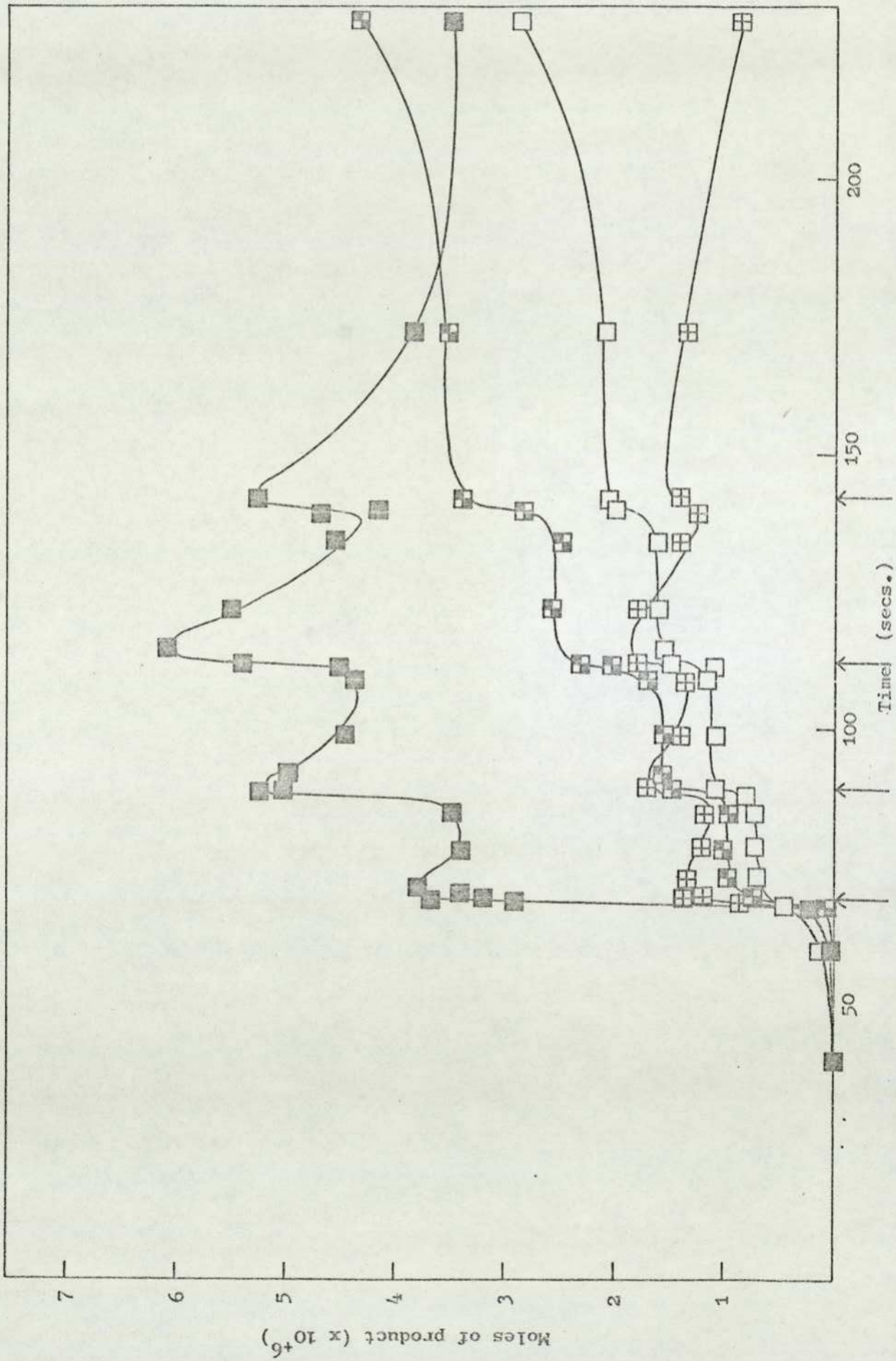


Figure 3.43

The variation with time of the yield of methyl ethyl ketone (300°C, 150 torr)

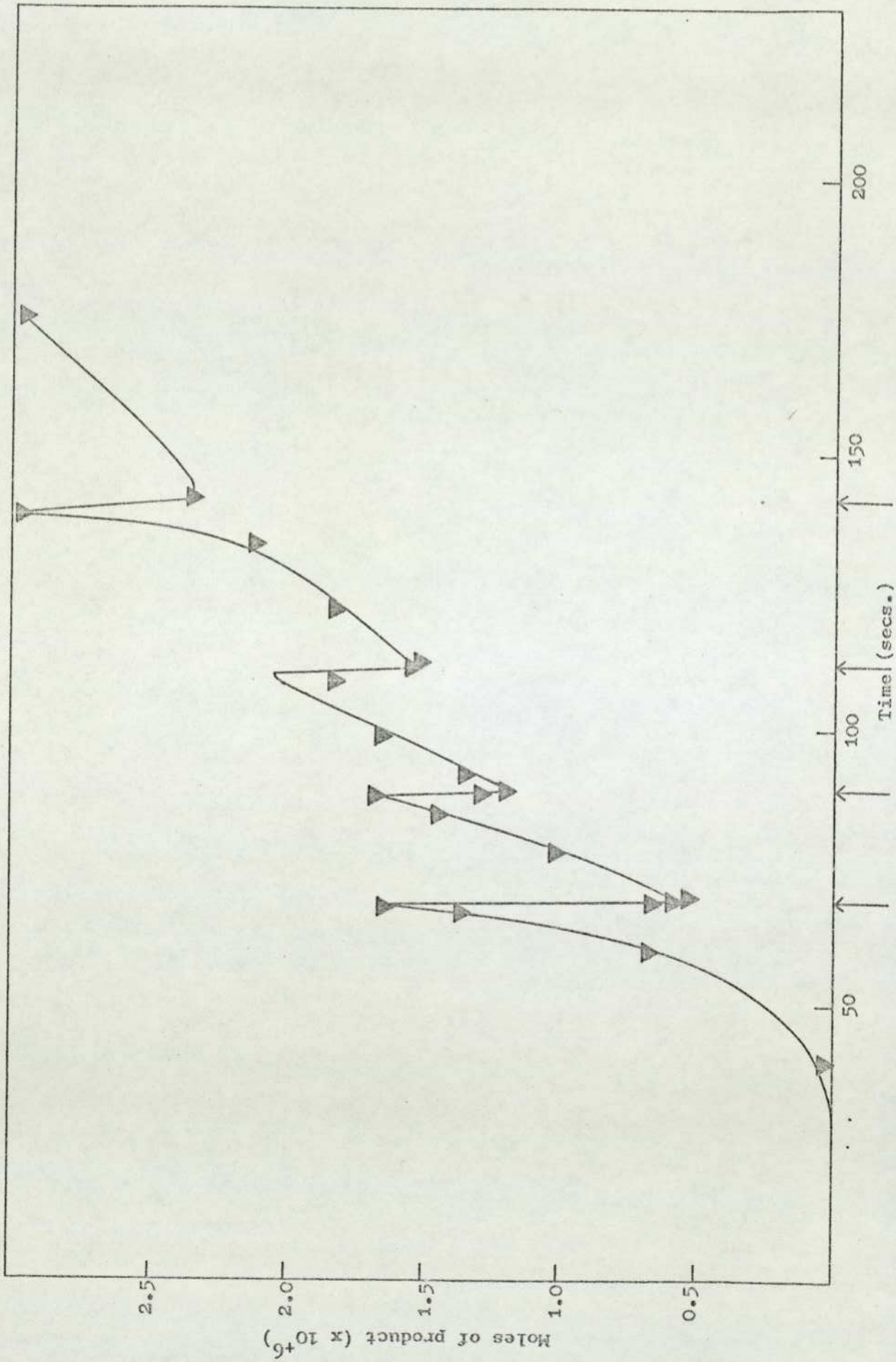
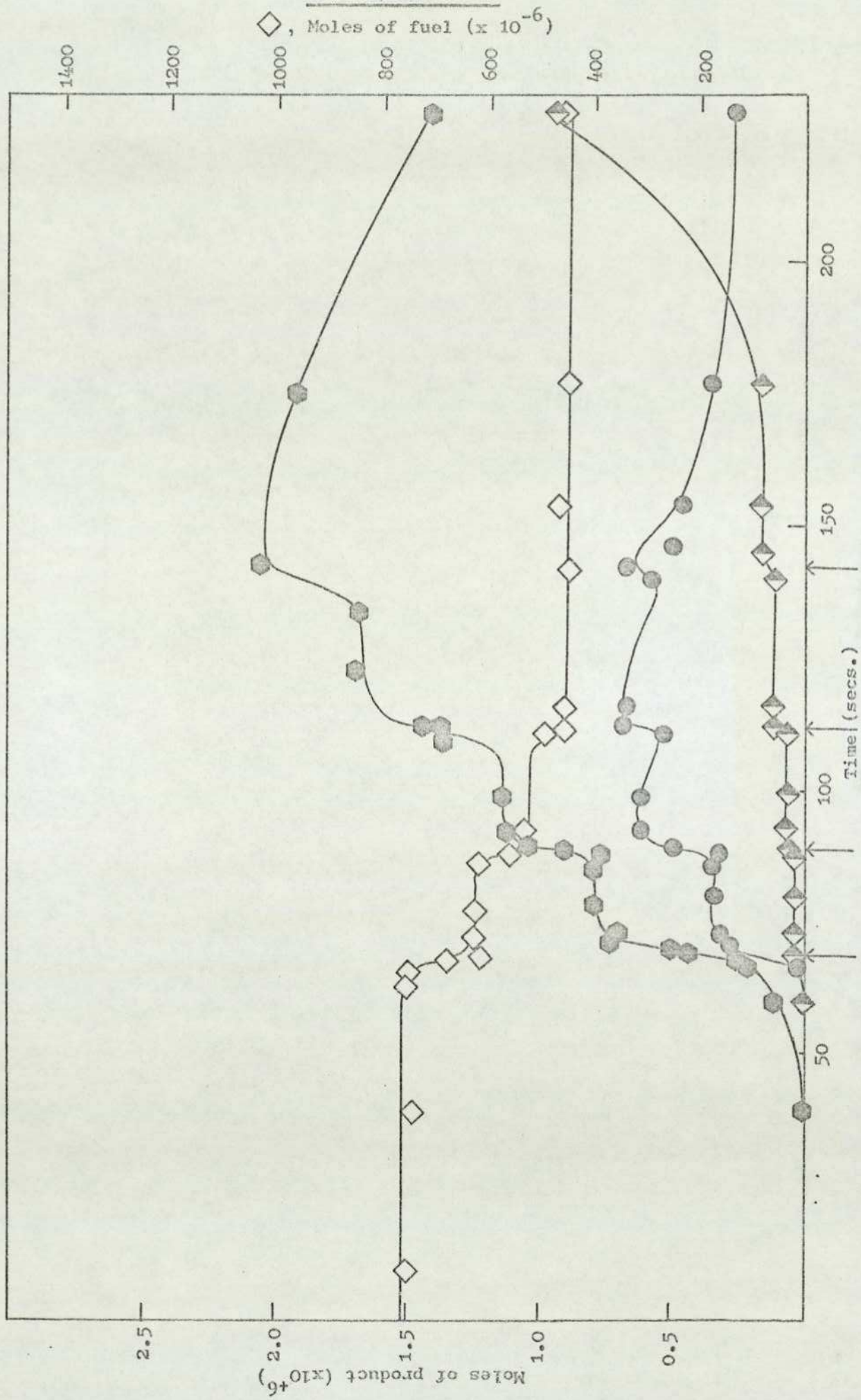


Figure 3.44

The variation with time of the yields of methyl vinyl ketone, buta-1,3-diene and propane plus the fuel consumption (300°C, 150 torr)



At 309°C the first cool flame is followed by two successive weak cool flames and then a normal fourth and fifth cool flame (figure 3.57). Furthermore, under these conditions a shoulder on the first cool flame becomes apparent. Product analyses were carried out until after the passage of the fourth cool flame as shown in figures 3.45 - 3.50. The product formation prior to and during the passage of the first cool flame is similar to that at 300°C, except that the yields of alkenes are greater. However, after the first cool flame and during the weak second and third cool flames, the concentrations of most products increase at steady rates (c.f. behaviour at 300°C) while the passage of the fourth cool flame is associated with an increase in the rate of formation of most of the products.

It is interesting to note that the observed oscillatory behaviour of the concentration of certain products during the reaction at 300°C is considerably less pronounced at 309°C. The concentration of methyl ethyl ketone, which shows an abrupt decrease immediately prior to the first cool flame, builds up continuously throughout the passage of the second and third cool flames but shows another less marked decrease prior to the passage of the fourth cool flame (figure 3.49).

Figure 3.50 shows that a rapid, but continuous, consumption of fuel accompanies the passage of the first three cool flames (ca. 47%), but again there appears to be no fuel consumed during the passage of the fourth cool flame.

Figure 3.45

The variation with time of the yields of but-1-ene, trans but-2-ene and cis but-2-ene (309°C, 150 torr)

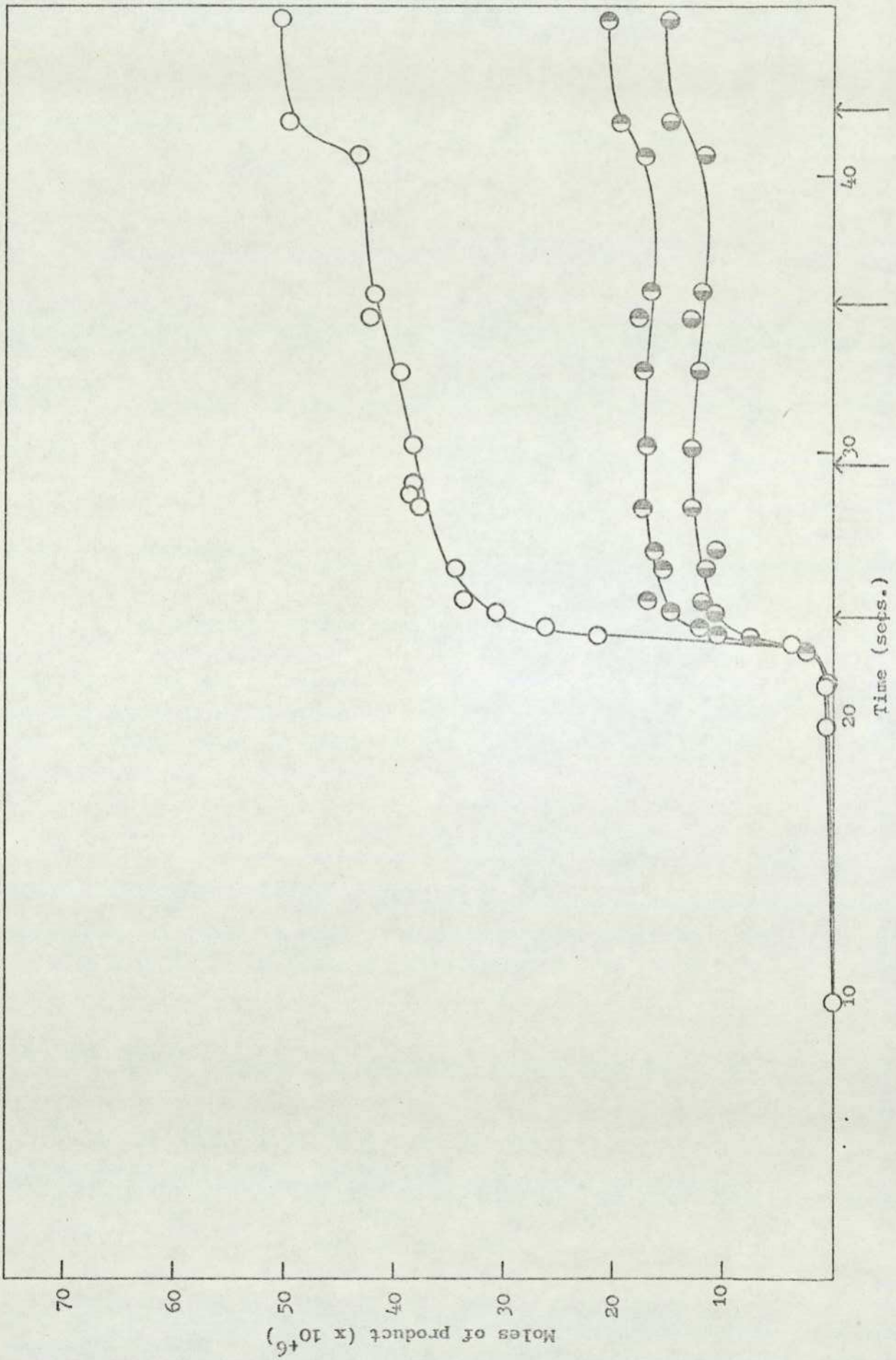


Figure 3.46

The variation with time of the yields of methanol, acetaldehyde, ethylene and methane (309°C, 150 torr)

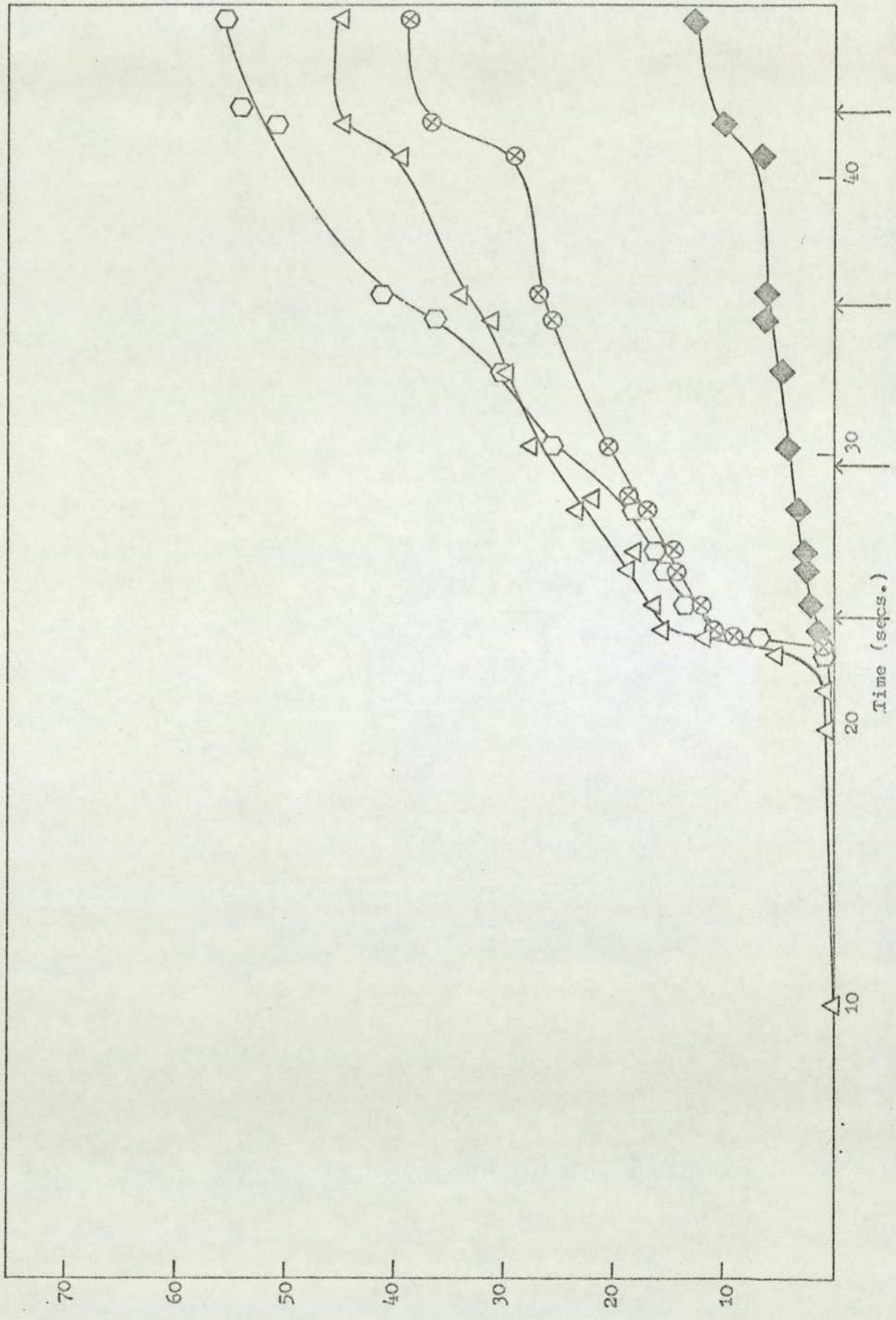


Figure 3.47

The variation with time of the yields of propene, acrolein, propionaldehyde and acetone (309°C, 150 torr)

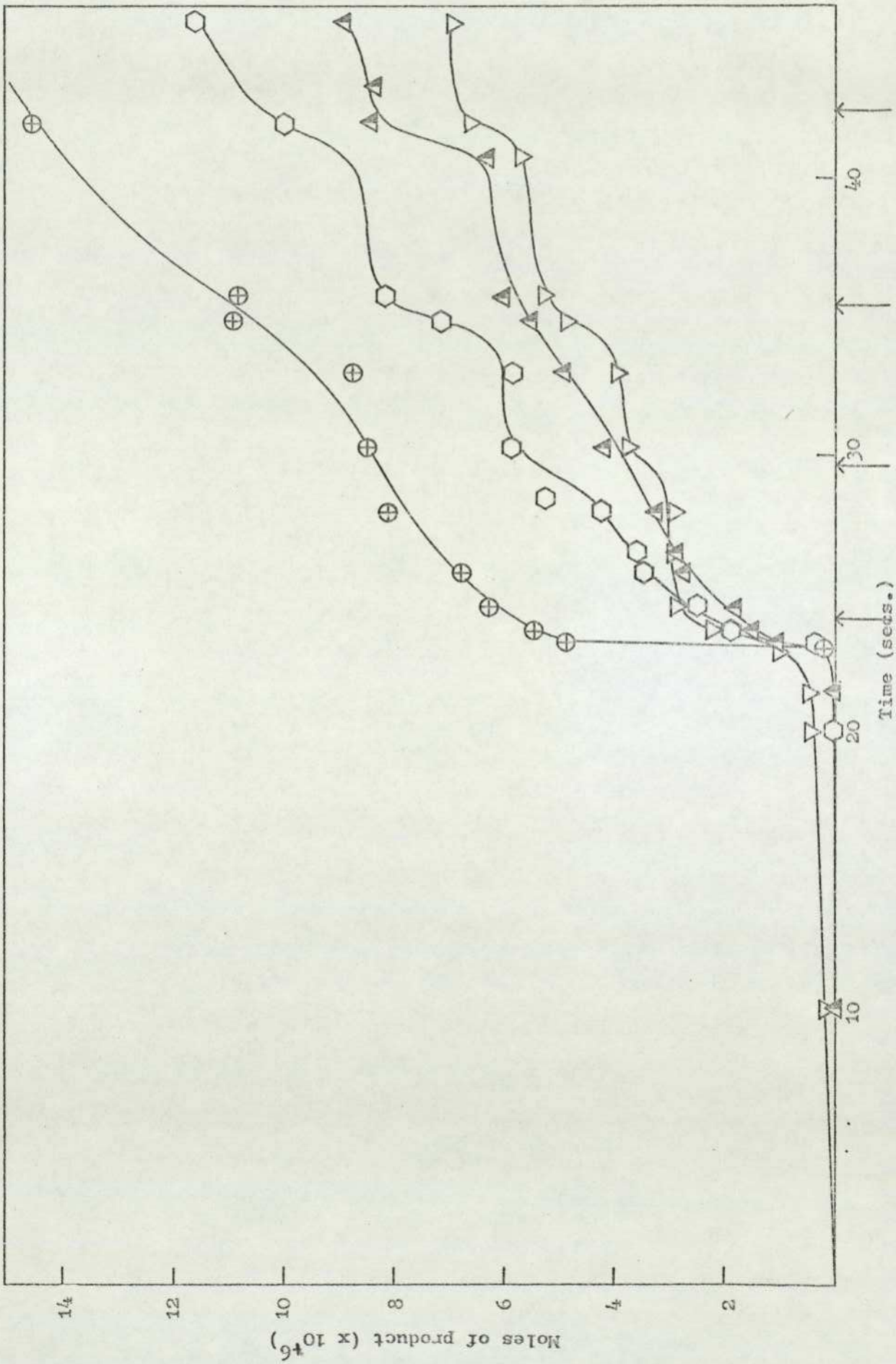


Figure 3.48

The variation with time of the yields of trans 2,3-dimethyloxiran, cis 2,3-dimethyloxiran, 2-ethyloxiran 2-methyloxetan, tetrahydrofuran and 2-methyloxiran (309°C, 150 torr)

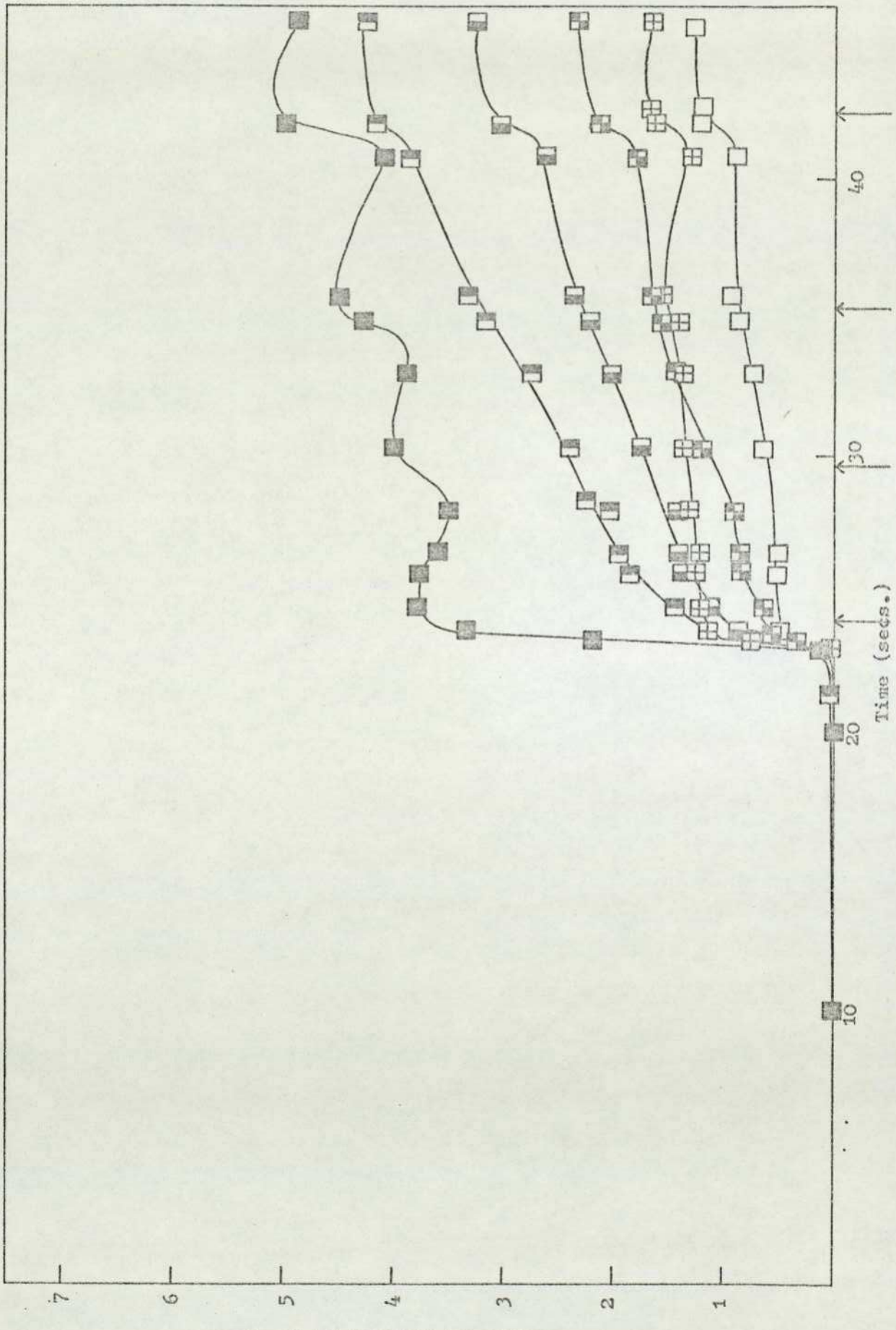


Figure 3.49

The variation with time of the yield of methyl ethyl ketone (309°C, 150 torr)

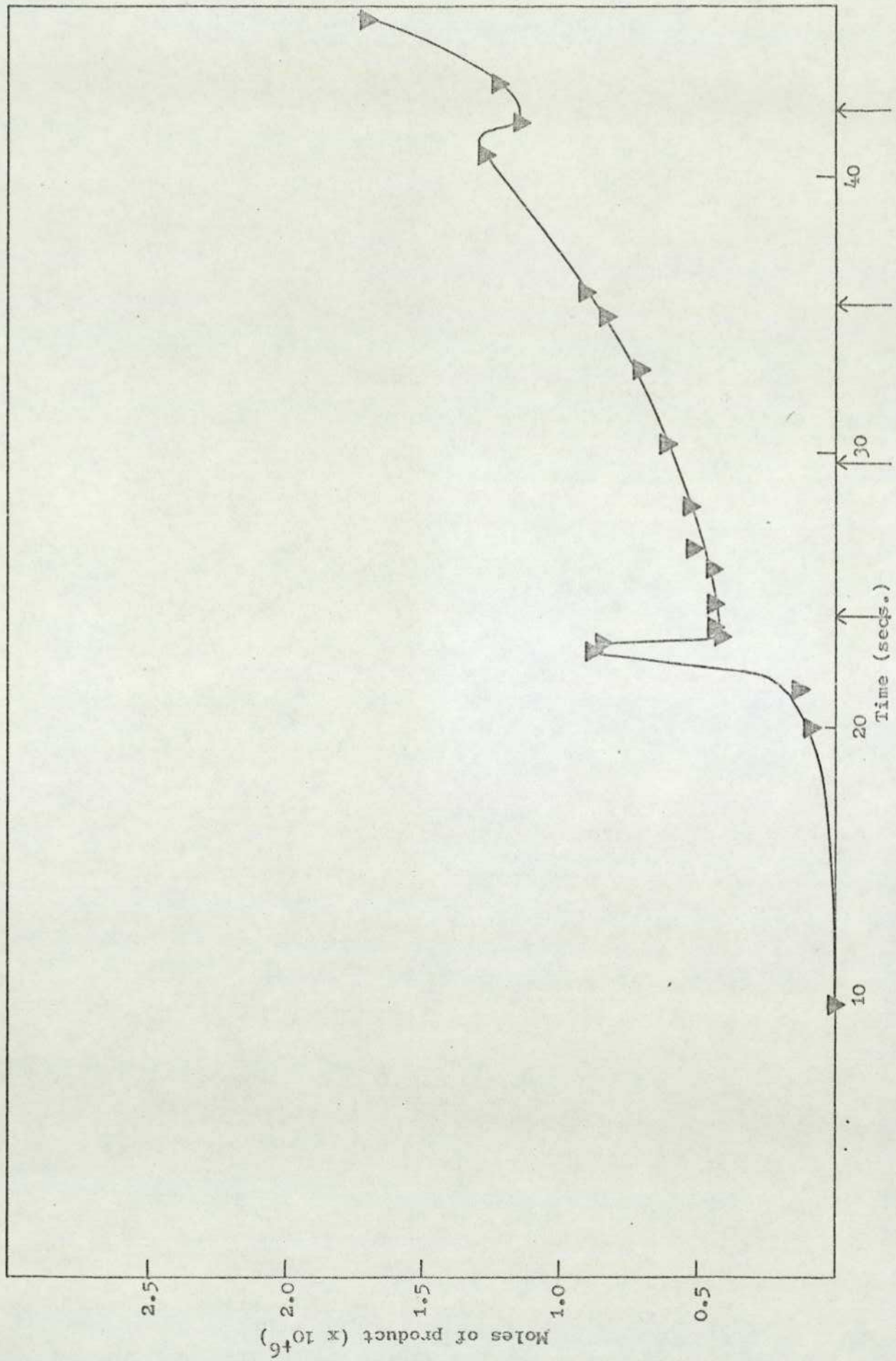
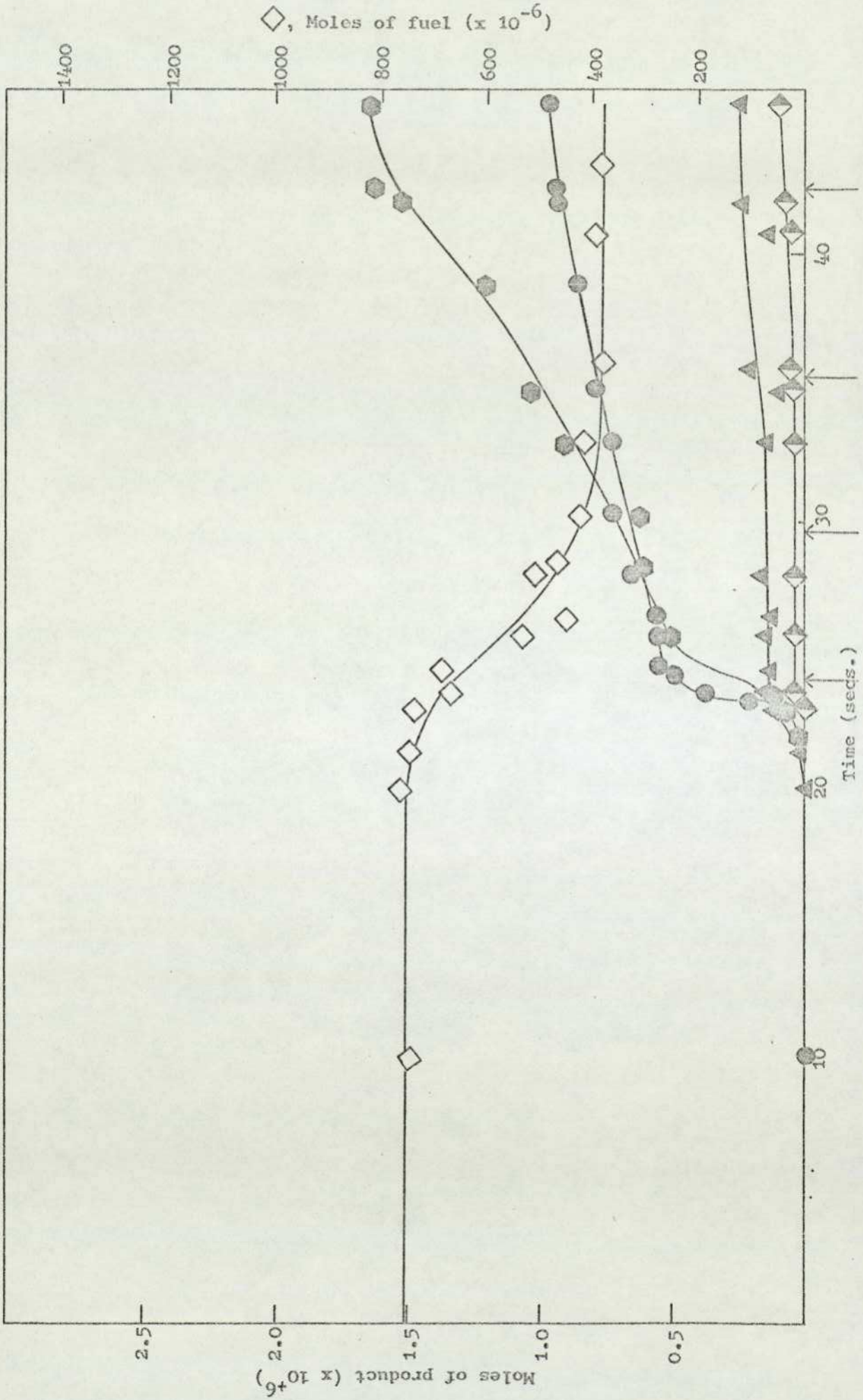


Figure 3.50
The variation with time of the yields of methyl vinyl ketone, buta-1,3-diene, n-butyraldehyde and propane plus the fuel consumption (309°C, 150 torr)



At 360°C the first cool flame is followed by rapid slow combustion (figure 3.57) and the variation of pressure with time is reflected in most of the product concentration-time curves over the first ten seconds of reaction (figures 3.51 - 3.56).

The most notable differences at this temperature are that the rates of accumulation of products are increased and that the butenes account for ca. 60% of the products detected immediately after the passage of the first cool flame (c.f. ca. 30% at 300°C). After the initial increase in concentration associated with the cool flame and the onset of the rapid slow combustion, most products continue to be formed throughout the reaction although at a lower rate. However, the concentrations of products such as the butenes, buta-1,3-diene, tetrahydrofuran and 2-methyloxetan pass through maximum values after ca. 8 seconds and continue to fall as the reaction proceeds. Once again it is clear that these products undergo further reaction which may be responsible for the continued increase in concentration of products such as O-heterocycles, carbonyl compounds and lower alkenes in the late stages of reaction.

Figure 3.55 shows that the first cool flame accounts for a consumption of ca. 22% of the original n-butane.

It is interesting to note that at 360°C, the concentration of methyl ethyl ketone shows no decrease at any stage in the reaction (figure 3.56), and that at all the initial temperatures investigated, methane is not detected until the first cool flame propagates.

Figure 3.51

The variation with time of the yields of but-1-ene, trans but-2-ene, cis but-2-ene and methanol (360°C, 150 torr)

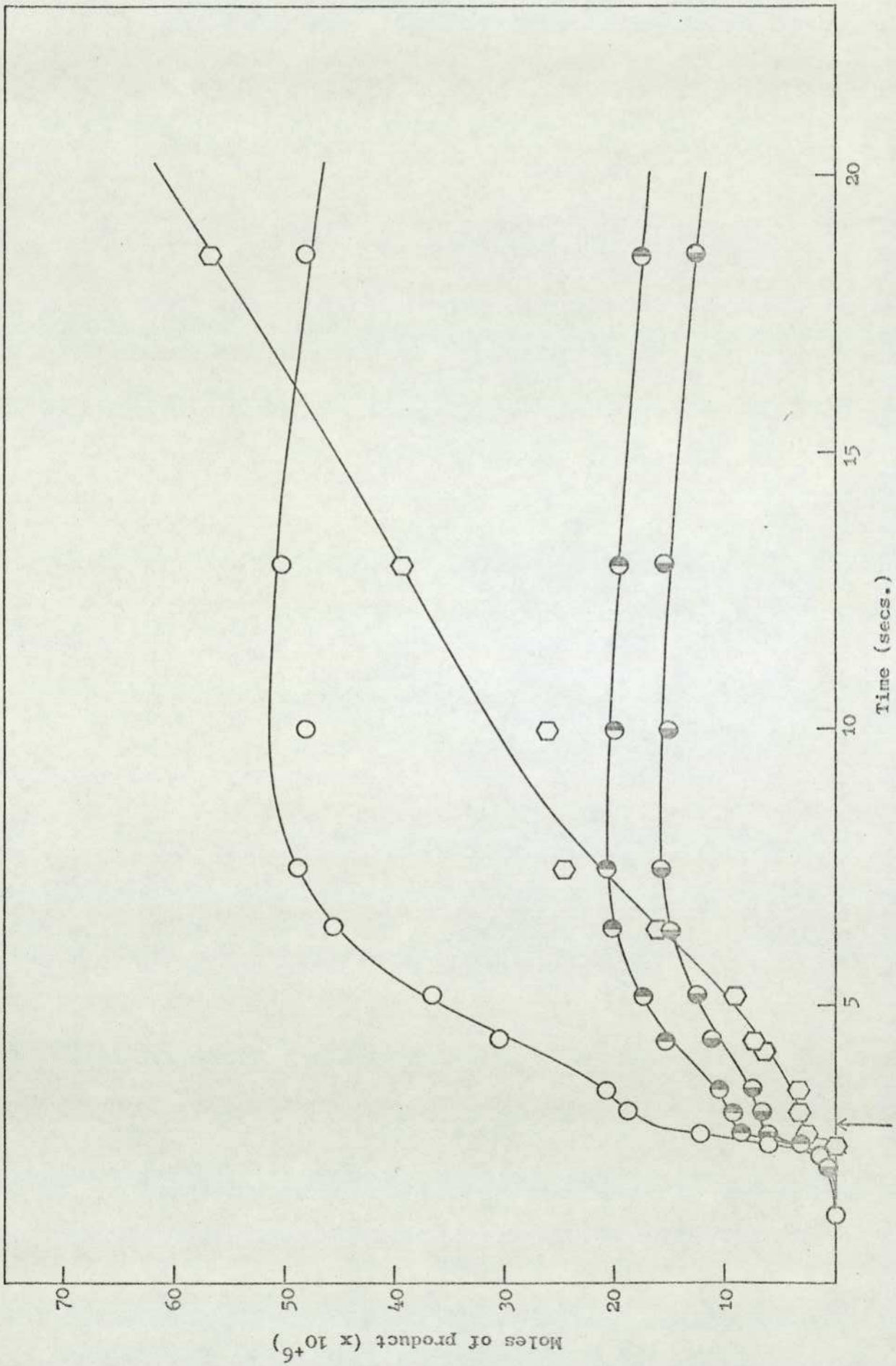


Figure 3.52

The variation with time of the yields of acetaldehyde, ethylene, acrolein and methane (360°C, 150 torr)

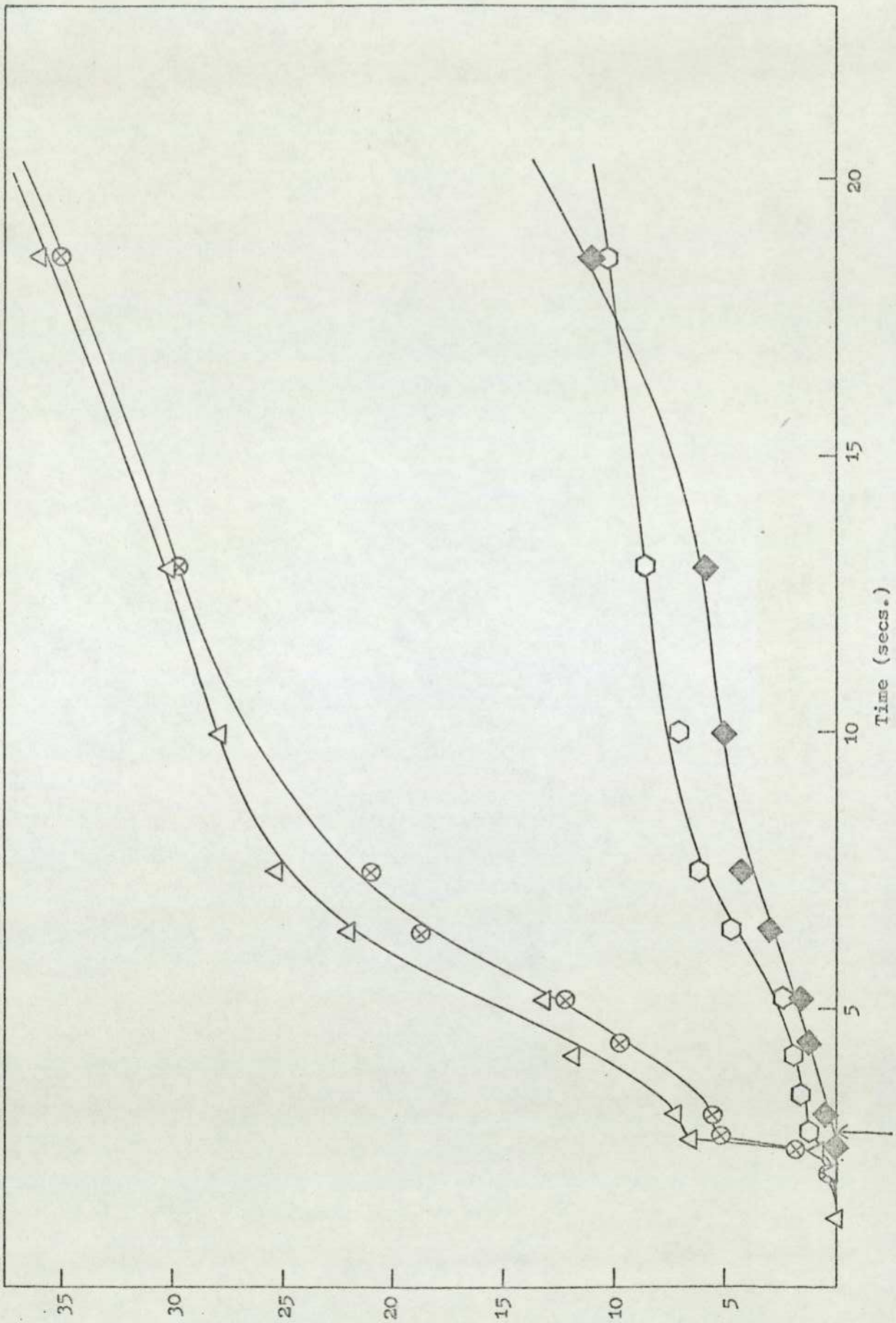


Figure 3.53

The variation with time of the yields of propene, propionaldehyde and acetone (360°C, 150 torr)

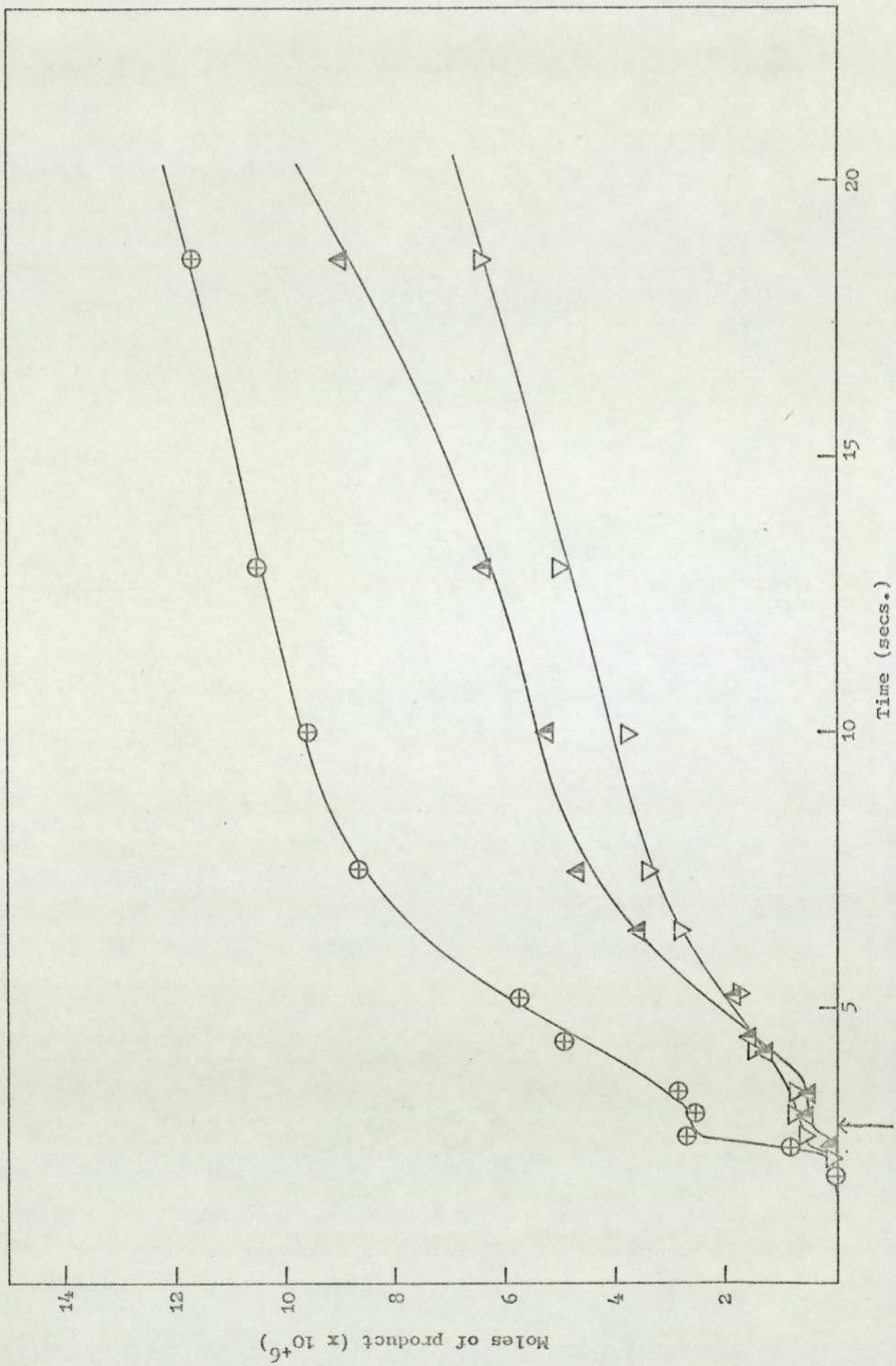


Figure 3.54

The variation with time of the yields of trans 2,3-dimethyloxiran, cis 2,3-dimethyloxiran, 2-ethyloxiran 2-methyloxetan, tetrahydrofuran and 2-methyloxiran (360°C, 150 torr)

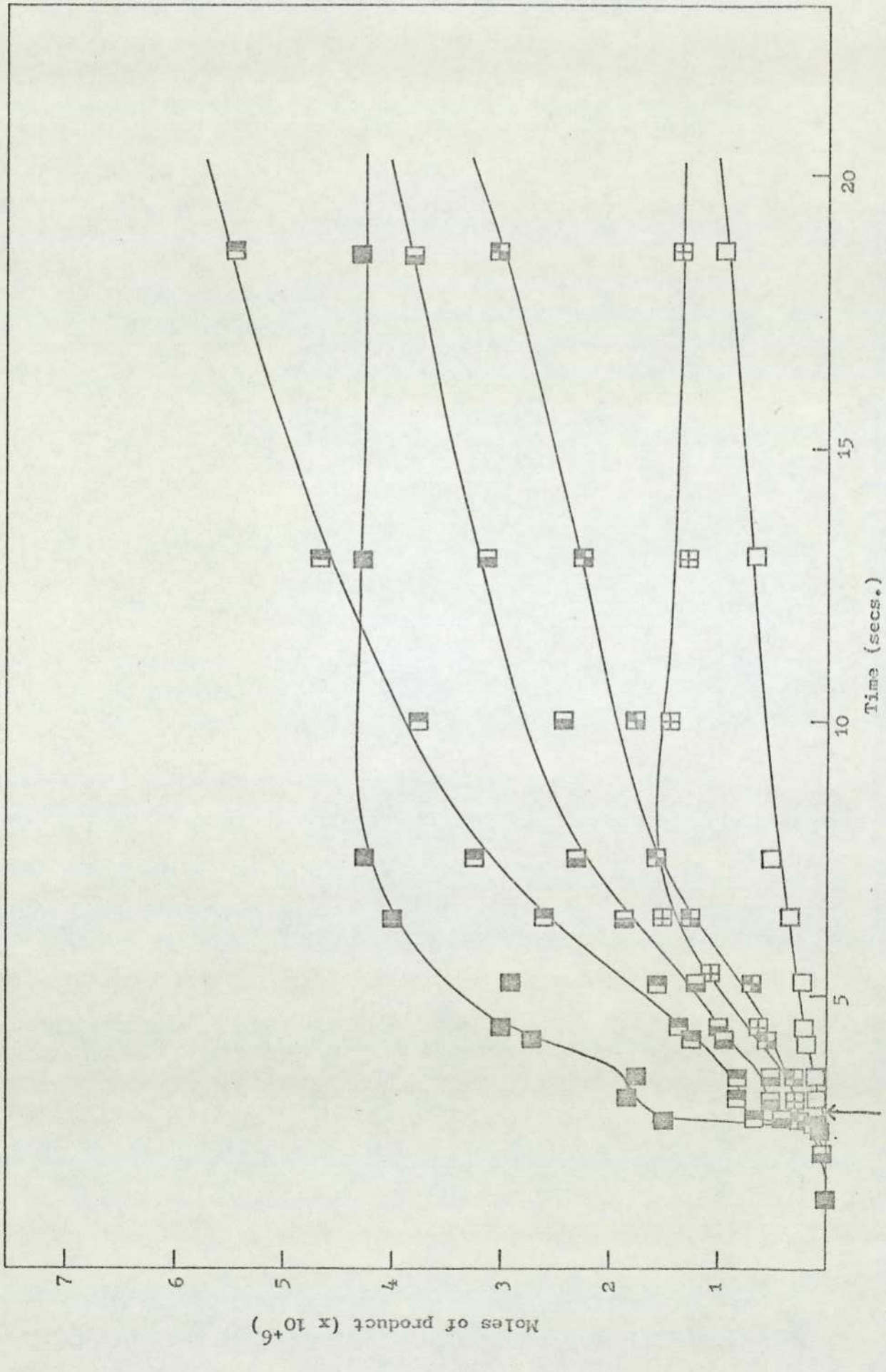


Figure 3.55

The variation with time of the yields of methyl vinyl ketone, buta-1,3-diene, n-butyraldehyde and propane plus the fuel consumption (360°C, 150 torr)

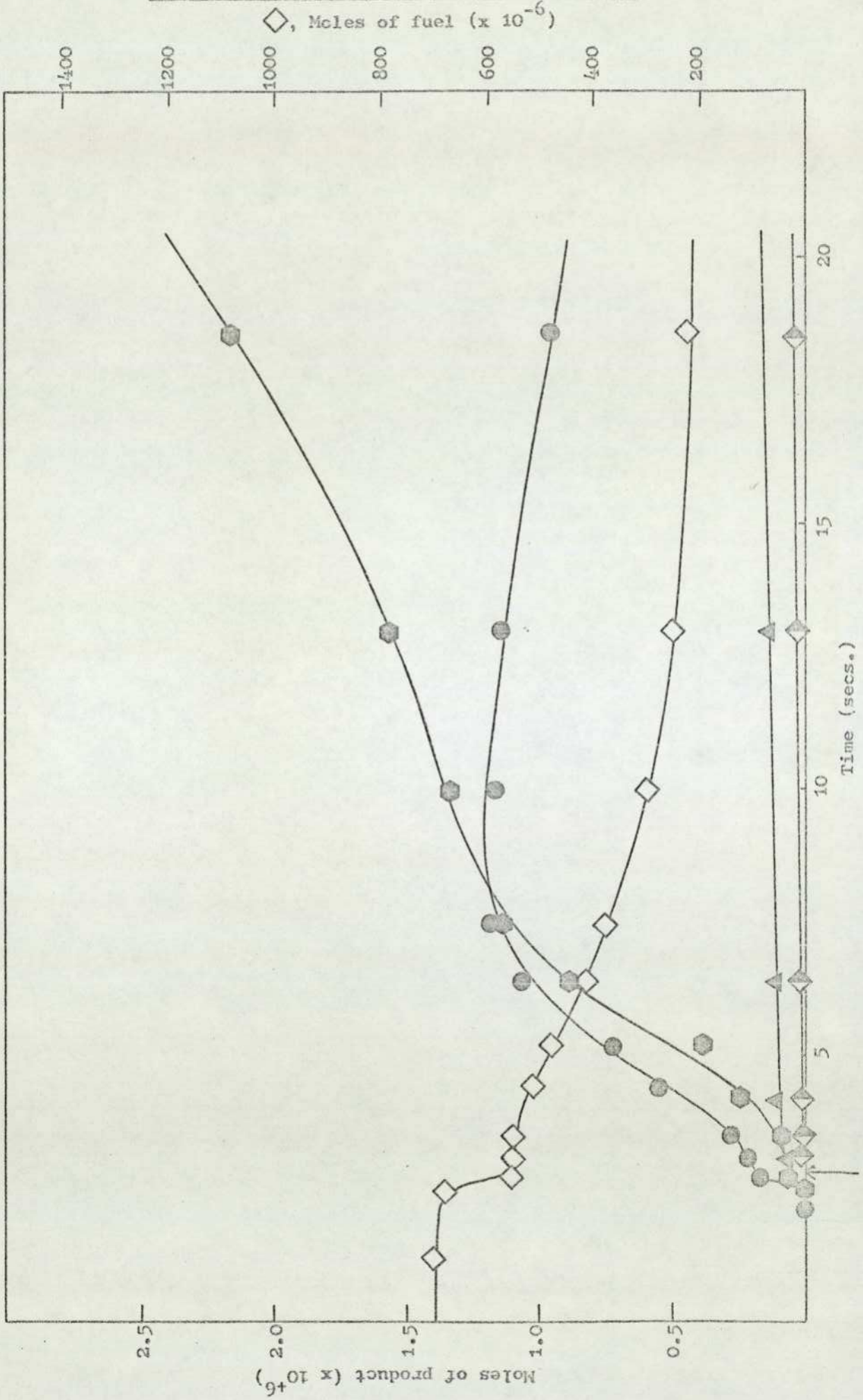


Figure 3.56

The variation with time of the yield of methyl ethyl ketone (360°C, 150 torr)

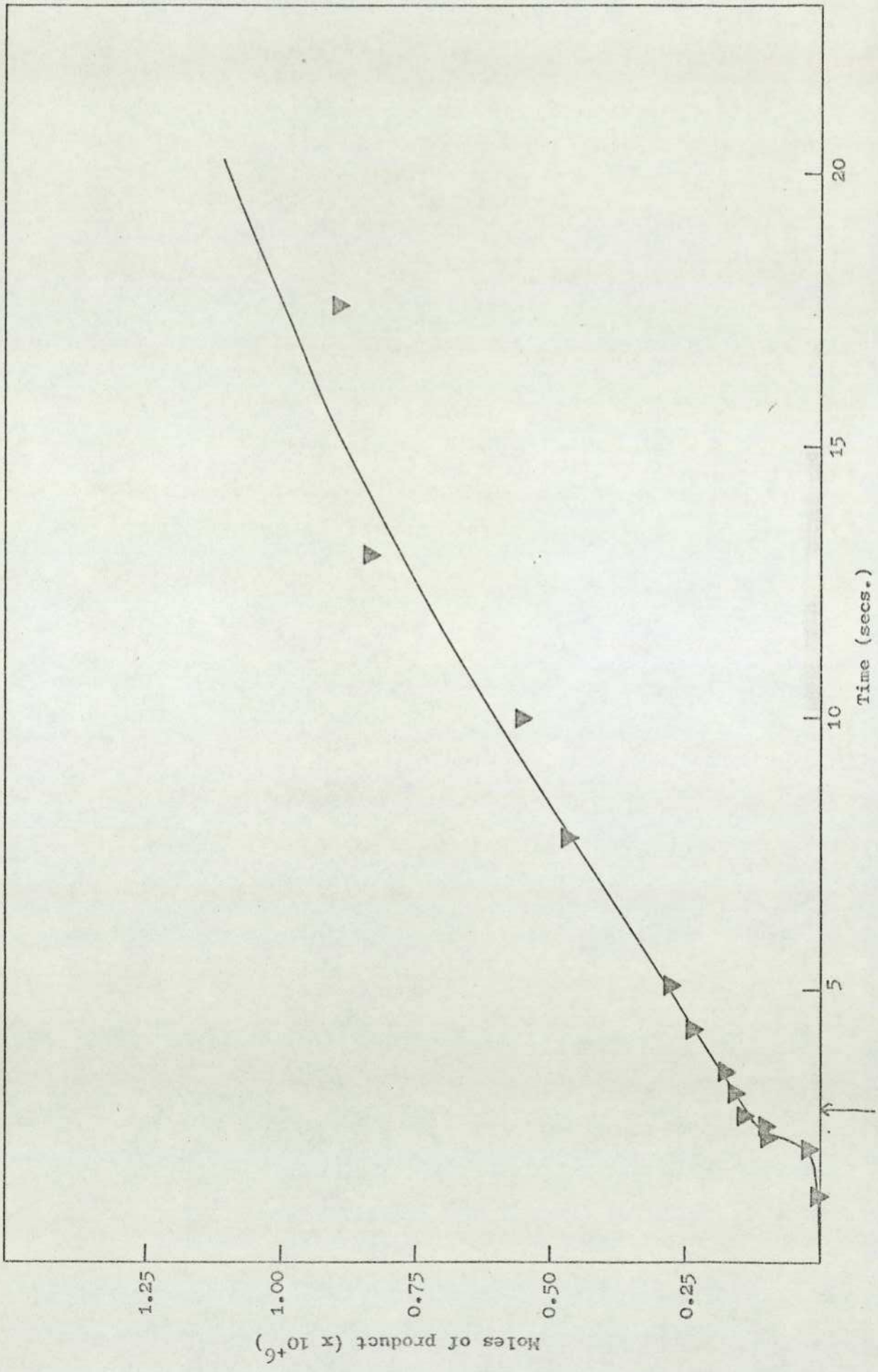
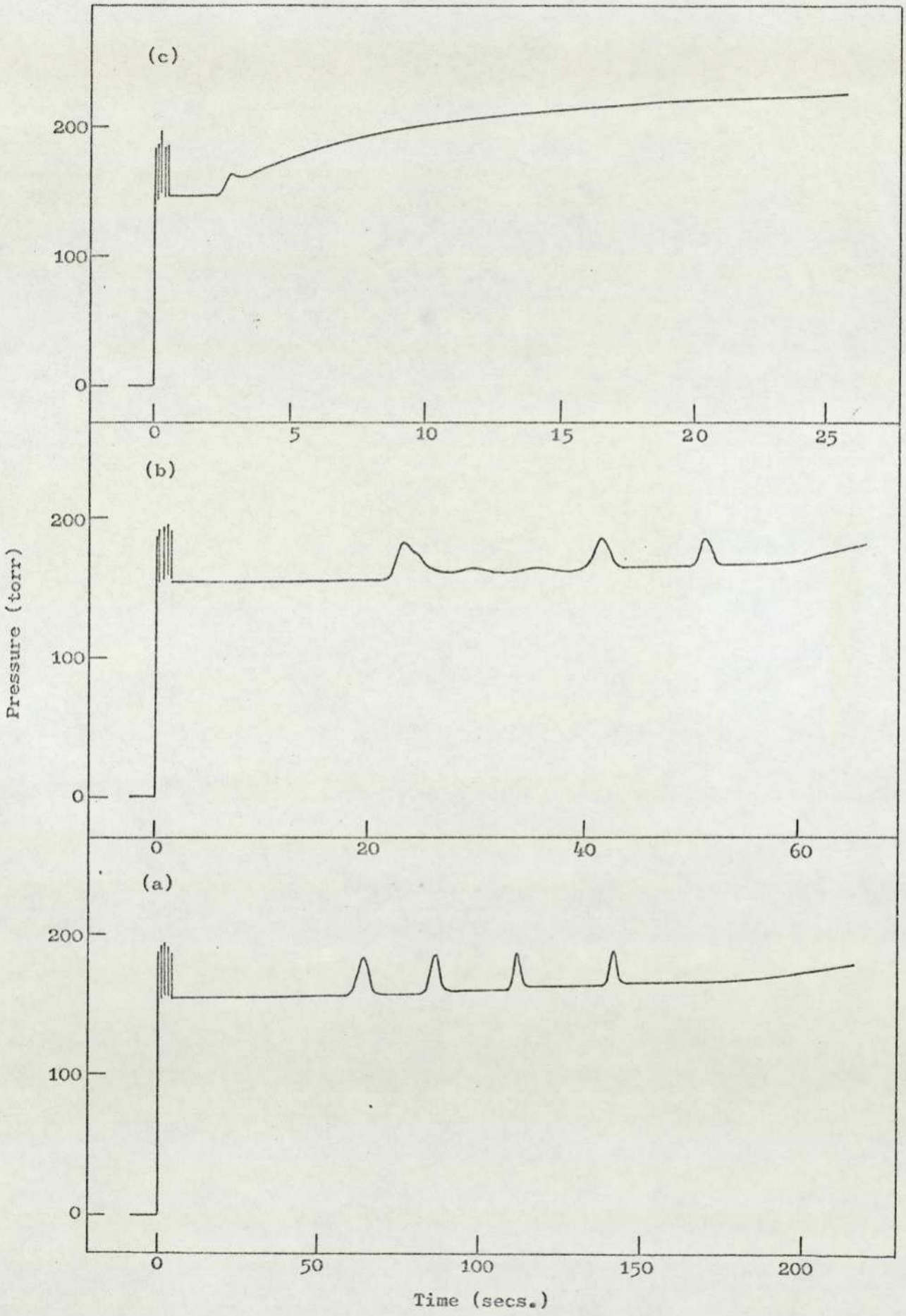


Figure 3.57

Pressure-time recordings in the cool flame region at (a) 300°C (b) 309°C and (c) 360°C (initial pressure = 150 torr)



3.2.2 Product distribution during the early stages of reaction

During the early stages of reaction it can reasonably be assumed that the products result from primary oxidation reactions only, since the products and radicals formed at this stage are present in very low concentrations. A study of the nature and distribution of products during the induction period preceding the first cool flame will therefore yield useful information concerning the primary chain propagation reactions. Numerous analyses were carried out, therefore, over a range of initial temperatures and pressures at a stage when the fuel consumption is less than 1%.

In order to make a direct comparison with the results of previous studies carried out under similar conditions [36,45], the yield of each product is expressed as a percentage of the total products detected, measured in g. atoms of carbon. In the early stages of reaction it is difficult to measure directly the amount of fuel consumed, so it has been assumed that the g. atoms of carbon detected in the products are equal to those in the fuel consumed. (This is not strictly true, however, in view of the likely presence amongst the products at this stage of undetected formaldehyde and oxides of carbon). The approximate fuel conversion is thus given by the ratio:

$$\frac{\Sigma(\text{g. atoms of carbon in detected products})}{\text{g. atoms of carbon in initial n-butane}}$$

3.2.2.1 The variation with respect to initial temperature

The variation of the percentage yields of products with initial temperature in the range of 285 - 380°C is shown in figures 3.58 - 3.61. At each temperature the initial pressure of the reactants was varied to maintain the molar concentration at 7.60×10^{-4} moles of n-butane and 1.520×10^{-3} moles of oxygen.

At 285°C the major products, acetaldehyde, acetone, but-1-ene and

but-2-ene, are formed in approximately equal amounts and together they account for ca. 90% of the total products. However, as the initial temperature is increased to 310°C the yields of acetaldehyde and acetone fall dramatically whilst the formation of the conjugate alkenes becomes more pronounced. This behaviour continues as the temperature is increased still further, although it becomes less marked. At 380°C, acetaldehyde and acetone together account for only 4% of the total products (c.f. ca.45% at 300°C) whereas but-1-ene and but-2-ene together account for ca. 85% (c.f. ca.45% at 300°C). Furthermore, as the initial temperature is increased from 285 to 380°C, the ratio of the yields of but-1-ene to but-2-ene is reasonably constant (Table 3.3).

The behaviour of the minor products also shows some interesting variations. The total yield of C_4 O-heterocycles increases by ca. 50% as the initial temperature is increased from 285 to 380°C although they do not all vary in the same manner. Thus, for example, the yield of 2,3-dimethyloxiran passes through a maximum at 310°C, whereas the yields of 2-methyloxetan and tetrahydrofuran increase throughout the temperature range. The yield of lower alkenes also increases steadily as the initial temperature is increased, whereas the yield of propionaldehyde declines markedly between 310 and 360°C. In contrast the yields of other products such as buta-1,3-diene, acrolein, n-butyraldehyde and methyl ethyl ketone show only very small variations with increase of temperature.

Figure 3.58

The variation with initial temperature of the percentage yields of but-1-ene, trans but-2-ene, cis but-2-ene and ethylene at <1% fuel conversion

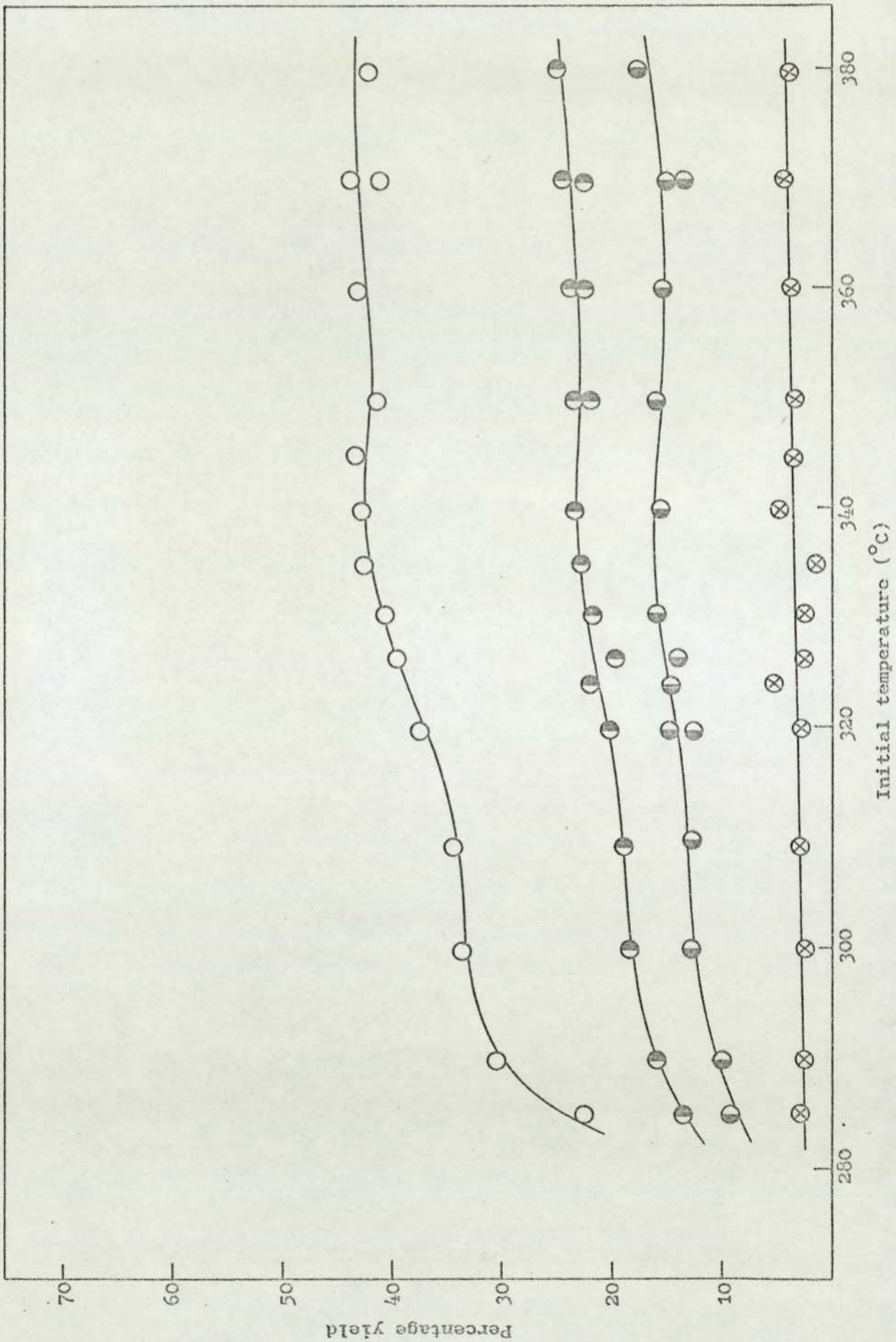


Figure 3.59

The variation with initial temperature of the percentage yields of acetaldehyde, acetone and methyl ethyl ketone at <1% fuel conversion

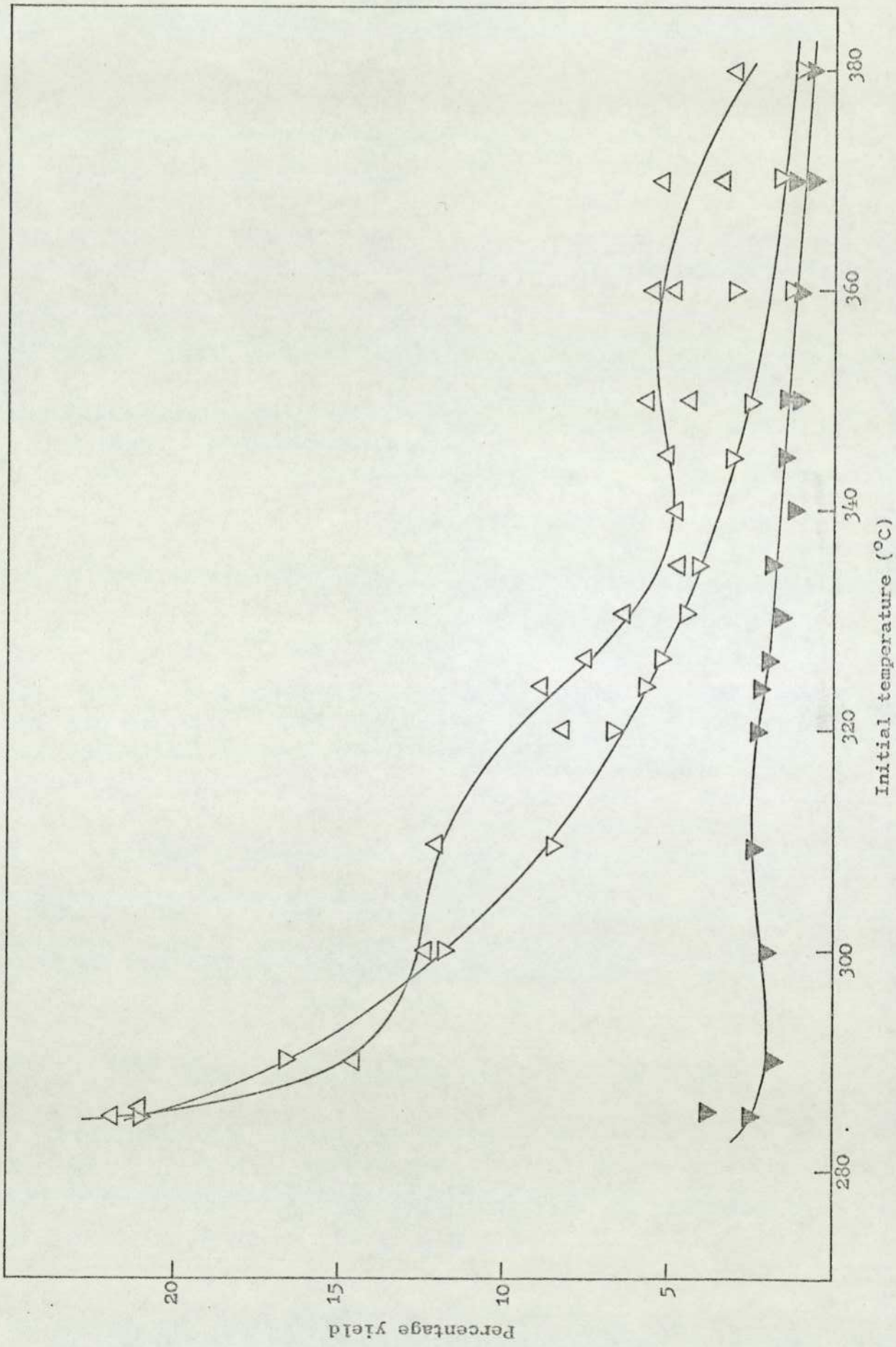


Figure 3.60

The variation with initial temperature of the percentage yields of trans 2,3-dimethyloxiran, cis 2,3-dimethyloxiran 2-ethyloxiran, 2-methyloxetan, tetrahydrofuran and 2-methyloxiran at <1% fuel conversion

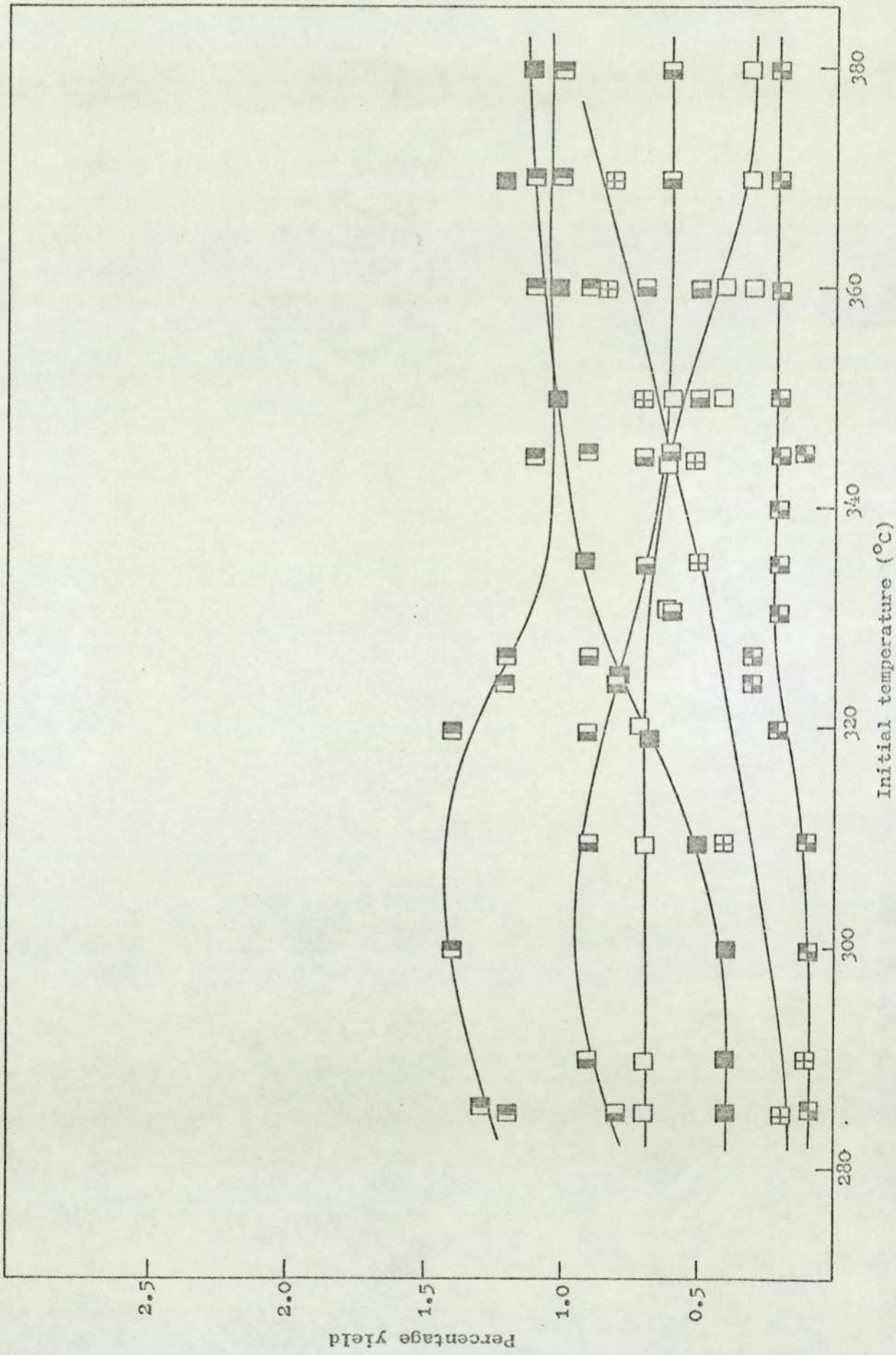


Figure 3.61

The variation with initial temperature of the percentage yields of propene, propionaldehyde and buta-1,3-diene at <1% fuel conversion

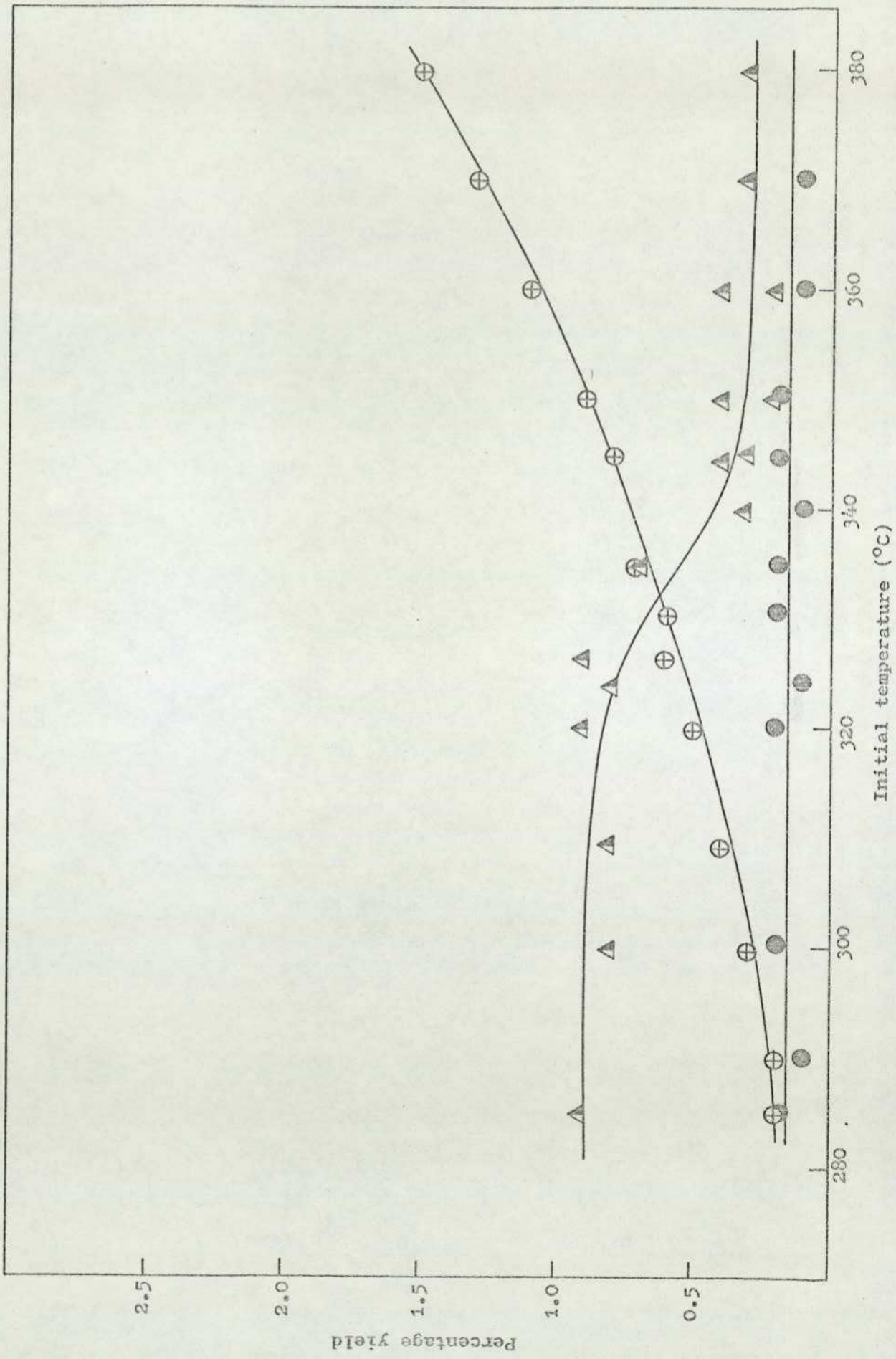


Table 3.3

The variation with temperature of the ratio of the yield of but-1-ene to but-2-ene in the early stages of reaction

Initial temperature	$\frac{\%\text{ yield of but-1-ene}}{\%\text{ yield of but-2-ene (t + c)}}$
285	1.0
300	1.1
320	1.2
340	1.1
360	1.1
385	1.2

3.2.2.2 The variation with respect to initial pressure

Analyses were performed during the induction period over a range of initial pressures at 300°C. The variation of product distribution with initial pressure is not large although certain trends are obvious as shown in Table 3.4. The yields of ethylene, acetaldehyde, 2-methyloxiran, n-butyraldehyde and methyl ethyl ketone all increase as the initial pressure is increased, particularly in the case of the last product, whereas the yields of but-1-ene, but-2-ene, 2,3-dimethyloxiran and methyl vinyl ketone show a slight decrease. The yields of all other products remain unchanged as the initial pressure is varied.

At 360°C, however, the predominant products, but-1-ene and but-2-ene, exhibit no variation with initial pressure, as shown in Table 3.5. Furthermore, the only significant differences from the variation of the product distribution at 300°C is that the yields of acetone and 2-methyloxetan decrease, whereas the yields of acetaldehyde and ethylene remain fairly constant as the initial pressure is increased.

It can be seen that the stage in the reaction at which the analysis was carried out, as indicated by the percentage fuel conversion, varies. This is not considered to invalidate the correlation made between the results, however, since it is reasonable to assume that only primary reactions are involved up to fuel conversions of 1-2%.

Table 3.4

The variation with initial pressure of the initial product distribution at 300°C (<1% conversion)

Product	Initial Pressure (torr)					
	76	91	111	131	148	190
ethylene	2.0	2.0	3.2	2.9	2.2	3.3
propene	0.4	0.2	0.3	0.2	0.2	0.3
but-1-ene	31.0	29.6	24.7	25.3	23.4	26.0
but-2-ene(t)	17.7	17.8	13.8	14.6	13.7	15.3
but-2-ene(c)	8.8	10.3	8.0	8.9	7.7	8.9
buta-1,3-diene	-	0.1	0.1	-	0.1	0.2
acetaldehyde	14.7	12.3	21.1	19.6	21.4	18.1
2-methyloxiran	0.4	0.5	0.6	0.8	0.8	0.9
methanol	1.1	0.6	1.2	0.8	0.9	1.3
propionaldehyde	0.9	1.0	0.9	0.7	0.9	0.9
2,3-dimethyloxiran(t)	2.0	2.0	1.6	1.4	1.5	1.4
acrolein	0.4	0.4	0.4	0.3	0.3	-
acetone	15.8	17.4	17.5	18.5	18.6	16.1
2,3-dimethyloxiran(c)	1.0	1.1	1.0	0.9	1.0	0.7
2-ethyloxiran	0.2	0.2	0.2	0.2	0.2	0.2
2-methyloxetan	0.8	0.8	0.7	0.8	0.7	0.5
n-butyraldehyde	0.1	0.1	0.3	0.3	0.3	0.4
tetrahydrofuran	0.3	0.4	0.3	0.3	0.3	0.2
methyl ethyl ketone	-	0.6	3.1	2.4	4.7	4.4
methyl vinyl ketone	2.4	2.4	1.3	1.4	1.5	0.9
% fuel conversion	0.1	0.6	1.7	0.9	0.6	0.4

Table 3.5

The variation with initial pressure of the initial product distribution at 360°C (<1% conversion)

Product	Initial Pressure (torr)					
	62	91	101	134	150	188
ethylene	1.7	3.5	3.9	5.4	3.8	4.2
propene	1.1	1.2	1.2	2.3	1.0	1.0
but-1-ene	40.1	41.0	40.8	41.8	42.2	39.6
but-2-ene(t)	22.7	21.8	24.5	24.5	23.8	23.6
but-2-ene(c)	15.4	16.3	17.1	17.1	16.5	16.3
buta-1,3-diene	0.1	0.1	0.1	0.1	0.1	0.3
acetaldehyde	5.6	5.8	4.3	3.5	4.7	4.2
2-methyloxiran	0.1	0.3	0.1	0.2	0.4	0.5
methanol	0.7	0.6	0.7	0.4	0.5	0.8
propionaldehyde	0.3	0.2	0.4	0.2	0.3	0.5
2,3-dimethyloxiran(t)	1.8	1.4	1.1	0.7	0.9	1.0
acrolein	0.5	0.4	0.4	0.2	0.2	0.3
acetone	3.4	2.3	1.8	1.1	1.6	1.3
2,3-dimethyloxiran(c)	1.3	0.9	0.7	0.4	0.6	0.8
2-ethyloxiran	0.5	0.3	0.2	0.1	0.3	0.3
2-methyloxetan	2.9	2.1	1.3	0.8	1.0	1.3
n-butyraldehyde	0.2	0.3	0.2	0.2	0.5	0.8
tetrahydrofuran	1.2	0.8	0.5	0.3	0.4	1.0
methyl ethyl ketone	0.2	0.7	0.6	0.8	1.1	1.8
methyl vinyl ketone	-	0.2	-	0.1	0.1	0.3
% fuel conversion	0.6	0.5	0.4	1.1	0.3	0.1

SECTION 4

DISCUSSION

SECTION 4

		Page No.
4.1	The kinetic and thermal properties of the oxidation of n-butane	200
4.1.1	The ignition diagram	200
4.1.2	The characteristics of the first cool flame	202
4.1.3	The thermal characteristics of cool-flame propagation	212
4.1.4	The characteristics of subsequent cool flames	220
4.1.5	The transition to hot ignition	225
4.2	The chemical interpretation of cool-flame oxidation	230
4.2.1	Product formation during the early stages of reaction	230
	4.2.1.1 The effect of temperature	240
	4.2.1.2 The effect of pressure	244
4.2.2	Product formation during cool-flame propagation	246
4.3	Conclusions	251
4.4	Future work	257

4.1 The kinetic and thermal properties of the oxidation of n-butane

4.1.1 The ignition diagram

The lobes which occur in the low temperature cool flame/multi-stage ignition boundary of most hydrocarbon + oxygen systems are due to the repeated waxing and waning of the net branching factor as the initial temperature is increased. This repeated fluctuation may be considered to be due to the onset of further branching and non-branching reactions which have successively higher activation energies. It is possible to visualise these branching processes as either involving different branching agents or different modes of formation of the same branching agent and from these considerations Antonik and Lucquin[60] have recently suggested that four basic branching processes, corresponding to the L_0 - L_3 lobes, can be identified. These processes are believed to predominate within specified temperature regions and the number which can occur for any particular hydrocarbon + oxygen system depends principally on the molecular structure of the fuel. For mixtures of n-butane + oxygen in the molar ratio 1:2, the cool flame/multi-stage ignition boundary exhibits a strong lobe in the temperature range 280 - 315°C and a much weaker lobe between 315 - 390°C. A comparison of these temperature ranges with those indentified for the lobes of other hydrocarbon + oxygen systems (Table 4.1), indicates that these correspond to the L_1 and L_2 branching mechanisms respectively. The L_1 mechanism is believed to involve primary peroxidation which is catalysed by hydrogen donors (see p.41). Thus compounds such as aldehydes, which contain a labile hydrogen atom, would be expected to be important intermediates during the reactions which precede the non-isothermal phenomena. The analytical results do indeed indicate that at low initial temperatures (ca. 300°C) acetaldehyde is an important intermediate during the induction period preceding the cool

Table 4.1

The temperature ranges associated with the lobes observed for various hydrocarbon + oxygen mixtures

Mixture \ Lobe	L_o	L_1	L_2	L_3	Reference
n-butane + oxygen (1:2)	———	280-315	315-390	———	Present study
n-butane + oxygen (1:1)	———	270-310	310-380	———	55
isobutane + oxygen (1:2)	290-315	315-325	325-380	380+	45
n-pentane + oxygen (3:4)	———	255-315	315-380	380+	52
2-methylpentane + oxygen (1:2)	250-270	270-310	310-350	———	95
neopentane + oxygen (1:1)	———	———	310-400	400+	49

flame. The L_2 mechanism is considered to involve the secondary peroxidation of aldehydes and again these compounds would be expected to be important intermediates. At ca. 360°C, acetaldehyde is in fact the third most abundant intermediate product during the induction period of the first cool flame; only but-1-ene and but-2-ene are more important.

Further inspection of the ignition diagram shows that the L_1 lobe occurs within the temperature range which is associated with intense, well-resolved multiple cool flames, whereas the L_2 lobe is associated with the upper single cool-flame region. This is in accordance with the suggestion made by Antonik and Lucquin[60] that the "reactivity" of the first cool flame increases as the initial temperature is increased and as such varies inversely with periodicity.

The present studies clearly refute the suggestion that the number of lobes exhibited at the cool flame/ignition boundary can be directly correlated with the number of alternative modes of alkylperoxy radical rearrangement[58]. This theory suggests that for n-butane three lobes should occur corresponding to 1:4, 1:5 and 1:6 hydrogen transfer. Since only two lobes are observed experimentally it is clear that this suggestion is not tenable.

In contrast with the ignition diagrams obtained when isobutane[45], 2,3-dimethylbutane[51] or 2-methylpentane[95] are used as the fuel, the lobes are not reflected at the slow combustion/cool flame boundary. In the case of n-butane, therefore, the change in mechanism responsible for the negative temperature coefficient associated with the L_1 lobe does not extend to low pressures.

4.1.2 The characteristics of the first cool flame

The induction period preceding the first cool flame may reasonably be assumed to be indicative of the rate of the reactions

which subsequently lead to the attainment of the critical rate of branching required for the occurrence of the cool flame. It has been seen that at constant initial temperature, the induction period decreases monotonically with increase of initial pressure and can be expressed by the relationship:

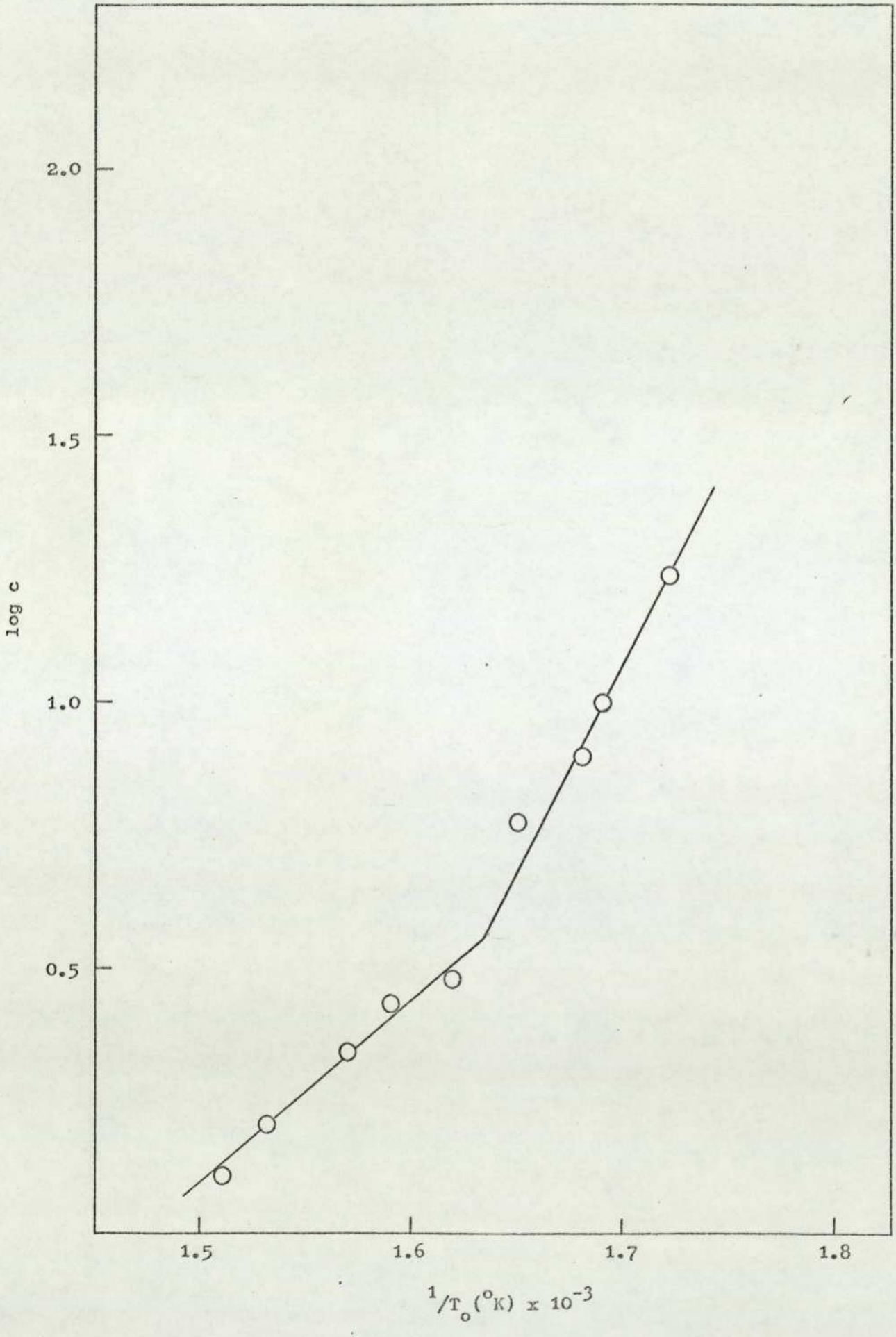
$$\tau_1 = kp_o^{-n} + c \qquad (4.1)$$

Recent studies [45,52] have shown that the constants in this relationship show marked changes as the initial temperature is increased and it has been suggested that these may be associated with a change in the branching mechanism. Although computational evaluation of these constants has not been carried out in the present studies, some information about the constant c has been obtained by assuming that $\tau_1 \approx c$ at initial pressures near to the cool flame/ignition boundary where changes in the branching mechanism are most clearly manifested. Equation 4.1 predicts that at a given initial temperature, τ_1 will become asymtotic to c as p_o is increased. Figures 3.4 and 3.5 show that τ_1 does indeed asymptote to a value which varies with the initial temperature. Approximate values of the constant c have thus been obtained at an initial pressure of 200 torr and the variation of log c with the reciprocal of the absolute initial temperature is shown in figure 4.1. It is interesting to note that the relationship displays two linear portions. This agrees with the computed results obtained from the study of the oxidation of isobutane [45] under similar experimental conditions. In this work [45], it was suggested that the value of c is, theoretically, the shortest time in which the critical rate of branching required for cool flame propagation can be attained and as such it would be expected to be closely related to the branching mechanism in operation. The fact that the above relationship displays two linear portions probably indicates that different branching mechanisms are associated with the cool-flame temperature regions

Figure 4.1

The variation of log c with $^1/T_o$

at p_o = 200 torr



on either side of the discontinuity which occurs at ca. 335°C. Indeed, these temperature ranges correspond closely to those associated with the L_1 and L_2 lobes.

The variation of τ_1 with the initial temperature is also informative. Yantovskii[96] has suggested that the relationship between these parameters can be expressed in the form:

$$\tau_1 = Ke^{E_{eff}/RT_o} \qquad (4.2)$$

where K is a constant, E_{eff} is the overall effective activation energy, R is the gas constant and T_o is the absolute initial temperature. The variation of $\log \tau_1$ with $^1/T_o$ is indeed linear, although it can be seen from figure 4.2 that at any initial pressure the relationship displays two linear portions. No doubt this discontinuity also indicates the occurrence of a change in mechanism. The variation with initial pressure of the initial temperature at which the discontinuity occurs is shown plotted on the ignition diagram for System I in figure 4.3. It is clear that the mechanism which predominates below the curve illustrated in figure 4.3, is associated with the temperature range within which the L_1 lobe occurs, whereas the mechanism which predominates above the curve is associated with the L_2 lobe. It is also extremely interesting to note that the position and shape of this curve is almost identical to that obtained for the initial conditions at which cool flames change from propagating from the walls of the reactor to propagating from the centre of the reactor, (c.f. figure 3.29). This point is discussed in more detail in section 4.1.3.

The value of E_{eff} at low initial temperatures is ca.46 kcal.mole^{-1}, whereas at high initial temperatures it varies from ca. 15 to 25 kcal.mole^{-1} as the initial pressure is increased. It is difficult to associate E_{eff} with any particular reaction occurring during the induction period since the reactions are complex, even at this early stage. The values of E_{eff}

Figure 4.2

The variation of log τ_1 with $^1/T_o$

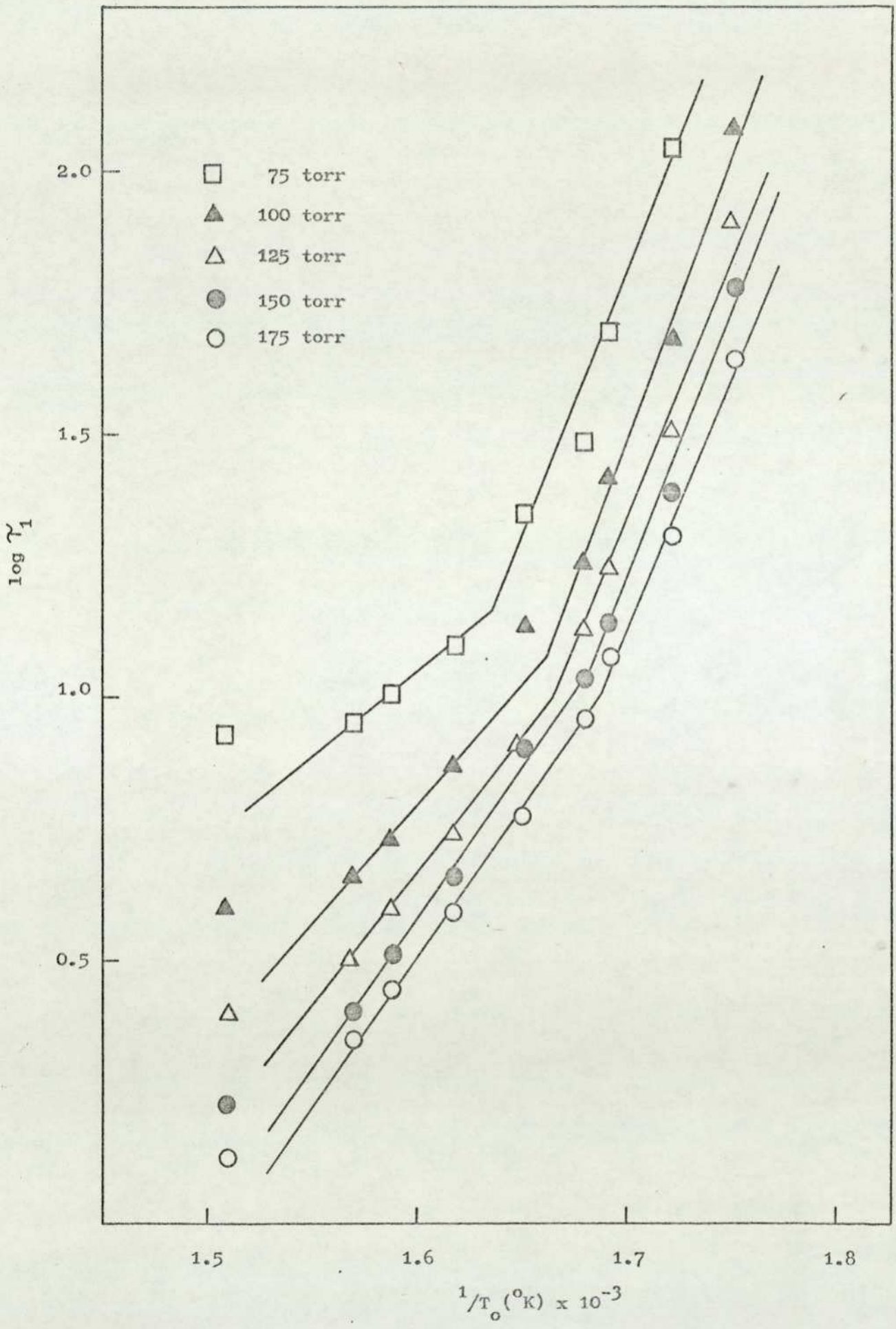
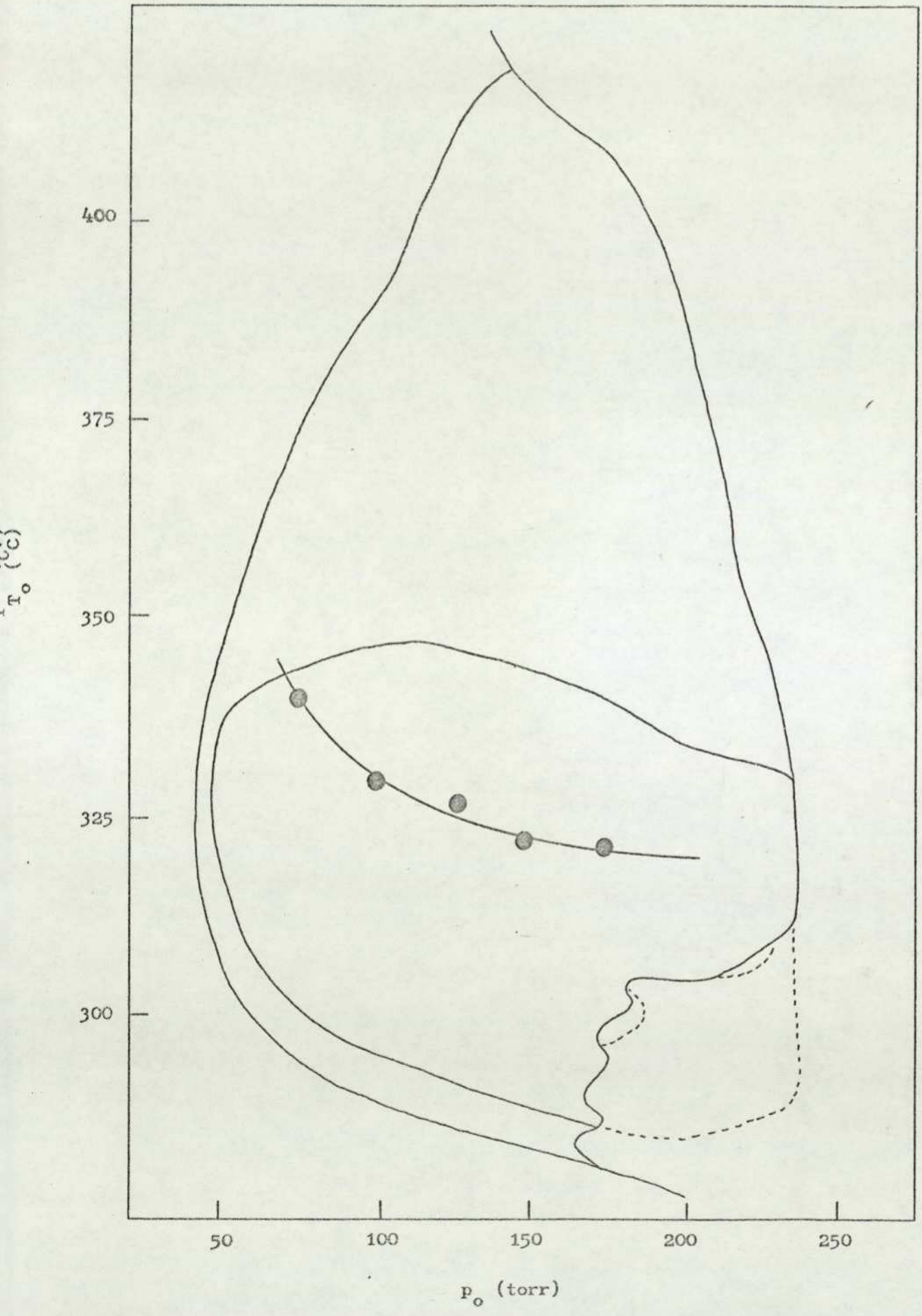


Figure 4.3

The variation with initial pressure of the temperature at which a discontinuity occurs in the relationship between $\log \tau_1$ and $1/T_o$



obtained, however, show good agreement with those quoted by Hughes and Simmons [97] (54 and 31 kcal.mole^{-1}) and Bastow [52] (49 and 20 kcal.mole^{-1}) for the lower and upper temperature regions respectively for n-pentane + oxygen mixtures. For n-heptane + air mixtures at pressures of up to 3 atmospheres, Yantovskii found that the variation of log τ_1 with $^1/T_o$ exhibited three linear portions corresponding to the temperature ranges 240 - 310°C, 310 - 390°C and above 400°C [96]. The values of E_{eff} in these regions were 37, 10 and 24 kcal.mole^{-1} respectively and he concluded that the branching mechanism in each region is different. In the lowest temperature range i.e. 240 - 310°C, he suggested that branching was due to the thermal decomposition of alkyl hydroperoxides, whereas between 310 - 400°C branching was due to the homogeneous decomposition of peracids (formed via the secondary oxidation of aldehydes). Thus, his chemical explanation of the branching mechanisms which predominate within these temperature ranges agree precisely with those given by Antonik and Lucquin [60] for the L_o and L_1 and L_2 mechanisms. Similar results were also obtained by Yantovskii for the iso-octane + air system [98].

A change in the character of the first cool flame also occurs as the initial temperature is increased. This is illustrated by consideration of the factors which account for the measured maximum transient pressure rise accompanying the cool flame. The two factors which contribute to the magnitude of Δp_1 are the increase in molecular concentration resulting from reactions which accompany the cool flame and the exothermicity of these reactions. At low initial temperatures, e.g. 290°C, Δp_1 is very large compared with $\Delta p_{1\infty}$. Furthermore, temperature measurements indicate that the cool flame is accompanied by a large temperature transient and that as soon as the increase in pressure ceases, the temperature of the reacting mixture falls rapidly back almost to the initial temperature conditions. It seems reasonable, therefore, to

infer that at this temperature the exothermic nature of the reactions which occur during the passage of the first cool flame is almost entirely responsible for the magnitude of Δp_1. Indeed, the theoretical values of Δp_1 calculated from the measured values of ΔT_1 assuming ideal gas behaviour, agree to within ca. 10% of the observed value of Δp_1. It is shown in Section 4.1.3, however, that the exothermicity associated with the cool flame reactions decreases steadily as the initial temperature is increased. At initial temperatures above ca. 330°C the relative importance of $\Delta p_{1\infty}$ compared with Δp_1 increases and the theoretical values of Δp_1 are always considerably smaller than the observed values of Δp_1. This suggests that fragmentation products, such as carbon oxides, become progressively more important as the initial temperature is increased, thereby increasing the contribution of the change in molecular concentration to the value of Δp_1. This behaviour would certainly be expected, since if it is assumed that the L_2 mechanism is operative in this temperature range then reactions (4.3) and (4.4) will become considerably more important as the temperature is increased from 330 to 390°C.

$$CH_3\dot{C}O \longrightarrow \dot{C}H_3 + CO \qquad (4.3)$$

$$CH_3C\dot{O}OO \longrightarrow CH_3\dot{O} + CO_2 \qquad (4.4)$$

Indeed, Dechaux [55] has recently shown that for n-butane + oxygen mixtures in the molar ratio 1:4, the yield of carbon monoxide increases by a factor of ca. 10 and the yield of carbon dioxide increases by a factor of ca. 5 as the initial temperature is increased from 350 to 400°C.

This change in the character of the cool flames is reflected by changes in the value of m in the relationship

$$\Delta p_1 = a p_o^m \qquad (4.5)$$

(where a and m are constants at a fixed initial temperature). In common with other fuels, the value of m increases with temperature as shown in Table 4.2.

Table 4.2

The values of m for various hydrocarbon + oxygen mixtures

Mixture	m	Temperature	Reference
n-butane + oxygen (1:2)	1.3 - 3.8	297 - 390°C	Present study
isobutane + oxygen (1:2)	2.8 - 5.0	302.5 - 386°C	45
2,3-dimethylbutane + oxygen (1:2)	2.6 - 4.5	301 - 342°C	51
2-methylpentane + oxygen (1:2)	1.4 - 3.5	275 - 395°C	87

From the foregoing considerations it is possible to suggest that low values of m may be associated with the occurrence of very exothermic reactions, whereas high values of m are largely the result of the formation of fragmentation products such as carbon oxides and formaldehyde. Since the values of m found for the n-butane + oxygen system are lower than those of the isobutane + oxygen system under similar conditions, it appears that the exothermicity of the reactions accompanying cool flames is greater during the oxidation of n-butane. Thermocouple measurements indicate that the temperature rises associated with cool flames during the oxidation of n-butane are indeed larger than those during the oxidation of isobutane [99]. Conversely, the higher values of m observed for the isobutane + oxygen system suggest that molecule fragmentation is more important for this fuel. Carbon balances calculated immediately after the passage of the first cool flame indicate that at temperatures at which the L_2 mechanism is operative, the yields of scission products, such as carbon oxides and formaldehyde, are indeed greater during the oxidation of isobutane [45].

The variation of Δp_1 with T_o exhibits a point of inflection at ca. 315°C which may also be explained by the change from the L_1 to L_2 mechanism. This changeover is most clearly illustrated, however, by the variation of $(dp_1/dt)_{max}$ with initial temperature (figure 3.12). At all initial pressures the L_1 mechanism, which is responsible for the occurrence of intense cool flames at the lower temperature limit, suffers increasingly effective competition from a non-branching reaction (or reactions) as the initial temperature is increased to ca. 315°C. Further increase of temperature, however, clearly promotes another branching process, which is presumably the L_2 mechanism, since $(dp_1/dt)_{max}$ increases quite markedly up to ca. 360°C. Between 360 and ca. 420°C, $(dp_1/dt)_{max}$ decreases continuously and this temperature range corresponds to the

principal negative temperature coefficient region.

4.1.3 The thermal characteristics of cool-flame propagation

One of the most significant results to emerge from the temperature measurements is the apparent change of the direction in which the cool flames propagate as the initial temperature is increased. This behaviour, which has not been reported hitherto, has been confirmed more recently in the studies of the oxidation of isobutane [99] and 2-methylpentane [100] under similar experimental conditions. The close similarity between this change and the change in mechanism indicated by the variation of log τ_1' with $^1/T_o$ has already been noted and it seems reasonable to assume that for n-butane + oxygen mixtures, the L_1 lobe can be associated with cool flames resulting from a predominantly heterogeneous mechanism, whereas the L_2 lobe can be associated with cool flames resulting from a predominantly homogeneous mechanism.

It was noted in the Introduction that it has been suggested that there is a substantial heterogeneous contribution to the oxidation of low molecular weight hydrocarbons. Furthermore, it appears that the degree of heterogeneity tends to parallel the resistance of the fuel to oxidise and therefore its knock-rating [101]. The degree of heterogeneity during the oxidation of isobutane would therefore be expected to be greater. This has been shown to be the case experimentally, since the changeover curve for heterogeneous to homogeneous flame propagation for n-butane + oxygen mixtures occurs at ca. 325°C, whereas for isobutane + oxygen mixtures [99] it occurs at ca. 340°C. For 2-methylpentane, however, which has a lower knock-rating than n-butane, this curve occurs at ca. 290°C [100]. For both isobutane and 2-methylpentane + oxygen mixtures, the locus of the initial conditions for the change in direction of cool-flame propagation is identical in shape to and lies within 8°C of

the locus of the initial conditions at which a discontinuity occurs in the relationship between log τ_1 and $^1/T_o$. Thus, assuming that these loci approximately coincide for other hydrocarbons, it is possible to suggest the temperature at which a change in direction of cool-flame propagation occurs for n-pentane + oxygen mixtures. Hughes and Simmons [97] reported that for this system, the discontinuity in the relationship between τ_1 and $^1/T_o$ at an initial pressure of 100 torr, occurs at 292 and 298°C for mixtures in the molar ratio 1:2 and 1:1 respectively. The observed change in direction of cool-flame propagation would thus be expected to occur at about these temperatures. It may be concluded, therefore, that the heterogeneous reactions are not favoured by an increase of the oxygen content of the reacting mixture. Similarly, Bastow [52] has recently shown that additions of 2 and 4% of HBr to mixtures of n-pentane + oxygen in the molar ratio 3:4, lower the temperature at which the discontinuity occurs from 314.5°C to 272 and 266°C respectively, at an initial pressure of 70 torr. Larger additions cause no further decrease in this temperature. The action of the additive clearly promotes homogeneous reactions at the expense of heterogeneous reactions.

A possible explanation for this change in the nature of the mechanism and for its variation with fuel structure, stoichiometry and hydrogen bromide will be discussed in Section 4.3.

Investigation of the relationship between p_o and the transient temperature rise accompanying the first cool flame measured at the wall of the reactor,

$$\Delta T_1 = Mp_o + C \qquad (4.6)$$

reveals that the constant C is markedly sensitive to changes in the initial temperature at temperatures at which cool flames are observed to propagate from the reactor walls. However, at higher initial temperatures, where cool flames are observed to propagate from the centre of the reactor, C is almost independent of the initial temperature. In contrast, the

constant C in the relationship between p_o and the temperature rise accompanying the cool flame measured at the centre of the reactor,

$$\Delta T_1 = Mp_o^x + C \qquad (4.7)$$

is predominantly affected by changes of initial temperature above ca. 335°C. It seems probable, therefore, that the behaviour of the constants in these relationships is connected with the mode of cool-flame propagation, although their exact significance is not clear.

The observation of a region within which cool flames propagate from the walls of the reactors as a result of heterogeneous reactions, suggests that the interpretation of the concurrent pressure - and temperature - time recordings obtained by Hughes and Simmons for the n-pentane + oxygen system [97], is incorrect. These workers, who studied cool flame development by following the pressure changes and temperature changes at the centre of the reactor, observed that the pressure pulse consisted of an initial very abrupt rise followed by a much slower rate of pressure rise. Furthermore, they observed that the first pressure rise apparently occurred before any appreciable temperature rise was recorded and that the second part of the pressure pulse and the thermal pulse were coincident. From these and other considerations, they concluded that two stages are involved in the appearance of a cool flame. In the first stage there is an abrupt increase in the molecular concentration which occurs practically isothermally. This leads to a thermally unstable system and hence the thermal pulse which forms the second stage of the cool flame. The present results indicate, however, that these two stages occur concurrently. At low initial temperatures, it is true that the temperature at the centre of the reactor begins to rise as much as 300 milliseconds after the start of the pressure rise, however, at the reactor wall the temperature rise is coincidental with the pressure rise. Clearly, the use of a single thermocouple positioned at the centre of the

reactor will give rise to misleading results under these conditions.

It has been suggested that the heat released during a cool flame is sufficient to raise the temperature of the reacting mixture to values of the initial temperature in the principal negative temperature coefficient region [63]. Indeed, this has been proposed as an explanation of the self-quenching and periodic characteristics of cool flames [93]. The present studies make it possible to test the validity of this proposal in detail. It has been assumed, for the convenience of calculation, that the maximum temperatures recorded by the three thermocouples occur instantaneously. It is thus possible to calculate a space-averaged maximum temperature rise, ΔT_{sa}, as follows:

$$\Delta T_{sa} = (T_C + T_{\frac{1}{2}R} + T_W)/3 \qquad (4.8)$$

where T_C, $T_{\frac{1}{2}R}$ and T_W are the maximum temperature rises at the centre, half-radius and wall respectively. The space-averaged temperature rises at various initial temperatures have been calculated for an initial pressure of 150 torr(since cool flames occur over the widest range of initial temperatures at this pressure) and are shown in Table 4.3. It can be seen that the maximum temperature reached by each reacting mixture, T_m, where

$$T_m = T_o + \Delta T_{sa} \qquad (4.9)$$

is more or less constant, irrespective of the initial temperature; the average value of T_m during the first cool flame being ca.422.5°C which is approximately 6°C above the observed upper cool-flame limit (see figure 3.27).

It was considered that the close similarity between T_m and the initial temperature corresponding to the upper cool-flame limit at an initial pressure of 150 torr might be very significant and so similar calculations were carried out for a range of initial pressures between 77 - 175 torr. The maximum temperatures reached in cool flames at these

Table 4.3

The variation of the space-averaged maximum temperature rise with initial temperature (p_o = 150 torr)

T_o	T_{sa}	T_m
292	136	428
297	126	423
302.5	119.5	422
307	112	419
313	104	417
319	103	422
325	97	422
333	87	420
339	78	417
344.5	79	423.5
351	71	422
360.5	65	425.5
371.5	53.5	425
381	45	426
392	31.5	423.5
402	22	424
409	14	423

pressures have been plotted on part of the ignition diagram for System I as shown in figure 4.4. (Although the overall ignition diagram for System I differs from that for System II, this difference is only significant below 360°C. Furthermore, the ignition diagram for System I is particularly useful since it includes the ignition boundary). It can be seen that the locus of these points (the dotted line) describes almost the same path as the experimentally observed slow combustion/upper cool-flame boundary. These results are both kinetically and chemically very significant, since they clearly illustrate that there is a discrete upper limit for cool-flame propagation which is determined by the average temperature rise and not the maximum temperature rise. This is in good agreement with the results of Hughes and Simmons for the n-pentane + oxygen system [97]. These workers calculated that in this case, the upper limit for cool-flame propagation is ca. 395°C, at an initial pressure of 140 torr. It should be noted, however, that this value was reached by adding half the maximum temperature recorded during a cool flame to the initial temperature. The present studies have shown that if this method of computation is used, the results are considerably more scattered and generally take lower values. Nevertheless, these two independent studies do suggest that a 'thermal switch' mechanism may explain the self-quenching nature of cool flames.

Two possible competing reactions responsible for the thermal switch are (4.3) and (4.10), which Enikolopyan [53] suggested may be capable of explaining the occurrence of the negative temperature coefficient region.

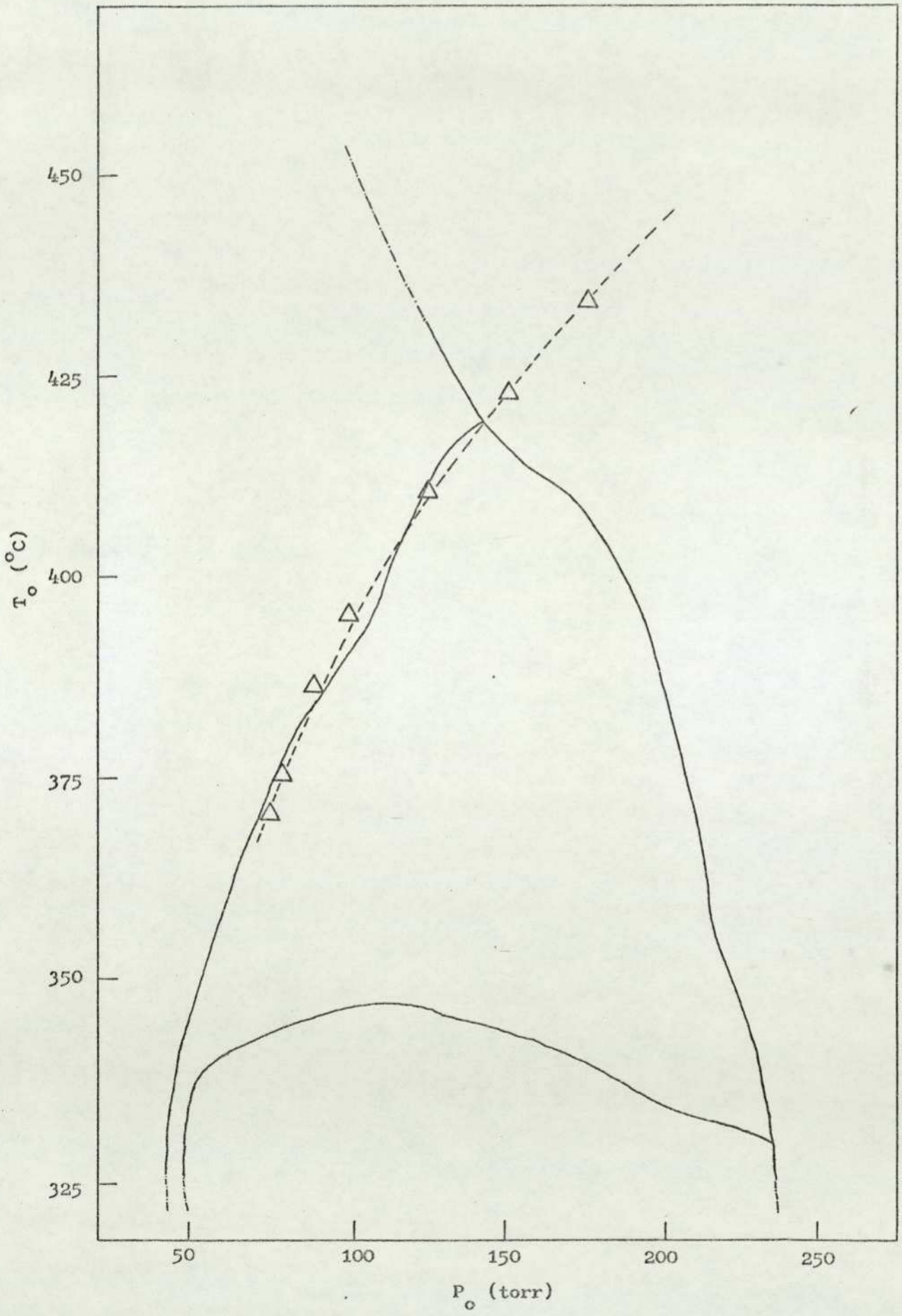
$$\dot{C}H_3CO \longrightarrow \dot{C}H_3 + CO \qquad (4.3)$$

$$\dot{C}H_3CO + O_2 \longrightarrow CH_3C\dot{O}_3 \qquad (4.10)$$

Semenov [102] considers that the activation energy for reaction (4.3) is ca. 18 kcal.mole^{-1}, whereas that for reaction (4.10) is close to zero.

Figure 4.4

The variation with initial pressure of the maximum temperature reached during the first cool flame



It is clear, therefore, that as the temperature is increased reaction (4.3) becomes increasingly competitive. For initial temperatures which lie within the range in which the L_2 lobe is observed, the above suggestion seems plausible, since the L_2 mechanism involves these reactions. For initial temperatures lying within the range of the L_1 lobe, however, the basic branching mechanism involves alkyl hydroperoxides and for the above competition to occur for cool flames at these low initial temperatures, the branching process must change during the propagation of the cool flame. Indeed, the fact that the maximum temperature reached during the first cool flame at a specific initial pressure, irrespective of the initial temperature, is more or less constant, suggests that this is so. If the stability and stationary concentration of alkylperoxy radicals is considered, it is clear that as the initial temperature is increased they will become less stable and therefore their stationary concentration will be smaller. Clearly this does not favour reaction (4.11).

$$C_nH_{2n+1}\dot{O}O + AH \longrightarrow C_nH_{2n+1}OOH + \dot{A} \qquad (4.11)$$

Nevertheless, the decomposition of alkylperoxy radicals via hydroperoxyalkyl radicals, which is favoured by an increase in temperature, will give rise to considerable yields of aldehydes which may then participate in the accepted L_2 mechanism.

The foregoing considerations thus indicate that for initial temperatures greater than ca. 330°C, a single thermal switch occurs between reactions (4.3) and (4.10). The precise temperature at which this switch occurs depends on the initial pressure and from figure 4.4 it can be seen that this temperature increases as the initial pressure is increased. This is to be expected since reaction (4.10) is favoured by high pressures and thus the temperature at which reaction (4.3) competes effectively is necessarily higher. For initial temperatures

below ca. 330°C, however, it seems that two thermal switches are operative. The first between reactions (4.11) and (4.12) at about 330°C,

$$C_nH_{2n+1}\dot{O}O + AH \longrightarrow C_nH_{2n+1}OOH + \dot{A} \qquad (4.11)$$

$$C_nH_{2n+1}\dot{O}O \xrightarrow[\text{radicals}]{\text{via hydroperoxyalkyl}} AH + \text{other products} \qquad (4.12)$$

and the second between reactions (4.3) and (4.10) which is dependent on the initial pressure.

The present studies also indicate that the role of the cool flame in two-stage ignition cannot be considered as entirely thermal, since at relatively high initial pressures the maximum temperature reached in the first cool flame is well in excess of the initial temperatures at the cool flame/ two-stage ignition boundary. These results are in agreement with those observed for the 2-methylpentane+oxygen system [95].

4.1.4 The characteristics of subsequent cool flames

Although detailed kinetic measurements were only carried out for the second and third cool flames, it is clear that the character of cool flames following the third is generally similar. Thus, the observations made in this section apply equally well to cool flames after the third except that the position of boundaries and changes of behaviour occur at progressively different initial conditions.

It has been seen in Sections 3.1.1.5 - 3.1.1.10 that below limiting initial temperatures and pressures (see figures 3.19 and 3.24), the behaviour of the second and third cool flames may be described in the same manner as that of the first cool flame. Thus, for example, the values of $\tau_{2,3}$ decrease, whilst those of $\Delta p_{2,3}$ and $(dp_{2,3}/dt)_{max}$ increase as the initial pressure is increased. Furthermore, the lower multiple cool-flame limits are distinct, like that of the first cool flame. Temperature measurements also indicate the similarity of these cool flames, since at initial temperatures below ca. 330°C, all cool flames propagate

from the walls of the reactor. It seems reasonable, therefore, to assume that the L_1 mechanism, which involves the participation of alkyl hydroperoxides, can account for the formation of multiple cool flames under these conditions.

Below initial temperatures of ca. 305°C, the intensities of the first three cool flames decrease in the order 3rd > 2nd > 1st, which is unusual. This may be due to the influence of compounds containing labile hydrogen atoms, particularly acetaldehyde which is a major product at all stages of reaction under these conditions. It seems reasonable to assume that its presence after the first cool flame will promote the rate of formation of branching agent and therefore increase the rate of branching, thereby leading to increased values of $\Delta p_{2,3}$ and $(dp_{2,3}/dt)_{max}$. With the passage of each cool flame, however, the oxygen consumption becomes a limiting factor and so the intensities of cool flames after the third or fourth cool flame decrease.

Above the aforementioned limiting initial conditions, the intensities of the subsequent cool flames decrease markedly as either the initial temperature or pressure is increased. A comparison of the variation of $(dp_1/dt)_{max}$ and $(dp_{2,3}/dt)_{max}$ with T_o, (figures 3.12, 3.17 and 3.23), shows that the sharp decline in the values of $(dp_{2,3}/dt)_{max}$ as the initial temperature is increased, coincides with the change of the temperature coefficient of reaction rate of the first cool flame from negative to positive. More specifically this can be considered as the change from the L_1 mechanism to the L_2 mechanism (see Section 4.1.2). These results are clearly a manifestation of the fact that the L_2 mechanism is not conducive to multiple cool flame formation.

The reduction of the intensities of cool flames subsequent to the first is also connected with the appearance, at these limiting conditions, of the 'shoulder' on the first cool flame. As the initial

temperature or pressure is increased, Δp_s increases whilst $(dp_{2,3}/dt)_{max}$ decreases (figures 3.16, 3.22 and 3.26). This shoulder, which eventually becomes the hot ignition stage of two-stage ignition, is probably the result of the further reaction of products formed during the first cool flame. Detailed considerations of this shoulder (see Section 4.1.5) indicate that the reactions responsible for its occurrence most probably occur homogeneously. It is interesting that its most pronounced 'inhibiting' effect on subsequent cool flames is in the region within which cool flames are observed to propagate from the walls of the reactor, although the exact significance of this is not clear from the present studies. Unfortunately, a precise chemical explanation for its inhibiting effect is not readily offered by the analytical results. One possibility which might be considered is that an intermediate which is a precursor of the branching agent responsible for subsequent cool flames is consumed during the shoulder pulse. In this case, however, the induction period of the second cool flame would be expected to be considerably lengthened and this was not observed experimentally. Furthermore, there is no indication in the product concentration - time curves of any abrupt decrease of concentration of any particular product when the shoulder is observed. It is clear that further work is necessary before this phenomenon can be explained unequivocally.

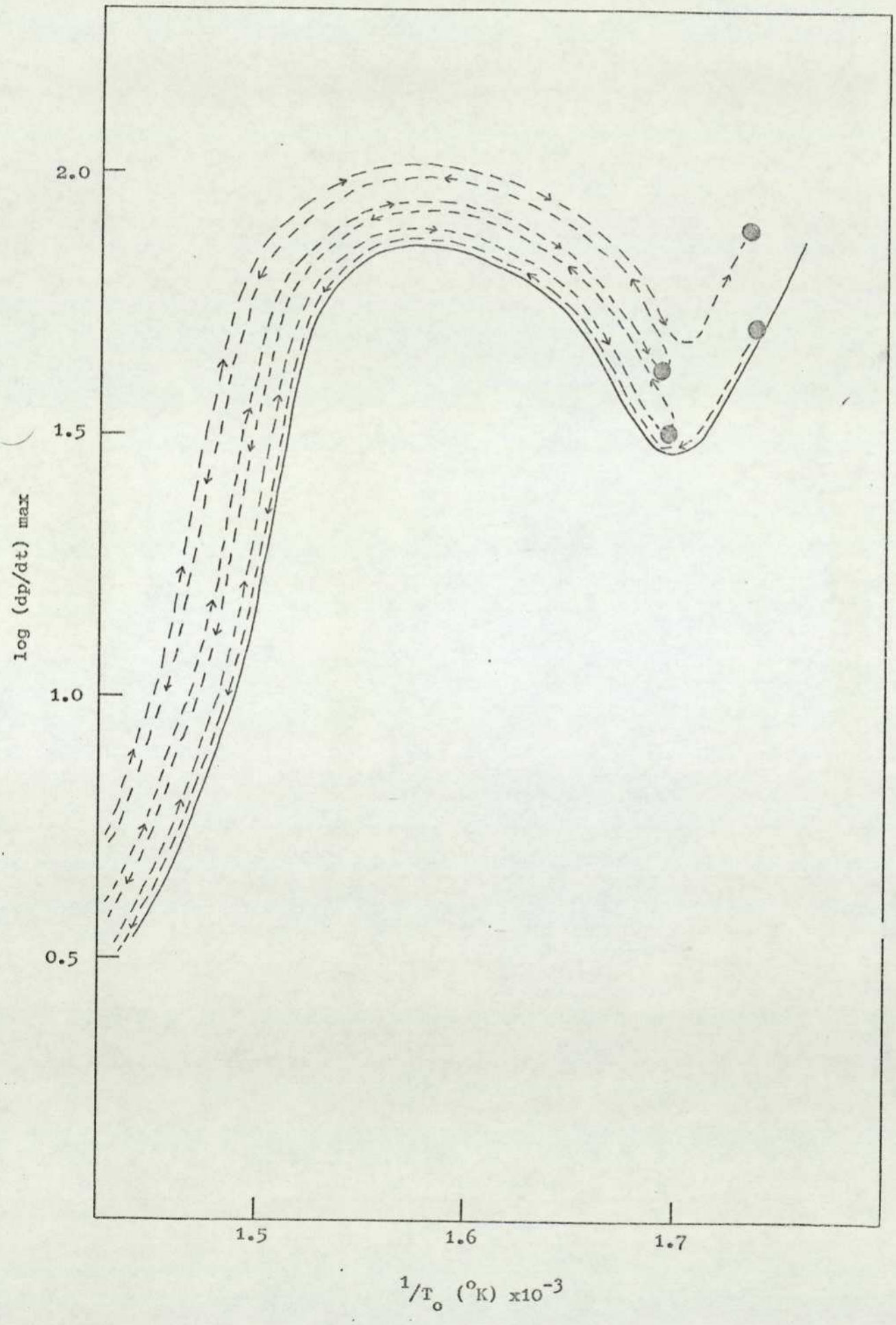
Detailed temperature measurements were not carried out on cool flames after the first although the values of ΔT_n and $(dT_n/dt)_{max}$ are, in general, considerably different from the values of ΔT_1 and $(dT_1/dt)_{max}$ when space-averaged temperatures are considered. In contrast to the first cool flame, the maximum temperature reached during the propagation of subsequent cool flames is very dependent on the initial temperature. Indeed, under certain conditions, principally at low initial temperatures, the maximum temperature reached during the second, third and fourth cool

flames exceeds that reached during the first cool flame by as much as 30 to 40°C. These results offer an explanation for the occurrence of multi-stage ignitions which is discussed in Section 4.1.5. The complex behaviour of these cool flames no doubt reflects the increasing complexity of the reacting mixture as the oxidation proceeds. For this reason it becomes increasingly difficult to describe with accuracy the path of the reaction and the concurrent morphological phenomena in terms of elementary reactions involving n-butane.

Finally, Barnard and Watts [93] have shown that for the acetone + oxygen system, the temperature of the reacting mixture during the passage of cool flames oscillates about a given point in the Arrhenius plot of the variation of log rate with the reciprocal of the absolute initial temperature. The present results show that at low initial temperatures and pressures this observation is also true in the present system as shown in figure 4.5. These results again point to the occurrence of a thermal switch between specific reactions which can explain the self-quenching and periodic nature of cool flames.

Figure 4.5

Cool flame temperature oscillations illustrated on an Arrhenious plot (p_o = 150 torr, T_o = 302.5°C)



4.1.5 The transition to hot ignition

It has been noted in Section 4.1.4 that a most important factor in this transition is the appearance of the shoulder pulse on the first cool flame which eventually becomes the second-stage hot ignition when the initial pressure is sufficiently high. Temperature measurements at the shoulder, especially at initial pressures close to the cool flame/two-stage ignition boundary, indicate considerable thermal activity at the centre of the reactor. Indeed, the heat release, which raises the temperature of the reacting mixture to a higher temperature than that reached during the first cool flame, lasts for 1 to 3 seconds compared to 0.5 to 1 second during the cool flame. Clearly, considerable further reaction of the intermediates formed during the first cool flame occurs. Affleck and Fish [82], who studied the controlling role of cool flames in two-stage ignition, concluded that the most likely explanation for the occurrence of the hot ignition is the production of additional branching agents during the passage of the cool flame. Certainly the controlling role of the cool flame is particularly well illustrated in figure 3.8 which shows that, over a wide range of temperature, $\Delta p_1 = 74$ torr at an initial pressure of 255 torr which is ca. 20 torr above the pressure at the cool flame/multi-stage ignition boundary. It appears, therefore, that for a multi-stage ignition to ensue Δp_1 must attain a critical value and it will be useful, therefore, to consider the possible additional branching agents which may be formed under these conditions.

The temperature studies show that for initial pressures greater than 100 torr, the maximum temperature to which the reacting mixture is raised is greater than ca. 400°C. Indeed, at an initial pressure of 175 torr, T_m is as high as ca. 435°C. At these temperatures, the direct oxidation of acetaldehyde ($E = 14$ kcal.mole^{-1} [110]) would be expected to give rise to further branching.

$$CH_3CHO + O_2 \longrightarrow \dot{C}H_3CO + \dot{H}O_2 \qquad (4.13)$$

Furthermore, the hydroperoxy radicals formed in reaction (4.13), together with those formed in reaction (4.14) may form hydrogen peroxide via reaction (4.15):

$$\alpha\text{-}\dot{C}_nH_{2n}OOH \longrightarrow \text{conjugate alkene} + \dot{H}O_2 \qquad (4.14)$$

$$\dot{H}O_2 + C_nH_{2n+2} \text{ or } AH \longrightarrow H_2O_2 + \dot{C}_nH_{2n+1} \text{ or } \dot{A} \qquad (4.15)$$

At the high transient temperatures reached during the cool flame, this may undergo homogeneous decomposition and hence lead to further degenerate branching.

$$H_2O_2 + (M) \longrightarrow 2\dot{O}H + (M) \qquad (4.16)$$

Similarly, the high temperatures may promote reactions which give rise to methyl radicals. Indeed, the thermal switch explanation for the negative temperature coefficient and the self-quenching nature of cool flames includes the formation of methyl radicals by reaction (4.3).

$$\dot{C}H_3CO \longrightarrow \dot{C}H_3 + CO \qquad (4.3)$$

The methyl radicals so formed may ultimately form methyl hydroperoxide which is known to be an important branching agent in analogous systems [103].

It is clear then, that the first cool flame may produce several intermediates which are capable of undergoing further reaction to form branching agents. Their subsequent branching will be slightly delayed with respect to the first cool flame and hence a shoulder is observed on the pressure-time trace. As the initial pressure is increased, the critical value of the net branching factor required for hot ignition is attained and hence two-stage ignition is observed. These general conclusions are supported by the work of Fish, Haskell and Read who studied the two-stage ignition of 2-methylpentane + oxygen mixtures at high pressures [11]. These workers observed that a further induction period occurs after the propagation of the first cool flame during which not only the pressure but also the concentrations of intermediate products

change only slowly. They concluded, therefore, that the second stage is, like the cool-flame stage, a degenerately branched chain reaction.

These considerations also offer an explanation for three (or more) -stage ignitions. Thus, the onset of the hot ignition will clearly depend on a critical concentration of the branching intermediate being formed in the cool flame. This may not necessarily occur during the first cool flame, but may eventually at a subsequent cool flame. Thus, for example, figures 4.6 (a) and 4.6 (b) show the nature of the formation of a typical intermediate I, as observed in the analytical studies, at low and high initial temperatures respectively. The different times required to reach the critical concentration necessary for ignition, $[I]_c$, after the passage of the first cool flame is readily apparent. However, the intermediate accumulates in a step-wise manner at low initial temperatures, where multiple cool flames are well resolved, and thus the critical concentration may not be attained during the first cool flame but at the second. In this case a three-stage ignition is observed as shown in figure 4.6 (c). Figure 4.6 (d) illustrates the expected effect on the concentration history of the intermediate of progressively increasing the initial pressure from the cool flame/three-stage ignition boundary to the three-stage ignition/two-stage ignition boundary at constant initial temperature. It is reasonable to assume also, that similar considerations may explain the change from four-stage to three-stage, to two-stage ignition as the initial pressure is progressively raised.

Another explanation for the occurrence of multi-stage ignition is suggested by the results of the temperature studies. It was shown in Section 4.1.4 that at low initial temperatures, the maximum temperature reached during the second and third cool flames exceeds that reached during the first cool flame. This means that under these

conditions the reacting mixture is heated to a temperature of ca. 420 - 450°C and it seems reasonable to assume that at these temperatures, the temperature coefficient of reaction rate has a positive value. Furthermore, at these temperatures, reaction (4.17) will be the predominant reaction of butyl radicals:

$$\dot{C}_4H_9 + O_2 \longrightarrow C_4H_8 + \dot{H}O_2 \qquad (4.17)$$

Completion of the chain cycle, by hydrogen abstraction reactions of the hydroperoxy radicals so formed, leads to the formation of hydrogen peroxide, which at these temperatures undergoes homogeneous decomposition [72], in a branching reaction.

$$\dot{H}O_2 + C_nH_{2n+2} \longrightarrow H_2O_2 + \dot{C}_nH_{2n+1} \qquad (4.15)$$

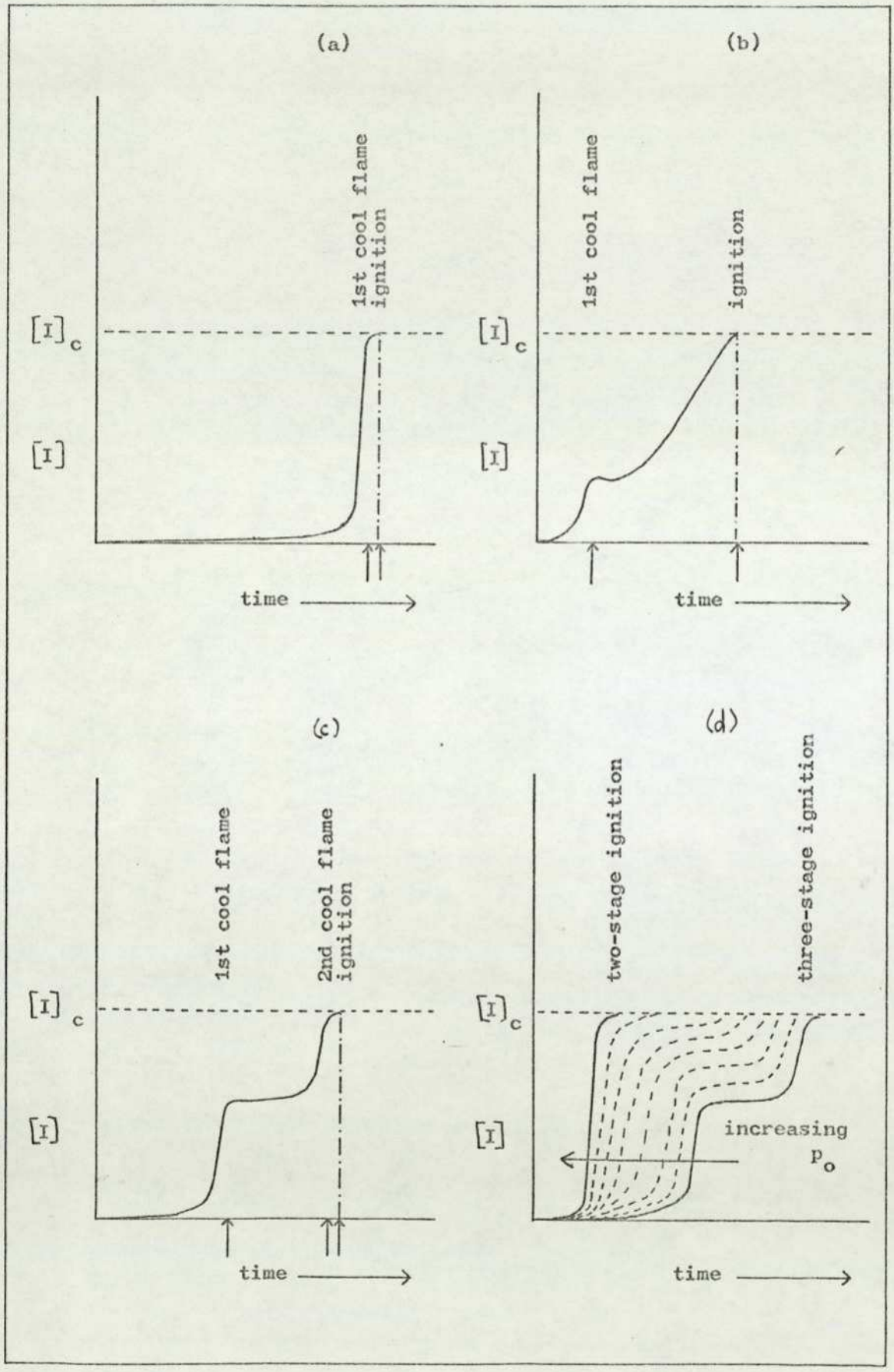
$$H_2O_2 + (M) \longrightarrow 2\dot{O}H + (M) \qquad (4.16)$$

Thus, provided that the temperature reached during the second or third cool flame is sufficiently high for the above mechanism to become established, then the hot ignition stage will occur and a multi-stage ignition is observed.

It is probable that neither of these factors is alone responsible for the phenomenon of multi-stage ignition and no doubt both the temperature rise and the concentration history of the degenerate branching agent are important.

Figure 4.6

The concentration histories of a typical oxidation intermediate I prior to ignition



4.2 The chemical interpretation of cool-flame oxidation

4.2.1 Product formation during the early stages of reaction

At low initial temperatures, close to the lower limit of cool-flame propagation, the reaction exhibits long induction periods during which slow reaction occurs virtually isothermally. These conditions are, therefore, ideal for studying the mechanism of product formation via the principal chain propagating reactions.

At these temperatures, (e.g. 285°C), the predominating reaction of n- and sec-butyl radicals is the addition of oxygen to form but-1-ylperoxy and but-2-ylperoxy radicals respectively.

$$\dot{C}H_2CH_2CH_2CH_3 + O_2 \longrightarrow CH_2(O\text{-}\dot{O})CH_2CH_2CH_3 \qquad (4.18)$$

$$CH_3\dot{C}HCH_2CH_3 + O_2 \longrightarrow CH_3CH(O\text{-}\dot{O})CH_2CH_3 \qquad (4.19)$$

Indeed, rate constant data [43] suggests that at 285°C, these reactions are approximately thirty times faster than the competing abstraction reactions:-

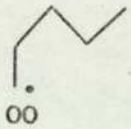
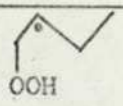
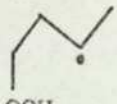
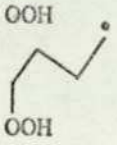
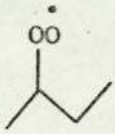
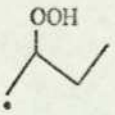
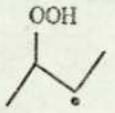
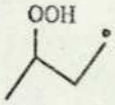
$$\dot{C}H_2CH_2CH_2CH_3 + O_2 \longrightarrow CH_2{=}CHCH_2CH_3 + H\dot{O}_2 \qquad (4.20)$$

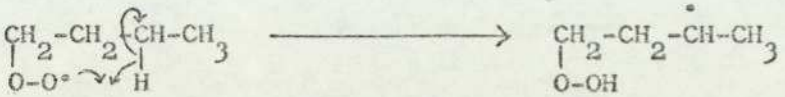
$$CH_3\dot{C}HCH_2CH_3 + O_2 \longrightarrow CH_3CH{=}CHCH_3 + H\dot{O}_2 \qquad (4.21)$$

The importance of alkylperoxy radical isomerisation has been discussed in detail in the Introduction and the analytical results suggest that this is also the major fate of butylperoxy radicals formed in reactions (4.18) and (4.19). It can be seen from Table 4.4 that the principal mode of isomerisation of but-1-ylperoxy and but-2-ylperoxy radicals is 1:5 hydrogen transfer to form the 1-hydroperoxybut-3-yl and 2-hydroperoxybut-4-yl radicals respectively.

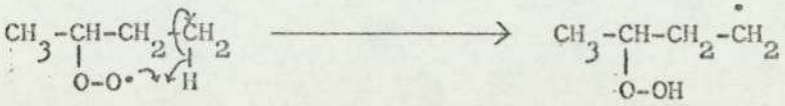
Table 4.4

Rate constants of butylperoxy radical isomerisation

Butylperoxy radical	Hydroperoxybutyl radical	log k (k in sec^{-1} at $558^{o}K$[43])
		4.3
		6.7
		2.8
		2.8
		4.3
		5.1

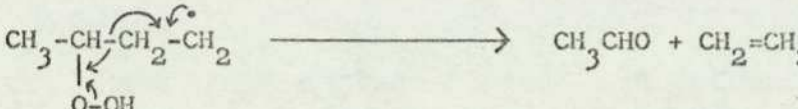


(4.22)

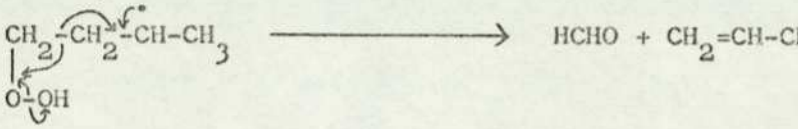


(4.23)

In principle, these β-hydroperoxybutyl radicals may either reisomerise, add oxygen, cyclise or undergo β-scission decomposition. The last reaction would lead to equal amounts of acetaldehyde and ethylene from the 2-hydroperoxybut-4-yl radical and equal amounts of formaldehyde and propene from the 1-hydroperoxybut-3-yl radical.



(4.24)

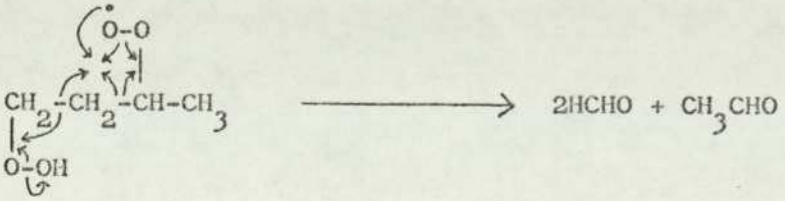


(4.25)

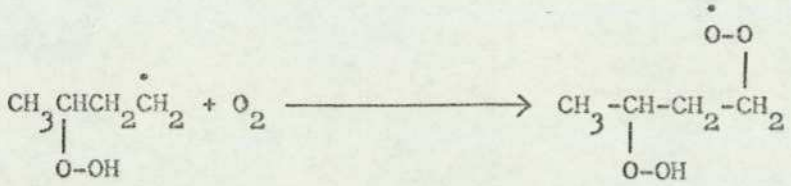
However, the ratio of acetaldehyde : ethylene is ca. 7.5 : 1 and propene is only found in small yield which suggests that it is not the major fate of these radicals. Similarly, the total yield of C_4 O-heterocycles is ca.2% and so cyclisation also plays only a minor role, while C^{14}- tracer studies [38] have shown that the reverse isomerisation (at least for α-hydroperoxybutyl radicals) is not important. The addition of oxygen, therefore, appears to be the major fate of these radicals and is indeed capable of explaining the formation of the two major products, acetaldehyde and acetone, the formation of the latter requiring further hydrogen abstraction and decomposition of the dihydroperoxide.



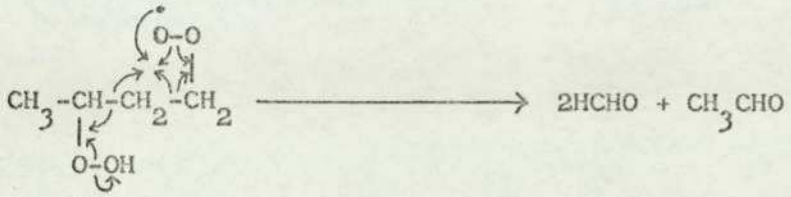
(4.26)



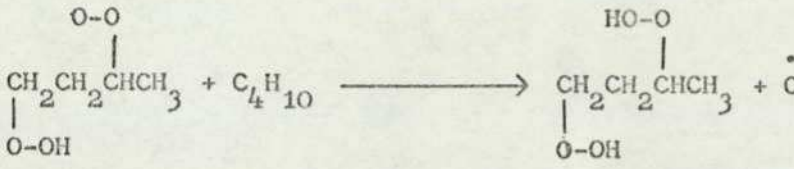
(4.27)



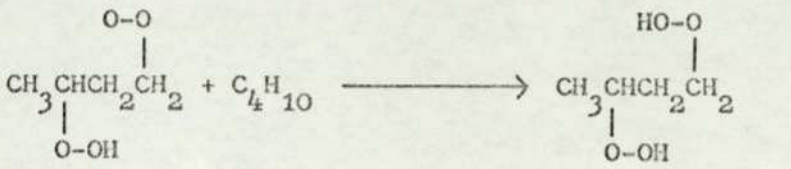
(4.28)



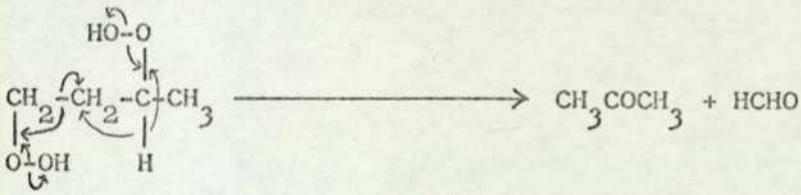
(4.29)



(4.30)



(4.31)



(4.32)

This may well be expected, since the concentration of oxygen is high in the early stages and its addition proceeds with an activation energy close to zero (analogous to the addition of oxygen to an alkyl radical). The formation of dihydroperoxides has been confirmed by Cartlidge and Tipper [35] and the existence of bifunctional group radicals is confirmed by the work of Crandell and Thomas [46] who showed that β-dicarbonyl compounds, such as butanal-3-one, are responsible for the characteristic absorption waveband at 2600 Å during the oxidation of n-butane. These authors also showed that the concentration of formaldehyde steadily increases during the induction period preceding the first cool flame at 300°C which supports the suggestion that reactions (4.26) to (4.29) account for the major route to acetaldehyde. Further support may be found in the work of Neiman and his co-workers who studied the mechanism of product formation with the aid of C^{14}-labelled fuels [104]. Measurement of the activities of acetaldehyde and

formaldehyde formed during the cool-flame oxidation of n-butane showed that formaldehyde is derived about equally from each carbon atom, while the mechanism of formation of acetaldehyde is specific, the carbonyl group being derived from the 2- and 3- carbon atoms. This is indeed the case if the formation of these compounds occurs principally via reactions (4.27) and (4.29).

The overall importance of the further oxidation of β-hydroperoxybutyl radicals is demonstrated by the fact that together, acetaldehyde and acetone account for ca. 52% of the detectable products during the early stages of reaction at 285°C.

The formation of acetaldehyde and acetone is also associated with the formation of hydroxyl radicals which are capable of attacking the fuel to regenerate butyl radicals.

$$CH_3CH_2CH_2CH_3 + \dot{O}H \longrightarrow \dot{C}H_2CH_2CH_2CH_3 + H_2O \qquad (4.33)$$

$$CH_3CH_2CH_2CH_3 + \dot{O}H \longrightarrow CH_3\dot{C}HCH_2CH_3 + H_2O \qquad (4.34)$$

Since the activation energy of hydrogen abstraction by hydroxyl radicals is generally agreed to be small and of the order of 1-2 kcal.mole^{-1}, it is likely that even at relatively low initial temperatures such as 285°C, the attack on the fuel will be largely unselective.

In contrast to β-hydroperoxybutyl radicals, it seems that α-hydroperoxybutyl radicals, which are formed by butylperoxy radical isomerisation involving 1 : 4 hydrogen transfer, preferentially decompose by β-scission of the C - O bond:

$$CH_2(\dot{})\text{-}CH(O\text{-}OH)\text{-}CH_2\text{-}CH_3 \longrightarrow CH_2{=}CH\text{-}CH_2\text{-}CH_3 + \dot{H}O_2 \qquad (4.35)$$

$$\dot{C}H_2\text{-}CH(O\text{-}OH)\text{-}CH_2\text{-}CH_3 \longrightarrow CH_2{=}CH\text{-}CH_2\text{-}CH_3 + \dot{H}O_2 \qquad (4.36)$$

$$CH_3\text{-}CH(\dot{})\text{-}CH(O\text{-}OH)\text{-}CH_3 \longrightarrow CH_3\text{-}CH{=}CH\text{-}CH_3 + \dot{H}O_2 \qquad (4.37)$$

Reaction (4.36) would not be expected to contribute greatly to the observed yields of but-1-ene, since the predominant mode of isomerisation of but-2-ylperoxy radicals occurs via the intramolecular abstraction of a hydrogen atom attached to the 3-carbon atom. The estimated rate constant data (Table 4.4) suggests that the rates of formation of 2-hydroperoxybut-3-yl and 2-hydroperoxybut-1-yl radicals are in the ratio of about 32 : 1 and hence it is possible to estimate the relative rates of initial attack on the fuel by hydroxyl radicals since but-1-ene is derived principally from the but-1-yl radical and but-2-ene from the but-2-yl radical. At 285°C, the two butenes are formed in approximately equal amounts and since there are six 1° hydrogen atoms available for the formation of but-1-yl radicals compared with four 2° hydrogen atoms for but-2-yl radical formation, it is clear that the relative rates of attack by hydroxyl radicals at 1°C-H and 2°C-H bonds are in the ratio of 2 : 3. This result compares well with those of Greiner [105], who found that at 525°C the ratio of attack by hydroxyl radicals at 1°, 2° and 3°C-H bonds is 2 : 3 : 5.

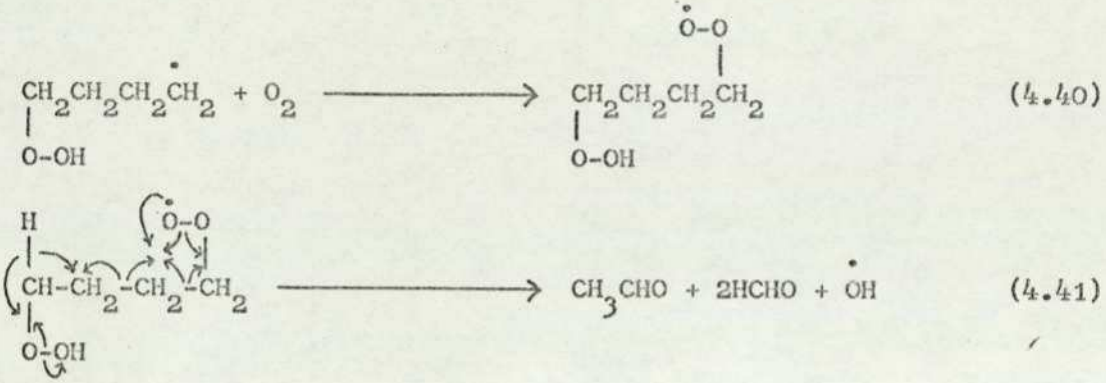
The formation of the butenes is also accompanied by the formation of hydroperoxy radicals. These radicals attack the fuel more selectively than hydroxyl radicals and at a slower rate. Nevertheless, they may be responsible for the production of hydrogen peroxide, which was not determined in the present studies but has been shown to be formed in the n-butane+oxygen system by Déchaux [55].

$$CH_3CH_2CH_2CH_3 + \dot{H}O_2 \longrightarrow \dot{C}H_2CH_2CH_2CH_3 + H_2O_2 \qquad (4.38)$$

$$CH_3CH_2CH_2CH_3 + \dot{H}O_2 \longrightarrow CH_3\dot{C}HCH_2CH_3 + H_2O_2 \qquad (4.39)$$

Butylperoxy radical isomerisation involving 1 : 6 hydrogen transfer would not be expected to compete effectively with 1 : 4 and 1 : 5 hydrogen transfer at 285°C because of the strain energy involved in the formation of the 7-membered transition ring complex (6.5 kcal.mole^{-1}) and because both the initial hydrogen abstraction leading to the formation of

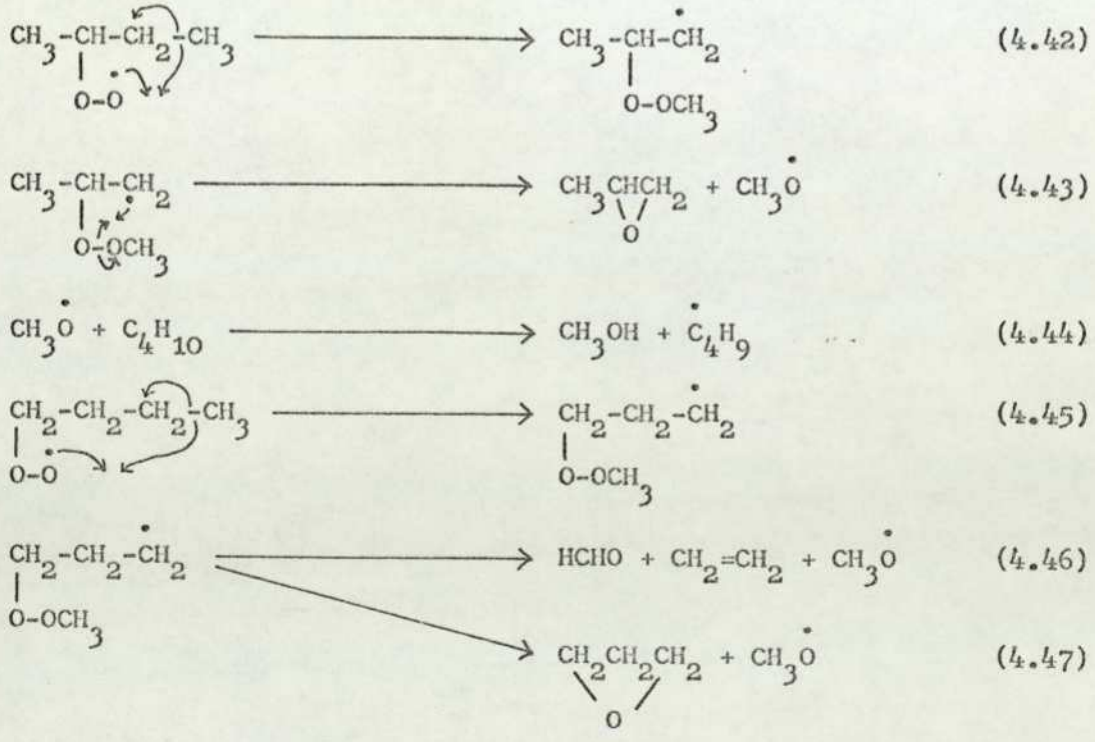
the but-1-yl radical and the intramolecular hydrogen abstraction stage, involve 1° hydrogen atoms. Nevertheless, it does occur to a small extent as indicated by the appearance of traces of tetrahydrofuran in the products. The major fate of γ-hydroperoxybutyl radicals, however, is likely to be further oxidation and decomposition of the hydroperoxybutylperoxy radicals so formed probably accounts for part of the observed yield of acetaldehyde.



(4.40)

(4.41)

Methanol is a reasonably important product during the induction period at 285°C and its formation may be explained by the occurrence of butylperoxy radical isomerisation involving 1 : 4 and 1 : 5 methyl group transfer. Decomposition reactions of the radicals so formed leads to the formation of methoxy radicals, which may intermolecularly abstract a hydrogen atom to form methanol.



(4.42)

(4.43)

(4.44)

(4.45)

(4.46)

(4.47)

Reaction (4.43) also probably accounts for the formation of 2-methyloxiran during the early stages of reaction. Theoretically a 1 : 3 methyl group transfer is possible but this seems highly unlikely in view of the high strain energy involved in the transition complex. The occurrence of methyl group transfer seems to be well established and is important when 1 : 5 hydrogen transfer is restricted as in the case of neopentane for example [49].

Unsaturated products such as acrolein, methyl vinyl ketone and buta-1,3-diene are formed only in very small concentrations during the early stages and C^{14} - tracer studies [38] show that they most probably arise as a result of the further oxidation of the butenes. Studies of the oxidation of alkenes [106, 107, 108] have shown that, except at very low initial temperatures i.e. ca. 240-260°C, the major attack by radicals on the alkene occurs at the carbon atom in the α-position to the double bond and that this is followed by the addition of oxygen. In the case of but-1-ene and but-2-ene the following reactions may be expected to occur:

$$CH_2{=}CH{-}CH_2{-}CH_3 + \dot{O}H \longrightarrow CH_2{=}CH{-}\dot{C}H{-}CH_3 + H_2O \qquad (4.48)$$

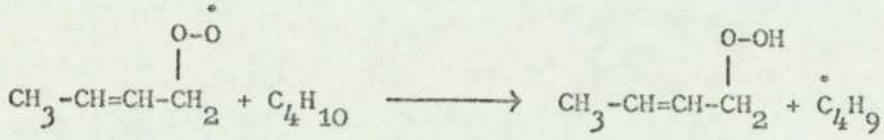
$$CH_2{=}CH{-}\dot{C}H{-}CH_3 + O_2 \longrightarrow CH_2{=}CH{-}\underset{\displaystyle O-\dot{O}}{\underset{|}{C}}H{-}CH_3 \qquad (4.49)$$

$$CH_2{=}CH{-}\underset{\displaystyle O-\dot{O}}{\underset{|}{C}}H{-}CH_3 + C_4H_{10} \longrightarrow CH_2{=}CH{-}\underset{\displaystyle O-OH}{\underset{|}{C}}H{-}CH_3 + \dot{C}_4H_9 \qquad (4.50)$$

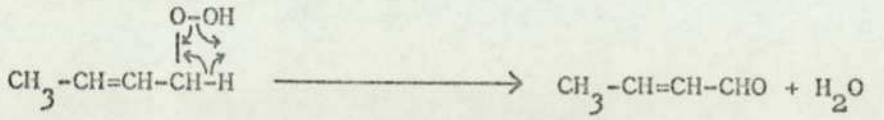
$$CH_2{=}CH{-}\underset{\displaystyle O-OH}{\underset{|}{C}}H{-}CH_3 \longrightarrow CH_2{=}CH{-}CHO + CH_3OH \qquad (4.51)$$

$$CH_3{-}CH{=}CH{-}CH_3 + \dot{O}H \longrightarrow CH_3{-}CH{=}CH{-}\dot{C}H_2 + H_2O \qquad (4.52)$$

$$CH_3{-}CH{=}CH{-}\dot{C}H_2 + O_2 \longrightarrow CH_3{-}CH{=}CH{-}\underset{\displaystyle O-\dot{O}}{\underset{|}{C}}H_2 \qquad (4.53)$$



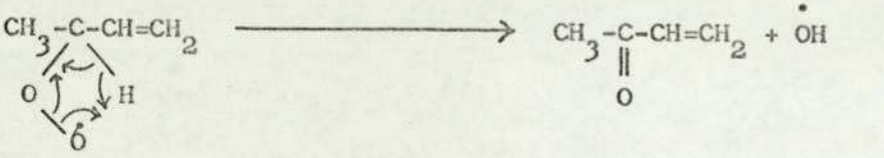
(4.54)



(4.55)

The presence of crotonaldehyde in the products under these conditions is confirmed in the present studies, but in view of its long retention time and its very small concentration, it was not determined.

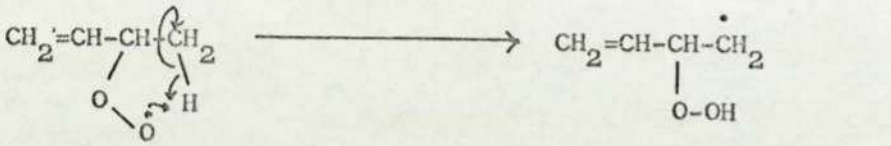
An alternative reaction of the but-1-enylperoxy radicals formed in the above sequence of reactions may explain the formation of methyl vinyl ketone.



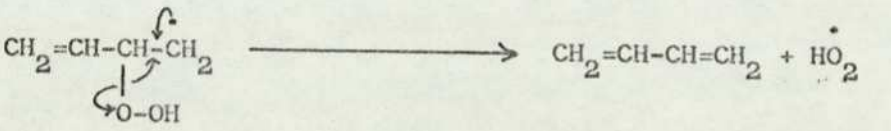
(4.56)

This reaction involves a four-membered transition ring complex which will have a high strain energy and consequently this reaction may only occur at the walls of the reactor. Indeed, the marked decrease in the yield of methyl vinyl ketone with pressure (see Section 4.2.1.2) supports this view.

Buta-1,3-diene may also arise by an alternative mode of decomposition of the but-1-enylperoxy radical



(4.57)

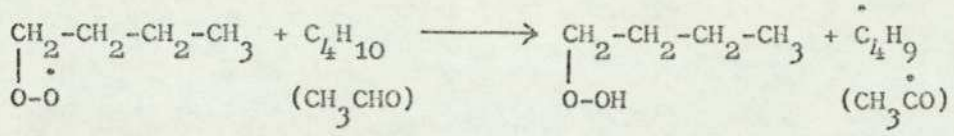


(4.58)

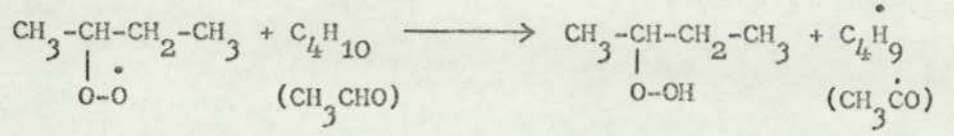
Reaction (4.57) is a conventional 1 : 4 hydrogen transfer isomerisation and decomposition of the radical so formed occurs via the β-scission of the C-O bond.

An important reaction, which has not so far been considered, is the bimolecular abstraction reaction of butylperoxy radicals to form butyl

monohydroperoxides.

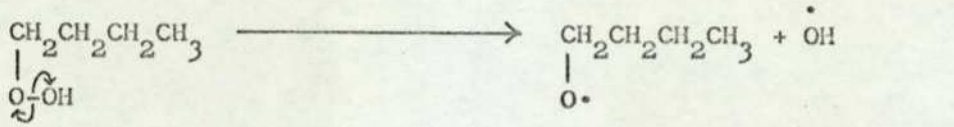


(4.59)

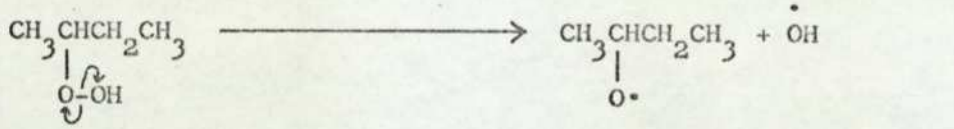


(4.60)

During the very early stages of the reaction, the butylperoxy radicals intermolecularly abstract hydrogen from fuel molecules. As the reaction proceeds, however, reaction intermediates containing a labile hydrogen atom, such as acetaldehyde, will compete with the fuel in reactions (4.59) and (4.60). The principal reaction of the n- and sec- butyl hydroperoxides so formed is unimolecular decomposition. This reaction is generally agreed to be the major degenerate branching reaction at initial temperatures below ca. 330°C.

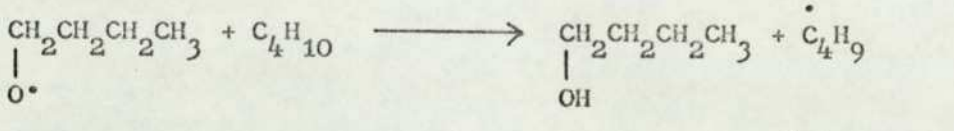


(4.61)

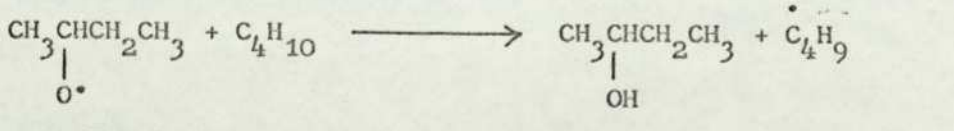


(4.62)

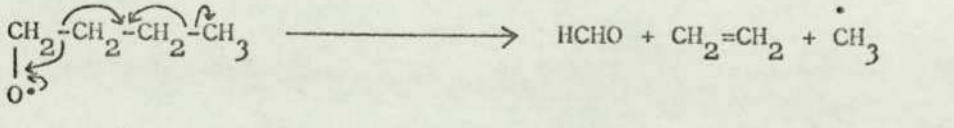
The resulting butoxy radicals may either abstract a hydrogen atom intermolecularly to form n- or sec- butanol or may undergo unimolecular decomposition themselves.



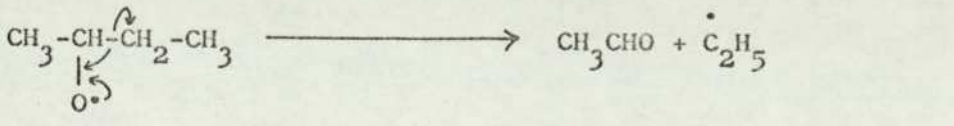
(4.63)



(4.64)



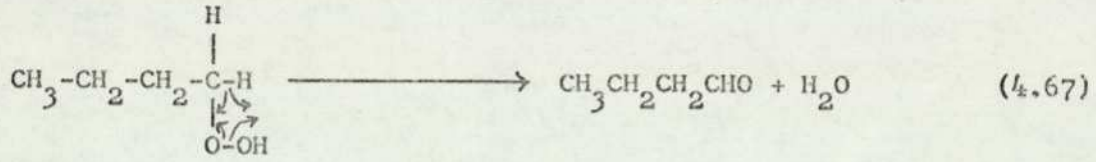
(4.65)



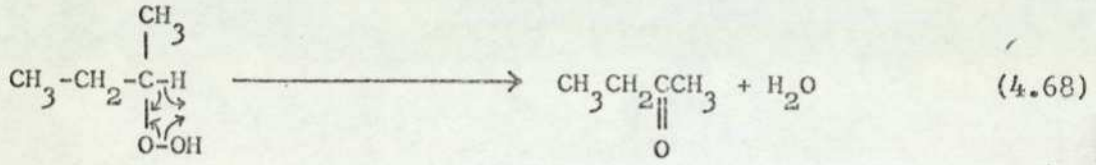
(4.66)

The fact that n- and sec- butanol were not identified in the reaction products suggests that unimolecular decomposition is the principal fate of butoxy radicals under these conditions.

Although the most common reaction of the butyl hydroperoxides is degenerate branching via reactions (4.61) and (4.62), another mode of decomposition, which has been considered by several workers [21, 109], is the four-centre elimination of a molecule of water:



$$CH_3-CH_2-CH_2-\underset{\displaystyle O-OH}{\overset{\displaystyle H}{\overset{|}{C}}}-H \longrightarrow CH_3CH_2CH_2CHO + H_2O \qquad (4.67)$$



$$CH_3-CH_2-\underset{\displaystyle O-OH}{\overset{\displaystyle CH_3}{\overset{|}{C}}}-H \longrightarrow CH_3CH_2\overset{\displaystyle O}{\overset{\|}{C}}CH_3 + H_2O \qquad (4.68)$$

Benson [109] considers that although the activation energy of the four-centre elimination of water will be about the same as that of O-O bond fission namely 43 kcal.mole^{-1}, the higher pre-exponential factor of the latter reaction will mean that O-O bond fission will predominate. Nevertheless, reactions (4.67) and (4.68) are capable of explaining the formation of n-butyraldehyde and methyl ethyl ketone.

An alternative mode of formation of methyl ethyl ketone is also indicated in the C^{14}- tracer studies of Cullis et al [38]. These workers showed that this product can arise from the further reaction of but-1-ene, although it is difficult to suggest a plausible mechanism for this reaction.

4.2.1.1 The effect of temperature

The most pronounced effect on the product distribution during the early stages of reaction as the initial temperature is increased from 285 - 320°C, is that the yields of acetaldehyde and acetone fall dramatically, whilst the yields of but-1-ene and but-2-ene gradually increase.

This suggests that the rate of butylperoxy radical isomerisation involving 1 : 4 hydrogen transfer increases relative to isomerisation involving 1 : 5 hydrogen transfer and that the further oxidation of hydroperoxybutyl radicals, particularly β-hydroperoxybutyl radicals, becomes less important as the temperature is increased. This may in part be due to the reversibility of reaction (4.69).

$$\dot{C}_4H_8OOH + O_2 \rightleftharpoons \dot{O}OC_4H_8OOH \qquad (4.69)$$

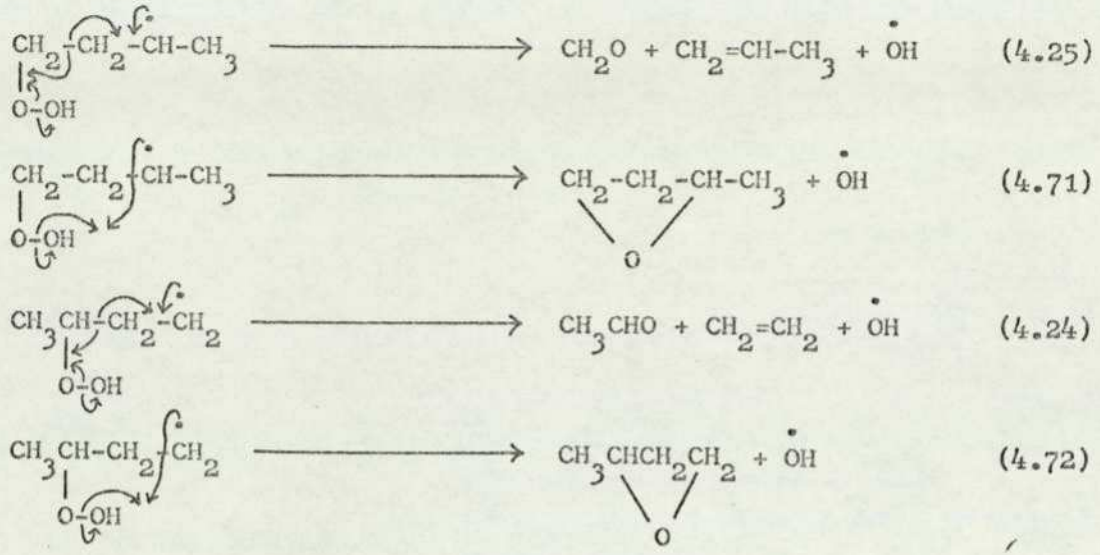
As the initial temperature is increased the breakdown of hydroperoxybutylperoxy radicals may become significant and lead to a decreased stationary concentration of these radicals which in turn will lead to the production of less of their decomposition products, principally acetaldehyde and acetone, as is observed experimentally. An important consequence of this is that since the concentration of acetaldehyde decreases as the initial temperature is increased to 320°C, the rate of reaction (4.70) becomes slower and the formation of butyl hydroperoxides becomes less competitive.

$$C_4H_9\dot{O}O + CH_3CHO \longrightarrow C_4H_9OOH + CH_3\dot{C}O \qquad (4.70)$$

Furthermore, increasing the initial temperature promotes the speed of butylperoxy radical isomerisation which tends to reduce the stationary concentration of butylperoxy radicals and thereby again reduces the effectiveness of reaction (4.70). The net effect is that branching reactions of the hydroperoxides and dihydroperoxides become less important over this temperature range and the rate of reaction will be expected to decrease as is shown by the marked decrease in $(dp_1/dt)_{max}$ as the initial temperature is increased from 285 to 315°C (see Section 4.1.2).

From the above considerations it is clear that products which result from cyclisation and β-scission decomposition reactions of hydroperoxybutyl radicals, should be formed in greater abundance as the

temperature is raised. In the case of β-hydroperoxybutyl radicals, the observed yields of propene, 2-methyloxetan and ethylene do indeed show an increase over the temperature range under consideration.



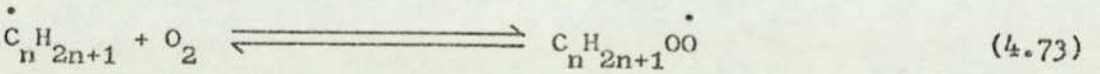
(4.25)

(4.71)

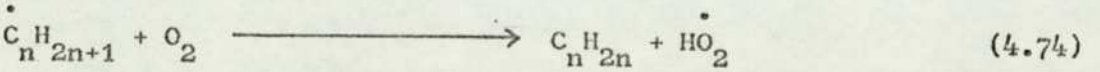
(4.24)

(4.72)

Nevertheless, these increases clearly do not balance with the marked decrease in the yields of acetaldehyde and acetone and the substantial increase in the yields of but-1-ene and but-2-ene indicates that β-scission decomposition of α-hydroperoxybutyl radicals is more important. The increase in the overall concentrations of the butenes from ca.30% at 285°C to ca. 60% at 320°C may, however, be explained in two ways. It has been suggested [32] that in view of the importance of the reversibility of reaction (4.73), the accepted high temperature mechanism of conjugate alkene formation may be important at temperatures as low as 300°C for relatively low molecular weight hydrocarbons.

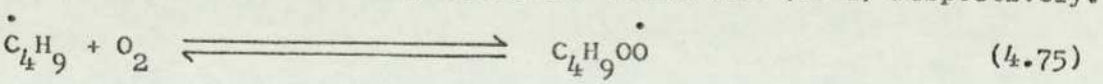


(4.73)

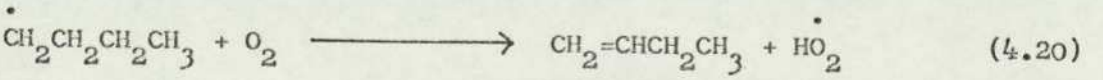


(4.74)

Thus, in the present system, increasing the initial temperature will lead to reaction (-4.75) occurring to a greater extent and as a result but-1-ene and but-2-ene will be formed by reactions (4.20) and (4.21) respectively.



(4.75)



(4.20)

$$CH_3\dot{C}HCH_2CH_3 + O_2 \longrightarrow CH_3CH{=}CHCH_3 + \dot{H}O_2 \qquad (4.21)$$

The alternative explanation is that increasing the initial temperature leads to a greater rate of butylperoxy radical isomerisation involving 1 : 4 hydrogen transfer. Since the predominant mode of decomposition of α-hydroperoxybutyl radicals is β-scission of the C-O bond to form the conjugate butene, their yields would be expected to increase.

Of these two explanations, the latter is favoured since the concentrations of products, such as 2-methyloxetan and tetrahydrofuran, which are generally considered to be diagnostic of the occurrence of alkylperoxy radical isomerisation, are also observed to increase up to ca. 380°C, whilst the former explanation predicts that the reverse should occur.

As the initial temperature is increased further from 320 to 385°C, the yields of acetaldehyde and acetone continue to fall to a combined total of ca. 4%. This clearly indicates that the further oxidation of hydroperoxybutyl radicals is of negligible importance above ca. 330°C. Furthermore, the fact that acetaldehyde and ethylene are formed in approximately equal yields at 380°C, suggests that reaction (4.24) gradually becomes the major route to their formation as the temperature is increased.

$$CH_3\underset{\underset{O\text{-}OH}{|}}{C}HCH_2\dot{C}H_2 \longrightarrow CH_3CHO + CH_2{=}CH_2 + \dot{O}H \qquad (4.24)$$

The increase in the yields of 2-methyloxetan and tetrahydrofuran as the initial temperature is raised to 380°C, clearly shows that butylperoxy radical isomerisation occurs at temperatures as high as 380°C.

It is also interesting to note that the ratio of the yields of but-1-ene to but-2-ene only changes from 1.0 to 1.2 as the initial temperature is raised from 285 to 380°C. This reflects the basic unselectivity of attack on fuel molecules over this temperature range and

strongly suggests, therefore, that this attack is by hydroxyl radicals even at 380°C.

4.2.1.2 The effect of pressure

The effect of increasing the initial pressure from 76 to 190 torr on the product distribution during the early stages of reaction at 300°C, is not markedly significant although certain trends are revealed. The major products at this stage are but-1-ene and but-2-ene and it may be seen from Table 3.4 that as the initial pressure is increased, the yields of these products tend to decrease. The two modes of formation of the butenes have been discussed in Section 4.2.1.1 and it has been suggested that the most probable route to their formation is via butylperoxy radical isomerisation involving 1 : 4 hydrogen abstraction followed by β-scission of the C-O bond. The effect of pressure on their yields is consistent, therefore, with the occurrence of either isomerisation of butylperoxy radicals involving 1 : 4 hydrogen transfer or the β-scission decomposition of the resulting α-hydroperoxybutyl radicals at the walls of the reactor. This suggestion is supported by the observation that an increase in the initial pressure also leads to decreased yields of the C_4 oxirans, which are alternative decomposition products of α-hydroperoxybutyl radicals. In this context it is also of interest to note that the yield of methyl vinyl ketone, which is probably formed by further reaction of but-1-ene at the reactor walls, suffers an even more marked decrease as the initial pressure is increased.

It has been seen in Sections 4.1.2 and 4.1.3 that the existence of a heterogeneous reaction or reactions is clearly illustrated by the kinetic results. Thus, since the yields of those products resulting from β- and γ-hydroperoxybutyl radicals do not exhibit a similar behaviour, it seems reasonable to suggest that at low temperatures it is the

decomposition of α-hydroperoxybutyl radicals which occurs almost exclusively at the walls of the reactor, and as initial temperatures of ca. 320°C are approached, their homogeneous decomposition becomes more important. It is not so surprising, therefore, that at 300°C the observed decrease in the percentage yield of butenes is not very pronounced, since increasing the pressure will tend to favour the homogeneous decomposition of α-hydroperoxybutyl radicals. It would be interesting, however, to determine the effect of increasing the initial pressure at a lower temperature, e.g. 280°C, since the above reasoning suggests that a much more pronounced decrease in the yield of butenes should be observed. Déchaux [55] has indeed found quite pronounced decreases in the butene yields for the n-butane + oxygen system at 290°C, although his experimental work was performed using a smaller reactor (volume ca. 33 ml) and it is to be expected that this higher surface to volume ratio will favour heterogeneous reactions.

Luckett and Pollard [45], who have studied the oxidation of isobutane also found a very pronounced decrease in the percentage yield of isobutene (from ca. 50% to 20%) as the initial pressure is increased from 140 to 340 torr at 310°C. If the decomposition and further oxidation of β-hydroperoxyalkyl radicals occur homogeneously, as is indicated by several studies including that herein, then this observation is to be expected, since isomerisation of isobutylperoxy radicals involving 1 : 5 hydrogen transfer is severely restricted and is impossible for tert-butylperoxy radicals. Thus, in the oxidation of isobutane, the formation of α-hydroperoxybutyl radicals will be expected to predominate and their heterogeneous decomposition will be considerably more pronounced, therefore, than the heterogeneous decomposition of α-hydroperoxybutyl radicals in the present study. Bastow [52] has also found that in the slow oxidation of n-pentane at 250°C, the yield of pent-2-ene decreases by a factor of two

as the initial pressure is increased from 70 to 197 torr. Since pent-2-ene only accounts for 15% of the total detected products, however, it may be concluded that α-hydroperoxypentyl radicals are not nearly so important for this alkane and that the marked decrease in the yield of pent-2-ene merely reflects the increased occurrence of heterogeneous reactions at initial temperatures as low as 250°C.

Table 3.4 shows that increasing the initial pressure has a marked effect on the yield of methyl ethyl ketone which increases by a factor of about 8 between 91 and 148 torr. It was suggested in Section 4.2.1 that this product is formed principally by a decomposition of sec-butyl hydroperoxide and clearly reaction (4.60) will be favoured by an increase in pressure.

$$CH_3\underset{\underset{O\text{-}O}{|\ \bullet}}{CH}CH_2CH_3 + C_4H_{10} \longrightarrow CH_3\underset{\underset{O\text{-}OH}{|}}{CH}CH_2CH_3 + \dot{C}_4H_9 \qquad (4.60)$$

The yields of acetaldehyde and acetone show a slight increase as the initial pressure is increased at 300°C which gives further support to the suggestion that these products result from the further oxidation of β-hydroperoxybutyl radicals at this initial temperature.

The effect of increasing the initial pressure from 62 to 182 torr at 360°C has no influence on the yields of but-1-ene and but-2-ene, which suggests that their formation is entirely homogeneous. In contrast to the results at 300°C, the yield of acetaldehyde and more particularly acetone, decrease as the initial pressure is increased. Clearly, their major mode of formation is not via diperoxy radicals at this elevated temperature.

4.2.2 Product formation during cool-flame propagation

An inspection of the product concentration-time curves obtained at 300°C and 150 torr, (figures 3.38 - 3.44), shows that the major products

during the induction period of the first cool flame, namely but-1-ene, but-2-ene, acetaldehyde and acetone, are also the major products immediately after its passage. In view of the high transient temperatures reached during the cool flame (ca.400+^{o}C), however, it is probable that at these temperatures β-hydroperoxybutyl radicals preferentially decompose by a β-scission reaction as opposed to undergoing further oxidation. This suggestion is supported by the observation that at < 1% fuel conversion, the ratio of the concentration of ethylene, a β-scission decomposition product, to that of acetone, a further oxidation product, is ca. 1 : 4, whereas immediately after the passage of the first cool flame this ratio is ca. 3 : 2. Likewise, the ratio of the concentration of propene to that of acetone shows an even more pronounced increase under the same conditions. Furthermore, these two ratios both increase with time, at least until the passage of the third cool flame and this suggests that further oxidation of β-hydroperoxybutyl radicals becomes increasingly less competitive as the reaction proceeds. Clearly, this is to be expected since the concentration of oxygen is steadily decreasing with time.

The enhancement of reactions (4.23) and (4.24) during the transient temperature rise accompanying the cool flame affords an explanation for the fact that the concentration of acetaldehyde does not decline during the passage of the cool flame as is usually expected of a degenerate branching agent.

$$CH_3\text{-}\underset{\underset{O\text{-}O}{|}}{CH}\text{-}CH_2\text{-}CH_3 \longrightarrow CH_3\text{-}\underset{\underset{O\text{-}OH}{|}}{CH}\text{-}CH_2\text{-}\dot{C}H_2 \qquad (4.23)$$

$$CH_3\text{-}\underset{\underset{O\text{-}OH}{|}}{CH}\text{-}CH_2\text{-}CH_2 \longrightarrow CH_3CHO + CH_2{=}CH_2 + \dot{O}H \qquad (4.24)$$

Clearly, the important reaction is not reaction (4.13),

$$CH_3CHO + O_2 \longrightarrow CH_3\dot{C}O + H\dot{O}_2 \qquad (4.13)$$

but the formation and decomposition of peracetic acid:

$$CH_3CHO + \dot{O}H \longrightarrow CH_3\dot{C}O + H_2O \qquad (4.76)$$

$$CH_3\dot{C}O + O_2 \longrightarrow CH_3COO\dot{O} \qquad (4.10)$$

$$CH_3COO\dot{O} + C_4H_{10} \text{ or } AH \longrightarrow CH_3COOOH + \dot{C}_4H_9 \text{ or } \dot{A} \qquad (4.77)$$

$$CH_3COOOH \longrightarrow CH_3CO\dot{O} + \dot{O}H \qquad (4.78)$$

Although peracids were not analysed, the appearance of methane in the products only at the time of the passage of the first cool flame provides strong evidence for this suggestion.

$$CH_3\dot{C}O \longrightarrow \dot{C}H_3 + CO \qquad (4.3)$$

$$CH_3COO\dot{O} \longrightarrow CH_3\dot{O} + CO_2 \qquad (4.4)$$

$$\dot{C}H_3 + AH \longrightarrow CH_4 + \dot{A} \qquad (4.79)$$

The variation of the concentration of methyl ethyl ketone with time at 300°C is extremely interesting, since immediately before the onset of the pressure rise which accompanies the first cool flame its concentration suffers a dramatic decline (figure 3.43) which is the behaviour expected of a branching agent. Ketones are generally considered to be relatively stable intermediates, however, and there is no previous evidence for their behaviour as agents of degenerate branching.

It is also of interest to note that the ratio of the concentration of but-1-ene to that of but-2-ene increases during the passage of the first cool flame. The most likely explanation for this behaviour is that the high transient temperature reached during the cool flame allows 1 :4 hydrogen transfer involving a 1^oC-H to compete more effectively with 1 : 4 hydrogen transfer from a 2^oC-H during the isomerisation of but-2-ylperoxy radicals. Thus, at the elevated temperatures, but-2-ylperoxy radicals eventually give rise to both but-1-ene and but-2-ene (c.f. their behaviour at low temperatures), whereas

but-1-ylperoxy radicals can only give rise to but-1-ene. In this way, the ratio of the concentration of but-1-ene to that of but-2-ene will increase during the passage of the cool flame.

The further reaction of intermediates during the course of the reaction is clearly shown in figures 3.38 - 3.42 and 3.44. Thus, for example, at 300°C the concentrations of but-1-ene and but-2-ene pass through maximum values at the third and second cool flames respectively. Furthermore, these results indicate that but-2-ene is more reactive than but-1-ene which is in accordance with the results of Cullis et al [38]. These workers also showed that at 315°C, when approximately 10% of the fuel has been consumed, at least 38% of the 2-ethyloxiran originates from but-1-ene, whilst 59% of cis 2,3-dimethloxiran and 43% of the trans isomer originate from but-2-ene. This fact probably explains the continual increase in the concentration of the C_4 oxirans as opposed to the oscillatory behaviour of the concentrations of 2-methyloxetan and tetrahydrofuran.

Other unsaturated intermediates such as ethylene, propene, acrolein, methyl vinyl ketone and buta-1,3-diene all enter into further reaction since their concentration-time curves exhibit maximum values. Products such as methane, propane and methanol continue to build up throughout the reaction and are, no doubt, formed in part by the secondary reactions involving these primary products.

The behaviour of the yield of acetone is interesting, since it increases fairly steadily throughout the multiple cool flame reaction. This suggests that its mode of formation is not so much connected with the passage of the cool flame but more with the underlying primary chain cycle. At low initial temperatures this may well be the result of branching due to dihydroperoxides.

At an initial temperature of 309°C the overall product distribution throughout the reaction is similar to that at 300°C except

that compounds such as acetaldehyde and acetone, which result from β-hydroperoxybutylperoxy radicals are less important and the butenes are more important.

During the course of the reaction, the concentrations of acetaldehyde and ethylene, although not equal, do not show such a large disparity as at 300°C which again indicates the increasing importance of β-scission reactions of β-hydroperoxybutyl radicals relative to their further oxidation as the initial temperature is increased.

The oscillatory behaviour of the concentrations of 2-methyloxetan and tetrahydrofuran are not as pronounced as at 300°C probably because the slow combustion following the first cool flame, (upon which subsequent cool flames are superimposed and which becomes more important as the initial temperature is increased) presumably contributes to their formation.

At 360°C the cool flames are characterised by extremely short induction periods during which negligible amounts of products are formed. The principal products immediately after the passage of the cool flame are but-1-ene and but-2-ene and their presence indicates the importance of α-hydroperoxybutyl radical formation. The predominant mode of decomposition of β-hydroperoxybutyl radicals at this temperature is clearly via a β-scission reaction since the concentrations of ethylene and acetaldehyde remain almost equal throughout the course of the reaction.

$$CH_3\underset{\underset{O\text{-}OH}{|}}{C}HCH_2\dot{C}H_2 \longrightarrow CH_3CHO + CH_2{=}CH_2 + \dot{O}H \qquad (4.24)$$

These results clearly demonstrate that the reactions leading to the propagation of a cool flame are also the predominant reactions at the elevated transient temperatures reached during its propagation.

4.3 Conclusions

The present study has thrown a considerable amount of light on the mechanism of oxidation of n-butane both before and during the propagation of cool flames. In particular, it gives strong support to the important suggestion made in the Introduction that for relatively low molecular weight alkanes the participation of α-hydroperoxyalkyl radicals in the oxidative mechanism is of major importance and that the decomposition of these radicals probably occurs heterogeneously at relatively low initial temperatures.

The kinetic and analytical results clearly show that changes in the mechanism occur as the initial temperature is increased above ca. 320 - 335°C. These changes are summarised in Schemes I, II and III which correspond to initial temperatures of 285, 330 and 380°C respectively. Below 320°C the cool flames propagate from the walls of the reactor and the major products at all stages of the reaction are acetone and acetaldehyde. These results may be explained as follows. The fuel is attacked unselectively and the major fate of the butyl radicals is addition of oxygen. The butylperoxy radicals so formed then isomerise predominantly by 1 : 4 and 1 : 5 hydrogen transfer to give α- and β-hydroperoxybutyl radicals. It appears that the former radicals decompose mainly heterogeneously to form the conjugate butenes and C_4 oxirans, whilst the latter are further oxidised before decomposing homogeneously to acetone and acetaldehyde. Although hydroperoxides were not estimated the results are consistent with those found for other hydrocarbon+oxygen systems in which branching at these temperatures occurs via the decomposition of alkyl hydroperoxides (i.e. the L_1 mechanism) which may also be heterogeneous.

As the initial temperature is increased to ca. 320-335°C, the

reaction rate decreases and the conjugate alkenes become the major products. It is suggested that this is due to the increased competition of isomerisation involving 1 : 4 hydrogen transfer and to the increased rate of decomposition of the hydroperoxybutyl radicals over their further oxidation. The resulting lower yields of acetaldehyde lead to the reduced rate reaction.

At initial temperatures above ca. 320-335°C the reaction rate again increases due to the onset of the L_2 branching mechanism. This is almost certainly homogeneous in nature and at these temperatures the α-hydroperoxybutyl radicals also decompose homogeneously. The general lack of heterogeneity is shown by the fact that the cool flames now propagate from the centre of the reactor.

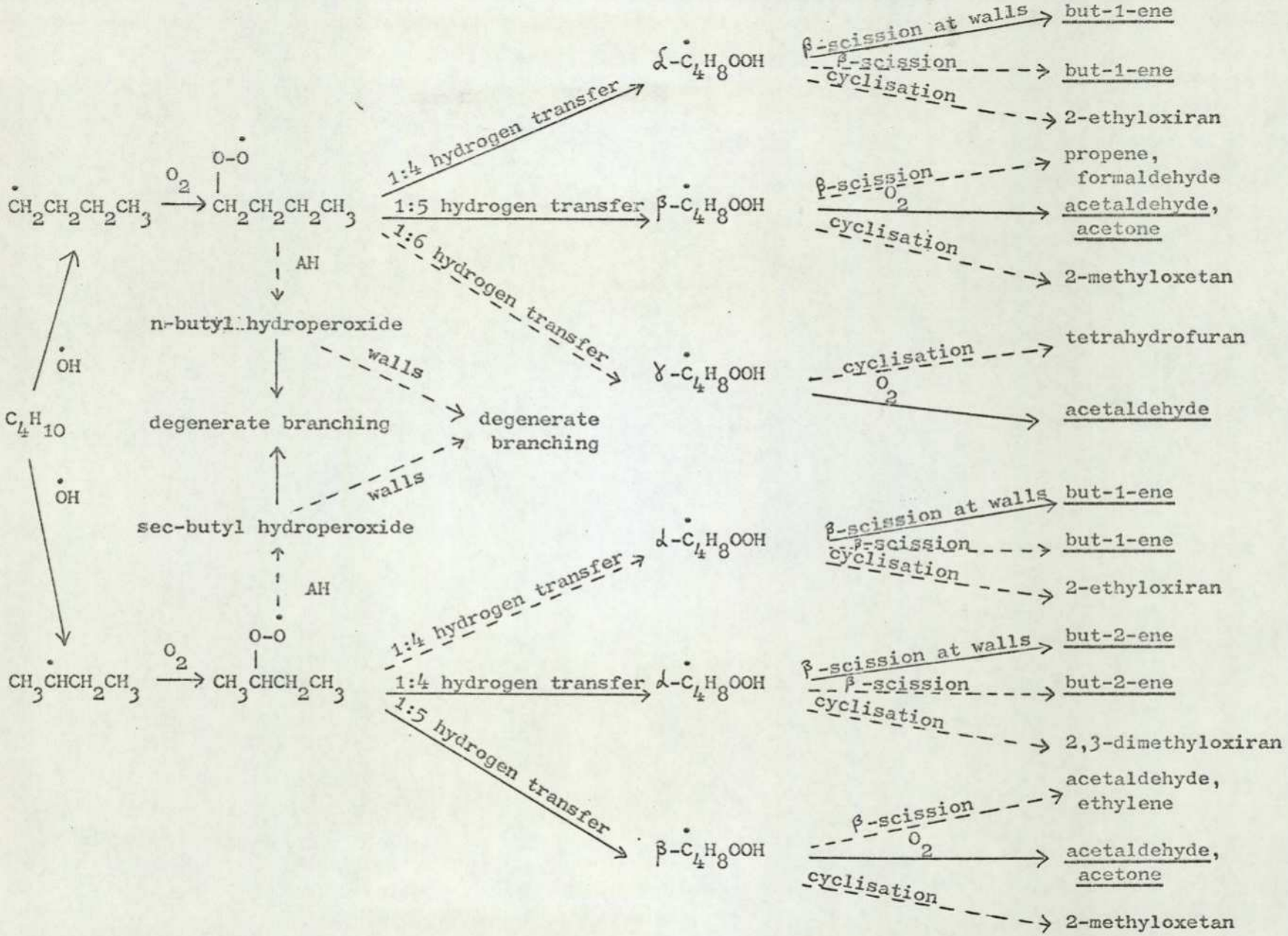
Measurements of the temperature of the reacting mixture strongly suggest that the periodicity and self-quenching nature of the cool flames may be attributed to a thermal switch between two competing reactions. The sudden appearance of methane in the products at the cool flame and the importance of acetaldehyde as a primary product suggest further that these reactions are the further oxidation and decomposition of acyl radicals. This thermal switch also appears to be responsible for the principal region of negative temperature coefficient above ca. 360°C.

Finally, the suggested mechanisms in Schemes I and II allow an explanation for the variation in mechanism with molecular weight of the hydrocarbon, stoichiometry and the presence of HBr. Clearly, the heterogeneous contribution to the oxidation of higher molecular weight hydrocarbons will be smaller since their structure permits the easier alkylperoxy radical isomerisations involving 1 : 5 and 1 : 6 hydrogen transfer and hence the production of α-hydroperoxyalkyl radicals will not predominate. Increase of the oxygen concentration will promote the further oxidation of hydroperoxyalkyl radicals which will be followed by

their homogeneous decomposition, whilst the presence of compounds containing a labile hydrogen atom, such as HBr, will promote the homogeneous formation of alkyl hydroperoxides. In both cases, therefore, the heterogeneity will be expected to decrease.

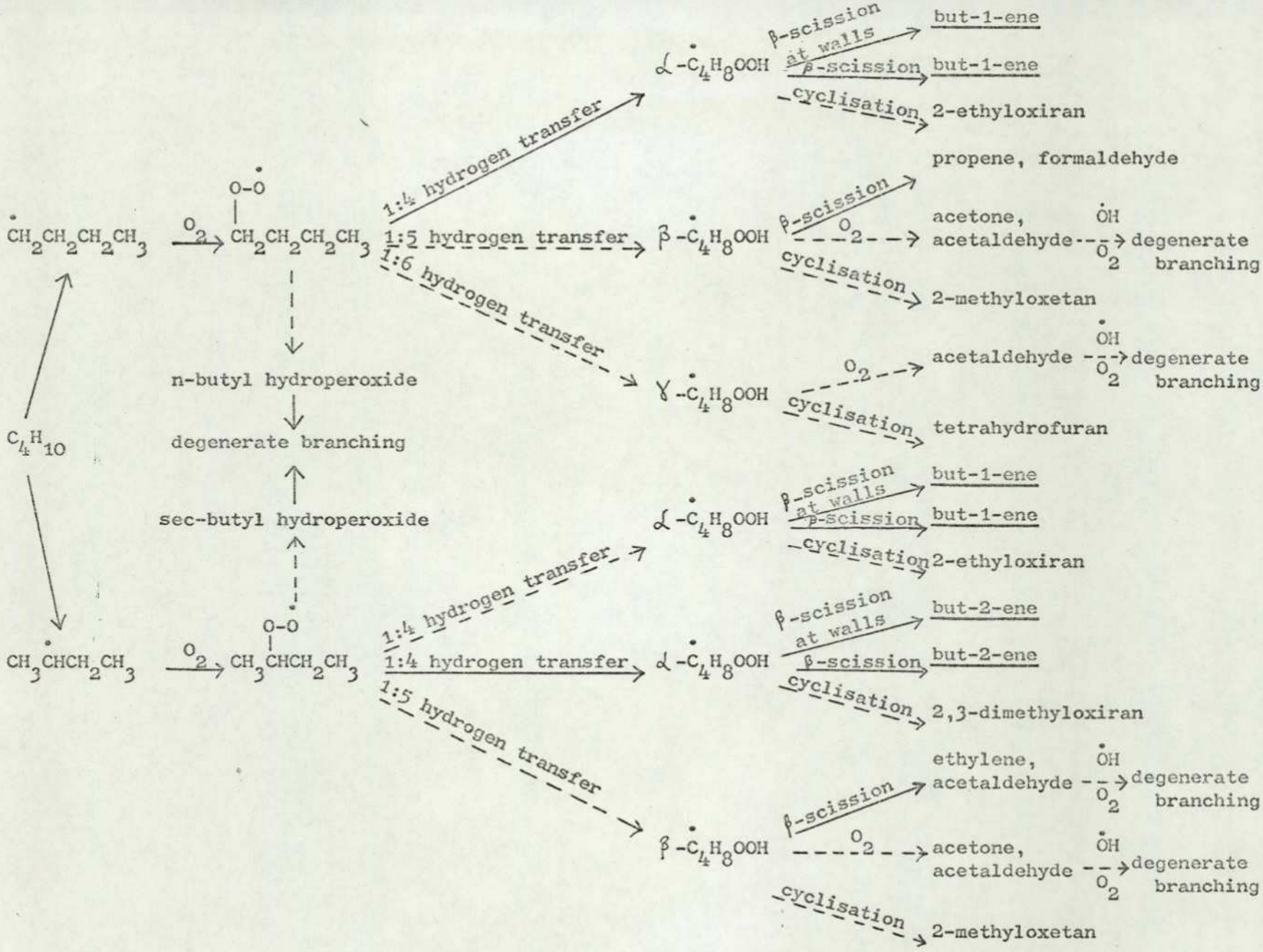
Scheme I

The overall mechanism at 285°C



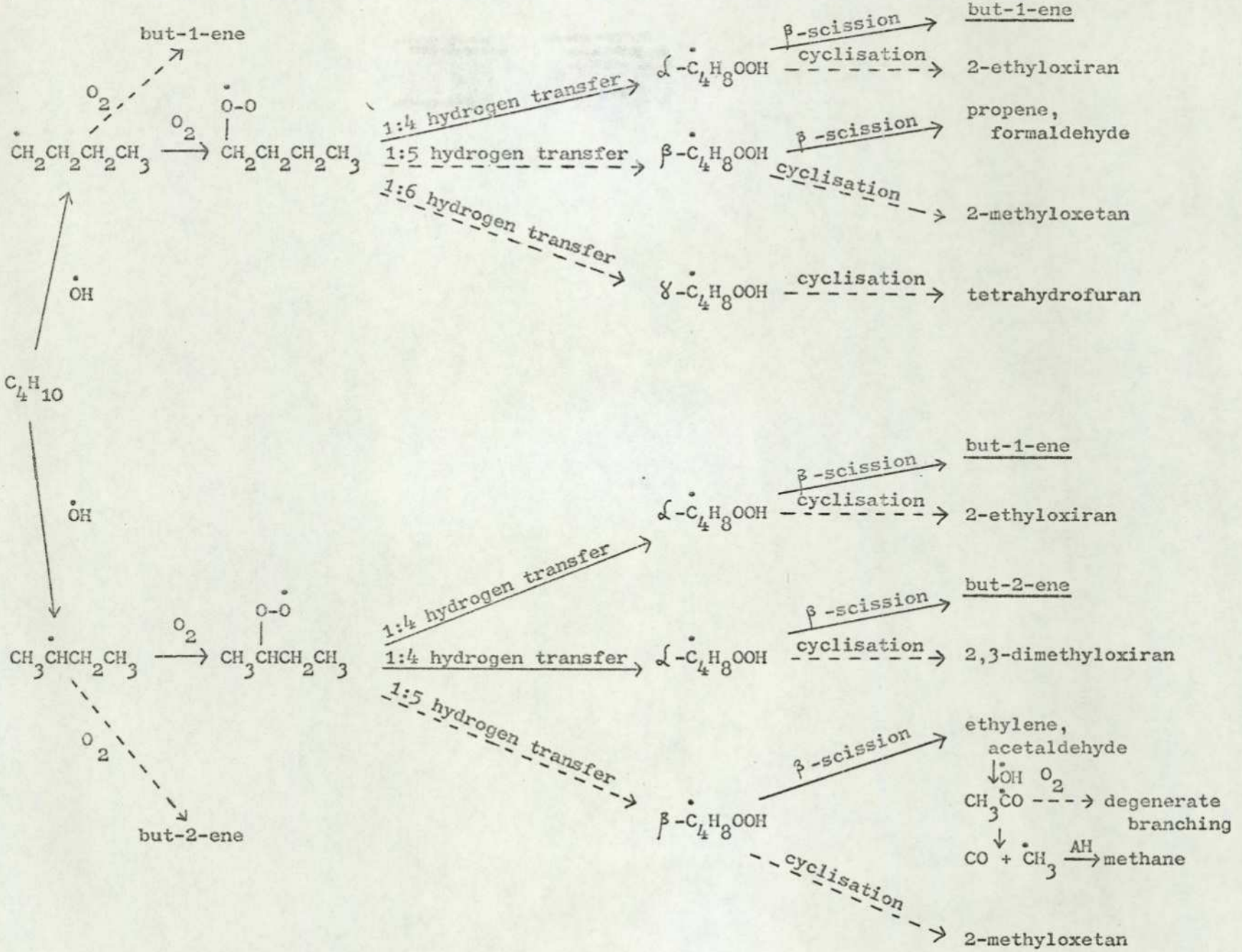
Scheme II

The overall mechanism at 330°C



Scheme III

The overall mechanism at 380°C



4.4 Future work

The present study has revealed several further lines of approach for a more complete elucidation of the mechanism of oxidation of n-butane and for the verification of the suggestions herein.

In view of the considerable evidence for the occurrence of heterogeneous reactions, it would be extremely useful to observe the effect of stoichiometry. The results of the present study suggest that an increase in the oxygen to fuel ratio would decrease the heterogeneity. This would be reflected in a lowering of the limit below which cool flames are observed to propagate from the walls of the reactor and a lowering of the temperatures at which discontinuities are observed in the variation of log τ_1 with $^1/T_o$. Studies of the effect of inert gases and changes in reactor dimensions would also provide useful information about the occurrence of heterogeneous reactions. In this context, the application of specially developed sampling techniques, whereby samples of the reaction mixture could be withdrawn from specific points in the reactor, for example from the three thermocouple locations, could indicate whether, as might be expected from the present results, concentration gradients of certain products or intermediates exist.

The present study has not unequivocally identified the nature of the branching agents which are responsible for cool flames in the n-butane + oxygen system although indirect evidence suggests that n- and sec- butyl hydroperoxides are important below ca. 330°C, whereas peracetic, and perhaps perpropionic, acid is important at temperatures above ca.330°C. A useful study, therefore, would be the determination and identification of these highly unstable intermediates in the above temperature ranges. Furthermore, the addition of aldehydes would help to elucidate the extent and nature of their participation in both the L_1 and L_2 mechanisms.

C^{14}- tracer studies have been carried out [38] in order to investigate the role of the butenes in the oxidation of n-butane at 315°C and it would be most rewarding to repeat such studies at a higher initial temperature, for example at 360°C, in the upper single cool-flame region. The present study suggests that at this temperature the butenes would be observed to give rise to a greater proportion of the yields of the C_4 oxirans than at 315°C. Furthermore, it would be interesting to determine whether but-1-ene is almost solely responsible for the formation of methyl ethyl ketone at 360°C. These studies would also provide valuable information regarding the reversibility of reaction (4.80) at 360°C.

$$C_4H_9\dot{O}O \rightleftharpoons \alpha\text{-}\dot{C}_4H_8OOH \qquad (4.80)$$

At 315°C, the reverse reaction has been shown to be negligible, but clearly, if it does become more competitive as the temperature is increased, then 2-methyloxetan and tetrahydrofuran would be expected to be amongst the active products at 360°C.

REFERENCES

1 Pet. Rev., 24, 327, (1970)

2 Stobaugh, R.B., Ray, G.C. and Spinek, R.A., Hydro.Process, 49, 105, (1970)

3 Schwerdtel, W., Hydro. Process, 49, 117, (1970)

4 Uhl, W.C., Process Rev., 41, 6, 8, (1970)

5 Fussel, D.R., Pet. Rev., 24, 192, (1970)

6 Caplan, J.D., S.A.E. Paper 650641, (1965)

7 Semenov, N.N., Chain Reactions, Oxford University Press, (1935)

8 Newitt, D.M. and Thornes, L.S., J. Chem. Soc., 1656, 1669, (1937)

9 Lucquin, M., Genie Chim., 88, 190, (1962)

10 Ben-Aim, R. and Lucquin, M., Oxidation and Combustion Reviews, Edited by C.F.H. Tipper, Elsevier, Amsterdam, 1, 1, (1965)

11 Fish, A., Haskell, W.W. and Read, I.A., Proc. Roy. Soc., A313, 261, (1969)

12 Barat, P., Cullis, C.F. and Pollard, R.T., Thirteenth Symposium (International) on Combustion, The Combustion Institute, Pittsburgh, p.171, (1971)

13 Ubbelohde, A.R., Proc. Roy. Soc., A152, 354, (1935)

14 Pease, R.N., J. Amer. Chem. Soc., 57, 2296, (1935)

15 Lewis, B. and von Elbe, G., J. Amer. Chem. Soc., 59, 970, (1937)

16 Walsh, A.D., Trans. Faraday Soc., 43, 297, 305, (1947)

17 Norrish, R.G.W., Disc. Faraday Soc., 10, 269, (1951)

18 Shtern, V. Ya., The Gas-Phase Oxidation of Hydrocarbons, Pergamon Press, London, P.331, (1964)

19 Cullis, C.F. and Hinshelwood, C.N., Disc. Faraday Soc., 2, 117, (1947)

20 Semenov, N.N., Some Problems of Chemical Kinetics and Reactivity, Pergamon Press, London, (1959)

21 Walsh, A.D., Trans. Faraday Soc., 42, 269, (1946)

22 Mayer, S.W. and Schieler, L., J. Phys. Chem., 72, 2628, (1968)

23 Markevich, A.M., Zh.fiz.Khim., 22, 941, (1948)

24 Butyagin, P. Yu., and Yelovich, S.Yu., Dokl. Akad. Nauk. S.S.S.R., 75, 711, (1950)

25 Dingledy, D.P. and Calvert, J.G., J. Amer. Chem. Soc., 85, 856, (1963)

26 Hoare, D.E. and Walsh, A.D., Trans. Faraday Soc., 53, 1102, (1957)

27 Fish, A., Adv. Chem. Ser., 76, 69, (1968)

28 Knox, J.H. and Norrish, R.G.W., Trans. Faraday Soc., 50, 928, (1954)

29 Knox, J.H., Trans. Faraday Soc., 55, 1362, (1959)

30 Falconer, J.W. and Knox, J.H., Proc. Roy. Soc., A250, 493, (1959)

31 Knox, J.H., Smith R.F. and Trotman-Dickenson, A.F., Trans. Faraday Soc., 54, 1509, (1958)

32 Knox, J.H., Combust. Flame, 9, 297, (1965)

33 Knox, J.H. and Wells, C.H.J., Trans. Faraday Soc., 59, 2786, 2801,(1963)

34 Skirrow, G. and Williams, A., Proc. Roy. Soc., A268, 537, (1962)

35 Cartlidge, J. and Tipper, C.F.H., Proc. Roy. Soc., A261, 388, (1961)

36 Hay, J., Knox J.H. and Turner, J.M.C., Tenth Symposium (International) on Combustion, Butterworths, p.331, (1965)

37 Turner, J.M.C., Ph.D. Thesis, Edinburgh, (1964)

38 Berry, T., Cullis, C.F. and Trimm, D.L., Proc. Roy. Soc., A316, 377, (1970)

39 Benson, S.W., Adv. Chem. Ser., 76, 143, (1968)

40 Fettis, G.C. and Trotman-Dickenson, A.F., J. Amer. Chem. Soc., 81, 5260, (1959)

41 Benson, S.W., J. Amer. Chem. Soc., 87, 972, (1965)

42 Kinnear, C.G. and Knox, J.H., Symposium on Gas Kinetics,Univ.of Szeged, Hun. Chem. Soc., p.356, (July, 1969)

43 Fish, A., Organic Peroxides, Edited by D. Swern, Wiley-Interscience, p.141, (1970)

44 Berry, T., Cullis, C.F., Saeed, M. and Trimm, D.L., Adv. Chem. Ser., 76, 86, (1968)

45 Luckett, G.A. and Pollard, R.T., unpublished results

46 Thomas, J.R. and Crandall, H.W., Ind. Eng. Chem., 43, 2761, 2766, (1951)

47 Rust, F.F., J. Amer. Chem. Soc., 79, 4000, (1957)

48 Fish, A., Proc. Roy. Soc., A298, 204, (1967)

49 Fish, A., Combust. Flame, 13, 23, (1969)

50 Cullis, C.F., Fish, A., Saeed, M. and Trimm, D.L., Proc. Roy. Soc., A289, 402, (1966)

51 Fish, A. and Wilson, J.P., Thirteenth Symposium (International) on Combustion, The Combustion Institute, Pittsburgh, p.221, (1971)

52 Bastow, A.W., Ph.D. Thesis, The City University, London (1970)

52* (i) Tcherniak, N. and Shtern, V.Ya., Dokl. Akad. Nauk. S.S.S.R., 78, 91, (1951)

(ii) Antonovski, V.L. and Shtern, V.Ya., Dokl.Akad.Nauk. S.S.S.R., 78, 303, (1951)

53 Enikolopyan, N.S., Dokl.Akad.Nauk. S.S.S.R., 119, 520, (1958)

54 (i) Bawn, C.E.H. and Skirrow, G., Fifth Symposium (International) on Combustion, Reinhold, New York, p.521, (1955)

(ii) Mullen, J.D. and Skirrow, G., Proc. Roy. Soc., A244, 312, (1958)

55 Dechaux, J.C., Theses, La Faculte Des Sciences de L'Universite de Lille, (1971)

56 Blanchard, L.P., Farmer, J.B. and Ouellet, C., Canad. J. Chem., 35, 115, (1957)

57 Walsh, A.D., Ninth Symposium (International) on Combustion, Butterworths, p.1046, (1963)

58 Fish, A., Angew. Chem., 80, 53, (1968); International Ed. 7, 45, (1968)

59 Lucquin, M., Discussion on Low Temperature Ignition of Organic Substances in the Gas Phase, Donnan Laboratories, Liverpool, December, (1967)

60 Antonik, S. and Lucquin, M., Bull. Soc. Chim. (France), 10, 4043, (1968)

61 Antonik, S., Theses, La Faculte Des Science de L'Universite de Lille, (1971)

62 Sochet, L.R., Sawerysyn, J.P. and Lucquin, M., Adv.Chem. Ser., 76, 111, (1968)

63 Minkoff, G.J. and Tipper, C.F.H., Chemistry of Combustion Reactions, Butterworths, (1962)

64 Bonner, B.H. and Tipper, C.F.H., Tenth Symposium (International) on Combustion, The Combustion Institute, Pittsburgh, p.145, (1965)

65 Seakins, M., Proc. Roy. Soc., A261, 281, (1961)

66 Hoare, D.E., Proc. Roy. Soc., A291, 73, 85, (1966)

67 Benson, S.W., J. Amer. Chem. Soc., 86, 3922, (1964)

68 Sochet, L.R. and Lucquin, M., Combust. Flame, 13, 319, (1969)

69 Kondrat'ev, V.N., Acta Physicochimica U.S.S.R., 4, 556, (1936)

70 Sokolik, A.S., Self-Ignition, Flame and Detonation in Gases, Israel Program for Scientific Translations, Jerusalem, (1963)

71 Hoare, D.E., Protheroe, J.B. and Walsh, A.D., Trans.Faraday Soc., 55, 548, (1959)

72 Baldwin, R.R. and Mayor, L., Trans. Faraday Soc., 56, 103, (1960)

73 Sampson, R.J., J. Chem. Soc., p.5095, (1963)

74 Cullis, C.F., Fish, A. and Gibson, J.F., Proc. Roy. Soc., A284, 108, (1965)

75 Sampson, R.J., From meeting on Oxidation in Organic Chemistry, Manchester, (1964)

76 Baldwin, R.R., Everett, C.J., Hopkins, D.E. and Walker, R.W., Adv. Chem. Ser., 76, 124, (1968)

77 Baker, R.R., Baldwin, R.R. and Walker, R.W., Trans. Faraday Soc., 66, 2812, (1970)

78 Fish, A., Read, I.A., Affleck, W.S. and Haskell, W.W., Combust Flame, 13, 39, (1969)

79 Bardwell, J., Fifth Symposium (International) on Combustion, Reinhold, New York, p.529, (1955)

80 Griffiths, J.F., Gray, B.F. and Gray, P., Thirteenth Symposium (International) on Combustion, The Combustion Institute, Pittsburgh, p. 000, (1971)

81 Antonik, S., private communication

82 Affleck, W.S. and Fish, A., Combust. Flame, 12, 243, (1968)

83 Voinov, A.N., Skorodelov, D.I. and Sokolov, F.P., Kinet. Katal., 5, 340, (1964)

84 Affleck, W.S., Bright, P.E. and Fish, A., Combust. Flame, 12, 307, (1968)

85 Jones, J.H. and Fenske, M.R., Ind. Eng. Chem., 51, 262, (1959)

86 Affens, W.A., Johnson, J.E. and Carhart, H.W., J.Chem.Eng. Data, 6, 613, (1961)

87 Miles, R.T., unpublished results.

88 Whitehead, D.M., Discussion on Low Temperature Ignition of Organic Substances in the Gas Phase, Donnan Laboratories, Liverpool, December, (1967)

89 Batten, J.J., Gardner, H.J. and Ridge, H.J., J. Chem. Soc., p. 3029, (1955)

90 Dahm, D.B. and Verhoek, F.M., Combust. Flame, 12, 380, (1968)

91 Barnard, J.A., private communication

92 Kaskan, W.E., Sixth Symposium (International) on Combustion, Reinhold, p.134, (1957)

93 Barnard, J.A. and Watts, A., Twelfth Symposium (International) on Combustion, The Combustion Institute, Pittsburgh, P.365, (1969)

94 Schmoyer, L.F. and Case, L.C., Nature, 187, 592, (1960)

95 Fish, A., Proc. Roy. Soc., A293, 378, (1966)

96 Yantovskii, S.A., Kinet. i Katal., 5, 399, (1964)

97 Hughes, R. and Simmons, R.F., Combust. Flame, 14, 103, (1970)

98 Yantovskii, S.A., Kinet. i Katal., 7, 21, (1966)

99 Atherton, J., unpublished results

100 Rehman, S., unpublished results

101 Pollard, R.T., Comprehensive Chemical Kinetics, Vol. 17, Chpt. 3, Elsevier, In press.

102 Semenov, N.N., Photochemistry and Reaction Kinetics, Edited by P.G. Ashmore, F.S.Dainton and T.M. Sugden, The University Press, Cambridge, p.229, (1967)

103 Barnard, J.A., Adv. Chem. Ser., 78, 98, (1968)

104 Neiman, M.B. and Feklisov, G.I., Doklady Akad. Nauk.S.S.S.R., 91, 877, (1953)

105 Greiner, N.R., J. Phys. Chem., 46, 3389, (1967)

106 Farmer, E.H., Trans. Faraday Soc., 38, 340, (1942)

107 Blundell, A. and Skirrow, G., Proc. Roy. Soc., A244, 331, (1958)

108 Cullis, C.F., Fish, A. and Turner, D.W., Proc. Roy. Soc., A262, 318, (1961)

109 Benson, S.W. and Shaw, R., Organic Peroxides, Edited by D. Swern, Wiley-Interscience, p. 105, (1970)

110 McDowall, C.A. and Thomas, J.A., J. Chem. Soc., p.2208,p.2217, (1949)